

UNCLASSIFIED

AD NUMBER
AD824698
NEW LIMITATION CHANGE
TO Approved for public release, distribution unlimited
FROM Distribution authorized to U.S. Gov't. agencies and their contractors; Critical Technology; SEP 1967. Other requests shall be referred to US Army Aviation Materiel Labs., Fort Eustis, VA 23604.
AUTHORITY
US Army Air Mobility Research and Development Lab ltr dtd 4 May 1971

THIS PAGE IS UNCLASSIFIED

AD 824-698

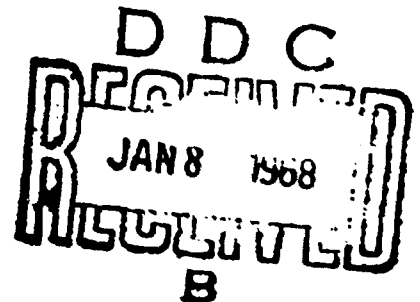
USAAVLABS TECHNICAL REPORT 67-45

ADVANCED LIFT FAN SYSTEM (LFX) STUDY CONTINUATION

AD824698

By

Harris C. True



September 1967

**U. S. ARMY AVIATION MATERIEL LABORATORIES
FORT EUSTIS, VIRGINIA**

**CONTRACT DA 44-177-AMC-422(T)
GENERAL ELECTRIC COMPANY
CINCINNATI, OHIO**

This document is subject to special export controls and each transmittal to foreign governments or foreign nationals may be made only with prior approval of U.S. Army Aviation Materiel Laboratories, Fort Eustis, Virginia 23604.



Disclaimers

The findings in this report are not to be construed as an official Department of the Army position unless so designated by other authorized documents.

When Government drawings, specifications, or other data are used for any purpose other than in connection with a definitely related Government procurement operation, the United States Government thereby incurs no responsibility nor any obligation whatsoever; and the fact that the Government may have formulated, furnished, or in any way supplied the said drawings, specifications, or other data is not to be regarded by implication or otherwise as in any manner licensing the holder or any other person or corporation, or conveying any right or permission, to manufacture, use, or sell any patented invention that may in any way be related thereto.

Trade names cited in this report do not constitute an official endorsement or approval of the use of such commercial hardware or software.

Disposition Instructions

Destroy this report when no longer needed. Do not return it to originator.

COST		WHITE SECTION <input type="checkbox"/>
BY		GRAY SECTION <input checked="" type="checkbox"/>
UNANNOUNCED		<input type="checkbox"/>
JUSTIFICATION		
BY		
RESTRICTION/AVAILABILITY CODES		
DISC.	AVAIL. and SPECIAL	
2		



DEPARTMENT OF THE ARMY
U. S. ARMY AVIATION MATERIEL LABORATORIES
FORT EUSTIS, VIRGINIA 23604

This report has been reviewed by the U.S. Army Aviation Materiel Laboratories and is considered to be technically sound. This study was undertaken to "design in depth" an advanced tip-turbine-driven lift fan propulsion system based on component technology.

Task LM121401D14415
Contract DA 44-177-AMC-422(T)
USAAVLABS Technical Report 67-45
September 1967

ADVANCED LIFT FAN SYSTEM (LFX) STUDY CONTINUATION

by

Harris C. True

Prepared by

General Electric Company
Flight Propulsion Division
Advanced Technology & Demonstrator Programs Department
Lift Fan Systems Operation
Cincinnati, Ohio

for

U.S. ARMY AVIATION MATERIEL LABORATORIES
FORT EUSTIS, VIRGINIA

This document is subject to special export controls and each transmittal to foreign governments or foreign nationals may be made only with prior approval of U.S. Army Aviation Materiel Laboratories, Fort Eustis, Virginia 23604.

ABSTRACT

A preliminary design of an advanced lift fan propulsion system is presented. The V/STOL system is designed to utilize the General Electric J97 gas generator, together with fans having a high degree of inherent control capability during vertical mode flight.

A technology development and acquisition plan leading to MQT in 1970 is identified.

FOREWORD

The program was conducted during the period 20 May 1966 through 30 December 1966 under U.S. Army Aviation Materiel Laboratories Contract DA 44-177-AMC-422(T) by the Lift Fan Systems Operation of the General Electric Company's Advanced Technology and Demonstrator Programs Department. The Lift Fan Systems Operation has been engaged in active development of lift fan V/STOL propulsion since 1958.

CONTENTS

	<u>Page</u>
ABSTRACT	111
FOREWORD	v
LIST OF ILLUSTRATIONS	viii
LIST OF TABLES	xv
LIST OF SYMBOLS	xvi
SUMMARY	1
EVALUATION OF PROPULSION AND AIRFRAME INTERFACE ALTERNATIVES	3
PRELIMINARY DESIGN	53
ADVANCED FAN DEMONSTRATOR DEVELOPMENT PLAN	295
CONCLUSIONS	311
BIBLIOGRAPHY	314
DISTRIBUTION	315

ILLUSTRATIONS

<u>Figure</u>		<u>Page</u>
1	Fan Pressure Ratio Influence Factor	4
2	LFX Study Number 4	5
3	Mission for LFX Preliminary Analysis	9
4	Typical Conventional Fan Mounting	13
5	Integrated Mounting Concept	14
6	Fan Door Installation Study	19
7	Center Mounted Helical Door Actuator Concept	25
8	Helical Hinge Door Actuator Concept	27
9	Geared Door Actuator Hub Spacing	29
10	Partial Admission Fan Study	33
11	General Arrangement - Ryan Model 209D	41
12	Alternate RPM Pickup Concepts	47
13	Fan Lift Versus Fan Pressure Ratio	56
14	Fan Weight Versus Fan Pressure Ratio	57
15	Fan Area Versus Fan Pressure Ratio	58
16	Fan Lift and Weight Ratio Variation With Fan Pressure Ratio	59
17	Fan Lift, Area and Weight Variation With Scroll Mach Number	60
18	Fan Lift, Area and Weight Variation With Fan Inlet Mach Number	61
19	Fan Lift, Area and Weight Variation With Turbine Discharge Mach Number	63
20	Fan Lift, Area and Weight Ratio Variation With Turbine Discharge Mach Number	64
21	Lift, Weight and Area Ratio Cycle Variations	66

<u>Figure</u>		<u>Page</u>
22	Lift, Weight and Area Ratio Cycle Variations	67
23	Lift to Weight Ratio Cycle Variation	68
24	Lift to Area Ratio Cycle Variation	69
25	Lift, Weight and Area Ratio Cycle Variations	70
26	LFX-6 Fan Assembly - Chordwise Section	75
27	LFX-6 Fan Assembly - Spanwise Section	77
28	LFX-6 Fan Assembly Parts List	79
29	Predicted Compressor Map	80
30	LFX Annulus	82
31	Total Pressure Rise Distribution	83
32	Rotor Loading Distribution	84
33	Deviation Angles	86
34	Stator Velocity Distribution	87
35	Total Pressure Loss Coefficient Distribution	88
36	Schematic for Cross-Flow Performance	89
37	Rotor Inlet Air Angles - Cross-Flow	90
38	LFX Pressure Ratio Versus Radius Ratio	91
39	Diffusion Factor and Static Pressure Rise	92
40	Static Pressure Distribution	93
41	Incidence Angle Distribution	94
42	Relative Mach Number Distribution	95
43	Rotor Velocity Diagram	96
44	Stator Velocity Diagram	97
45	Quasi-Orthogonal Flow Schematic	100
46	Turbine Flow Path	101

<u>Figure</u>		<u>Page</u>
47	Turbine Velocity Diagram	102
48	Turbine Nozzle Airfoils	104
49	Turbine Nozzle Airfoils	105
50	Turbine Bucket Profiles	106
51	Scroll Planform	108
52	Wing Fan Door Loads	110
53	Maneuver Loads - Lift Mode	112
54	Rotor Assembly	119
55	Rotor Assembly Parts List	121
56	Bucket Carrier Section Identification	124
57	Turbine Sector Torque Transmission	125
58	Rotor Disc Design Comparison	127
59	Sump Configuration	131
60	Grease Seal Configuration	133
61	Blade Geometry	135
62	Rotor "g" Field Versus Radius	136
63	Blade Air Loads	137
64	Blade Geometry	138
65	100-Percent N_f Blade Stress	139
66	100-Percent N_f Blade Shear	140
67	100-Percent N_f Blade Moment	141
68	100-Percent N_f Blade Displacement	142
69	Blade Campbell Diagram	143
70	First Flexural Mode Blade Deflection	144
71	First Torsional Mode Blade Deflection	145

<u>Figure</u>		<u>Page</u>
72	Second Flexural Mode Blade Deflection	146
73	First Flexural Mode Blade Stress Ratio	147
74	First Torsional Mode Blade Stress Ratio	148
75	Second Flexural Mode Blade Stress Ratio	149
76	Gyroscopic Blade Stress	150
77	Gyroscopic Blade Stress	151
78	Gyroscopic Blade Deflection	152
79	Gyroscopic Blade Slope	153
80	Tang Schematic	155
81	Dovetail Configuration	156
82	Blade and Disc Dovetail Stresses	157
83	Goodman Diagram	158
84	Disc Effective Spring Constant	160
85	Blade Effective Spring Constant	161
86	Disc Stress and Deflection Summary	164
87	Blade Retainer	165
88	Bearing Deflection Path	167
89	Turbine Sector Stations	169
90	Turbine Bucket Gas Load	171
91	Turbine Bucket Tangential Force	172
92	Turbine Bucket "g" Field	173
93	Turbine Bucket Campbell Diagram	174
94	Bucket Carrier Shear Diagram	175
95	Bucket Carrier Moment Diagram	176

<u>Figure</u>		<u>Page</u>
96	Bucket Carrier Shear Stress	177
97	Bucket Carrier Bending Stress	178
98	Torque Transmission System Schematic	179
99	Alternate Bucket Configuration	183
100	Front Frame Load Schematic	188
101	Front Frame Load Paths	189
102	Front Frame - LFX-6	191
103	Front Frame Components	195
104	Front Frame Parts List	199
105	Front Frame Major Strut	201
106	Front Frame Minor Strut - 9:00 O'Clock	203
107	Front Frame Hub	204
108	Front Frame Minor Strut - 3:00 O'Clock	205
109	Major Strut Loads, Shear and Moment	208
110	Major Strut Loads, Shear and Moment	209
111	Minor Strut Loads, Shear and Moment	210
112	Minor Strut Loads, Shear and Moment	211
113	Front Frame Deflections	213
114	Front Frame Deflections - Lift Forces	214
115	Front Frame Deflections	215
116	Door-Strut Combination Concept	217
117	Door-Strut Combination Concept	218
118	Door-Strut Combination Study	219
119	Rear Frame Assembly	223
120	Rear Frame Parts List	225

<u>Figure</u>		<u>Page</u>
121	Rear Frame Cooling	229
122	Rear Frame Outer Box	230
123	Scroll Assembly	237
124	Scroll Assembly Parts List	239
125	Alternate Scroll Split-Line Concept	242
126	Alternate Scroll Split-Line Concept - Close Inlets	243
127	Scroll Nozzle Partition (Type I) Section Properties	244
128	Scroll Nozzle Partition (Type IV) Section Properties	245
129	Scroll Area Distribution	247
130	Variable Scroll Nozzle Area Actuation	249
131	Scroll Bending Stress - Alternate Close Spaced Inlets	251
132	Scroll Bending Stress	252
133	Scroll Section Properties	253
134	Conventional Scroll Mounting	256
135	Variable Area Scroll Schematic	259
136	Lift and Variation With Power Transfer	260
137	Power Transfer Lift Variation	260
138	Turbine Admission Arc Variation With Time	262
139	Electrical and Mechanical Jazzer Systems	264
140	Jazzer Response Characteristics	265
141	Torque-Speed Characteristics for Computer Input	267
142	Turbine Admission Arc Time Rate	268
143	Speed-Time Constant for Changes in Turbine Arc	269
144	Speed Time Constant	270

<u>Figure</u>		<u>Page</u>
145	Speed Time Constant	271
146	Speed Time Constant	272
147	Effect of Jazzer Magnification	274
148	Jazzer Magnification Effect on Lift and Speed Time Constants	275
149	Initial Speed Effects	276
150	LF2 Analog Results	280
151	LF2 Analog Results	281
152	Analog Jazzer Magnification Factor Effects	282
153	Steady-State Frequency Response - Analog Results for 100 ± 5 Percent Area Without a Jazzer	284
154	Steady-State Frequency Response - Analog Results for 100 ± 5 Percent Area With a Jazzer Magnification Factor of 1	285
155	Steady-State Frequency Response - Analog Results for 100 ± 50 Percent Area With a Jazzer Magnification Factor of 3	286
156	Comparison of Analog and Hardware Test Results - Fan Speed Time Constant for Positive Step Changes in Fan Area Without a Jazzer	287
157	Steady-State Frequency Response - Comparison of Analog and Test Results for Test Actuator Stroke of 50 ± 20 Percent Without a Jazzer	288
158	Steady-State Frequency Response - Comparison of Analog and Test Results for Actuator Stroke of 50 ± 20 Percent With Jazzer Magnification Factor of 1	289
159	Energy Modulation Power Transfer Concept	292
160	Energy Modulation Performance	293
161	LFX Integrated Master Plan	297
162	Composite Compressor Blade Concept	301
163	Combination Bellmouth/Scroll Concept	303

TABLES

<u>Table</u>		<u>Page</u>
I	Background Data for LFX Discussions	10
II	Mission Background for LFX Discussions	11
III	Characteristics for 170-Degree Admission Arc	37
IV	Increased Mach Number Comparison - Partial Admission Fan	37
V	Derivative LFX Fans Summary	39
VI	Fan Parameters	53
VII	LFX Turbine Design Point	99
VIII	LFX Turbine Energy Summary	99
IX	Design Parameters	117
X	Rotor Weight Summary	118
XI	Bucket Section Properties	180
XII	Bearing Loads	181
XIII	Front Frame Loads	193
XIV	Front Frame Weights	194
XV	Alternate Front Frame Concept Weight	227
XVI	Rear Frame Weights	227
XVII	Scroll Weights - Pounds	234
XVIII	Scroll Component Stresses	257
XIX	Scroll Materials Properties	257
XX	Fan Performance During Power Transfer	278
XXI	Fan Dynamic Parameters	278
XXII	LFX-6 Program Cost Estimate	310

SYMBOLS

a	dimension from center of gravity to propulsion component mount, inches
A/A*	ratio of area at sonic velocity to design area
AR	aspect ratio
b	dimension from center of gravity to propulsion component mount, inches
c	dimension from center of gravity to propulsion component mount, inches
CG	center of gravity
cps	cycles per second
C _{U1}	compressor inlet radial velocity
C _{U2}	compressor outlet radial velocity
C _{V13}	fan thrust coefficient
C _{Z1}	compressor inlet axial velocity
C _{Z2}	compressor outlet axial velocity
D-factor	compressor diffusion factor
DGW	aircraft design gross weight, pounds
d ₁	inlet dimension, turbine blade row, inches
D _{max}	wing fan maximum diameter, measured in the direction of the wing chord, inches
DN	product of bearing diameter and RPM
d _o	turbine nozzle throat dimension, inches
D _{TT}	turbine tip diameter, inches
D ₁	turbine nozzle discharge dimension, inches
e	2.71828
F _A	aft force exerted on propulsion components, pounds

F_N	net thrust, pounds
F_S	side force exerted on propulsion components, pounds
ft/sec	feet per second
F_V	vertical force exerted on propulsion components, pounds
g	acceleration due to gravity, feet per second per second
I	moment of inertia, inches ⁴
ID	inside diameter of scroll inlet, inches
KSI	thousands of pounds per square inch
L	lift, pounds
lb	pounds
L_N	net lift or nominal lift, pounds
L/W	aircraft lift/weight ratio, the ratio of total uninstalled lift on a sea level standard day to vertical takeoff gross weight
L_1	lift of fan receiving additional flow during power transfer, pounds
L_2	lift of fan receiving less flow during power transfer, pounds
L_3	blade tang load, based on bearing stress, pounds
L_4	blade tang load, based on average tensile stress, pounds
M	Mach number
M_{ABS}	compressor inlet absolute Mach number
M_{EX}	compressor stator discharge absolute Mach number
M_{IN}	compressor blade inlet absolute Mach number
M_J	jazzer magnification factor
M_P	pitch moment, inch-pounds
M_R	roll moment, inch-pounds
M_{REL}	compressor inlet relative Mach number

M_{R1}	turbine inlet relative Mach number
M_{R2}	turbine discharge relative Mach number
M_S	scroll gas flow Mach number
M_Y	yaw moment, inch-pounds
M_1	turbine inlet absolute Mach number
M_2	turbine discharge absolute Mach number
$M_{5.5}$	turbine stator discharge absolute Mach number
M_{10}	fan inlet Mach number
N_f	fan speed, revolutions per minute
P/P	wing fan compressor pressure ratio
P_S	static pressure, pounds per square inch, absolute
psi	pounds per square inch
P_T	total pressure, pounds per square inch, absolute
$P_{5.1}$	core engine discharge total pressure, pounds per square inch
q	dynamic pressure, pounds per square foot
R_H	compressor hub radius, inches
R_H/R_T	compressor radius ratio
RPM	revolutions per minute
r/S	radians per second
r/S^2	radians per second ²
R_T	compressor tip radius, inches
R_1-R_6	propulsion system component mount reactions, pounds
S	wing planform area, square feet
t	time, seconds
TBO	time between overhauls
T_d	design point torque, pound-feet

TE	trailing edge
te	edge thickness, inches
tm/c	ratio of maximum thickness to chord
TPLC	total pressure loss coefficient
T_T	total temperature, degrees Rankine
$T_{5.1}$	core engine discharge total temperature, degrees Rankine
U	turbine pitch line wheel speed, feet per second
U_{FT}	fan tip speed, feet per second
$U_{FT}/\sqrt{\theta}$	corrected fan tip speed, feet per second
U_{NO}	ratio of turbine air velocity to tip speed
U_1	compressor inlet tangential velocity
U_2	compressor outlet tangential velocity
VAC	variable area control system
VL	vertical landing
V_{R1}	turbine inlet relative velocity, feet per second
V_{R2}	turbine discharge relative velocity, feet per second
VTO	vertical takeoff
V_1	turbine inlet absolute velocity, feet per second
V_2	turbine discharge absolute velocity, feet per second
W_d	design point speed, radians per second
W/S	aircraft wing loading, pounds per square foot
$W_{5.1}$	core engine discharge flow, pounds per second
$W/\sqrt{\theta}/\sqrt{\phi}$	compressor corrected flow, pounds per second
Y_a	time constant parameter for scroll actuator
Y_F	time constant parameter for lift
Y_J	time constant parameter for jaxzer
Y_N	time constant parameter for speed

α	aircraft angle of attack, degrees
α_R	aircraft angular acceleration about the roll axis, radians per second ²
α_j	scroll nozzle angle, degrees
β_1	inlet absolute air angle, degrees
β_2	discharge absolute air angle, degrees
β_{w1}	compressor blade inlet relative air angle, degrees
β_{w2}	compressor blade discharge relative air angle, degrees
Γ	turbine discharge swirl angle, degrees
γ_1	turbine inlet flow angle, degrees
γ_2	turbine discharge flow angle, degrees
$\Delta P/q$	compressor static pressure rise coefficient
δ	ratio of ambient pressure to sea level standard day ambient pressure
η_{AD}	compressor adiabatic efficiency
θ	turbine arc of admission, degrees
$\dot{\theta}$	aircraft angular velocity about the roll axis, radians per second
$\ddot{\theta}$	aircraft angular acceleration about the roll axis, radians per second ²
τ_a	actuator time constant, seconds
τ_F	lift time constant, seconds
τ_j	jazzer time constant, seconds
τ_N	speed time constant, seconds
$\dot{\phi}$	aircraft angular velocity about the pitch axis, radians per second
$\ddot{\phi}$	aircraft angular acceleration about the pitch axis, radians per second ²

Y	aircraft angular velocity about the yaw axis, radians per second
..	aircraft angular acceleration about the yaw axis, radians per second ²
1	compressor total pressure loss coefficient
10	compressor inlet total pressure loss, expressed as a percentage of the local dynamic pressure
11	compressor discharge total pressure loss, expressed as a percentage of the local dynamic pressure

SUMMARY

This report presents a preliminary "design in depth" of an advanced lift fan propulsion system (designated LFX). The LFX design is an extension and refinement of the conceptual design defined during a previous study. This advanced lift fan system design is based on technology which will permit performance demonstration by 1968 and operational readiness compatible with U.S. Army mobility concepts by 1970.

The broad LFX objectives identified during the previous study have been refined and made more specific during this preliminary design. This refinement has been achieved by directed parametric optimization studies, technical interchange with airframe manufacturers, and the use of technology input from other "in-house" advanced tip turbine fan efforts.

The parametric optimization studies for the LFX wing fan resulted in an area reduction of 10 percent and an increase of $7\frac{1}{2}$ percent in maximum lift compared to the fan identified in the previous study. Both of these improvements were achieved without an increase in fan weight.

The propulsion system airframe interface was explored in depth through qualitative technical interchange with seven different airframe manufacturers. A quantitative evaluation of specific interface concepts was accomplished by identification of the effects of the various concepts on system weight and performance. The recommendations and improvements defined by these airframe reviews and interface studies were incorporated into the LFX design criteria. These recommendations include:

1. The basic wing fan should be an integral structure, not sharing airframe loads and not integrated into the aircraft structure.
2. Certain elements of the structural interface could benefit through integration of the airframe/propulsion structure. The fan cover doors and actuation could be mounted on the fan front frame. The fan exit louvers could be mounted directly to the airframe.
3. The fan should be capable of scavenging any leakage into the fan compartment during fan operation.
4. Further study should be conducted to identify additional quantitative trade-offs through integration of interface features.

The major contribution from other "in-house" advanced tip turbine fan efforts was the definition of an effective power transfer method. The LFX wing fan design concept incorporates a large control power modulation capability achieved by a variable area turbine scroll. The power modulation

would permit the generation of roll moments of more than 55,000 foot-pounds in a typical aircraft installation. Additionally, a single wing fan will accept the continuous full flow of one gas generator. The pitch control fan could be phased out as the aircraft control surfaces become effective during forward flight transition. The pitch fan gas flow (26 percent of one gas generator flow during trimmed hovering flight) made available by phasing out the pitch fan can be accepted by the wing fan, thus providing higher aircraft forward velocities during fan-powered flight.

The LFX wing fan mechanical design described in this report features a front frame, rotor, scroll and rear frame. The fan will fit into a representative wing planform having a 9 percent maximum thickness. The LFX propulsion system, consisting of two advanced technology gas generators, two wing fans and a fuselage pitch control fan, has a total system lift at sea level standard day conditions of 28,670 pounds. System weight is 2,943 pounds.

The major emphasis in the preliminary mechanical "design in depth" was on the wing fan. Component drawings were completed, major loads identified, component stresses calculated, deflections calculated and potential problem areas identified. Mechanical design and value analysis reviews were held to aid in establishing priorities for future study to yield maximum reliability and performance at a minimum of cost. Technology level of the LFX fan is compatible with the G.E. J97 turbojet with a 1968 first fan running date.

A technology acquisition and development plan is presented which would permit initial demonstration of the LFX technology by static testing of a full-scale wing fan during the last quarter of 1968 and full acquisition of the LFX technology through a PFRT completion in 1969 and MQT in 1970.

Supporting and interrelated lift fan technology programs are identified, and a complete master plan for tip turbine fan technology development is given.

EVALUATION OF PROPULSION AND AIRFRAME INTERFACE ALTERNATIVES

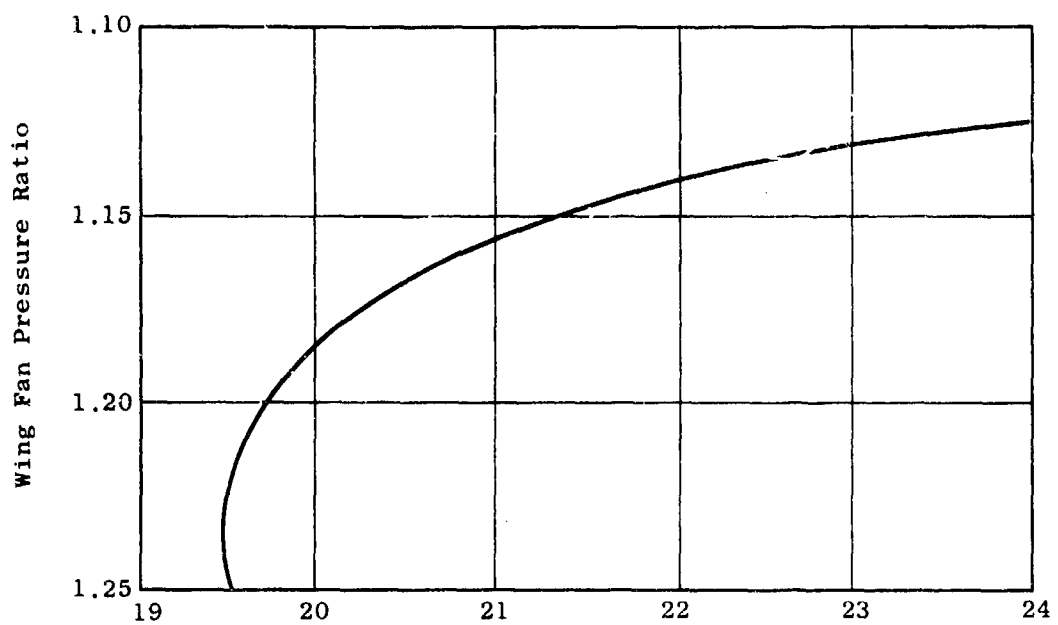
Experience gained during the design and fabrication of the XV-5A aircraft and during many installation studies of various aircraft has proven the effect of the propulsion system and its design on the aircraft design and performance. Aside from the consideration of obtaining maximum installed lift or thrust, the propulsion system design can dictate many of the required aircraft design features. In the case of the fan-in-wing VTOL aircraft, the fan design can influence such factors as aircraft wing loading, aircraft weight, maximum flight speed, maximum gross weight and others. Many of the influential factors are a function of a specific or general mission requirement and, as such, can be evaluated in terms of mission requirements. An example of this type of influence factor is the effect of fan pressure ratio on maximum allowable gross weight with a given total gas generator horsepower available. An example is shown in Figure 1. Other fan effects on the airframe requirements were identified and are presented in the final report for Phase 1 of the LFX study (Reference 1).

Many propulsion/airframe interface effects are not readily identifiable and, consequently, are cause for conjecture and speculation. During the course of the LFX study described in this report, three techniques were used to establish the best design criteria for the LFX lift fan to be compatible with a variety of potential aircraft installations. A qualitative summary was gained through direct contact with many aircraft manufacturers whose background and product orientation had familiarized them with the lift fan concept. A quantitative evaluation of interface and installation effects was obtained through the basic design effort on the LFX wing fan and identification of the weights or performance effects associated with alternate designs. Additional evaluation was obtained through study by an airframe company during another USAAVLABS contracted program (Reference 2). Propulsion manufacturer comments on the recommendations contained in Reference 2 are included in this report.

QUALITATIVE REVIEW OF INTERFACE FEATURES

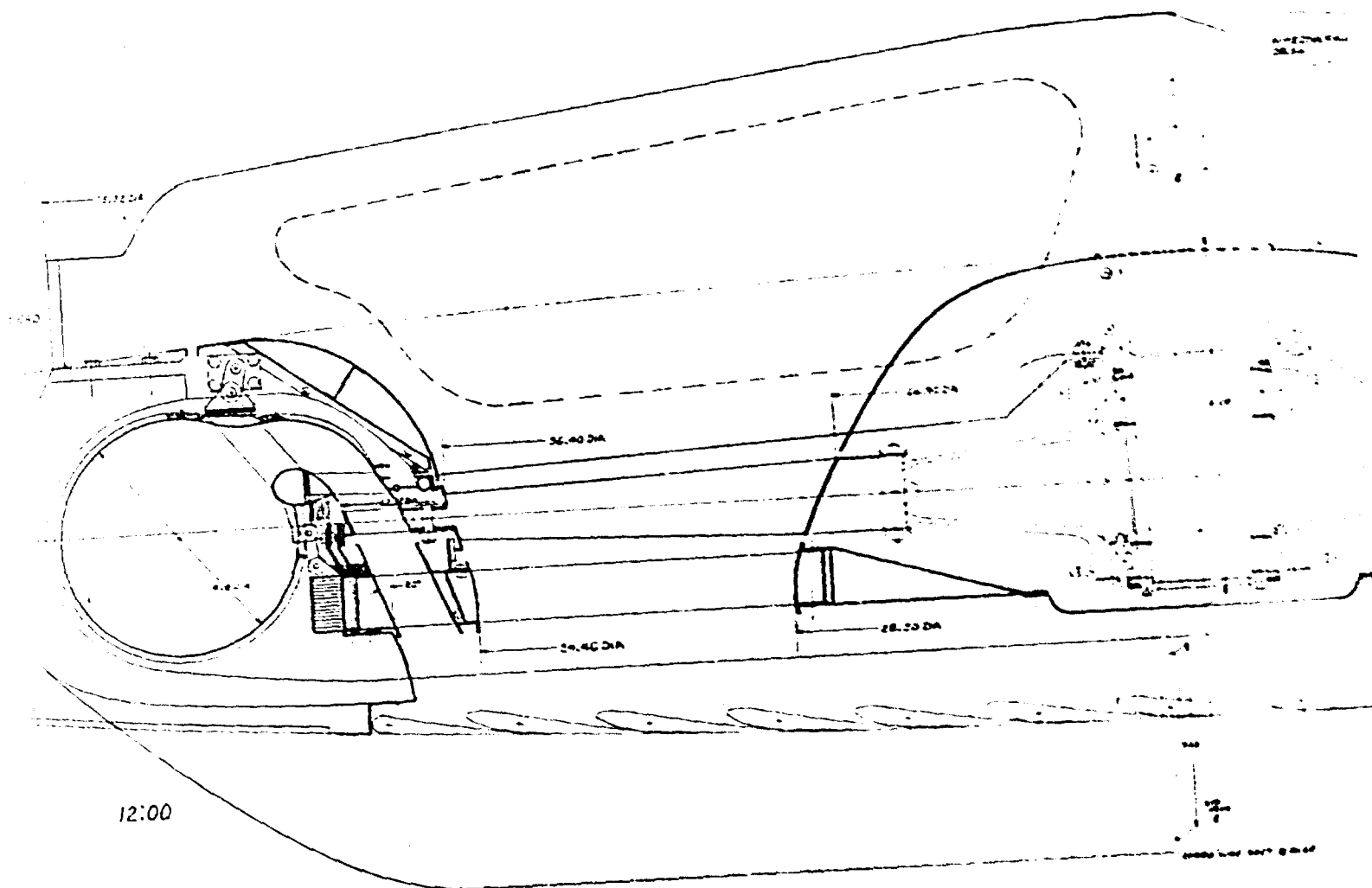
Airframe companies with current or past experience in VTOL applications and with knowledge of the lift fan propulsion system concept were contacted and briefed on the LFX-size fan and some of the basic mission analysis used in the sizing of the fan. Commentary and recommendations were solicited for the propulsion/airframe interface area.

The airframe manufacturers who were contacted were: Bell, Grumman, McDonnell, Northrop, North American, Republic and Ryan. The conceptual design fan shown in LFX Study Number 4 (Figure 2) was used as a basis for discussion. Excerpts from the data presented by General Electric for propulsion information are shown in Figure 3 and Tables I and II. A detailed description of each discussion is contained in LFX Memorandum 66-4 (Reference 3).



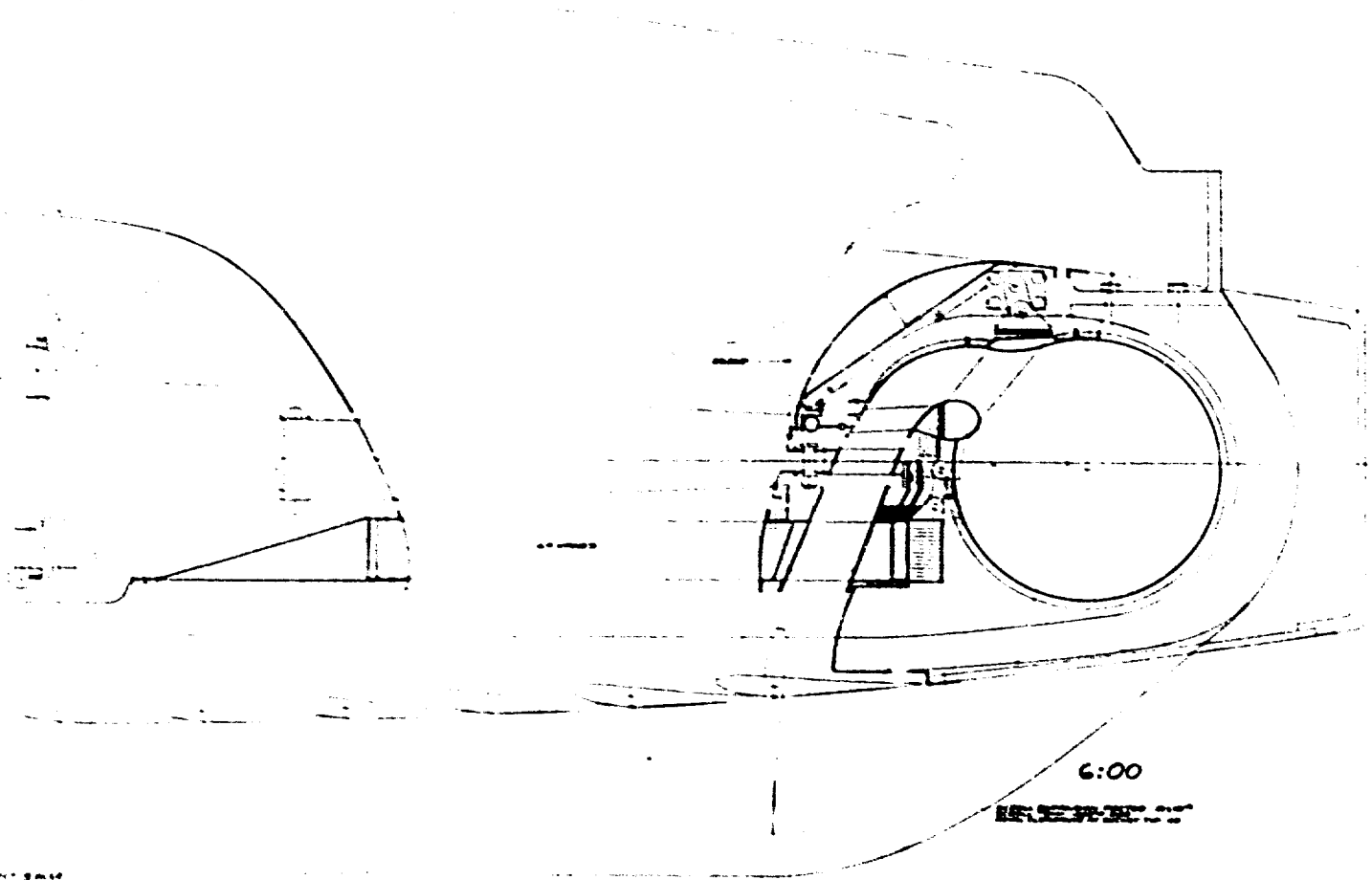
Aircraft Vertical Takeoff Gross Weight, 1000 Pounds

Figure 1. Fan Pressure Ratio Influence Factor.



B

W. J. HALL, ARCHT.
1870



c

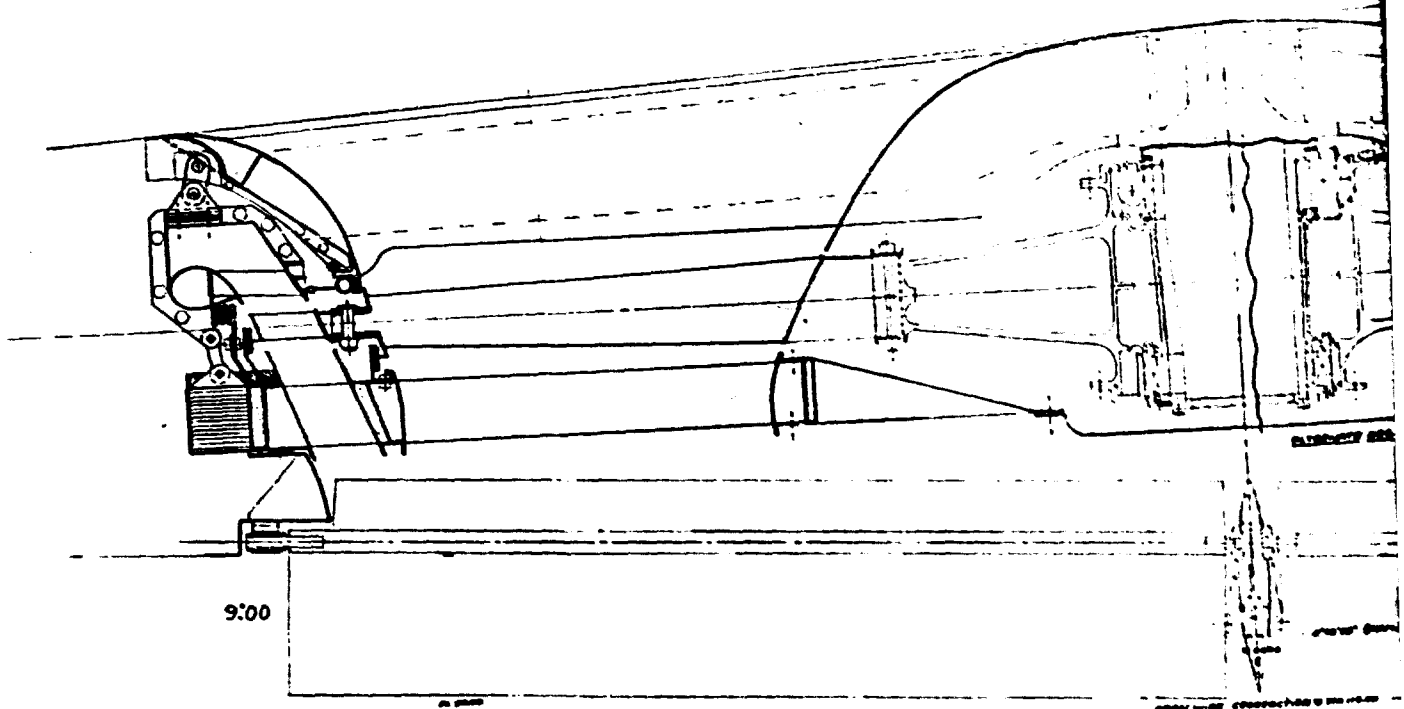
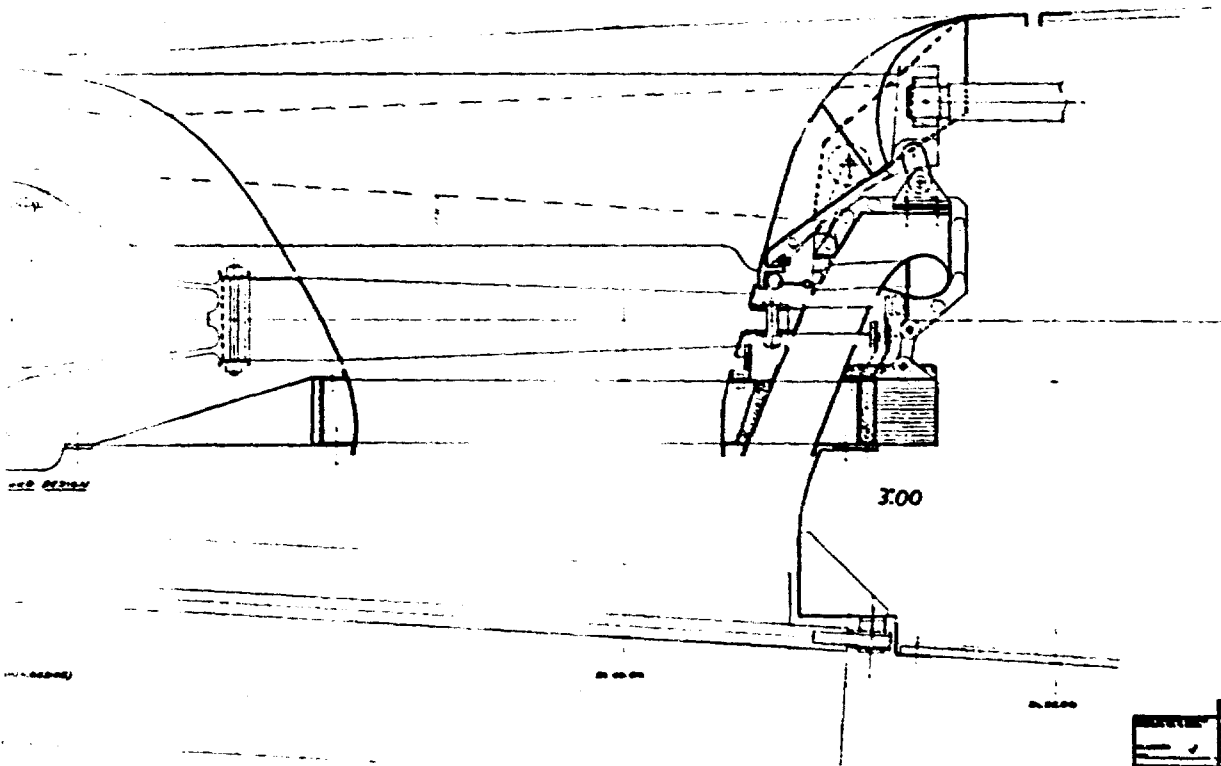
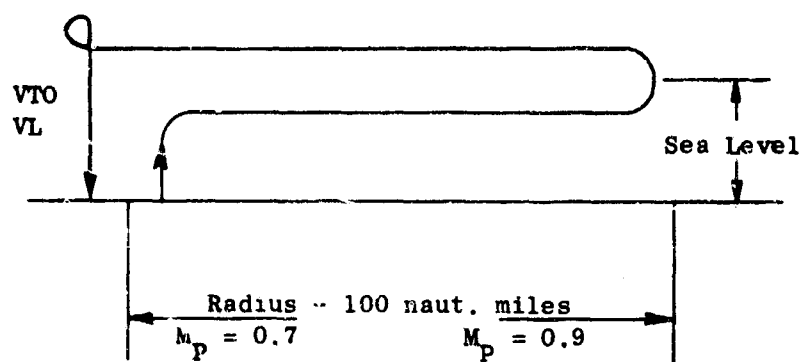


Figure 2. (Cont'd.)



LAYOUT		DATE
DESIGNED BY	DATE	
CHECKED BY	DATE	
APPROVED BY	DATE	
EX STUDY SET		
4013087-124		

B



VTO and VL - 5 min @ max power
 Range 200 naut mi
 Speed constant, from M.7 to M.9, OSL
 Reserves 3 min @ max power
 Payload 2500 lb desired

Figure 3. Mission for LFX Preliminary Analysis.

TABLE I
BACKGROUND DATA FOR LFX DISCUSSIONS

<u>Objectives</u>	<u>Specification</u>
Fan P/P	1.25
Fan Tip Diameter	57.1 in.
Turbine Tip Diameter	63.1 in.
Maximum Continuous Lift	12,750 lb
Nominal Lift	10,800 lb
Weight	570 lb
Continuous RPM	115%
Momentary Overspeed	120%
TBO	1000 Mission Hours
Life	10,000 Mission Hours
Control Modulation	Power Transfer System + 18% Thrust

TABLE II
MISSION BACKGROUND FOR LFX DISCUSSIONS

LFX Mission Study Propulsion Sizing

Two Advanced Engines Nearly Optimum

2500 ft/90° VTO Mission Requires 20,000-lb Aircraft

Two LFX Wing Fans Required

1.25 Pressure Ratio

56-in. Fan Diameter

63-in. Turbine Diameter

10,480-lb Lift per Fan

One or More Scaled LFX Fuselage Fans Required

7,688-lb Nominal Lift

Major areas of interest were covered through six specific questions. Other areas of interest peculiar to the specific company were covered during general discussion. Questions and commentary were:

1. Could you decrease wing weight by using one or more of the fan frame struts to carry wing loads?

Background - Figure 4 shows the typical type of fan mount where the fan loads are transmitted to the wing but wing loads may not be transmitted through the fan structure. A possible alternative type of mount is shown in Figure 5 where the fan is suspended directly from an integral wing structural member, such as a rib. The large wing cutout for the lift fan necessitates less-than-optimum torsional load transmittal around the cutout area. Some of these torsional moments could be taken through bending in the strut or fan-mount member, if the strut were properly designed.

General opinion leaned toward the probability of the airframe wing weight being slightly reduced by a fan mount such as that shown in Figure 5. However, the problem of maintaining the close seal clearances required for efficient aerodynamic performance by the rotor is not compatible with the tendency for a wing to flex or bend with aircraft flight loads. The majority opinion was that the wing fan structure could not share airframe structural loads without sacrificing performance in the fan. The majority opinion also was that the fan major strut could possibly be used to reduce the differential bending in the main wing spars due to torsional loading.

2. Could you decrease wing weight by using the fan inlet bellmouth to carry wing loads?

Background - The fan inlet bellmouth was an integral part of the LF1 fan. The PF1 fan (XV-5A pitch fan) and the LF2 fan were designed with the bellmouth not on the fan, but rather as a part of the airframe. In past fan design practice, the bellmouth has not had structural capability beyond that sufficient to react the inlet air loads. In most turbojet engine installations, the inlet, up to the engine compressor front frame, is part of the aircraft.

Opinion on the potential use of the fan inlet bellmouth as a load-sharing component for wing loads was not strong for either pro or con. The wing skin itself requires a doubler or other type of stiffening device around the fan cutout hole. However, to use the bellmouth as an integral part of the wing skin in lieu of the doubler would increase overall weight. Additionally, wing skin deflection would tend to necessitate increased clearance between the bellmouth and the rotor with a resultant decrease in fan performance. A summary might be that the wing had little to gain from structural use of the bellmouth and the fan had much to lose.

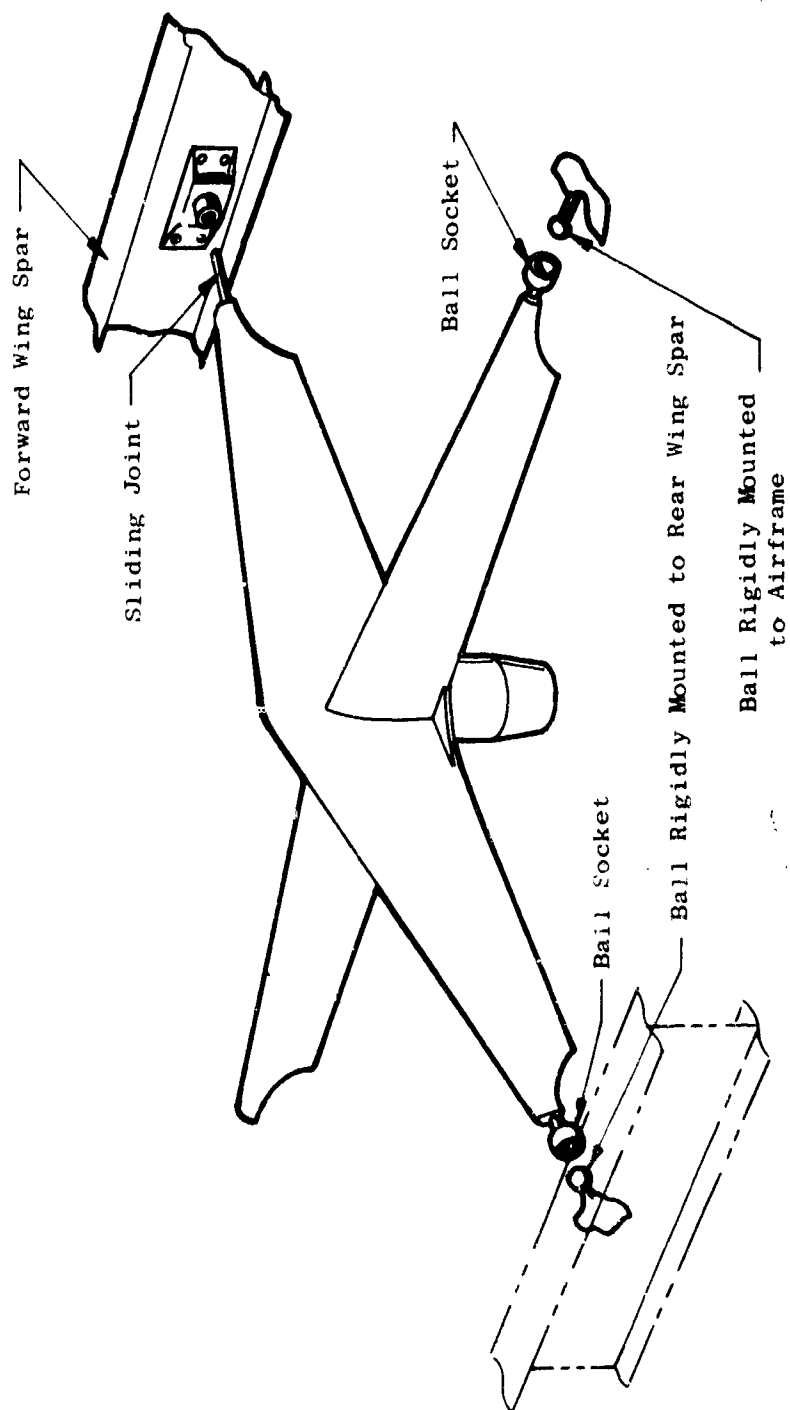


Figure 4. Typical Conventional Fan Mounting.

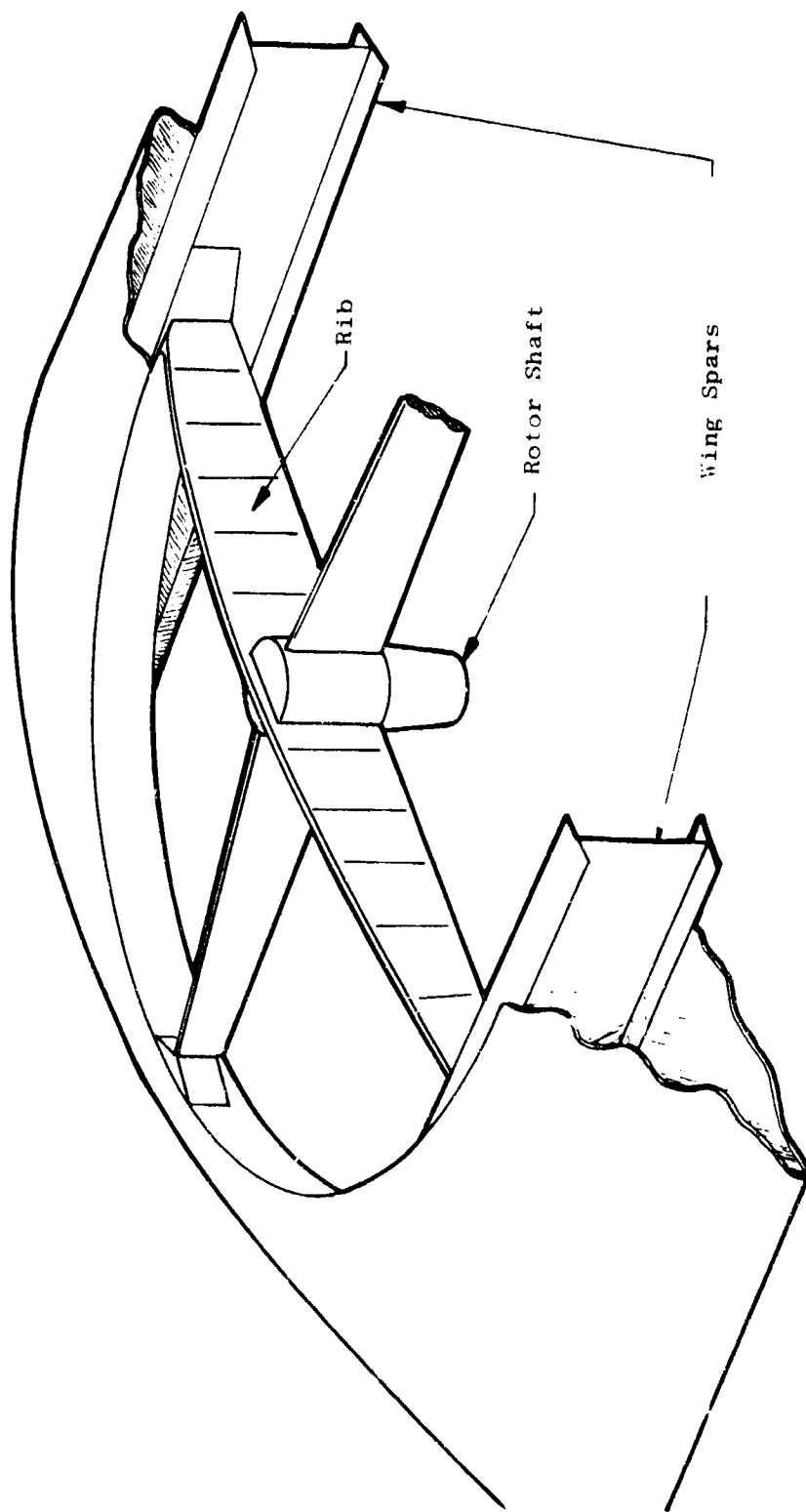


Figure 5. Integrated Mounting Concept.

3. What is your reaction to mounting the wing fan exit louvers directly to the wing lower skin structure?

Background - The wing fan exit louvers and actuation mechanism on the LFI fan are attached to the fan rear frame. Loads are transmitted to the fan front frame and then to the front and rear fan mounts as point loads into the spars. When not in use, the exit louvers serve as the lower wing skin in much the same manner that the fan inlet door covers serve as the upper skin.

The concept of mounting the exit louvers directly to the lower wing skin or box surrounding the fan received favorable comments from all people with whom it was discussed. A more even distribution of the exit louver load into the wing, less required fan structure and a more direct load path for the actuation were cited as possible advantages.

4. What advantages exist for placement of the power transfer portion of the scroll arc on the inboard side of the fan? On the outboard side of the fan?

Background - Although the LFX fan is designed with a 360-degree total arc of admission scroll, the nominal scroll arc of admission is 250 degrees. Only during maximum power transfer does the arc of admission increase to the full 360 degrees. Experience with the XV-5A has indicated some degree of lower fuselage heating during fan operation because of fan turbine gas impingement.

The XV-5A fans have an active scroll arc of admission of 168 degrees, located centroidally adjacent to the fuselage. Additionally, analysis of the XV-5A fan efflux in ground effect indicates an interaction between the discharge of the pitch control fan and the wing fans with fan turbine gases reflected upward into the turbojet engine inlets.

It was recognized that the interaction effects of fan efflux on the other fans will necessarily depend on the specific location of the fans in the airframe. Assuming that the normally inactive scroll arc will lead to less heating of adjacent airframe material, a preference might exist for the outboard location of the scroll inactive arc. One other possible advantage for the outboard inactive scroll arc location is the longer moment arm available for generation of control moment during conditions of maximum power transfer. Longer hydraulic lines to the actuators and the slightly greater weight associated with the outboard inactive arc are off-setting factors. Additionally, earlier LFX studies had shown a scroll gas flow velocity which varied with power transfer in the outboard arc. Scroll Mach number remains essentially constant with the power transfer portion of the scroll arc located inboard.

5. What other opportunities do you see for combining the lift fan structure into the wing structure?

Background - The lift fan structure has certain basic requirements inherent to the design concept. Other areas exist for potential combinations of airframe loads (structure) with the lift fan. In the XV-5A aircraft, for example, the wing fan exit louvers serve as the bottom wing skin when the aircraft is in the jet or cruise mode.

Ideas for possible uses of the wing structure as part of the fan or vice versa were as many and varied as the companies contacted and the conceptual aircraft configurations. However, only one concept recurred with various companies: that of mounting the exit louvers so that their drag and forward thrust loads could be transmitted more directly to the wing rather than through the fan structure. In the XV-5A aircraft and in other General Electric lift fan designs, the wing fan exit louver loads are transmitted into the fan rear frame, from the rear frame to the scroll (or front frame) and from the front frame to the wing spars via the fan major strut front and aft mounts. The additive effect of each component on the other evoked comments from many people.

The fan inlet cover doors were discussed at length, with suggestions offered ranging from eliminating the doors entirely by a blowing/suction device to replacing the split butterfly doors with louvers, window-shade devices, etc. Most persons agreed that the split butterfly door probably represented a reasonable compromise between the requirements for maximum fan performance and minimum installed weight. The use of the fan front frame major strut to mount the split butterfly doors and actuators was considered to be a logical development. Additionally, general opinion on door down-latching requirements was that the doors could be secured through latches outside the periphery of the fan bellmouth inlet. Redundancy in both the fan door actuation system and the down-latch system was thought to be desirable to enhance system reliability.

6. What are your comments and suggestions pertaining to the LFX concept?

Background - The LFX design criteria for performance, control capability, size, and design philosophy (mission orientation) were summarized.

The control power or moment generating capability of the fan was thought to be minimal for most fans. The thrust modulation of plus-or-minus 17 percent of nominal thrust would not allow sufficiently high roll rates with most conceptual aircraft inertias.

The ratio of the installed fore/aft dimension of the fan to the fan tip diameter was thought to be too high and a potential source of difficulty for a fan-in-wing installation because of the fan's effect on required wing spar spacing and, potentially, on maximum wing loading. The LFX goal of fitting the fan into a 9-percent-maximum-thickness wing was thought to be adequate for most sub-sonic conceptual aircraft.

Much interest was expressed in the validity of the control time constant estimated for the LFX fan and in the techniques used to calculate it and verify it. General opinion was that the time constant (fan response) given in the LFX criteria was compatible with the requirements of most aircraft control systems, provided that the time constant could be met.

The power transfer type of fan modulation for control with the minimum associated losses received favorable comment. However, comments were made indicating the desirability of utilizing the pitch control fan flow in obtaining forward thrust for higher fan-supported aircraft velocities.

QUANTITATIVE EVALUATION OF INTERFACE AREAS

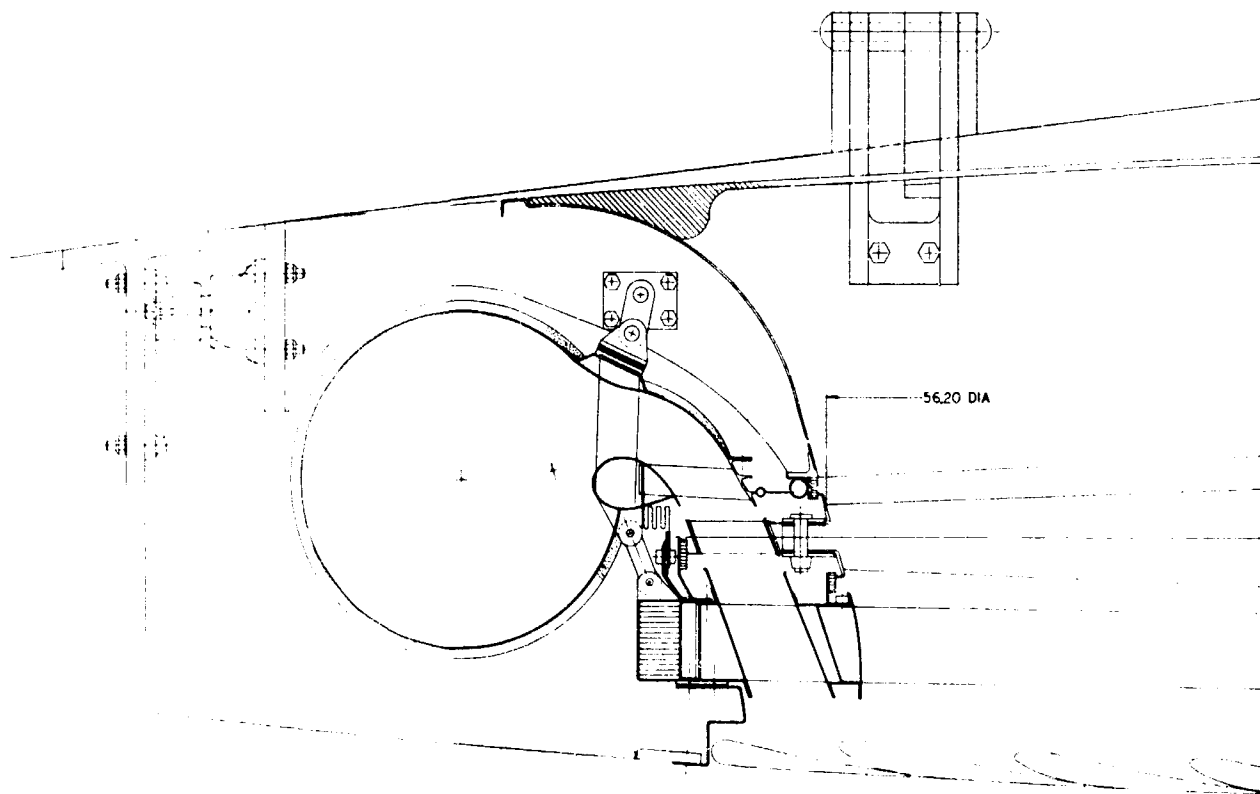
The quantitative evaluation of design options affecting the interface between the propulsion system and the aircraft frequently requires intimate knowledge of both aircraft design practice and propulsion system design practice. In many cases, the evaluation will tend to be weighted towards the experience background of the evaluator.

The LFX fan study has accurately identified the weight for each component in the LFX wing fan and the performance anticipated with that combination of components compatible with the weight. The Preliminary Design section of this report (page 53) summarizes both weight and performance for the basic LFX design concept.

In addition to identification of basic fan weight and performance, estimates were made of the cost in weight and performance to include other concepts and features. It should be noted that the estimates included here are based specifically on the LFX fan size and performance and on the concepts delineated. Other concepts may well prove to be more desirable.

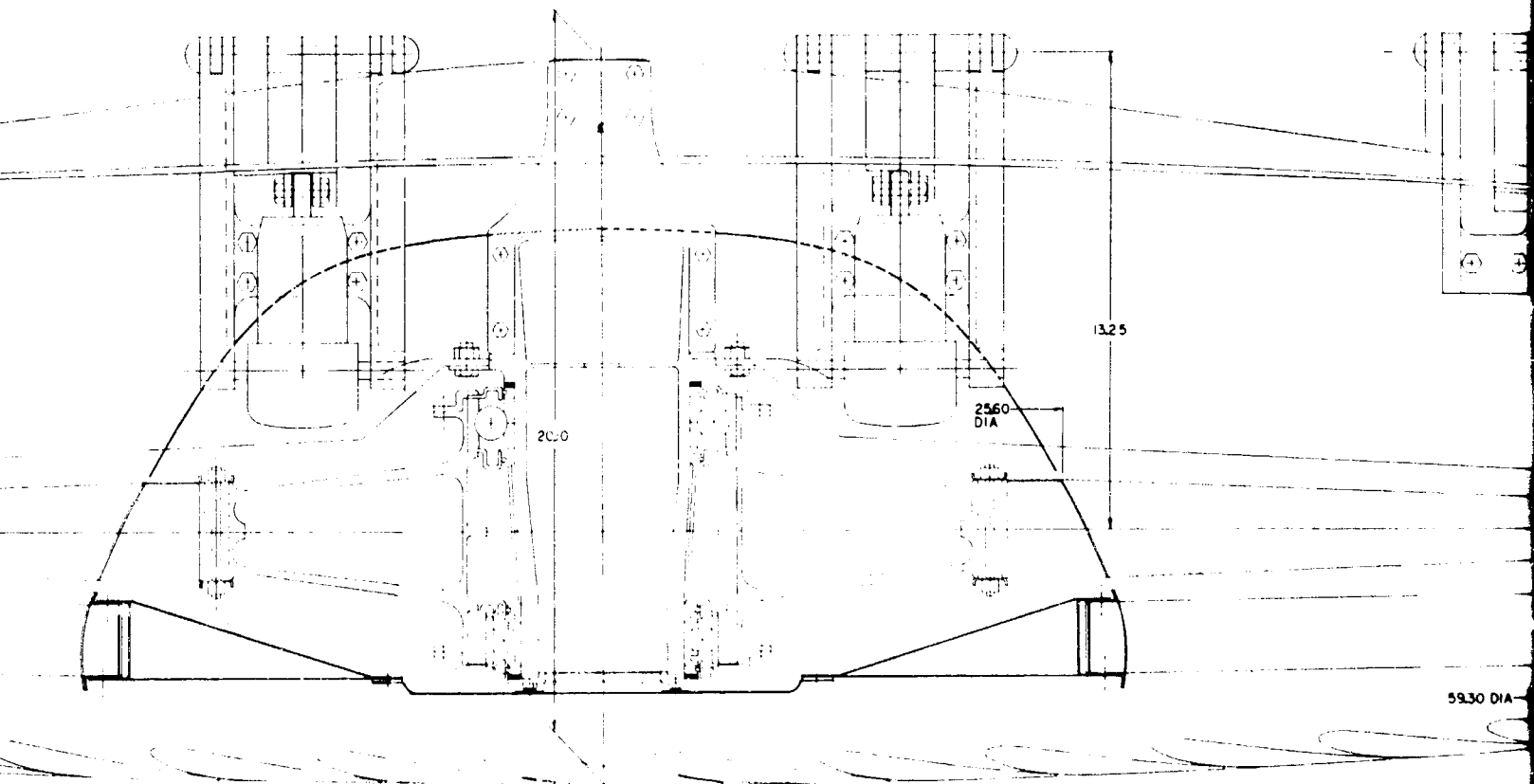
Wing Fan Closures

The wing fan cover door and its mounting actuation and latching system have been subjected to many studies and much discussion. An arrangement closely resembling the XV-5A is shown in Figure 6. The estimated weight of the fan front frame without doors, actuators or latches is 102 pounds. The following tabulation shows the estimated increased weight for adding the wing fan doors of a composite plastic construction and linear hydraulic actuators:



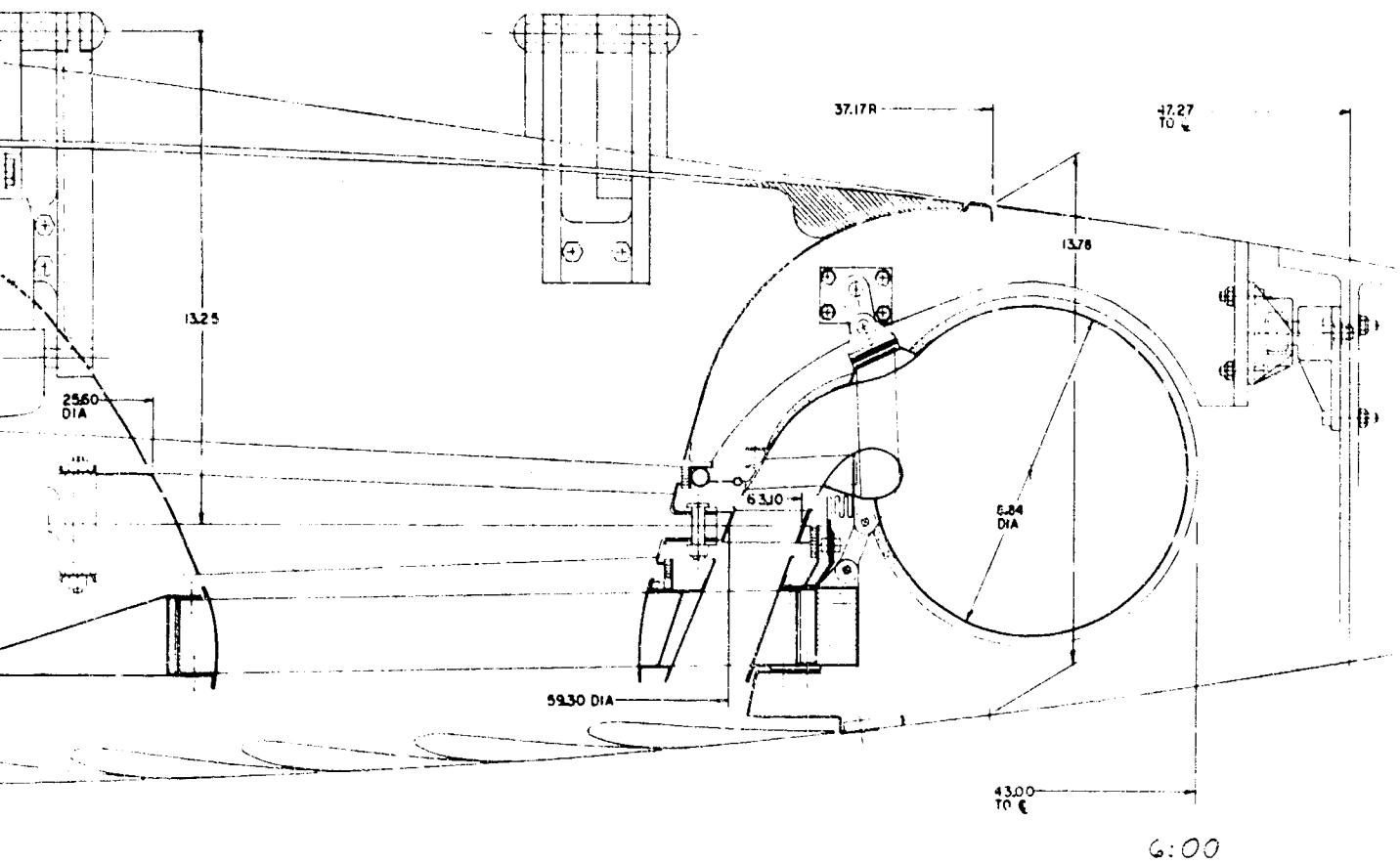
12:00

Figure 6. Fan Door Installation Study.



CHORDWISE SECTION LEFT WING OUTBOARD LOOKING IN

B



C

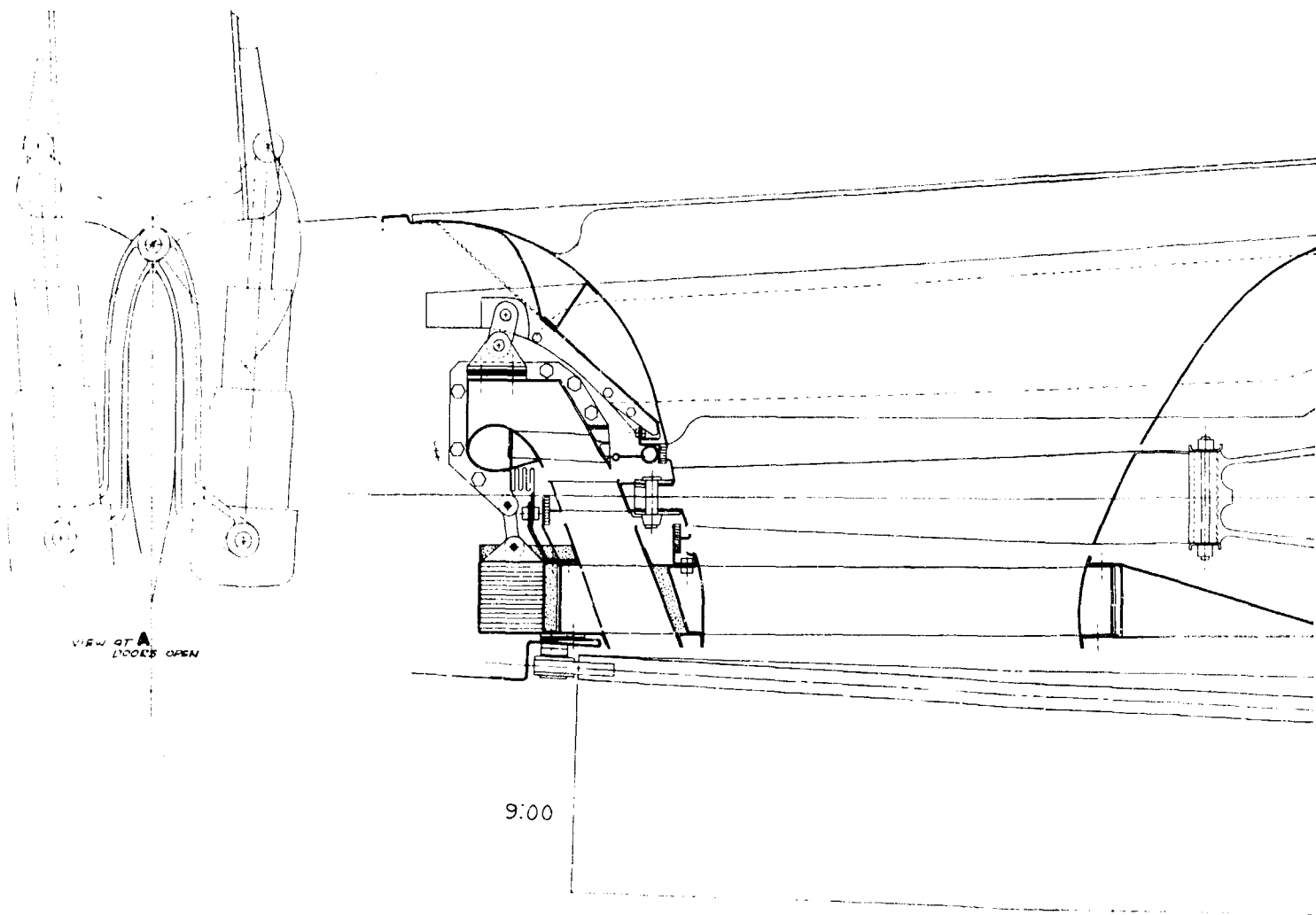
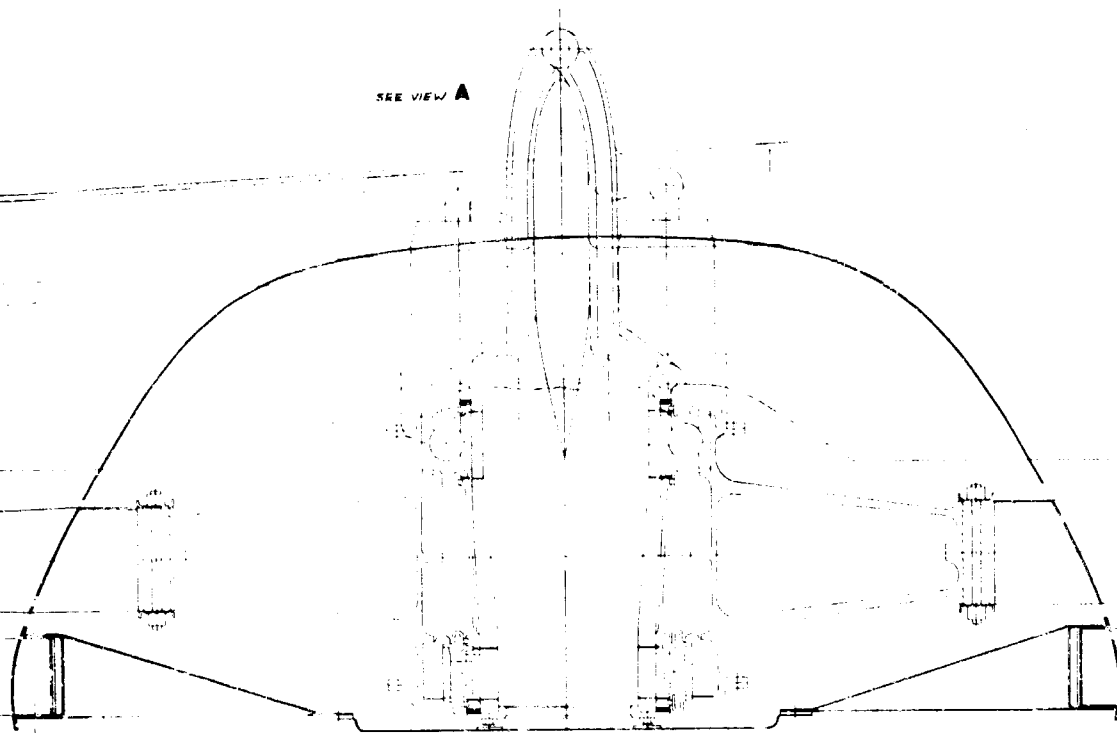


Figure 6. (Cont'd.)

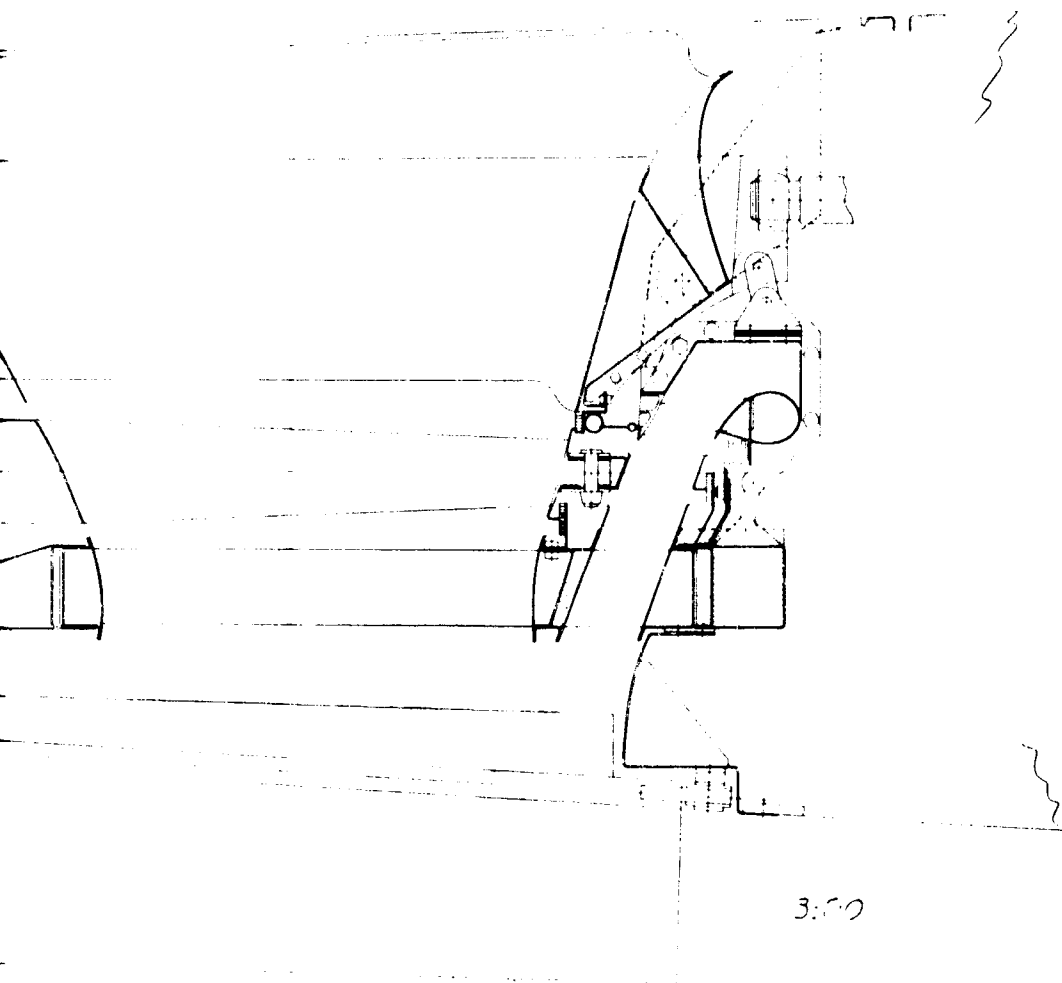
A

SEE VIEW A



SECTION OF SHIP'S SUPERSTRUCTURE, LEFT WALL OF FLOODING FWD

B



3:00

STUDY	
DATE	4013007-653
BY	STUDY
REVIEWED	STUDY
APPROVED	STUDY

C

	<u>Pounds</u>
Basic frame	98.0
Strut increment for door loads	4.0
Hard points for door mounts	9.0
Hard points for actuators	9.5
Hinges	21.5
Door	65.0
Actuators	22.0
Down locks	10.2
	<u>239.2</u>

A concept which utilizes the fan door as a structural member of the fan was identified as a potential weight-saving change. A description of that concept is given in Section III of this report.

Other fan door actuating schemes were studied. Figure 7 shows a center mounted helical actuator. The necessarily large diameter of the door actuator, although located over the fan hub, could cause performance losses particularly during high-speed fan-powered flight. The estimated weights are:

	<u>Pounds</u>
Basic frame	98.0
Strut increment for door loads	4.0
Hard points for door mounts	10.1
Hard points for actuator	8.5
Hinges	21.5
Door	86.0
Actuator	24.6
Door locks	10.2
	<u>262.9</u>

A variant of the helical hinge actuator is shown in Figure 8. Performance losses during hover flight would be caused by the comparatively large diameter actuators. Weight estimates show a total of 269.1 pounds.

A door actuation device similar to one described in an airframe study of lift fan technology (Reference 1) was briefly studied. Figure 9 shows the effect of the geared door opening device on required space above the fan. A bulge in the doors above the fan dome and door gearbox area would be a requirement. The gearbox door actuator weight was not estimated.

Fan Inlet - Bellmouth

The wing fan bellmouth inlet is used to assure a smooth flow-path entry for air entering the fan compressor. It is lightly loaded in its functional capacity which is analogous to the nacelle on a jet engine. Past lift fan design practice has included a bellmouth as a part of the fan (LF1 fan) or a bellmouth as a part of the airframe (PF1 and LF2 fans).

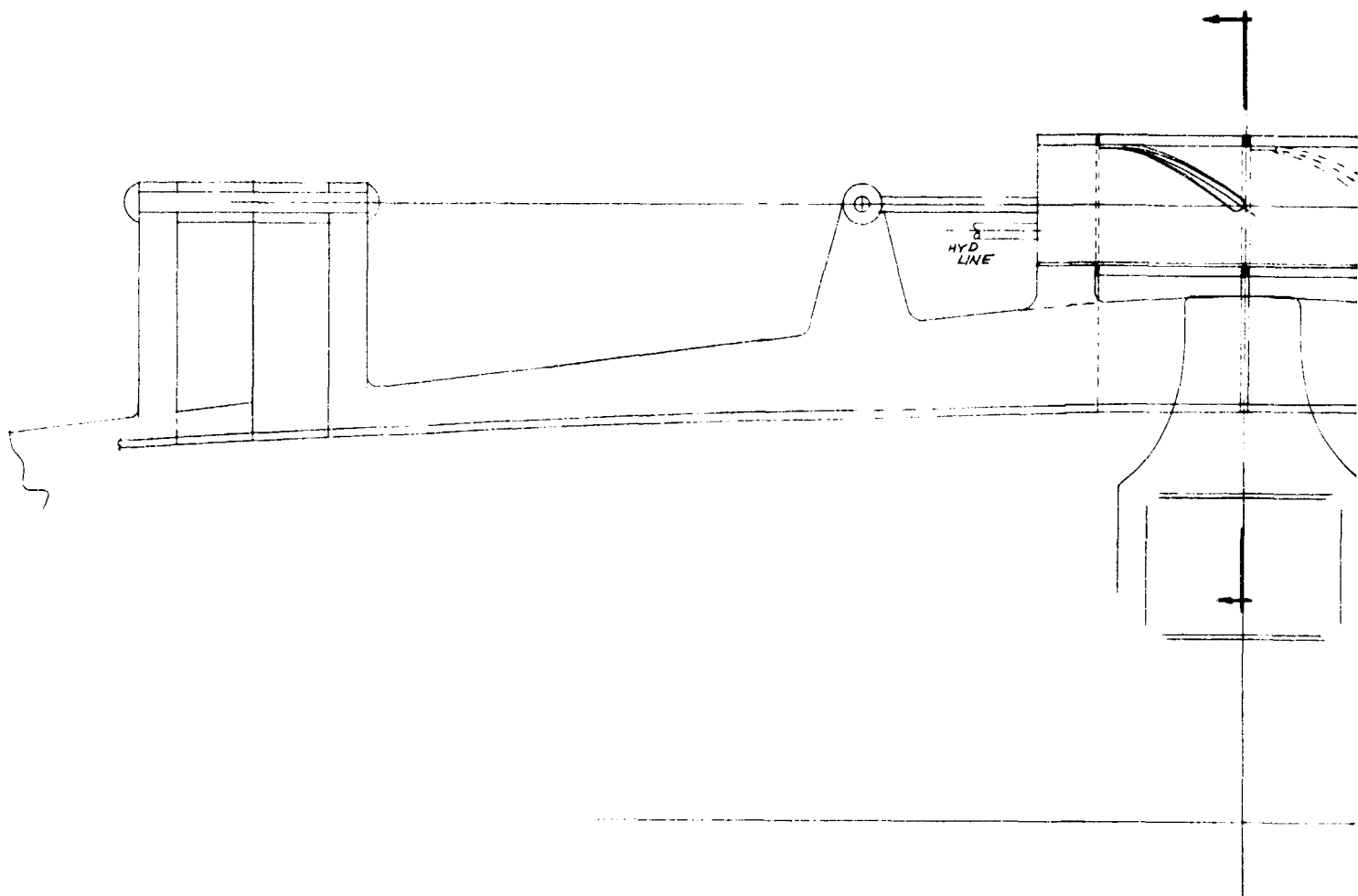
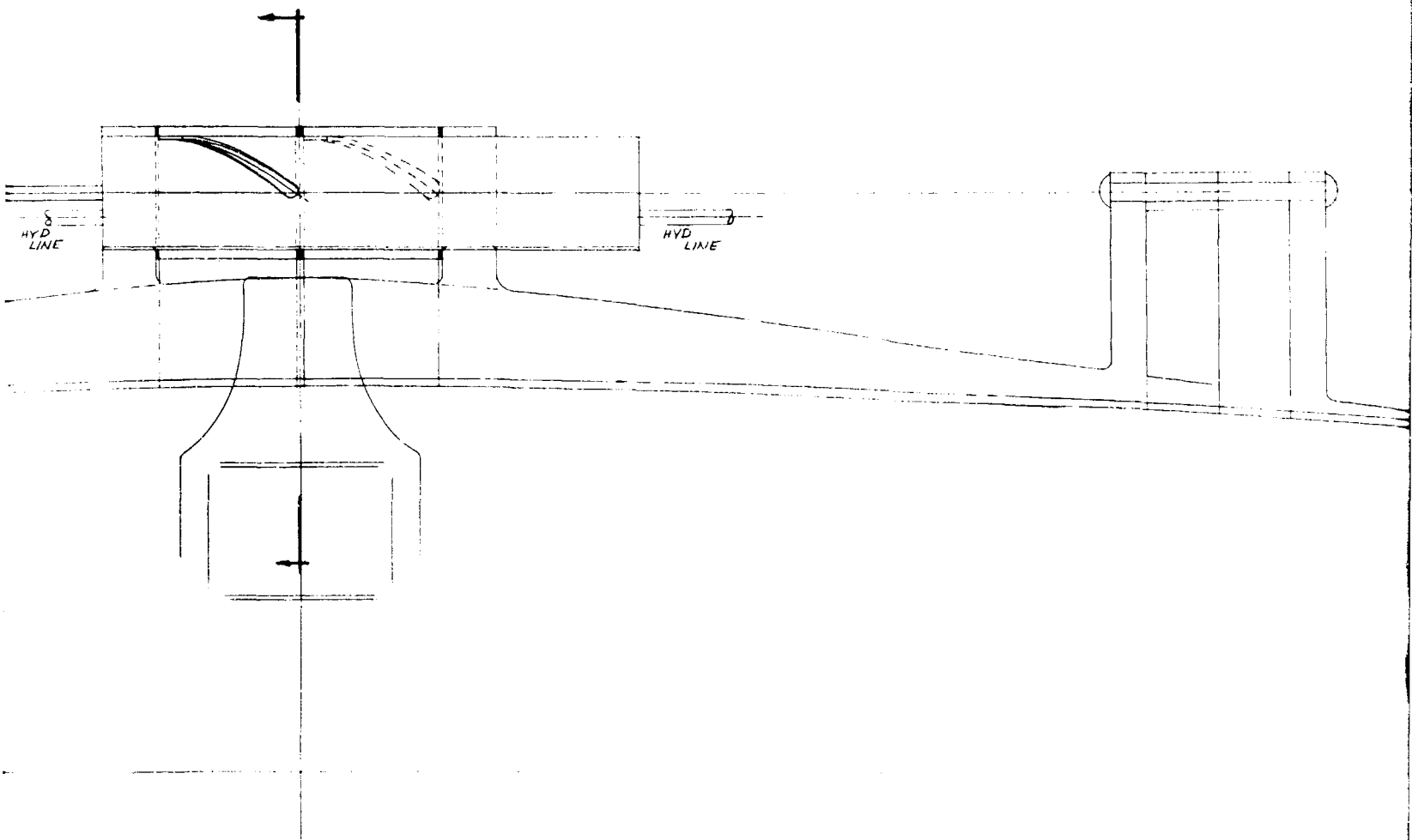
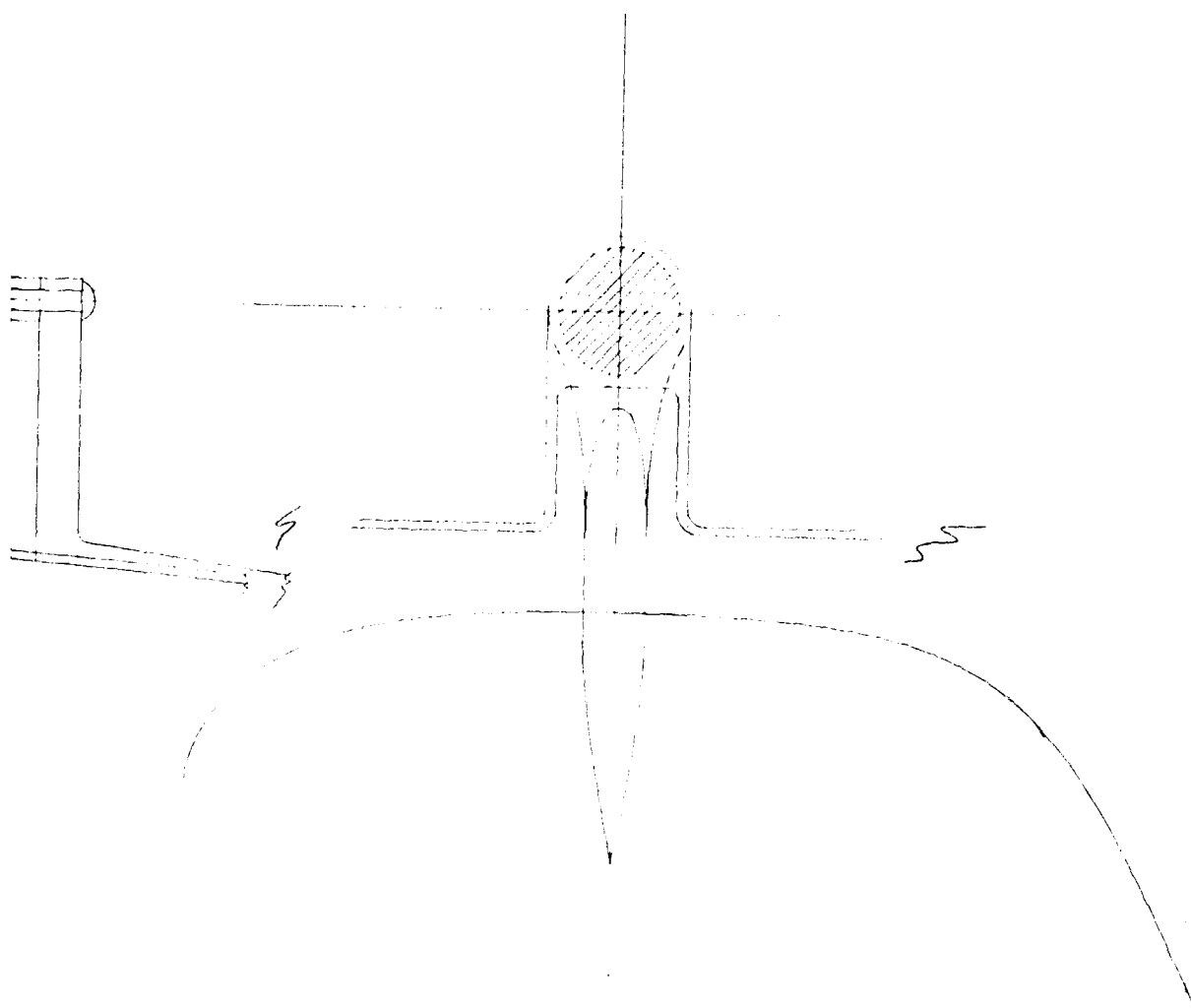


Figure 7. Center Mounted Helical Door Actuator Concept.



B



HELICAL DOOR	
ACTUATOR	

C

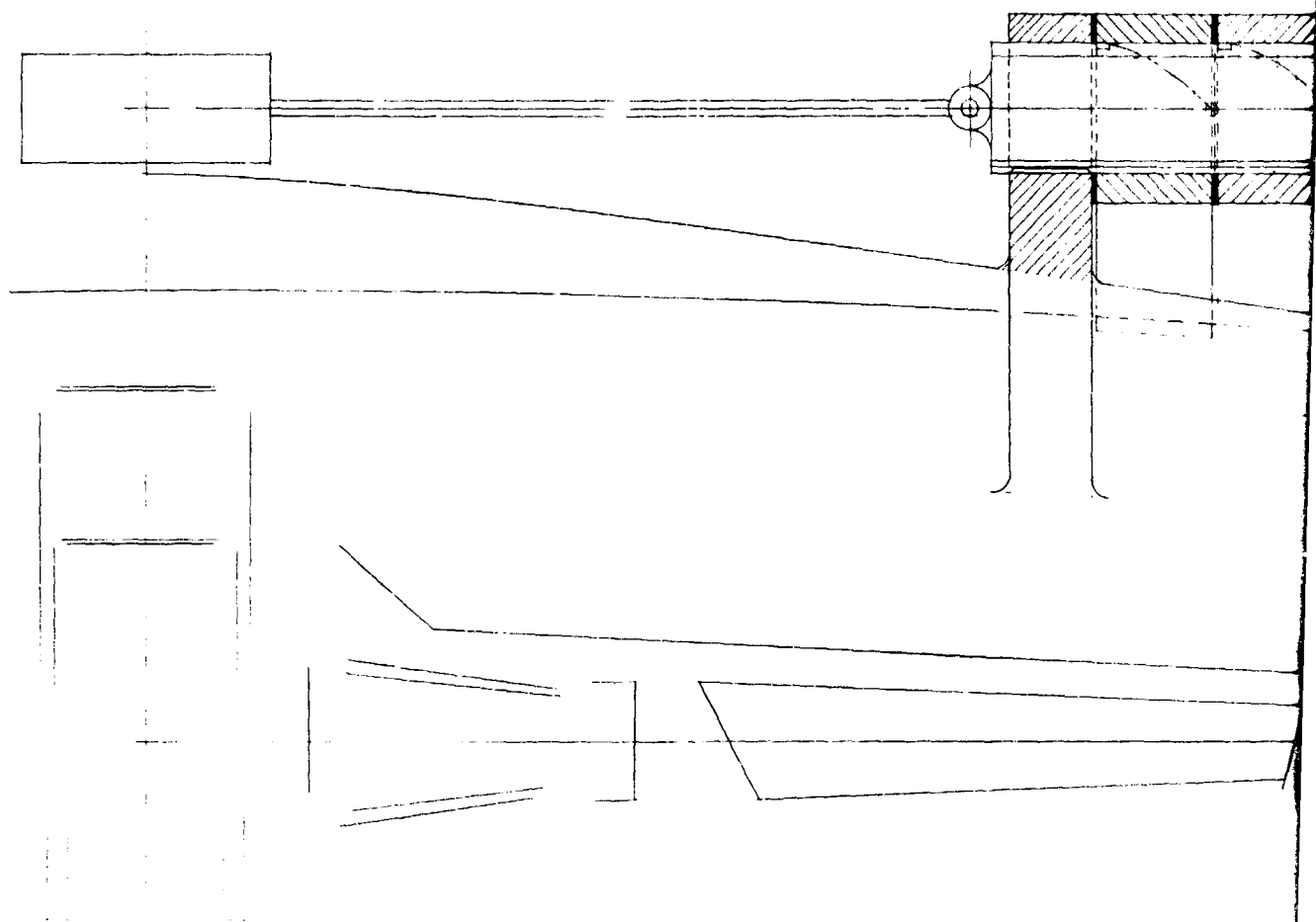
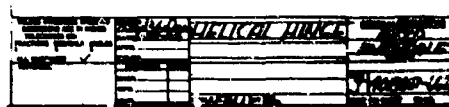
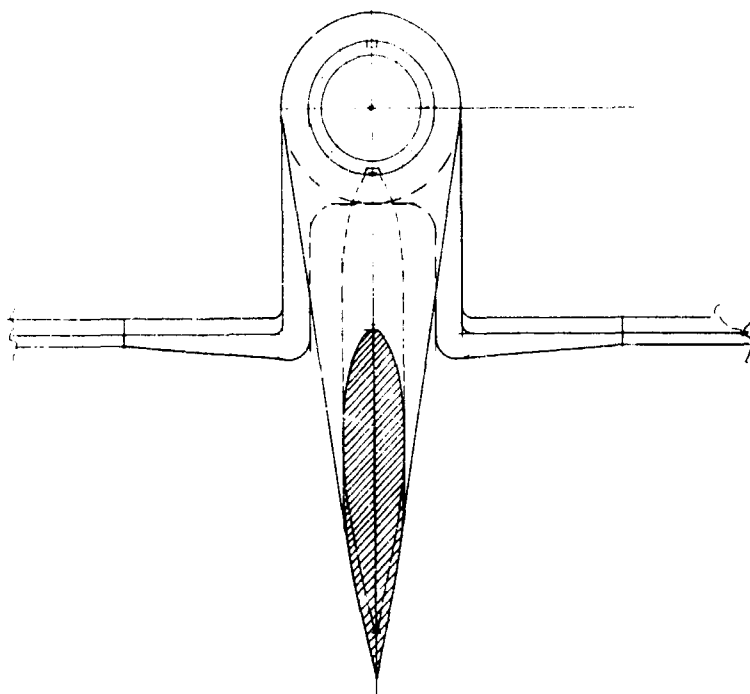
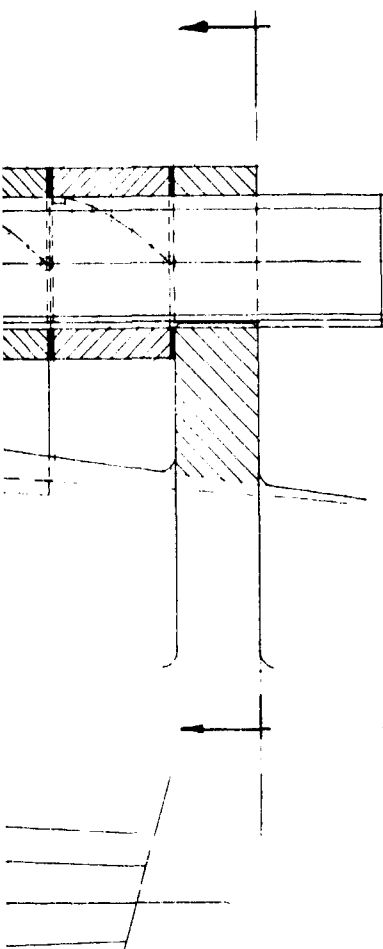


Figure 8. Helical Hinge Door Actuator Concept.



B

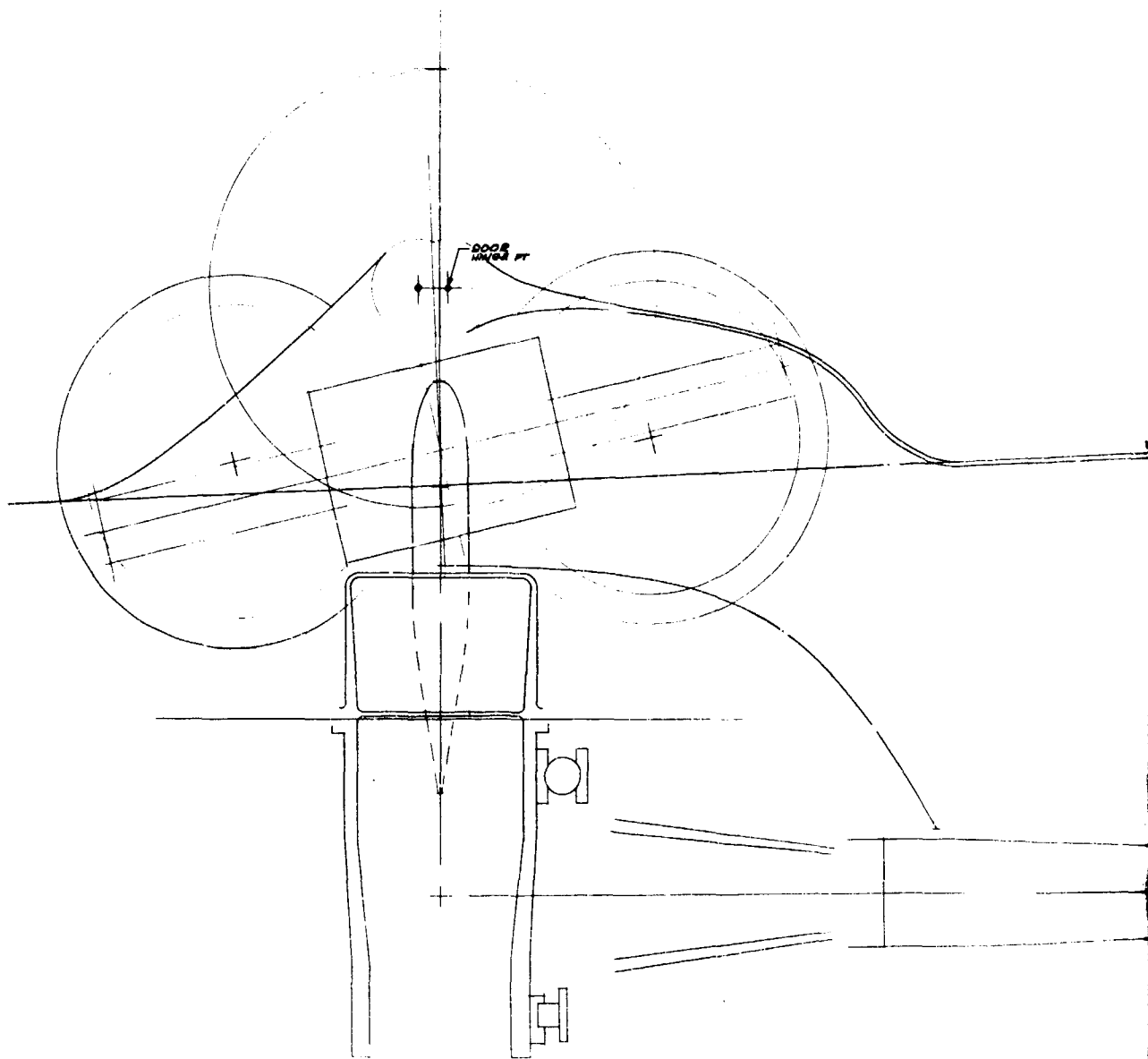
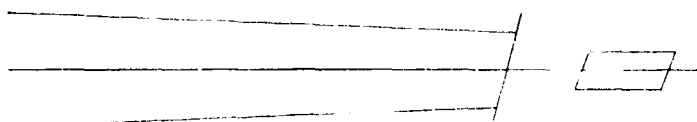
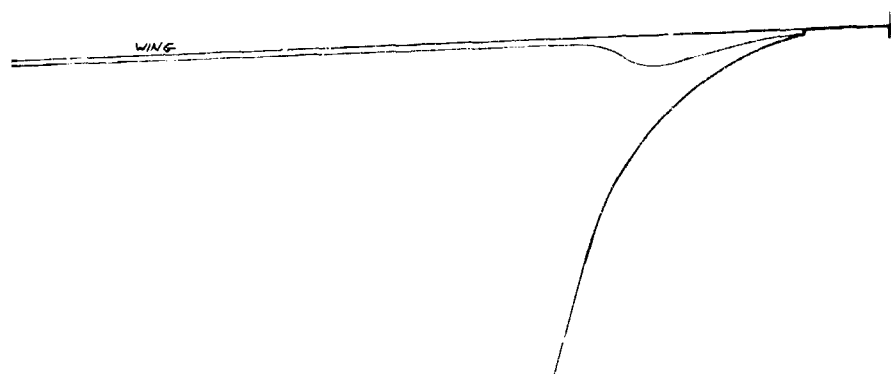


Figure 9. Geared Door Actuator Hub Spacing.



DOOR CONTROL	DOOR
FOR BACKWARD	DOOR
DRIVER ECT.	DOOR
DOOR	DOOR

B

The LFX design concept for the bellmouth uses the bellmouth as an integral part of the fan itself. In addition to its function as a flow-path guide, it also supports the forward compressor air seal, affords a circumferential nesting support for the wing fan cover door in the closed position and includes attach capability for the wing skin/bellmouth seal. As it is conceived, the bellmouth could not readily be separated from the fan structure unless the remaining fan structural weight were increased. The estimated weight of the bellmouth and components and the estimated frame weight without the bellmouth are:

	<u>Pounds</u>
Bellmouth	13.7
Other Frame	<u>88.5</u>
Total	102.2

The estimated increase in other fan weight if the bellmouth were removed is 6.5 pounds, or a total frame weight without the bellmouth of 95.7 pounds.

Scroll Inlet Location

The scroll inlet configuration for the LFX has two in-plane inlets with the inlet centerlines approximately 56 inches apart (Figure 123). Other scroll inlet locations are feasible but might increase the overall weight. One such alternate configuration is shown in Figure 126. Weight increase for this alternate scroll could be as much as 20 pounds.

Scroll Arc of Admission

The LFX studies included a parametric optimization of performance and weight trade-offs in the fan system aeromechanical interrelationship. The basic design which evolved included a scroll with a nominal arc of admission of 250 degrees and a maximum arc of admission of 360 degrees utilizing the power transfer system of varying scroll admission arc. Although this system represents a near optimum control and propulsion device for the parametric aircraft described in the initial LFX studies (Reference 1), it is recognized that other mission orientation or aircraft configurations might dictate the desirability of a different type of control system or of minimum fan fore-aft dimensions. Accordingly, studies were made to determine quantitative effects of other LFX configurations.

Partial Admission Fan

Some installations require fans to have minimum width across the major strut. Minimum width between mounts will occur with fans which have a maximum scroll arc of admission less than 180 degrees. The installed width or diameter is determined by scroll bubble size when the arc of admission exceeds 180 degrees. At scroll arcs less than 180 degrees the turbine casing diameter is the limiting dimension. Decreasing scroll arcs to less than 180 degrees causes the turbine bucket height to increase as does the

turbine casing diameter. Layouts have shown that minimum fan width (fore-aft dimension) occurs near 170 degrees arc of admission.

A derivative fan has been defined at 170 degrees arc of admission. This fan retains the same basic LFX fan rotor design with a modified turbine and scroll. Bucket height has been increased to accept the same flow in 170 degrees that the basic LFX accepts in 250 degrees. Turbine discharge Mach number is maintained at 0.50, retaining the same energy extraction as the basic LFX design. Fan rpm runs about 0.2 percent higher than basic design at its nominal flow condition with slightly higher lift.

Table III shows some of the more pertinent characteristics of this derivative fan. A cross-sectional layout is shown in Figure 10.

Decreasing arc of admission from 250 degrees to 170 degrees decreases installed wing spar spacing from 84 to 75.2 inches at the expense of a lift to weight decrease from 23.3 to 19.5. Since power transfer by variable scroll area is not included in the 170-degree fan, the weights of power transfer mechanism are not included in the 250-degree fan, and lift for full 360-degree scroll is used for this comparison.

A further consideration of the partial admission fan is the effect of increased turbine Mach number. The decreased arc of admission causes the turbine bucket height to increase about 1 inch. It is conceivable to retain the same bucket height as the basic fan by increasing the turbine discharge Mach number to 0.73. The reduced energy extraction associated with the high Mach number requires low camber in the bucket. Low camber will produce high bucket bending stress. Bucket leading edge thicknesses required for turbine aerodynamics are too small for easy manufacturability. Finally, the annulus is uncomfortably close to choke, which could reduce overall fan performance significantly by limiting the turbine power input to the fan.

Some increase in turbine Mach number is advisable. It does two things which help reduce the fan rotor weight. First, it reduces bucket height; second, it reduces fan RPM. Fan lift is only slightly reduced. A Mach number of 0.6 is a good compromise in that it does not force the very low camber and leading edge thickness problem and at the same time reduces the bucket height by about 0.5 inch and reduces fan tip speed from 977 to 950 feet per second. Lift drops off about 1 percent while weight decreases by 10 percent. Table IV shows a comparison of the two cases for 170 degrees arc of admission.

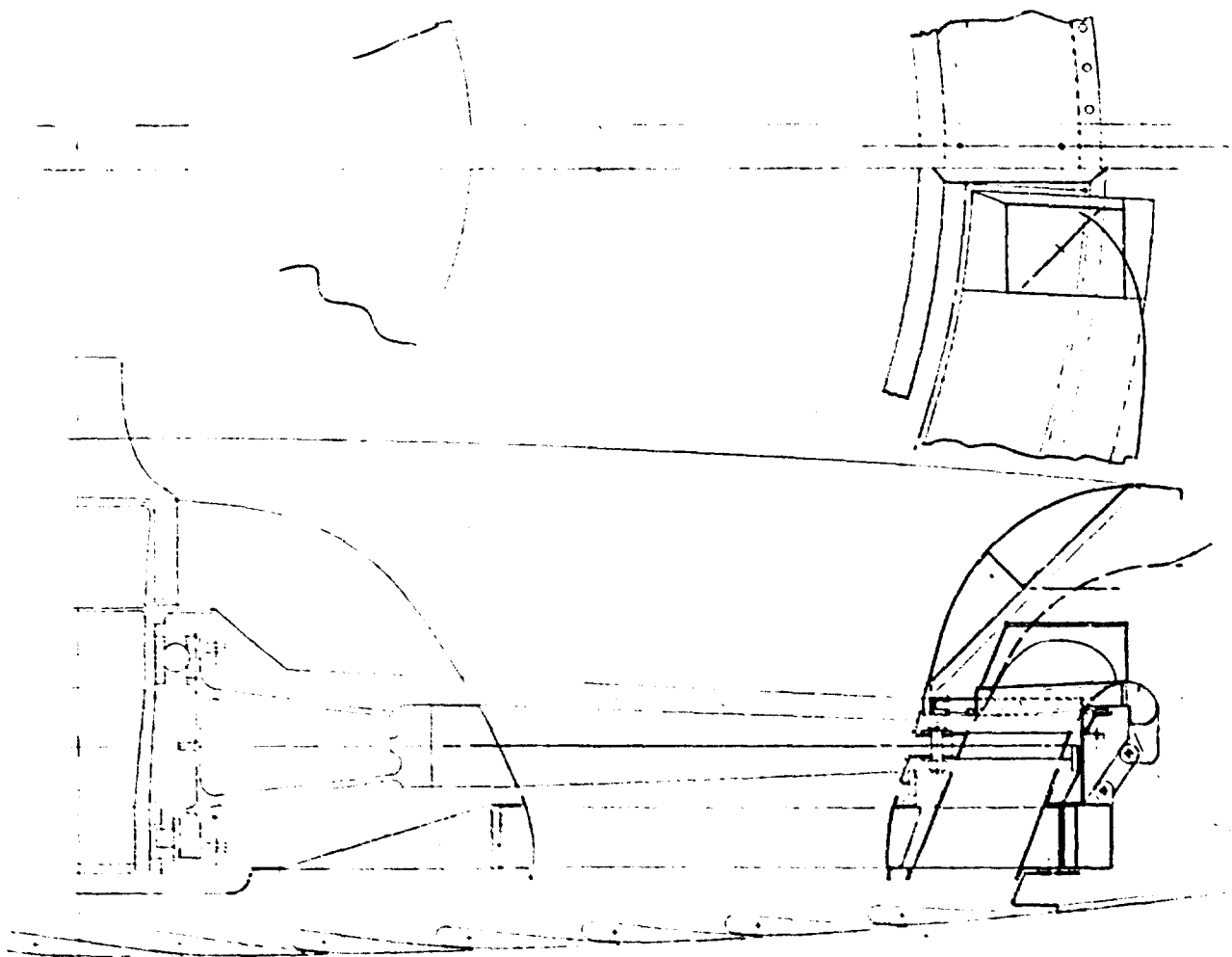
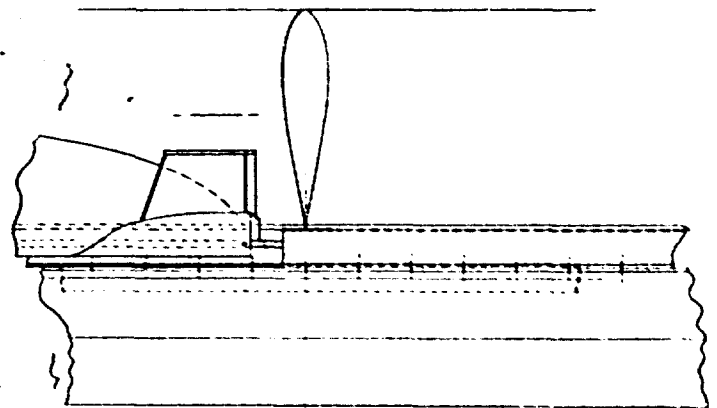
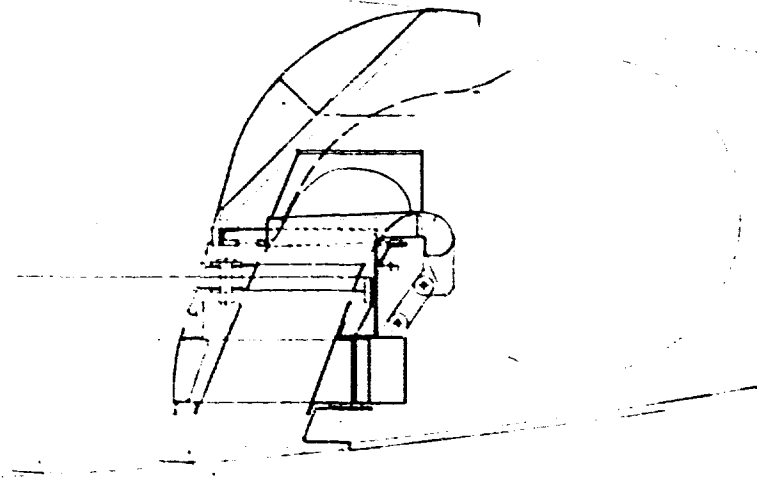
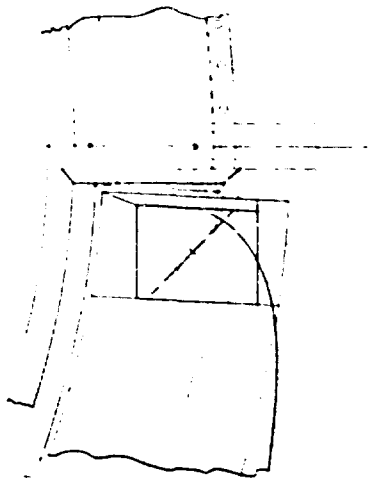


Figure 10. Partial Admission Fan Study.



on Fan Study.

B

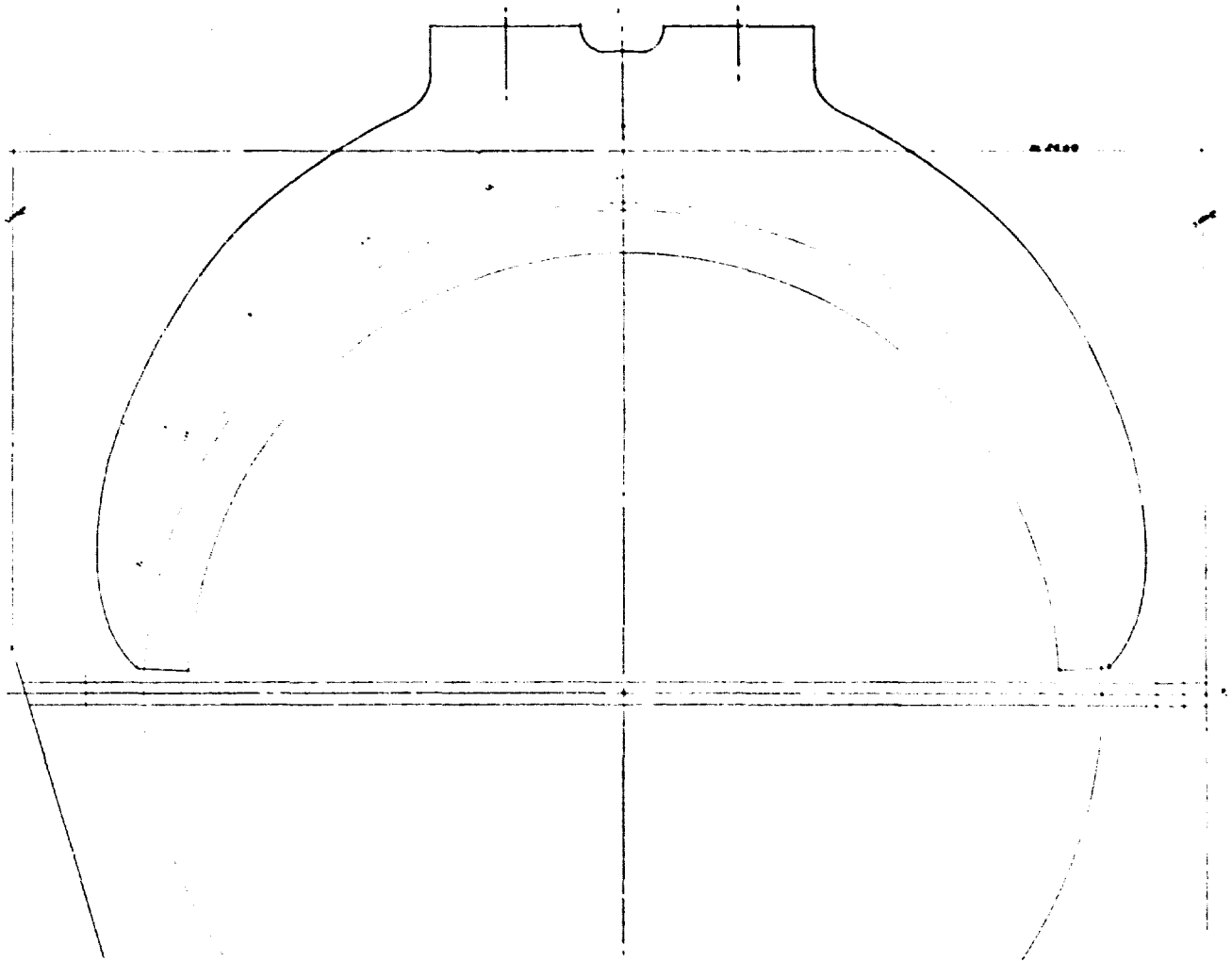
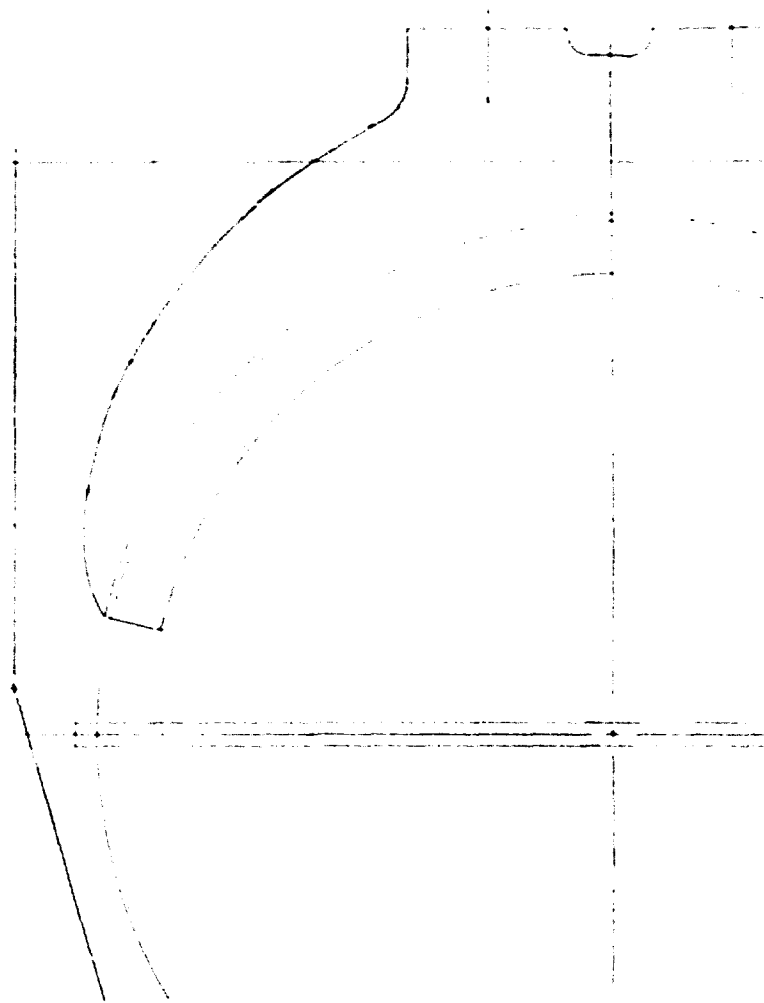
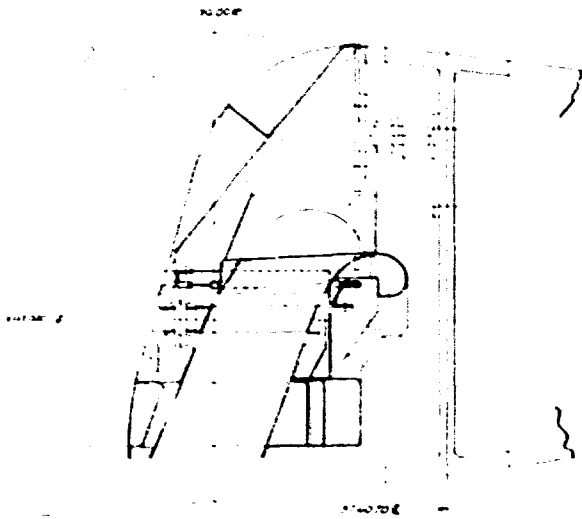
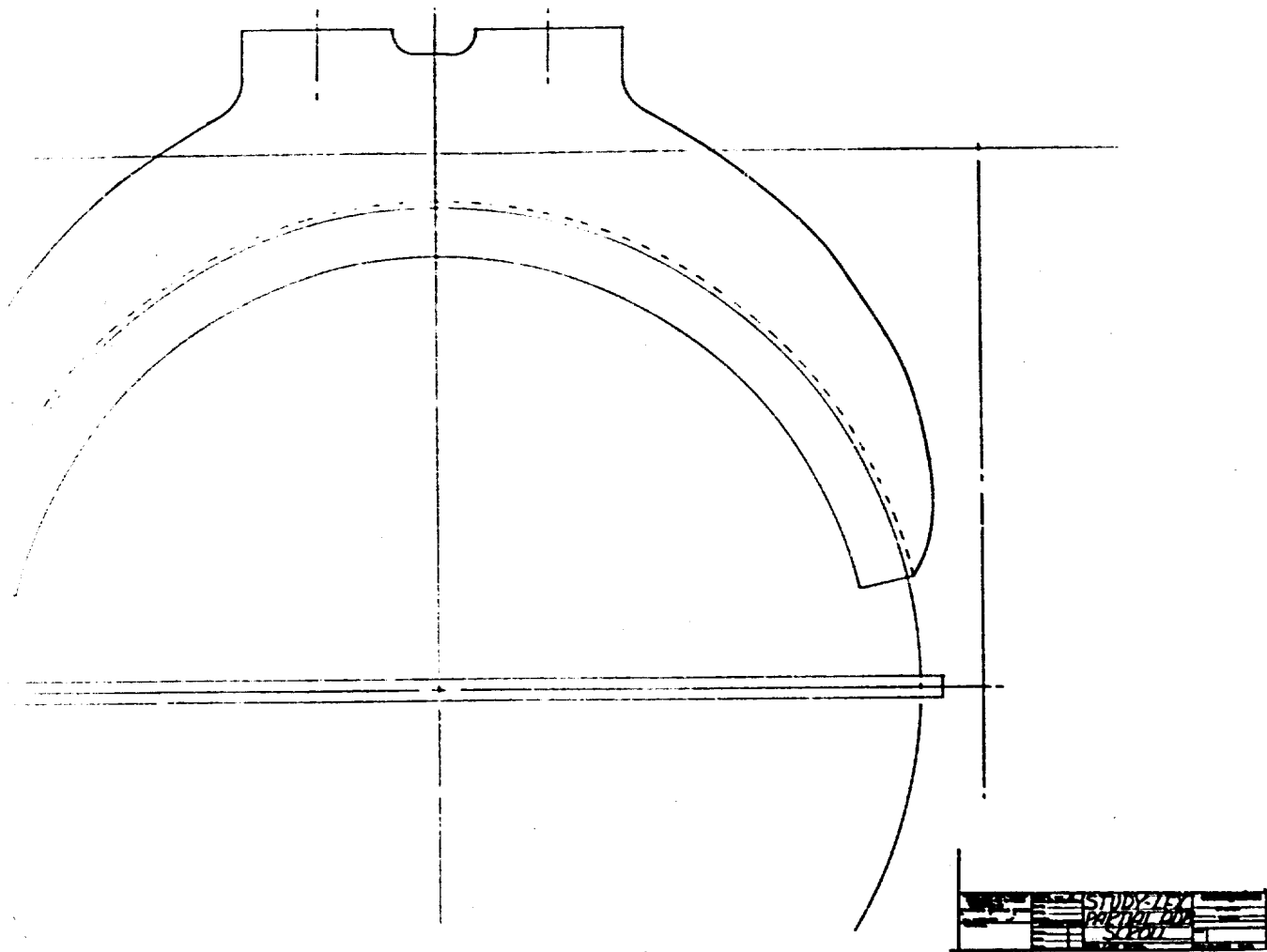


Figure 10. (Cont'd.)

A



B



C

TABLE III
CHARACTERISTICS FOR 170-DEGREE ADMISSION ARC

Scroll Inlet Flow, lb/sec	50.01
Turbine Arc of Admission, deg	170
Fan Pressure Ratio	1.245
Fan Tip Speed, ft/sec	977
Fan Tip Diameter, in.	54.9
Turbine Tip Diameter, in.	64.13
Fan Lift, lb	10,800
Fan Weight, lb	553
Lift/Weight	19.5

TABLE IV
INCREASED MACH NUMBER COMPARISON - PARTIAL ADMISSION FAN

Turbine Discharge Mach Number	0.5	0.6
Fan Tip Speed, ft/sec	977	950
Fan Tip Diameter, in.	54.9	54.9
Turbine Tip Diameter, in.	64.1	63.0
Fan Pressure Ratio	1.245	1.233
Fan Lift, lb	10,800	10,700
Fan Weight, lb	553	498
Lift/Weight	19.5	21.5

Full Admission Performance - Maximum Thrust

With a fan power modulation concept other than the power transfer scroll, it may be desirable to operate the LFX fan at its maximum continuous thrust and without the variable area scroll. In other aircraft concepts, the LFX basic wing fan might be utilized as a pitch control fan or as one fan in multiple series installation.

The LFX basic fan design includes a variable area scroll with the nominal lift condition sized for 74.2-percent flow from the diverter valve discharge. Nominal scroll arc is 250 degrees. Capability is provided for accepting total flow from the gas generator with a 360-degree scroll.

The fan lift with the variable area scroll in the fully open, 360-degree admission arc position is 12,750 pounds. Gas generator flow is 67.52 pounds per second. Fan RPM will be 112 percent of design RPM.

If ducting pressure loss due to diverter valve and cross ducting can be reduced, the power input to the fan could be increased such that the fan would run at its maximum rpm of 115 percent. Lift at this rpm is 13,100 pounds.

Removing hardware such as exit louvers, variable scroll control, vanes and actuators to bring the fan to a pure lift configuration will reduce the weight of the fan by 80 pounds. Running the fan at its maximum rpm for a pure lift device at the reduced weight will increase the lift to weight to 26.9. Table V summarizes lift/weight for various hardware combinations and fan power settings.

COMMENTARY - STUDY OF AIRFRAME REQUIREMENTS FOR LIFT FAN TECHNOLOGY ADVANCEMENT - CONTRACT DA 44-177-AMC-345 (T)

During the initial phase of the LFX study (summarized in Reference 1), a comparison study was made under a separate contract to USAAVLABS by the Ryan Aeronautical Corporation. Results of this study were given in report entitled "Study of Airframe Requirements for Lift Fan Technology Advancement" (Reference 2). As a part of the Phase II LFX studies, the subject report was reviewed by General Electric with particular attention given to reported propulsion and airframe system interface problem areas. A complete summary of commentary is given in Reference 4.

Recommendations pertaining to these problem areas are included with the recommendations generated during qualitative review with other airframe designers and manufacturers. These recommendations are summarized in a subsequent section of this report.

The airframe company chosen for the requirements study was particularly well qualified by virtue of experience in design, fabrication and flight testing of the U. S. Army XV-5A aircraft. Much of the data and recommendations were based on parametric mission studies and on the preliminary

TABLE V
DERIVATIVE LFX FANS SUMMARY

Hardware	Power Setting	Weight	Lift	Lift/Weight
Total fan, including exit louvers, and power transfer	Nominal lift %N = 100	569	10,745	19.0
Total fan, including exit louvers, and power transfer	Maximum power transfer %N = 112	569	12,750	22.5
Modified scroll for lower inlet Mach number	Maximum power transfer %N = 113.5	569	12,850	22.7
Modified scroll for lower inlet Mach number	%N = 115	569	13,100	23.1
Modified scroll for lower inlet Mach number - no variable area	Full gas generator flow %N = 113.5	544	12,850	23.6
No exit louvers - no variable scroll	Full gas generator flow %N = 113.5	487	12,870	26.4
No exit louvers - no variable scroll	%N = 115	487	13,100	26.9

aircraft design evolved during the study as an evaluation aid (Figure 11). Many of the concepts were discussed during the course of the initial LFX studies.

General Comments

The realization of the maximum potential of the operational lift fan aircraft requires a high level of knowledgeable coordination between the airframe and propulsion manufacturer. Additionally, the aircraft configuration (i.e., mission orientation) will have a marked effect on the interface requirements.

Although individual components of the complete propulsion system can be studied for optimization initially, the interaction of each component with the system needs to be evaluated to define a truly optimum system. The parametric fan optimization study described subsequently in this report shows the desirability of system optimization rather than component optimization.

Specific Comments

Specifications

The choice of specification requirements for lift fan propulsion systems has been dictated largely by the existing specifications for the turbojet engine, modified as required for compatibility with the lift fan diverter valve and for compatibility with the aircraft. Many recommendations have been made pertaining to the desirability of certain characteristics and features for both the gas generator and the lift fan.

The LFX studies contain a preliminary specification for a complete propulsion system including turbojet engines, wing lift fans, and a fuselage pitch control fan (USAAVLABS Technical Report Number 67-48). This study specification includes a format and general content based on MIL-E-5007C, -5008C and -5009C. Major areas such as performance, weight, accessory drive capability, compressor bleed limits and load limits are given both for the gas generators and for the lift fan. The conclusion remains, however, that complete definitions of aircraft mission and operating requirements are the best tools for trade-off studies to define firm propulsion system and accessory specifications.

The preliminary design specification for the LFX system includes engine inlet pressure and distortion limits on the premise that the engine manufacturer historically has little or no input to the aircraft engine inlet design on subsonic applications. As a result, it is necessary that the engine manufacturer establish inlet pressure and temperature limits, distortion limits and change rate limits within which the engine will operate with freedom from compressor stall or performance penalties. These limits, when met by proper inlet design, assure operation of the engine in a manner which is commensurate with the engine's development and testing. When

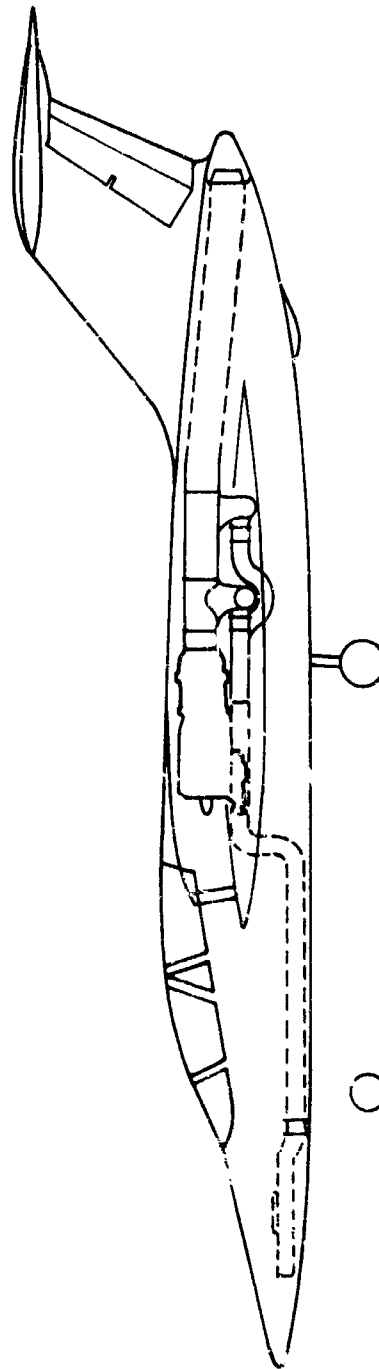
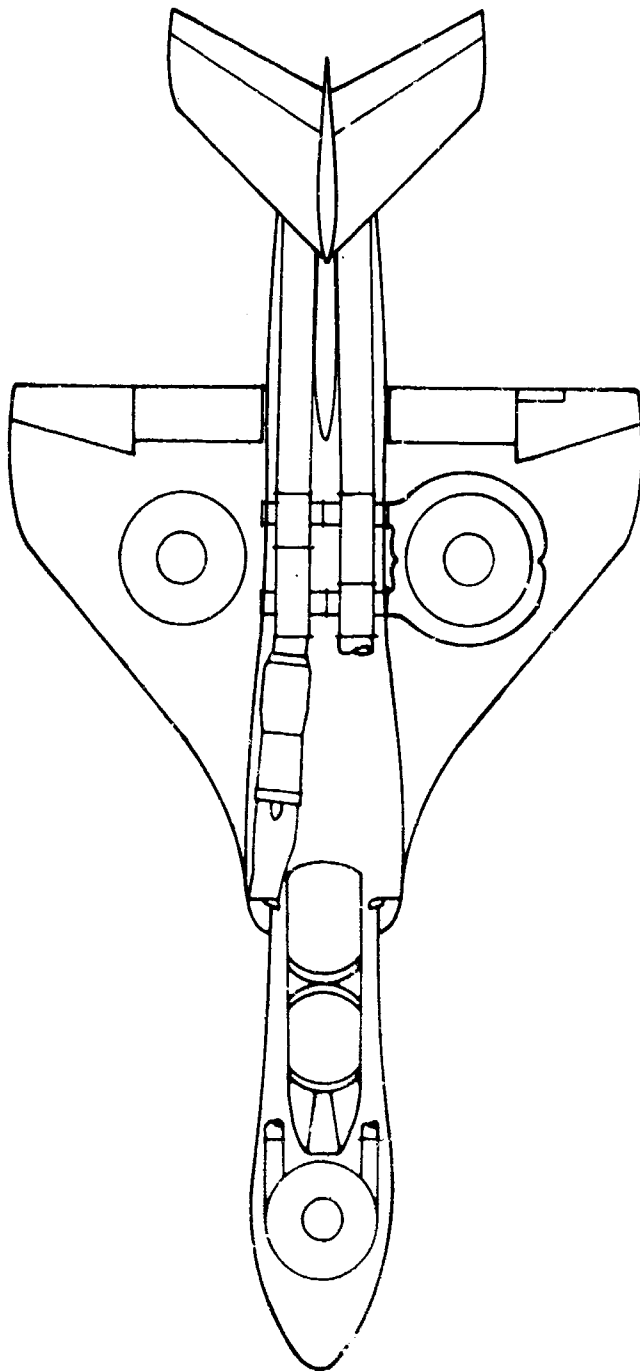


Figure 11. General Arrangement - Ryan Model 209D.

these specified limits are exceeded due to specific inlet design, operational requirements or other reasons, it may still be possible to assure safe engine operation although at somewhat reduced performance capability.

The aircraft engine inlet and its accompanying characteristics have a major effect on engine performance. Consequently, with all aircraft and even more with VTOL aircraft, judicious choice of engine inlet location and attention to detail design will assure the maximum engine performance. Because of the respective lead times for design and development of engine inlets and for engines themselves, the engine manufacturer should retain responsibility for establishing specification limits for inlet temperature and pressure distortion.

Hot Gas Reingestion

The testing of the XV-5A aircraft in the fan flight mode revealed a tendency under certain combinations of altitude, control position and wind velocity for the fan turbine exhaust gases to reenter the turbojet engine inlet. This necessitated certain control adjustments on the turbojet engine to permit operation with higher engine inlet temperatures and temperature gradients. Some performance degradation resulted, both from the hot gas reingestion and from the control adjustments. The cause of the engine inlet reingestion was identified as an interaction of the wing fan exhaust with the opposite wing fan and with the pitch control fan. Identification of the source and cause of the reingestion (prediction of the interaction zone) can lead to design criteria for location of the engine inlets out of the interaction zone. Wind tunnel evaluation of a lift jet VTOL configuration has identified a similar problem with respect to interaction zones and has additionally identified propulsive engine inlet locations to minimize or stop hot gas reingestion into the propulsive engine inlets (Reference 5).

Hot gas reingestion into the lift fans has only a secondary effect on available lift. The lift fan turbine power will remain constant and fan RPM will increase with an increase of ambient compressor air inlet temperature. Within the normal operating range of the fan, lift will almost be constant. Thus, location of the lift fan in the aircraft can be optimized on the basis of other parameters.

Some steps have been taken in the LFX fan design to aid in reducing hot gas reingestion. The normally inactive portion of the scroll/turbine arc has been located on the inboard or fuselage side of the fan. This 110-degree portion of the 360-degree turbine actively discharges hot gases only during the application of roll control in the aircraft. This location of the inactive portion of the turbine will aid in minimizing hot gases conducted back into the turbojet engine inlet and will also aid in reducing fuselage skin temperatures in areas adjacent to the fan turbine exhaust.

Diverter Valve Leakage

Diverter valve leakage is similar to hot gas reingestion in the gas generators in that the ideal for either is none. Within practical limits of weight, pressure, operating force and environment, some diverter valve leakage is highly probable. During fan mode operation, diverter valve leakage through the jet mode duct or nozzle causes fan performance losses but has little other effect on the exhaust duct area. During jet mode operation, leakage into the fan leg can cause heating problems in the duct portion of the propulsion system, in the fan itself and in the wing or fuselage area adjacent to the fan. Although it is possible to design fans which would be insensitive to diverter valve leakage during jet mode flight, it would be at the expense of increased fan weight. The additional effects of the gas leakage on the surrounding aircraft areas indicate the desirability of some compromise between materials and purging of the hot gases. A pilot-controlled variable purging capability would be desirable. Partial opening of the wing fan exit louvers is one possibility. Other potential purging configurations might take the form of small auxiliary cooling air scoops located at the wing and fuselage leading edges. These auxiliary cooling air circuits need be no more complicated or performance-degrading than similar circuits used for electronics bay cooling, cockpit boot-strap pressurization, etc. A third possibility is the use of shaft-driven cooling fans.

The biggest problem associated with the diverter valve gas leakage may well be the factor of recognition of its existence. After proper identification of the potential leakage and its paths, detail design evaluation should lead to maximum efficiency purging and cooling techniques.

Fan Inlet Cover Doors

The wing fan inlet cover doors and door actuators in the XV-5A aircraft are mounted on the fan front frame major strut. Latches for the doors in the down or jet mode position are locked into the cross-flow struts which are a part of the fan. Much discussion and many studies have been made of the wing fan door cover and attendant actuators. Suggestions range from a "no-door" cover (aerodynamic control of the boundary layer air) to louvers similar to the wing fan exit louvers. The split butterfly doors mounted on the XV-5A fans represent a compromise between weight, fan performance degradation and wing aerodynamic requirements for the jet mode.

Certain types of wing fan door actuating schemes have been identified which require as much as 9 inches of space above the fan structural components in the fan hub area. Additional requirements for door latching necessitate circular vanes, cross-flow struts or other structural members in the lift fan flow path.

The LFX fan concept is compatible with a representative 9-percent-maximum-thickness wing, provided that the door actuation scheme does not require height above the fan hub area. A linear hydraulic actuator such as that shown in Figure 6 could be used. In addition, the LFX aerodynamic optimization has evolved a design which has only the structural major and minor

struts in the fan flow path. The addition of vanes or struts for fan door latching would degrade fan mode performance. A lighter weight design could utilize down-latches which retract outside the fan outboard bellmouth when the fan is operating. The ideal door closure and actuating mechanism will not require additional space above the fan hub other than that for the structural thickness of the door.

Exit Louvers

In the XV-5A aircraft, the exit louvers were an integral part of the lift fan rear frame. The actuation system, exclusive of actuators, was mounted on the fan rear frame. The actuators were airframe mounted. Because the exit louvers actually form the bottom portion of the wing skin when the aircraft is in the jet mode, there is some logic in the assignment of design responsibility of the exit louvers to the airframe manufacturer. However, since the exit louvers have an immediate and direct effect on the fan performance during fan flight mode, it is necessary that the exit louver design be identified, controlled and tested as a part of the lift fan. However, there are potential weight advantages to be gained through mounting of the exit louvers and actuation directly to the airframe rather than to the frame. A possible compromise might lie in the provision of specification control drawings by the propulsion supplier.

The recommendation that the exit louvers be aerodynamically balanced to reduce actuation loads is valid. The LFX-6 wing fan design shows the maximum degree of aerodynamic balancing of the exit louvers compatible with available space in the representative 9-percent-maximum-thickness wing chosen for the LFX studies.

V-Band Couplings

The use of V-band couplings for connection of ducts is a time-saving feature during maintenance and frequently represents a weight saving when used in lieu of bolted flanges. The lift fan, diverter valve and pitch fan on the XV-5A incorporated V-band flanges of the machined variety. As a general rule, in ducts with diameters more than approximately 6 inches, a sheet metal formed flange is not recommended. A clamp manufacturer's estimate of leakage at a joint using sheet metal flanges with no gasket is 0.01 SCFM per inch of diameter. In an installation where hot gas leakage causes problems, it is vital to make a compatible choice of a leak-free joint. A leak-free joint using V-band couplings can be made with piloted machined flanges or with sheet metal flanges employing a gasket between the flanges. Use of a pilot with either flange design is conducive to easier assembly and longer life during repeated maintenance cycles.

Instrumentation

Fan instrumentation requirements will differ for fans used in a test-development program and for fans used in production-tested vehicles. Within the time period forecast for the LFX fan concept to be operational, instrumentation for fans in either stage of development should include RPM and vibration amplitude indication. Fans in development status should also include

bearing temperature indication as well as other protective temperature indications. The present XV-5A fan RPM measurement system does not function below approximately 30 percent of design RPM. Although this is well below any operating range of the fan, it could be desirable to measure very low fan RPM as an aid to check-out prior to flight or during jet mode flight. Fan rotation with the diverter valve in the jet mode could be an indication of diverter valve leakage. The LFX fan system design includes RPM pickups capable of readouts as low as 2 percent of design RPM. Alternate RPM readout concepts are shown in Figure 12.

Integral Structure Versus Integrated

The possibility of combining or integrating certain fan and aircraft structural components to improve weight and performance has been discussed in many places. In the absence of quantitative weight-savings estimates or performance improvements which can readily be identified, the LFX concept remains that of a fan integral to itself, i.e., needing only mount points and duct connections to operate.

The fan hub has been suggested as a possible point for interface split between the airframe supplier and the propulsion system supplier. Using this concept, the propulsion manufacturer would supply a rotor to be installed in the aircraft-furnished fan hub. One qualitative advantage cited is the necessary integration of the wing fan door actuation system with the fan hub. In fact, the wing fan closure door mechanism and the fan hub supporting beam (strut) are inseparable only for the split butterfly type of fan cover doors. Even then, the fan hub itself should be considered inviolate, with no shafts, hydraulic lines or other items piercing the highly loaded hub area. The LFX studies have identified potential door actuation mechanisms which are compatible with the fan structural designs and split butterfly doors. An alternate design wing fan cover door and actuation system has been identified (Figure 118) which has the potential of both reducing weight and improving performance.

Design control (and qualification of components) of the fan hub supporting mechanism should remain with the propulsion system supplier in order to assure known tolerances, operating conditions and clearances. In addition, the front frame, rear frame and scroll require precise and known relationships to the rotor to assure proper operation such that design and manufacturing control should remain with a single supplier.

The fan inlet bellmouth is analogous to an engine inlet in that it has a direct effect on performance and a less direct effect on mechanical requirements. However, in the LFX design concept, there are structural loads in addition to the aerodynamic loads transmitted through the bellmouth, making it in effect a dual-purpose part with some resultant weight saving.

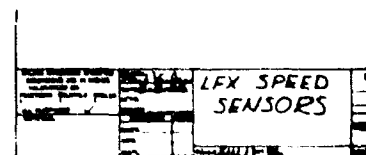
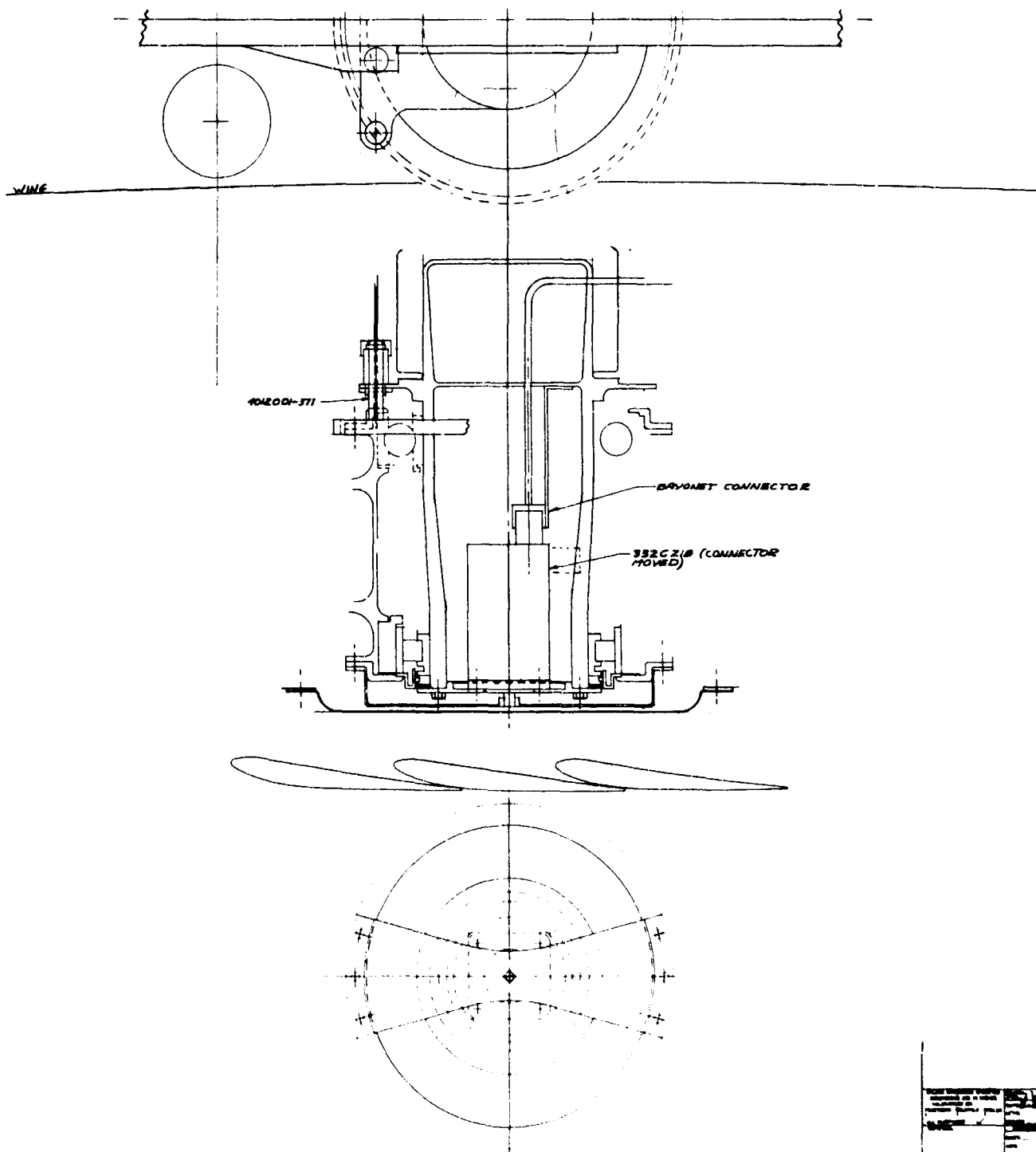


Figure 12. Alternate RPM Pickup Concepts.

The LFX structural design concept utilizes a fan rear frame with no major strut. Consequently, both the exit louvers, the exit louver actuation system (strut) and the actuators can be attached directly to the airframe with a resultant saving in weight.

SPECIFIC RECOMMENDATIONS - INTERFACE AND INSTALLATION

As a result of reviews and discussion with airframe manufacturers and of quantitative trade-off evaluations, specific recommendations were formulated for incorporation into the LFX design criteria and requirements. These recommendations and the reasons therefor are described in this section.

1. The LFX fan design should be capable of incorporating mounts for split butterfly wing fan doors and actuators. Figure 6 shows one possible configuration utilizing linear hydraulic actuators.

The fan front frame should be capable of reacting wing fan door loads ratioed to XV-5A loads as a function of fan pressure ratio and size (or aircraft wing loading, since both tend to vary in a geometric ratio).

Reason: The split butterfly fan doors are the best compromise identified to date for the fan cover doors. The fan structure can accept the door and actuator with reasonable weight penalties.

Identification of specific hard points in the strut for the door hinges and actuators presupposes an exact door/actuator configuration. Therefore, representative door loads will be used in the LFX front frame design criteria. Weights for typical hard points to mount the doors and actuators were calculated as an aid to possible trade-off evaluation when a specific installation is studied.

2. Cross-flow vanes and circular turning vanes should not be added to the LFX design for structural reasons. Means of piercing the fan bellmouth for wing fan door down-locks should be identified.

Reason: The LFX aerodynamic design does not presently include a requirement for either cross-flow vanes or a circular turning vane. Any vanes that may be added would represent a probable degrading factor on fan static performance.

As specific aircraft installations are identified, exact location and actuation methods for the wing fan door down-latches can be optimized.

3. The LFX fan should be designed for minimum thickness compatible with maximum utilization of structural material (i.e., minimum weight).

Reason: The "thinness" of the fan has a direct effect on wing design, on aircraft drag in the jet mode and on fan performance. Within certain limits, the structural and aerodynamic design of the fan can be tailored to reduce installed fan thickness. With the use of inlet guide vanes, single frames and other departures from previous fan design practice, even more reduction in fan cross-sectional area can be achieved. The design criteria for the LFX-6 include the capability of installation in a typical 9-percent-maximum-thickness wing.

4. The LFX wing fan exit louvers should be aerodynamically counter-balanced over as much length of louver as possible. Exit louver actuation and mounting should be direct to the airframe. The propulsion supplier should retain design specification control for the exit louvers. The exit louvers should be included in development and fan qualification testing.

Reason: Installed weight savings are probable when the exit louver loads are transmitted directly to the airframe as dispersed loads rather than point loads through the fan.

The exit louvers directly affect fan performance and operation and should be aerodynamically matched to the fan compressor characteristics.

5. The LFX wing fan design should retain the normally inactive portion of the scroll arc of admission on the "inboard" side of the fan.

Reason: The decrease of hot gas adjacent to the fuselage during steady-state fan operation is a benefit for the airframe. The shorter control lines to the actuation system almost offset weight differential. The "inboard" location for power transfer portions enables a scroll gas flow velocity which is essentially constant throughout the range of operation from maximum gas flow quantities to minimum gas flow quantities.

6. The LFX aerodynamic design should take advantage of the minimum tip speed for the compressor which will give highest component efficiencies with reduced diameter.

Reason: The initial LFX studies identified a maximum installed fore-aft dimension of 86 inches. Because of the effect on aircraft wing characteristics, it is desirable to reduce the fore-aft dimension while retaining good efficiencies for maximum lift to weight.

7. The control response characteristics for the LFX system should be identified and verified with the aid of available computer programs. The LF2 variable area scroll performance characteristics should be utilized as applicable.

Reason: The LFX-6 design includes a very high degree of power modulation utilizing the variable area scroll concept. Because of the immediate effect on aircraft control response and control design requirements, it is desirable to have an early and accurate prediction of the lift fan control characteristics.

8. The LFX wing fan design should include pumping capability for fan compartment evacuation. Pumping capability should be available over the entire operating spectrum of fan-powered flight.

Reason: Scroll seal leakage necessitates some form of evacuation of the fan compartment. Within a range of flow up to approximately 0.6 percent of the turbine discharge flow, the turbine exhaust flow can be used as an "aspirator" with little or no effect on fan performance.

9. The LFX fan design structural concept should be that of a fan-integral structure to include a front frame, rotor, rear frame, bellmouth and scroll.

The LFX fan design should include provisions for aircraft mount attachments at the fore and aft ends of the fan frame major strut and at the outboard end of the deflection limiter (minor) strut.

Reason: Many qualitative recommendations for the combination of fan and aircraft structural components have been studied. In the absence of a quantitatively defined weight saving or performance gain, the requirements of the fan rotor for a precise and known dimensional relationship to the scroll and exit stators indicate the desirability of a single source of manufacture and development testing. Because of the tendency of a wing to flex under various loading, it is desirable to isolate the fan from the wing in such a manner that the wing does not impart loads or deflections to the fan structure.

10. The LFX fan design should include provisions for rotor removal with the front frame remaining in the aircraft.

Reason: The front frame, seal, wing fan doors and actuation system require a substantial number of maintenance man-hours for removal and installation. It is desirable to remove the rotor for inspection, replacement of turbine sectors or replacement of blades without removing the complete fan assembly, including the front frame.

11. Weights, loads, and principal stresses of each component should be identified.

Reason: Further study with airframe manufacturers will be facilitated with a possibility of identification of quantitative weight savings.

12. The nominal design flow for the LFX turbine should be 50.01 pounds per second. The maximum flow under power transfer should be 68.2 pounds per second.

Reason: The nominal flow is matched to the results from the parametric mission analysis of the Phase I LFX study. The maximum flow will permit a very high degree of thrust modulation for control purposes and will permit phasing out of the pitch fan and acceptance of the pitch fan turbine gas flow into the wing fan.

13. MIL-E-5007C, -5008C, and -5009C should be used as the format for specifications for the LFX propulsion system.

Reason: The development of VTOL propulsion systems specifications is the subject of much effort by the industry. The turbojet specifications offer the best basis at the present time for the systems specifications.

PRELIMINARY DESIGN

PARAMETRIC CYCLE OPTIMIZATION

The design point of the LFX fan was established by the use of a parametric mission analysis computer program during the first phase of the LFX studies. Results of the mission analysis and a complete description of the design point are given in Reference 1.

With the design point previously determined, parametric evaluation of the interaction of aeromechanical features was desirable to determine the effects of varying tip speed, pressure ratio and other parameters.

Parameters Studied

Six fan cycle parameters were selected for study. Figures 13 through 20 show fan lift, fan weight, fan area, and the ratios lift/weight and lift/area as functions of these six cycle parameters. The data were generated by varying one parameter at a time while holding the remaining five parameters constant. Table VI contains the parameters, reference values, and range covered.

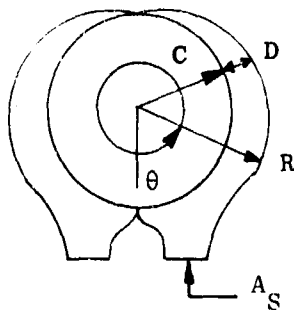
TABLE VI
FAN PARAMETERS

Parameters	Range Covered	Reference Cycle
Fan Pressure Ratio, P/P	1.20 to 1.30	1.25
Fan Tip Speed, ft/sec, U_{FT}	900 to 1000	950
Scroll Mach Number, M_S	0.25 to 0.35	0.30
Fan Inlet Mach Number, M_{10}	0.50 to 0.55	0.50
Turbine Discharge Mach Number, $M_{5.5}$	0.50 to 0.70	0.50
Turbine Exhaust Diffusion	0 and 30 percent	0

The fan radius ratio and the fan efficiency were defined as functions of pressure ratio and tip speed. The gas generator discharge conditions were held constant throughout the study.

The fan lift and fan diameters were calculated using the fan cycle design point computer program. The weight data were obtained using the fan weight computer program. The fan area is defined as the planform area of the fan including the scroll. A derivation of the expression for fan area as a function of turbine tip diameter and scroll size follows.

Derivation of Expression for Lift Fan Planform Area



For a full admission fan, the planform area is equal to

$$A = 2 \int_0^{\pi} \frac{R^2}{2} d\theta = \int_0^{\pi} (C+D)^2 d\theta \quad (1)$$

where

- A = fan area
- C = radius to scroll
- D = scroll diameter
- R = C+D = total fan radius
- θ = integration angle

The radius to the scroll, C, was assumed to be 5 percent larger than the tip turbine radius:

$$C = 1.05 \left(\frac{D_{TT}}{2} \right) \quad (2)$$

The scroll area varies linearly with the angle θ . The scroll diameter, D, can be expressed as

$$D = \sqrt{\frac{A_S}{\pi/4} \left(1 - \frac{\theta}{\pi} \right)} \quad (3)$$

where A_S = scroll inlet area, a function of scroll Mach number and scroll flow, pressure and temperature.

Combining equations (1), (2) and (3) and integrating yields the desired expression for fan area A:

$$A = 0.866 D_{TT}^2 + 2.48 D_{TT} \sqrt{A_S} + 2 A_S \quad (4)$$

Fan Pressure Ratio and Tip Speed

Figures 13, 14 and 15 show the lift, weight and area changes due to changes in pressure ratio and tip speed. The resulting lift/weight and lift/area values are shown in Figure 16. Lift and lift/weight increase with increasing tip speed for tip speeds up to about 975 feet per second. Cross-plots of these data show a peak in lift and lift/weight at about 975-feet-per-second tip speed. Lift/area increases with increasing tip speed for tip speeds up to 1000 feet per second.

The fan efficiency decreases and the turbine efficiency increases with increasing tip speed. The product efficiency increases with increasing tip speed, which explains the increase in lift. The decrease in fan radius ratio with increase in tip speed explains the effect of tip speed on size. The parametric fan weight computer program predicted that this size decrease would offset the weight penalty associated with higher tip speeds. However, the subsequent detailed mechanical design analysis showed that rotor weight is more sensitive to tip speed than the parametric data had indicated.

Scroll Mach Number

For this study, the diverter valve, straight duct, and crossover duct all have the same design point value of flow Mach number as the scroll.

The lift, weight and area changes are shown in Figure 17. Lift, weight and area all decrease with increasing scroll Mach number. Lift decreases because of the higher total pressure losses. Area decreases because of the decreasing scroll size. The decreasing lift and area combine to reduce weight. The decreases in lift and weight are nearly identical, and so there is little change in lift/weight, as seen in Figure 17. The lift/area ratio varies about 3½ percent between the scroll Mach numbers of 0.25 and 0.35.

Fan Inlet Mach Number

Figure 18 shows the effects of fan inlet Mach number on the lift, weight and area. In the interval of fan inlet Mach numbers between 0.50 and 0.55, the lift, weight and area decrease linearly with increasing fan inlet Mach number. Previous studies (Reference 1), in which the fan inlet Mach number was varied between 0.40 and 0.60, showed that these are actually nonlinear curves which are very nearly linear in the small interval of 0.50 to 0.55 fan inlet Mach number.

The lift decrease is relatively small, and is caused by the increase in fan inlet loss due to increase in fan inlet Mach number. The area and weight decreases are due to the reduction of fan annulus area caused by the increase in flow axial velocity through the fan.

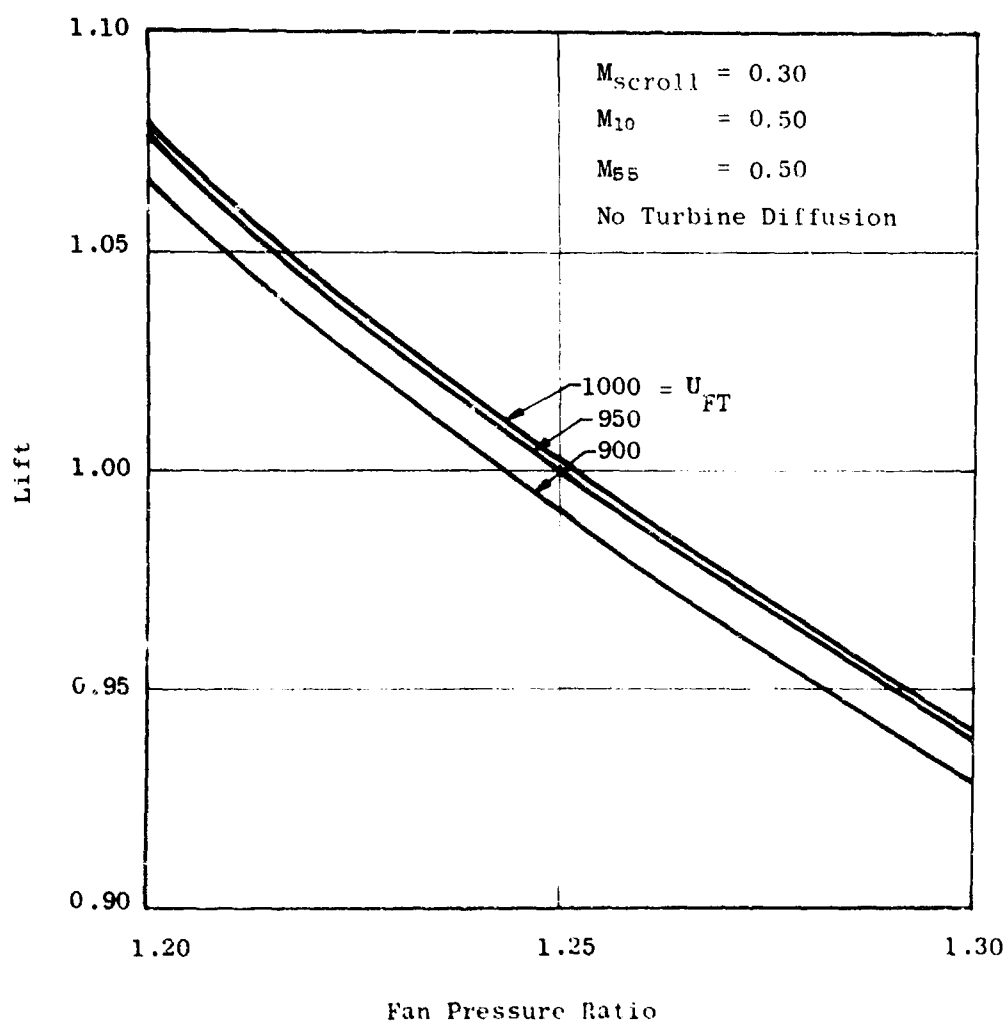


Figure 13. Fan Lift Versus Fan Pressure Ratio.

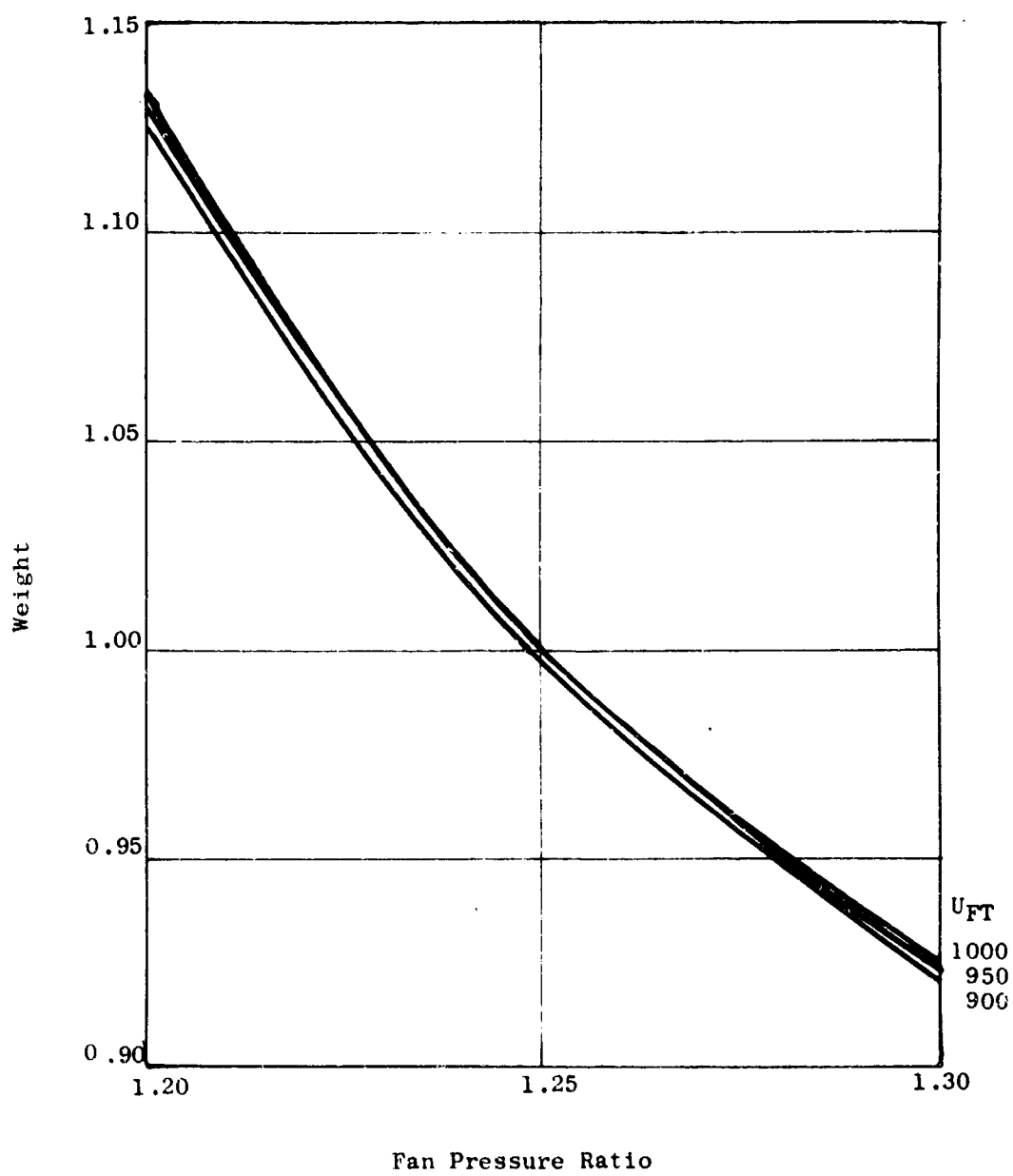


Figure 14. Fan Weight Versus Fan Pressure Ratio.

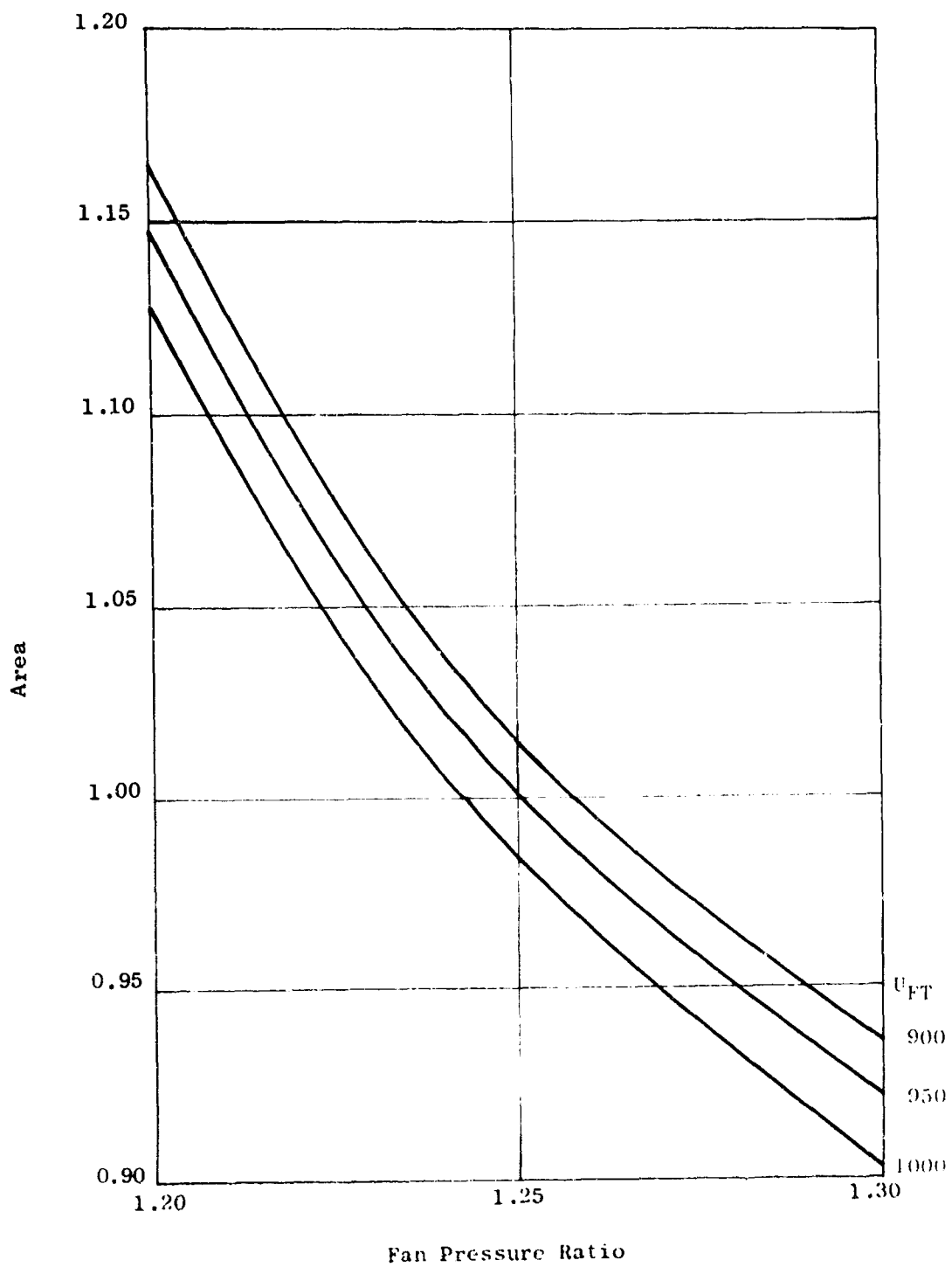


Figure 15. Fan Area Versus Fan Pressure Ratio.

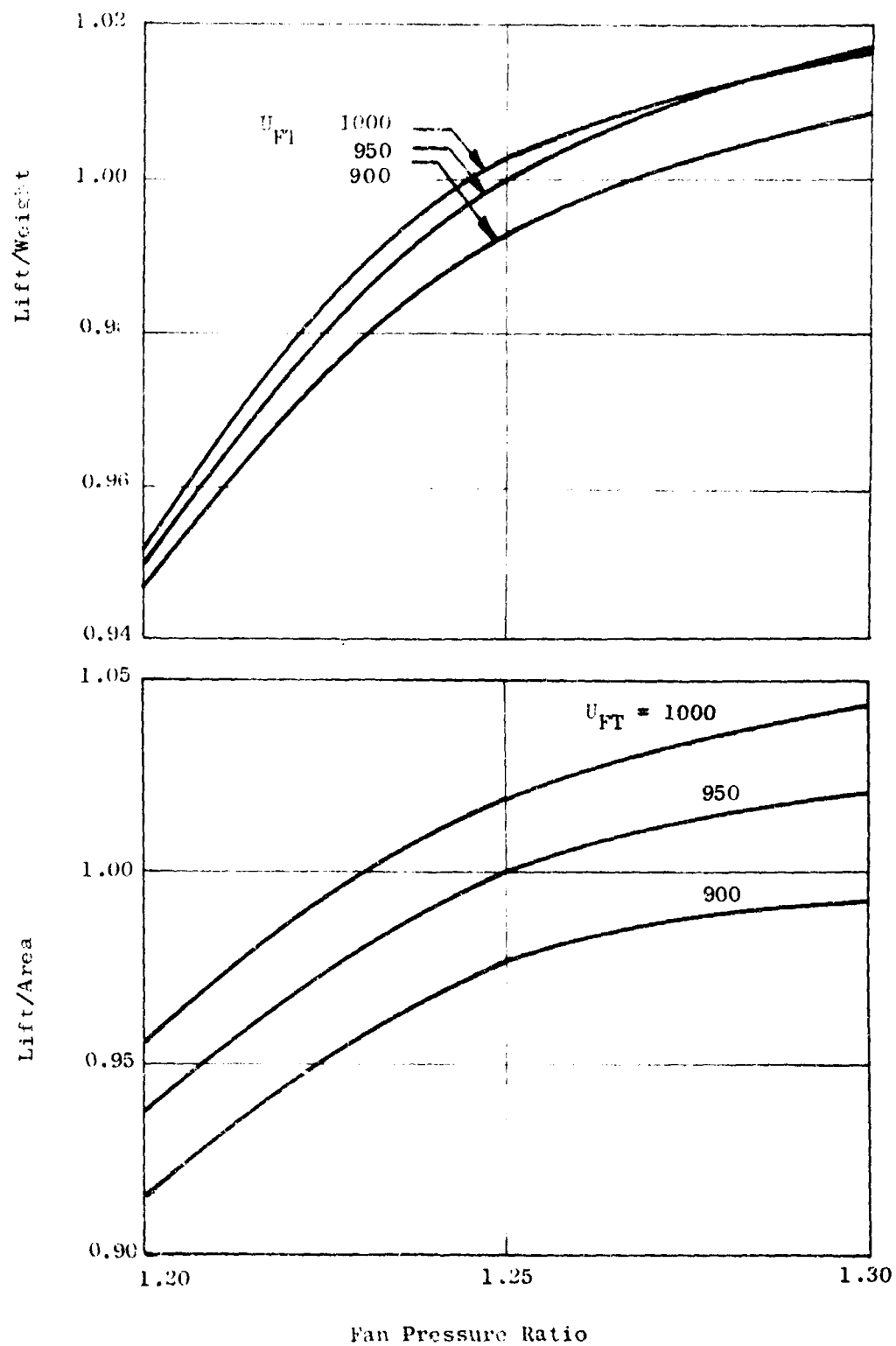


Figure 13. Fan Lift and Weight Ratio Variation With Fan Pressure Ratio.

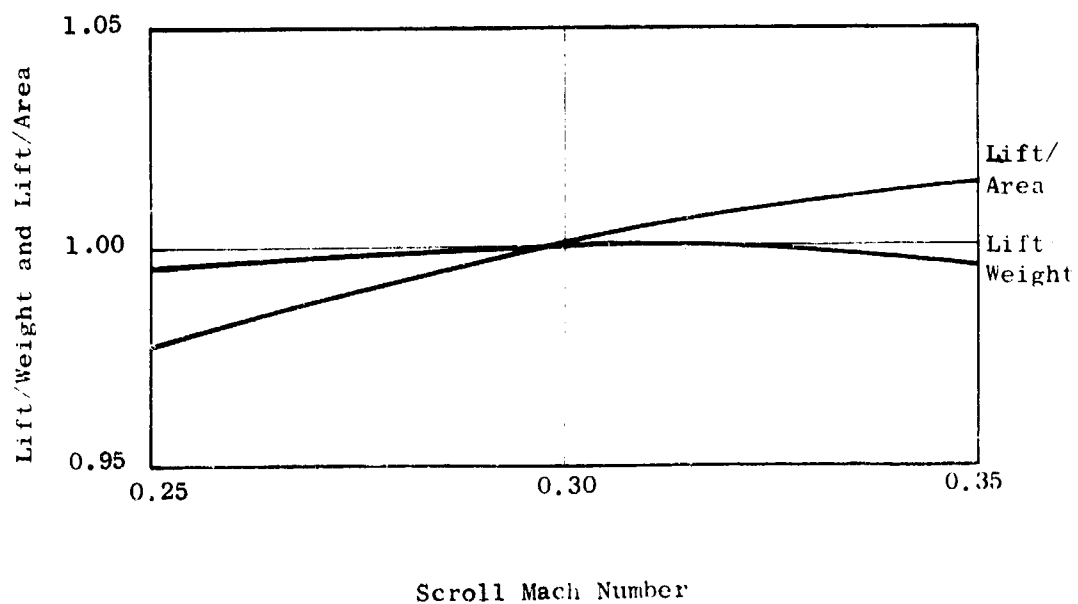
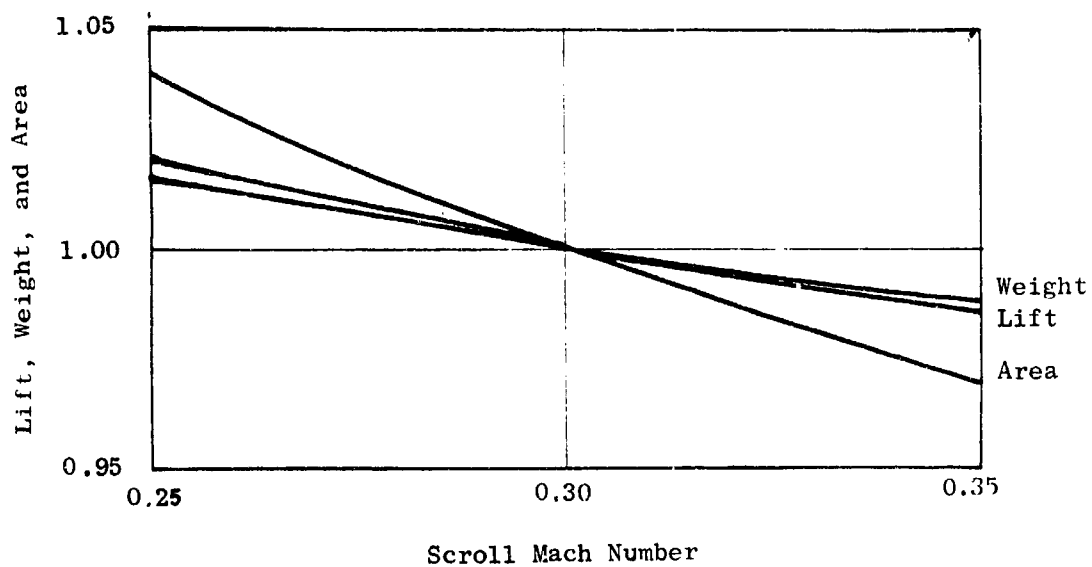


Figure 17. Fan Lift, Area and Weight Variation With Scroll Mach Number.

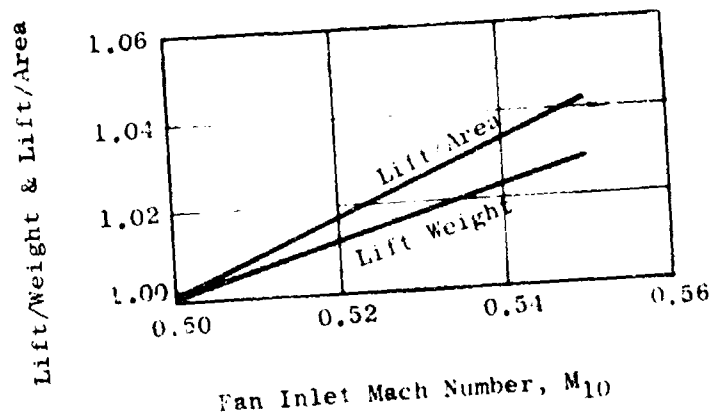
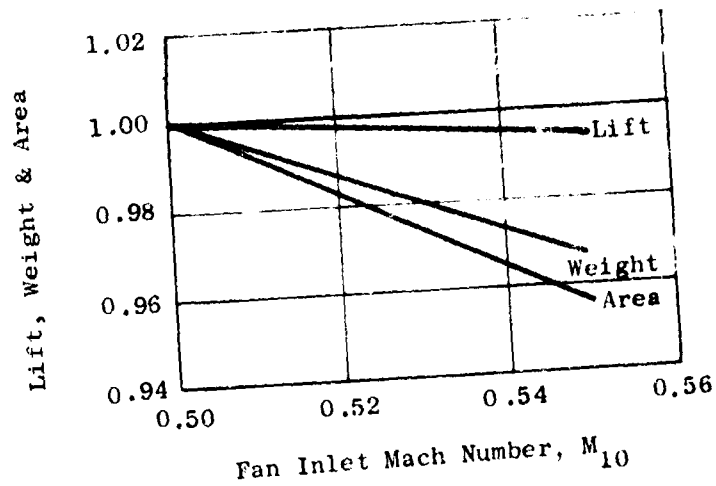


Figure 18. Fan Lift, Area and Weight Variation With Fan Inlet Mach Number.

Figure 18 shows the resulting lift/weight and lift/area trends. Changing the fan inlet Mach number from 0.50 to 0.55 will increase the lift/weight ratio 3 percent and increase the lift/area ratio 4 percent, with only a 0.6-percent decrease in lift.

Turbine Discharge Mach Number

The solid lines of Figure 19 show the changes in lift, weight and area as functions of the turbine discharge Mach number for a conventional tip turbine with no diffusion of the turbine exhaust. The dashed lines show similar data with diffusion.

Increasing the turbine discharge Mach number decreases the turbine bucket size and lowers the turbine pressure ratio and energy extraction, thereby lowering the compressor lift while increasing the turbine residual thrust. The net effect is a decrease in total lift accompanied by much larger decreases in fan weight and area. Figure 20 shows the resulting ratios of lift/weight and lift/area. There are large gains in lift/weight and lift/area ratio obtainable through increase of the turbine discharge Mach number. However, these gains are achieved through a decrease in total lift.

The diffusion is a static pressure rise in the turbine exhaust stream during the passage of the turbine exhaust gas through the turbine stators, and is accomplished by an area increase in the flow path formed by the walls of the outer and middle boxes of the rear frame. The diffusion rate was selected to give a static pressure rise in the turbine exhaust equal to 30 percent of the dynamic head at the turbine rotor discharge. This amount of diffusion is not large. A diffusion passage length of only about 1.5 to 2 inches is required, and therefore the diffusion could be accomplished in the turbine stators. Diffusion lowers turbine exhaust pressure and increases the turbine pressure ratio, thus increasing the turbine work extraction and increasing the compressor lift while decreasing the turbine residual thrust. The fan total lift is therefore increased, as shown in Figure 19. The fan weight and area also increase because the increase in compressor lift increases the fan size.

Figure 20 shows the resulting ratios of lift/weight and lift/area. Adding diffusion to the turbine exhaust increases lift but reduces the lift/weight and lift/area potential improvement. The effects of turbine diffusion will be a little better than these data show, because one important additional effect of diffusion is to reduce the static pressure difference between the turbine inlet and the fan inlet. This will decrease the amount of leakage of hot gas into the fan tip region. This decrease in leakage will improve the fan efficiency. It is estimated that the fan efficiency is reduced $1\frac{1}{2}$ percent due to this leakage. Some fraction of this $1\frac{1}{2}$ -percent efficiency can thus be regained by the addition of turbine diffusion.

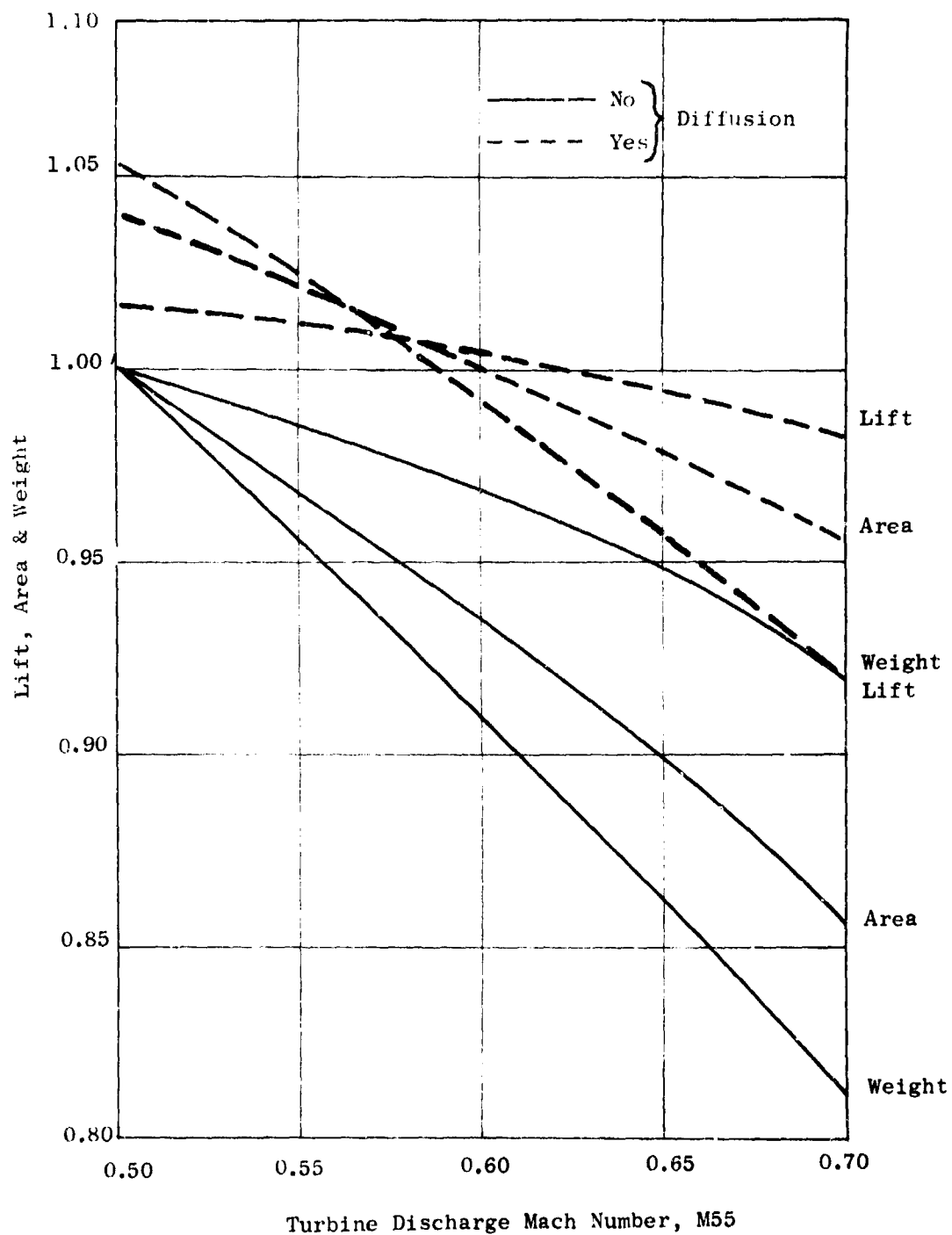


Figure 19. Fan Lift, Area and Weight Variation With Turbine Discharge Mach Number.

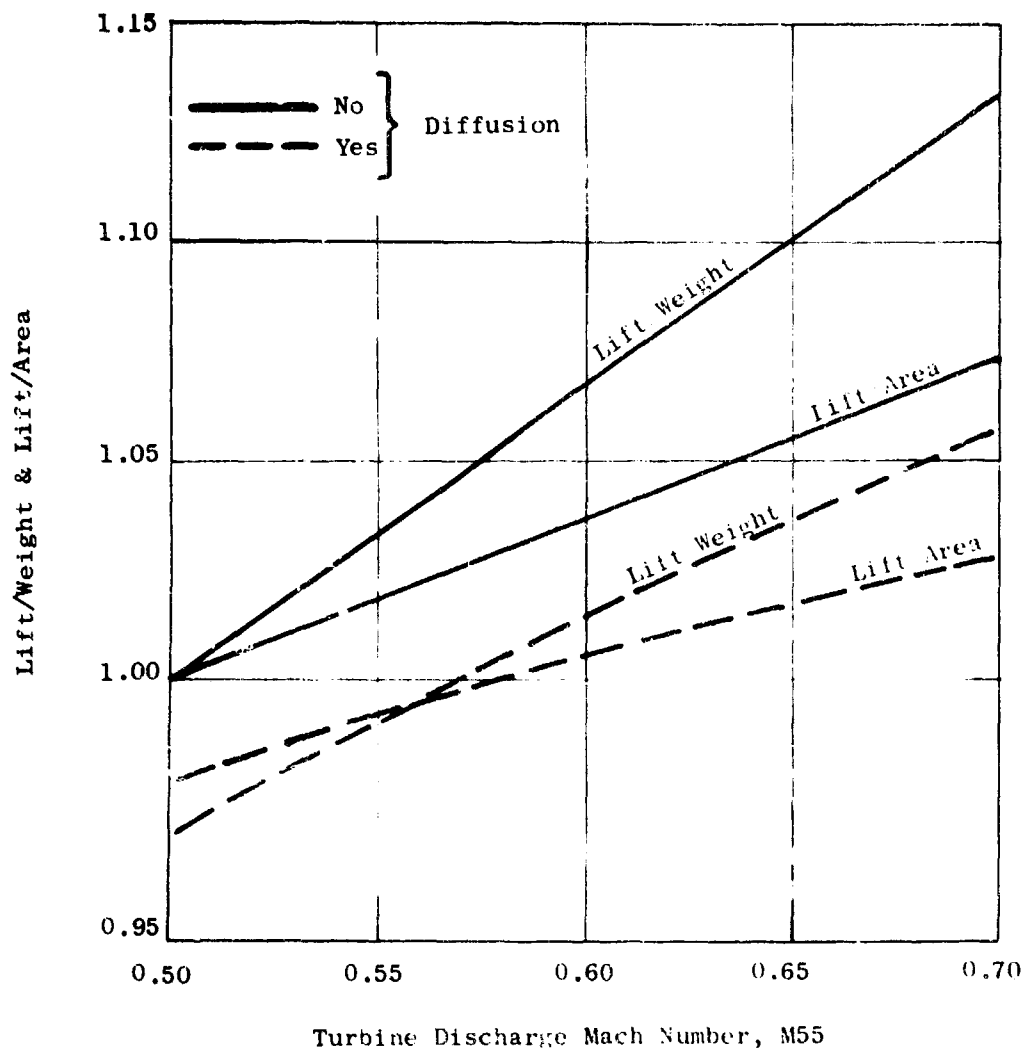


Figure 20. Fan Lift, Area and Weight Ratio Variation With Turbine Discharge Mach Number.

Effects of Combinations of Cycle Parameters

The previous discussion related the effects of individual cycle parameters on lift, weight and area. Figures 21 through 24 illustrate the effects of combinations of cycle parameter selections. Shown are the lift/weight and lift/area ratios plotted versus lift. These curves were obtained from the data of Figures 13 through 20, plus additional data generated using various combinations of cycle parameters. Figure 21 shows the effects of changes in fan pressure ratio and tip speed. A plot is formed by intersecting lines of constant pressure ratio and tip speed. The figure shows that for any pressure ratio, a tip speed of 575 feet per second was predicted to maximize lift/weight and maximize lift. A tip speed of 1000 feet per second was predicted to maximize lift/area.

Figure 22 shows lift/weight and lift/area versus lift, as affected by scroll Mach number and turbine discharge Mach number, with and without turbine exhaust diffusion. On the lift/weight-versus-lift curves, the nearly vertical lines are lines of constant scroll Mach number, and the horizontal lines are lines of constant turbine discharge Mach number. The dashed lines denote diffusion of the turbine exhaust. Symbols are used to help identify the lift/area lines which are closely spaced. The figure shows that

Scroll Mach number will be selected to achieve a desired lift level or a desired lift/area level; lift/weight is almost unaffected.

Turbine discharge Mach number should be selected as high as possible, limited by the lift level required.

Small gains in lift or lift/weight or lift/area are possible by increasing the turbine discharge Mach number and adding diffusion to the turbine exhaust. These same gains can also be obtained without diffusion by increasing turbine discharge Mach number and decreasing scroll Mach number.

Figures 23 and 24 show the lift/weight and lift/area versus lift, as affected by changes in scroll Mach number, turbine discharge Mach number without diffusion, and fan inlet Mach number. The solid lines are the same as on Figure 22. The dotted lines show the effect of increasing the fan inlet Mach number. The message is clear - for any combination of the other fan cycle parameters, fan inlet Mach number should be chosen as high as possible.

Figure 25 shows the same points as Figure 24, but they are connected a different way. It is included hopefully to clarify the effects of combined cycle parameters. To change fan inlet Mach number is to move along a vertical line; to change scroll Mach number is to move along a horizontal line; and to change turbine discharge Mach number is to move from one rectangle to another.

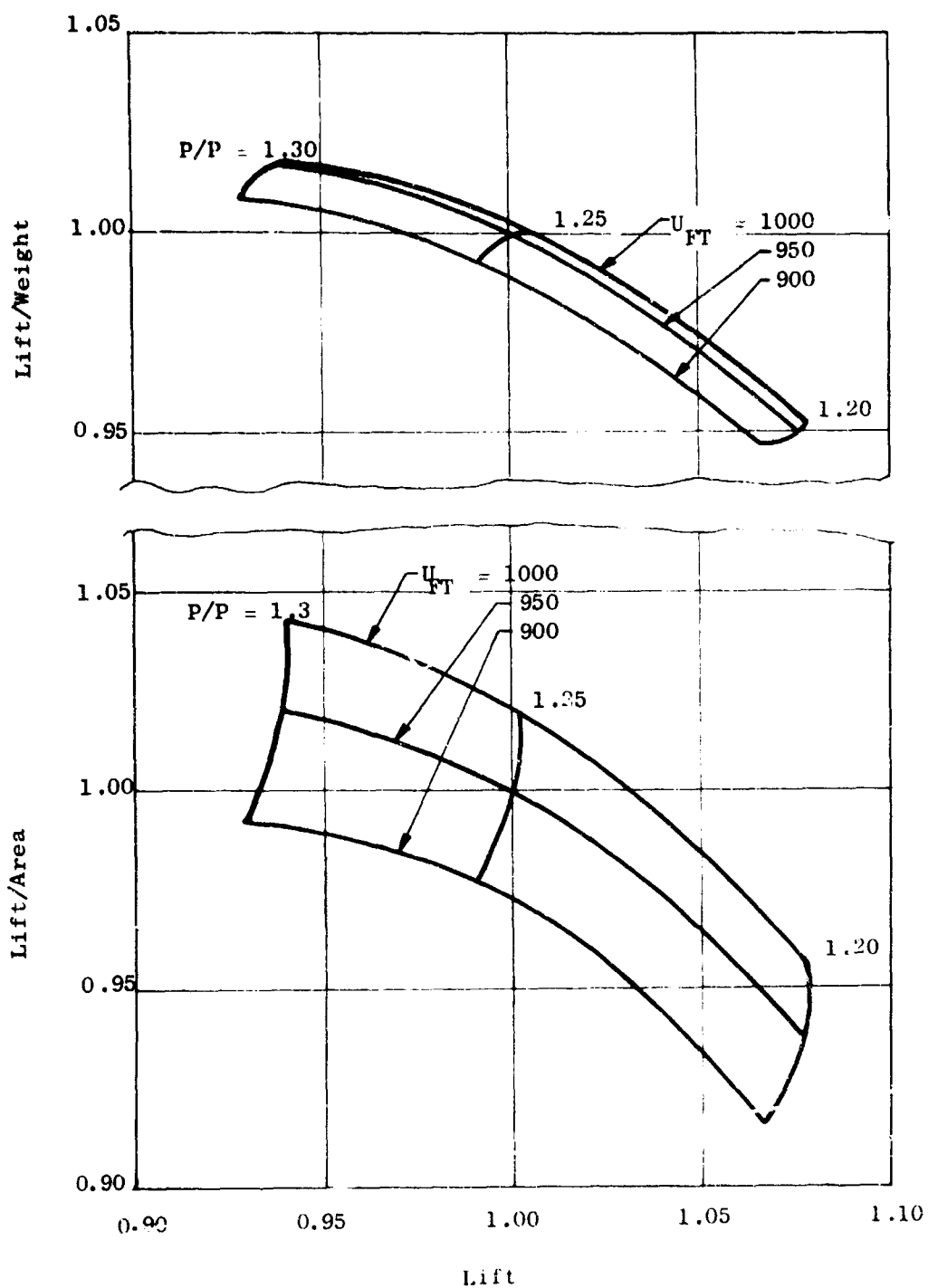


Figure 21. Lift, Weight and Area Ratio Cycle Variations.

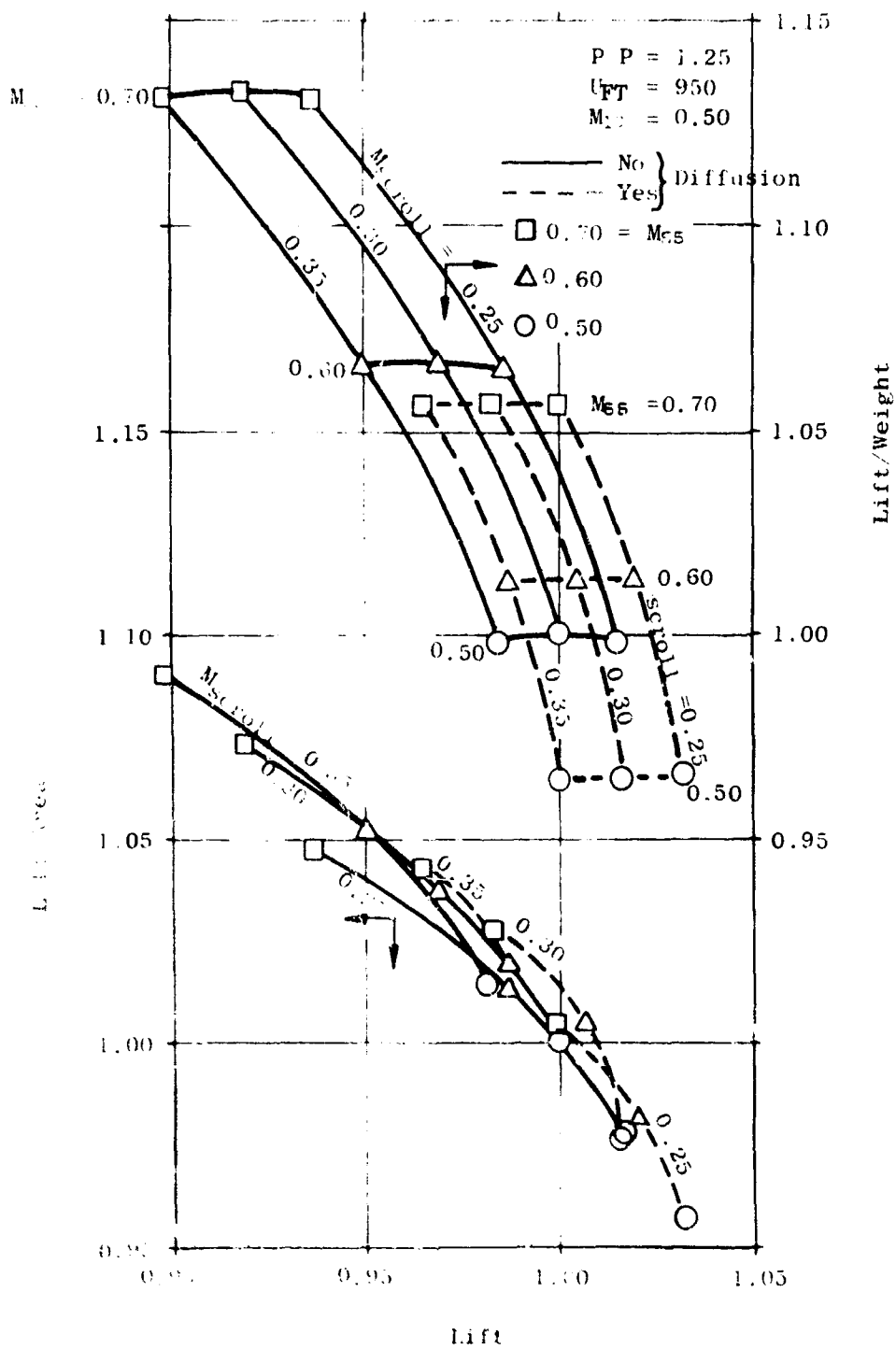


Figure 22. Lift, Weight and Area Ratio Cycle Variations.

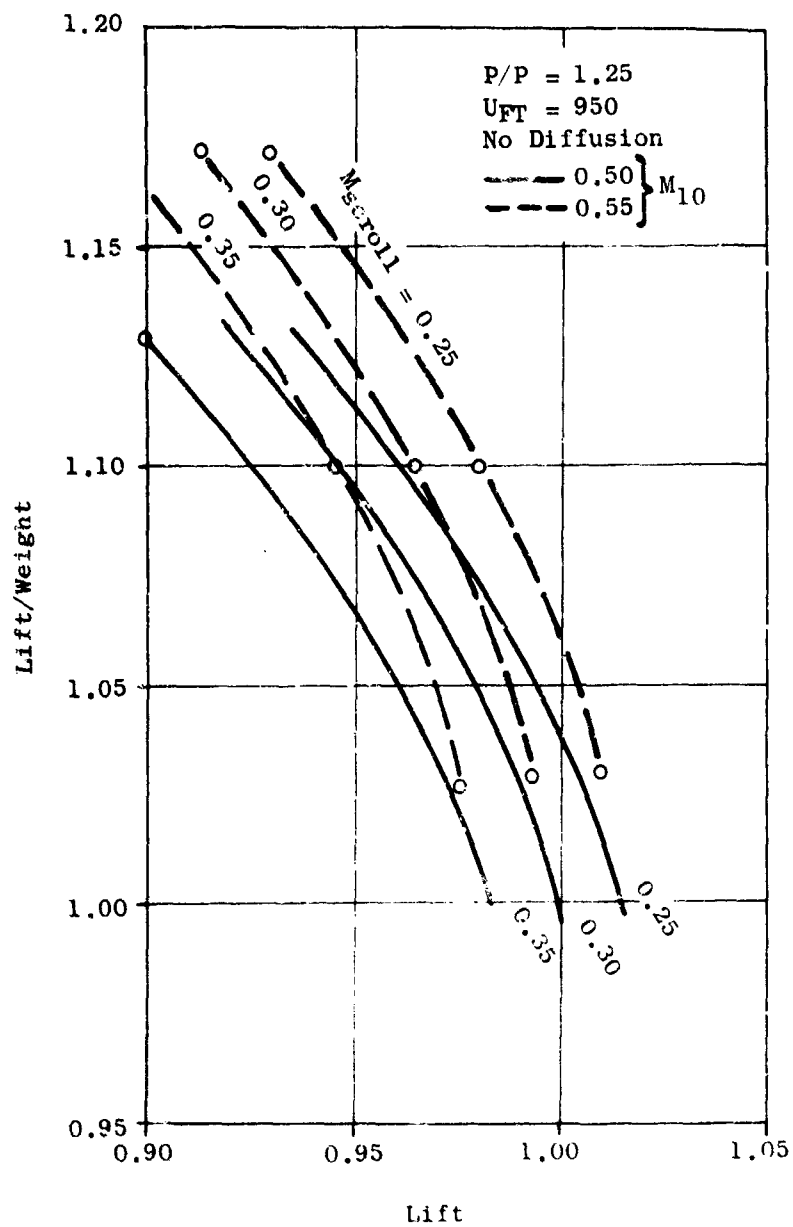


Figure 23. Lift to Weight Ratio Cycle Variation.

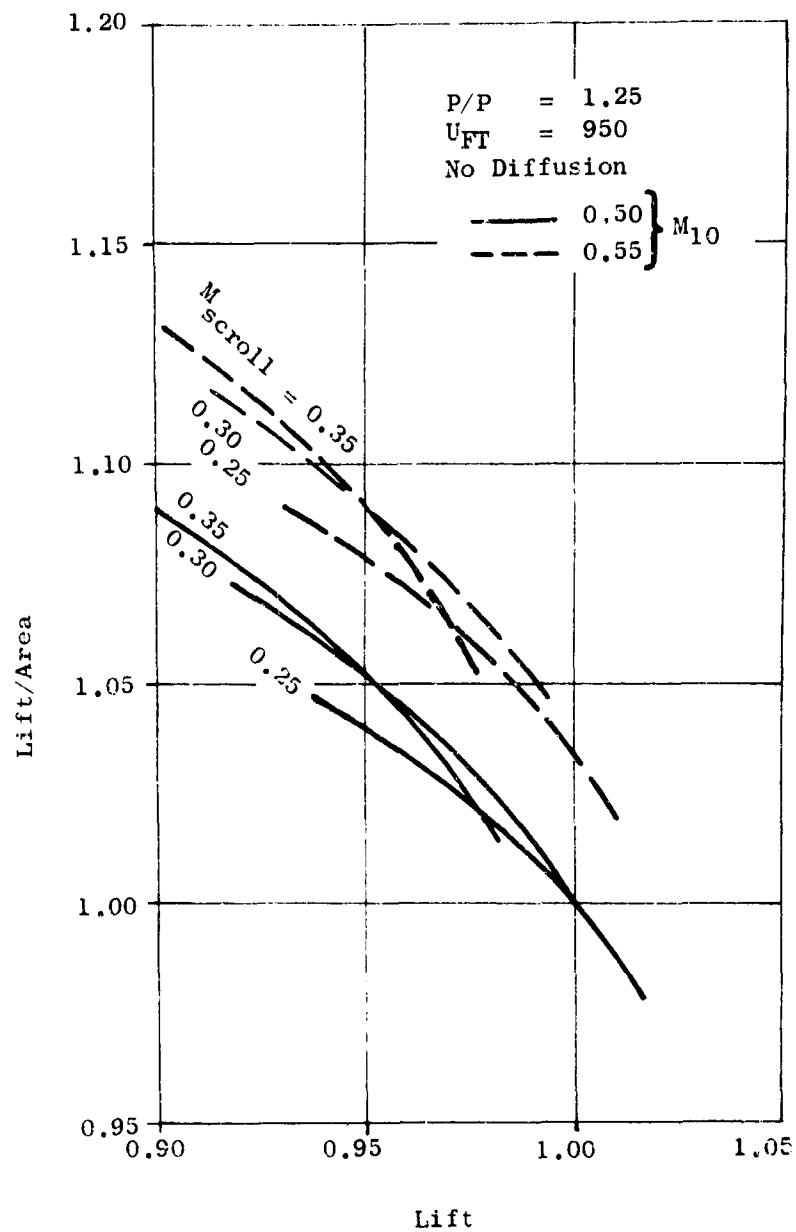


Figure 24. Lift to Area Ratio Cycle Variation.

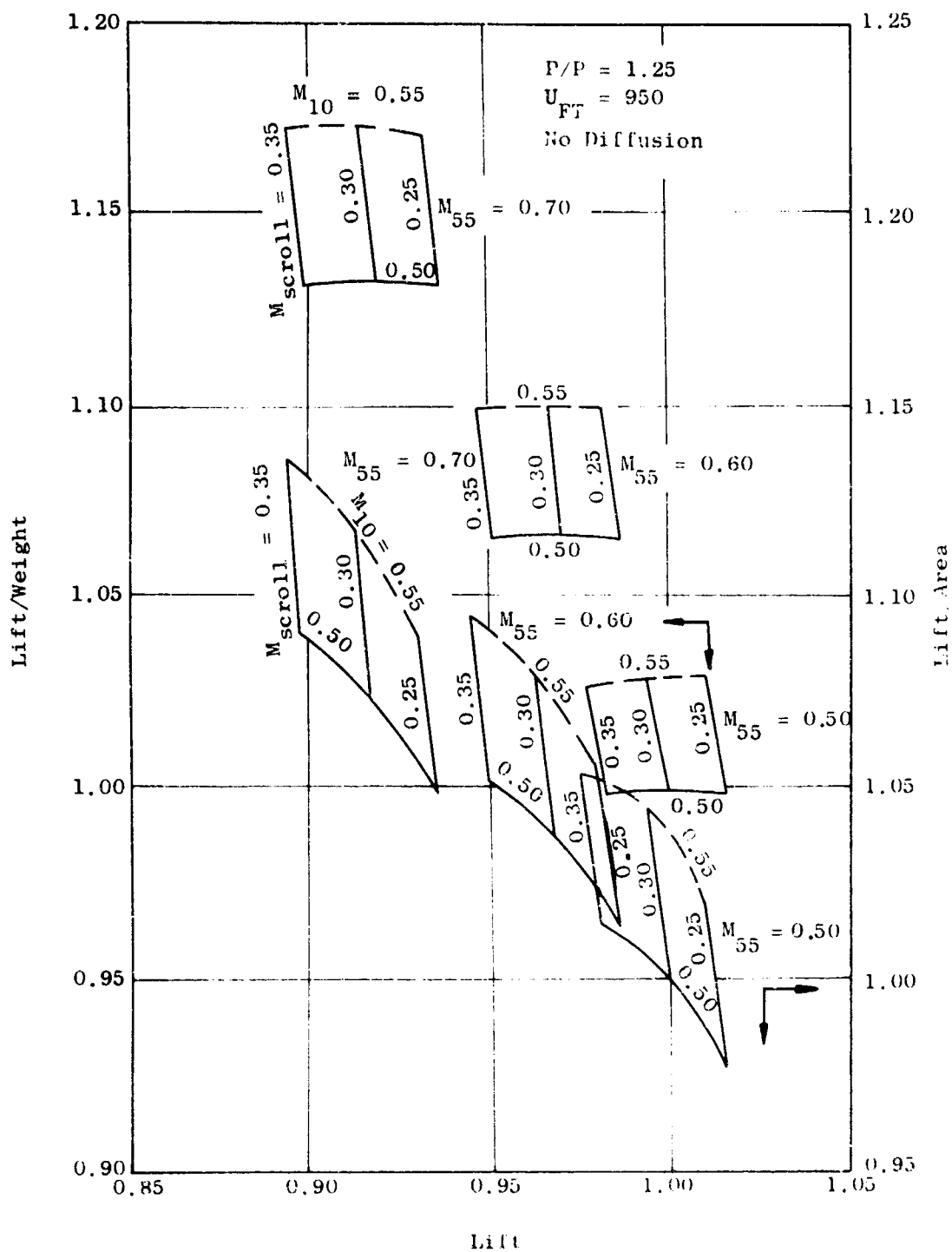


Figure 25. Lift, Weight and Area Ratio Cycle Variations.

Limitations on the Selection of Fan Cycle Parameters

The selection of a combination of design point values of cycle parameters must be based on

Level of technology to be demonstrated.

Amount of power transfer and the power transfer performance requirements.

Required level of nominal lift.

Any other constraints such as size limitations, requirement to demonstrate high pressure ratio, etc.

Selection of the LFX Design Point

The LFX design point selection was made using these ground rules:

Advanced technology commensurate with a 1968 time period, with no large component development programs.

A power transfer capability of ± 35 percent of the nominal flow. (Based on estimated roll control requirements of a 20,000-pound class of aircraft carrying wing-mounted external stores and having landing gear outboard on the wings.)

A nominal lift level compatible with a 20,000-pound class of aircraft. (Based on mission analyses conducted in Phase I.)

A nominal fan pressure ratio of about 1.25. (Based on the mission analyses conducted in Phase I.)

A tip speed of 975 feet per second was chosen. This value was expected to maximize lift and lift/weight while increasing the lift/area. However, the detailed rotor mechanical design analysis which followed this optimization study showed that rotor weight was more sensitive to tip speed than the optimization study had predicted. The resulting rotor weight was 170 pounds, compared to an objective rotor weight of 141 pounds. Reduction of the fan tip speed from the selected value of 975 feet per second to about 900 feet per second is expected to yield the objective rotor weight.

Power Transfer Effects

During power transfer, the Mach numbers in the diverter valve, straight duct and scroll will remain constant, but the Mach numbers in the cross-over ducts and scroll entrance will change. For the 35-percent flow transfer capability used in this study, a system having a nominal Mach number

of 0.30 will incur an additional total pressure loss of 4 percent during maximum power transfer operation because of the increase in crossover duct Mach number. Larger losses will occur with higher values of nominal flow Mach number. The requirement of good performance during power transfer thus imposes a restriction on the choice of high values of the design point scroll Mach number. A value of 0.30 was chosen.

During power transfer, the fan inlet Mach number will change because of the change in tip speed and fan flow. If the nominal (design point) value of fan inlet Mach number is too high, the fan will choke during the maximum power transfer condition. A fan inlet Mach number of 0.60 is about 85 percent of the choked value, and is a reasonable upper limit. With 0.60 as a fan inlet Mach number in the maximum power transfer condition, the nominal value of fan inlet Mach number must not exceed approximately 0.54 for the 35-percent flow transfer capability used in this study. A value of 0.54 was chosen.

Turbine Diffusion

An increase in turbine discharge Mach number can only be achieved by advancements in turbine material and fabrication technologies and by advancements in tip turbine carrier technology. A decrease in bucket length requires a decrease in bucket chord to hold aspect ratio (ratio of length to chord) to a reasonable value. Otherwise, the turbine efficiency, which is a function of aspect ratio, will be decreased and the potential gains in lift/weight and lift/area will not be realized. Further, a small bucket chord requires very sharp leading edges, since the ratio of leading edge thickness to bucket chord must be about 1 percent to avoid inlet blockage, in order to pass the desired flow. The tip turbine technology, then, must be such that small-chord buckets having extremely thin leading edges can be built, such that these leading edges will not erode away due to thermal gradients existing in the bucket, and such that these small buckets can be attached to the carrier. Present carrier technology requires that the bucket chord be long enough for the carrier side-rails to grip the bucket. Carrier side-rail separation is dictated by the tip tang thickness. Thus, the minimum bucket chord is also dictated by the carrier geometry. Increasing the number of tangs (blades) is not the solution because, unless blade weight penalties are accepted, the increased number of blades would require a midspan shroud - again, a new item in lift fan technology. The maximum value of turbine discharge Mach number which can be achieved without these technology advancements is approximately 0.50. A value of 0.50 was selected.

There is a risk incurred by the addition of turbine diffusion - if the diffuser does not work as planned, there will be a "dump loss" of lift equal to 2 percent of the nominal lift at a turbine discharge Mach number of 0.50 to as high as 6 percent of the nominal lift at a turbine discharge Mach number of 0.70. The turbine exhaust has swirl, which makes the design of an efficient diffuser more difficult. Further, any thermal growth of the rotor buckets with respect to the turbine stators could

cause misalignment of the flow path and easily upset the flow and make the diffuser ineffective. Turbine exhaust diffusion has never been demonstrated on tip turbine fans. A development program is required to obtain test data necessary to verify the effectiveness of the diffuser. Further still, to realize the potential gains of turbine diffusion, it is necessary to increase the turbine discharge Mach number, which the previous paragraph declared to be outside the LFX ground rules. The LFX design, then, does not use turbine diffusion.

The selected LFX fan pressure ratio was 1.245, which meets the desire for high pressure ratio and the requirement for nominal lift.

Summary

The following table compares the selected LFX design point to the original design point used in Phase I:

	<u>Phase I</u> <u>Design Point</u>	<u>New</u> <u>Design Point</u>
Fan pressure ratio	1.25	1.245
Fan tip speed, ft/sec	946	975
Scroll Mach number	0.25	0.30
Fan inlet Mach number	0.52	0.54
Turbine discharge Mach number	0.50	0.50
Total fan nominal lift, lb	10,800	10,750
Fan planform area, in ²	5223	4912
Flow transfer capability, percent of nominal flow	±23	±35
Nominal arc of admission	280	250
Fan tip diameter, in.	56.2	54.9
Turbine tip diameter, in.	63.1	61.8

Comparing the two design points, it is noted that even though the amount of power transfer has been increased, the fan diameter was decreased 2 percent and the fan area was decreased 6 percent. All of the 0.46-percent lift decrease is due to the refinement in the performance calculations to account for the scroll leakage flow through the inactive arc during nominal operation.

AERODYNAMIC PRELIMINARY DESIGN

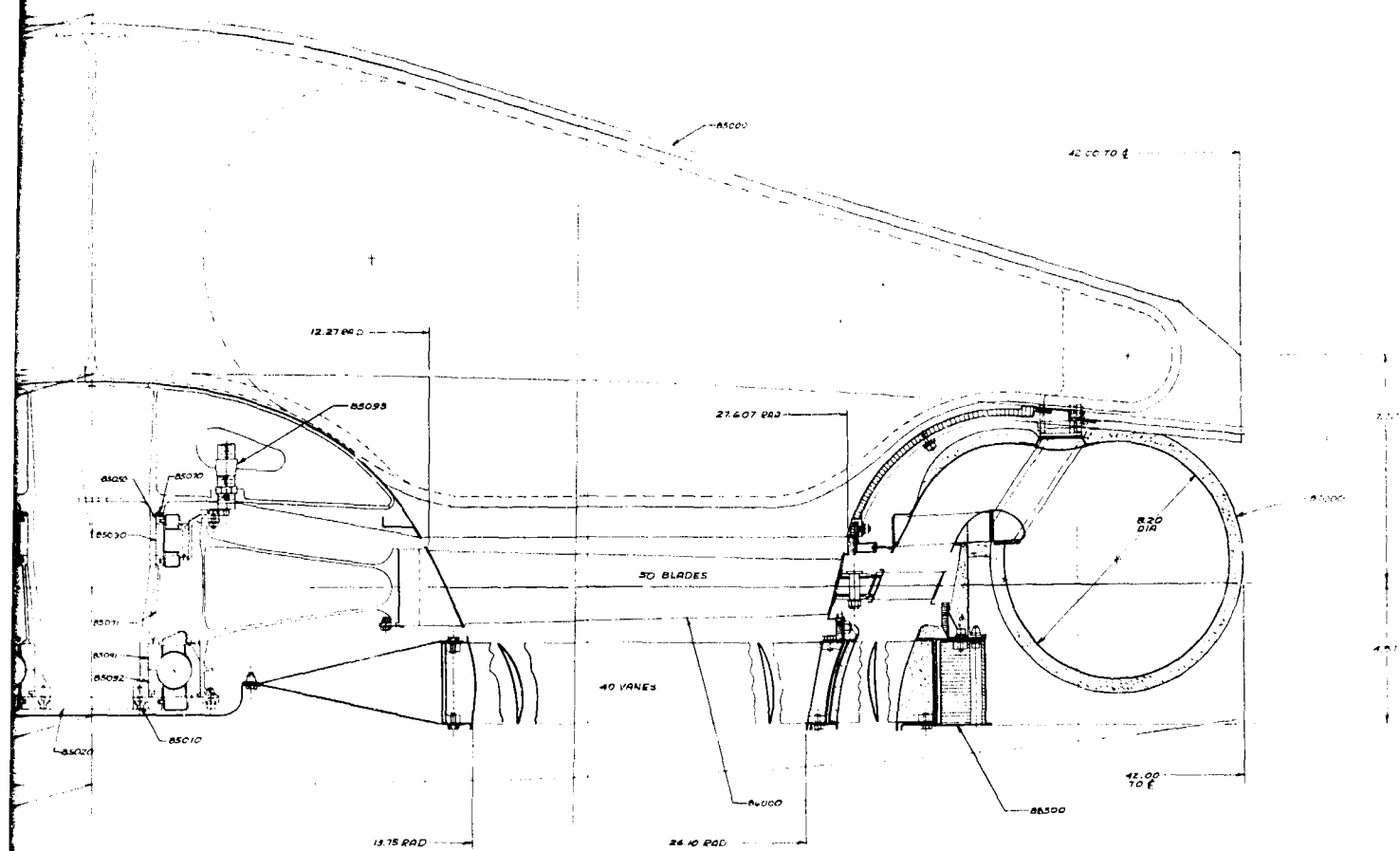
The LFX conceptual aerodynamic design for the compressor and turbine was completed during the initial phase of the LFX studies. The results of the initial studies are documented in an Army report (Reference 1). During the continuation of the LFX studies, a parametric optimization of fan aerodynamic-mechanical characteristics was completed to identify potential improvements in fan installed wetted area and lift to weight ratio. Additionally, results of airframe/propulsion studies were summarized and included in the design objectives for fan preliminary mechanical design. Following completion of the fan preliminary mechanical design, the compressor and turbine aerodynamic design were reexamined using the mechanical design represented in the LFX-6 preliminary assembly, Figures 26, 27 and 28.

Changes from the original conceptual aerodynamic design, although of minor nature, were sufficient to warrant documentation of the revised aerodynamic design. In addition, a brief study of the effect of cross-flow velocity on the fan characteristics was performed to aid in identification of possible problem areas.

COMPRESSOR AERODYNAMIC DESIGN

The fan is a single stage composed of a rotor and stator. The flow path was optimized to achieve a compact, lightweight lift fan assembly. Good performance in the tip region and cross-flow distortion resistance are features of the design. The important aerodynamic design parameters of the fan are presented below, together with a comparison of other fan stage designs. The predicted fan map is shown in Figure 29.

	<u>X353-5</u>	<u>80"</u>	<u>LFX-3</u>	<u>LFX-6</u>
Stage nominal pressure ratio	1.115	1.313	1.253	1.245
Stage efficiency (no leakage), percent	88	87	88	86
Corrected tip speed, feet per second	720	969	946	975
Corrected flow, pounds per second	529	1,074	492	503
Tip diameter, inches	62.5	80.0	56.2	54.8
Hub-tip radius ratio	0.40	0.48	0.477	0.445
Aspect ratio	5.85	4.2	5.8	5.2
Inlet average Mach number	0.400	0.600	0.520	0.575
Rotor solidity - tip	0.580	0.900	0.740	0.950
- hub	1.430	1.500	1.540	1.890
Stator solidity - tip	0.700	0.900	0.700	0.700
- hub	1.750	1.540	1.240	1.320



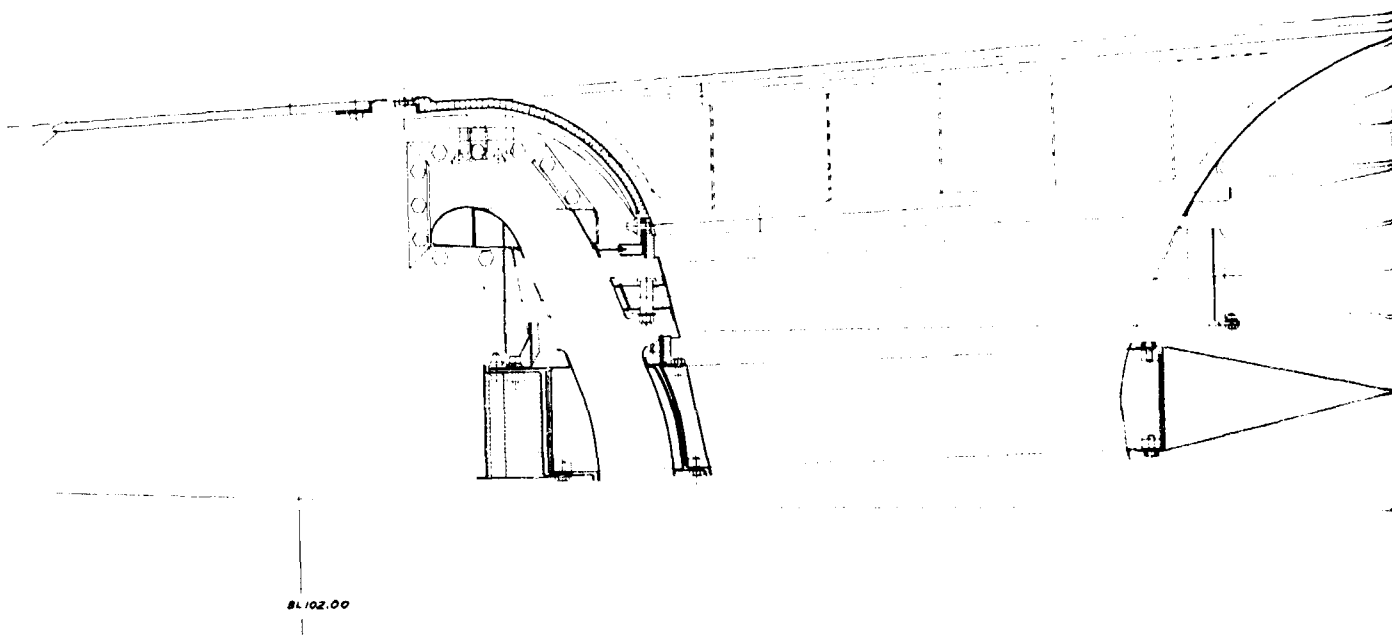
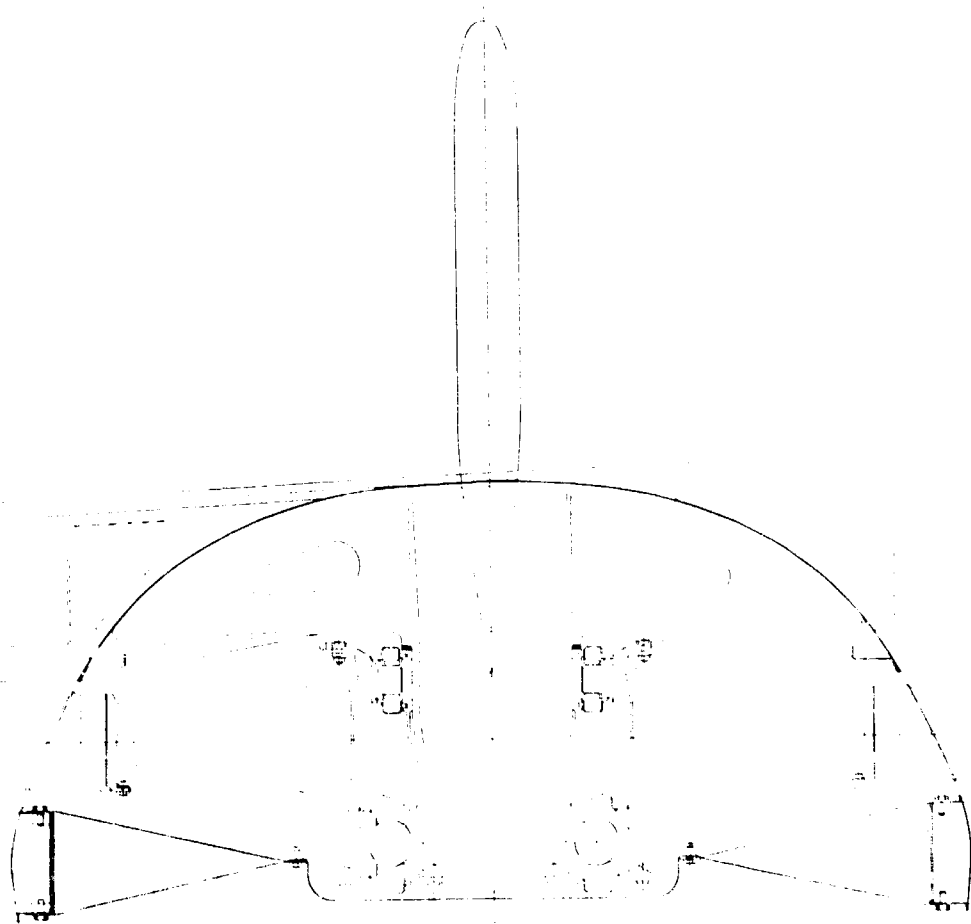


Figure 27. LFX-6 Fan Assembly - Spanwise Section.



00470

Section.

19

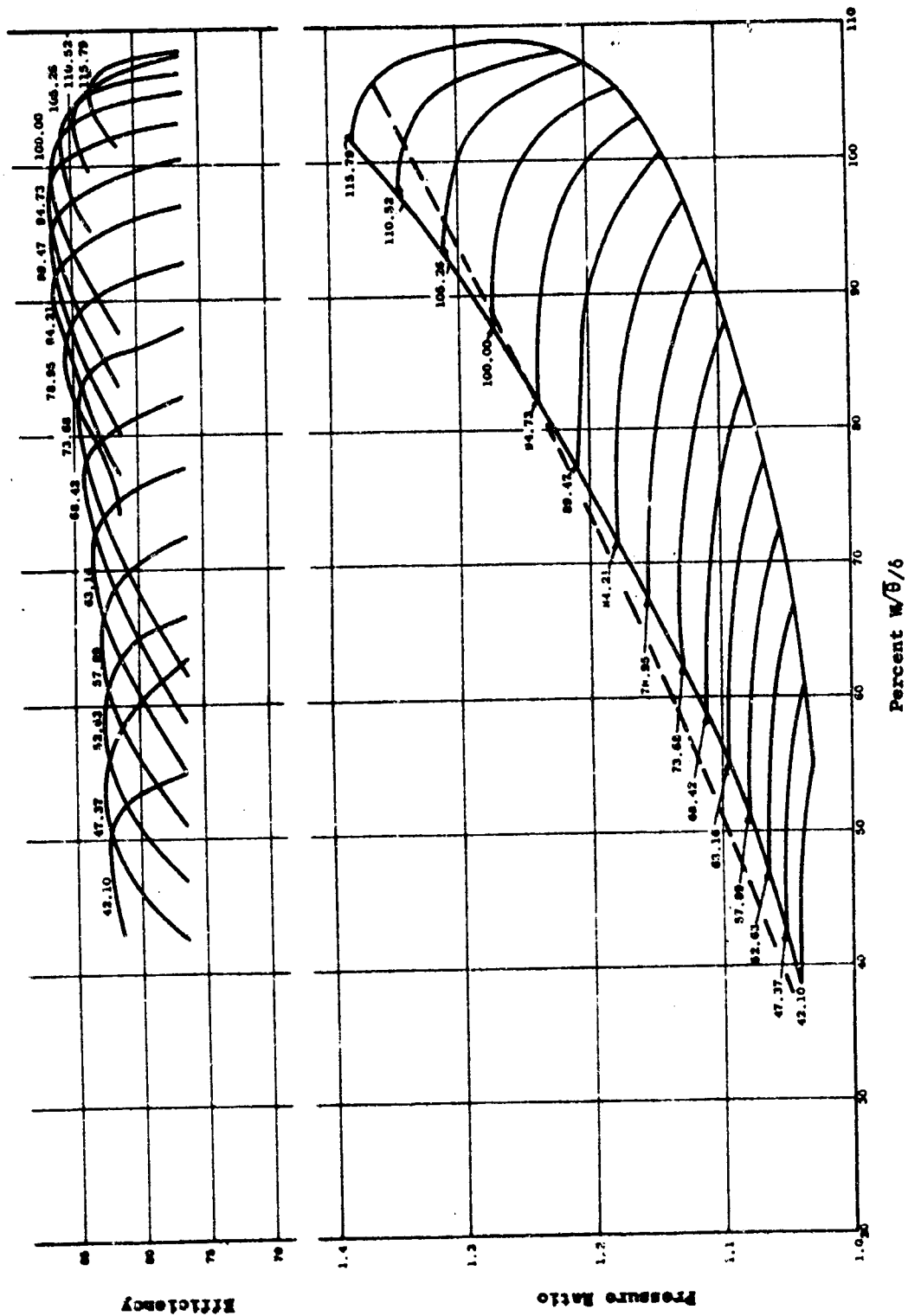


Figure 29. Predicted Compressor Map.

Annulus

The LFX annulus (Figure 30) is sized for an average meridional Mach number of 0.575 at the rotor inlet when passing the design flow, 503 pounds per second. At this level the rotor will not be subject to high Mach number losses, nor will choking be a problem. The inlet (bellmouth) lip ends with a 14-degree slope toward the hub at the rotor. The remainder of the turning toward the axial direction is accomplished in the stator region. The annulus at the rotor hub is sloped toward the tip at an angle of 28.5 degrees to 27.8 degrees. The flow path described offers two distinct advantages. First, the 14-degree shroud slope at the rotor will combat the diffusion normally occurring in stream tubes negotiating a 90-degree turn about a low radius lip. The slope reduces the amount of turning required and increases the effective lip radius. Thus, local diffusion in static operation is reduced and the probability of separation in crossflow is reduced. Furthermore, the sloped walls serve to reduce the loading of the rotor, thus providing a desirable stall margin.

By doing the remainder of the turning toward the axial direction (in the meridional sense) downstream of the rotor, the flow which has been energized will follow the shroud contour more faithfully than if this turning were attempted in front of the rotor.

Blading

The total pressure rise distribution is quite flat radially (Figure 31) except at the hub and tip regions. At the hub the pressure rise is limited to avoid the necessity of turning the air past the axial direction in the circumferential sense.

Turning beyond the axial direction at the design point would lead to blading which would unload when throttled by the vectored louvers. The relatively small pressure rise designed into the tip will enable blading to be generated which will tolerate the range of inlet incidence conditions expected in static and cross-flow operation. The rotor loading distribution described in terms of diffusion factor and static pressure rise coefficient (Figure 32) is suited to the requirements of a lift fan. Throughout the tip region where the possibility of stall is greatest the diffusion factor is held below 0.36 and the static pressure rise coefficient is about 0.28. The region that extends from about the pitch to the hub is, as verified by lift fan test results, quite resistant to stall in vectored crossflow as well as in static operation. As a consequence of this experience the higher loading in this region appears attainable. The highest design diffusion factor at this point is 0.42, while the static pressure rise coefficient is 0.375.

The rotor inlet relative Mach numbers are within the range in which double circular arc blading will be suitable. The incidence angles chosen at plus 4 degrees will provide minimum loss and will also be of

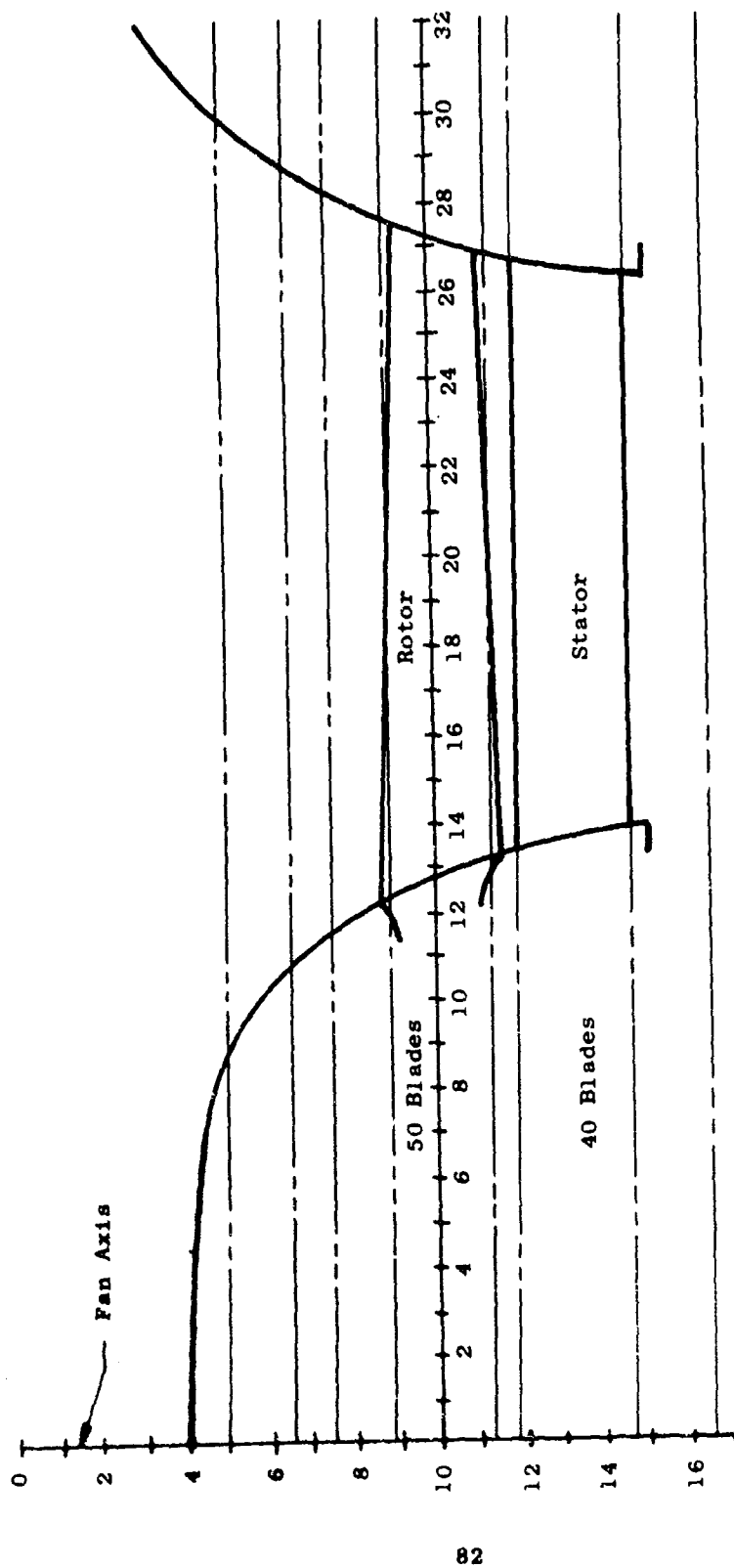


Figure 30. LFX Annulus.

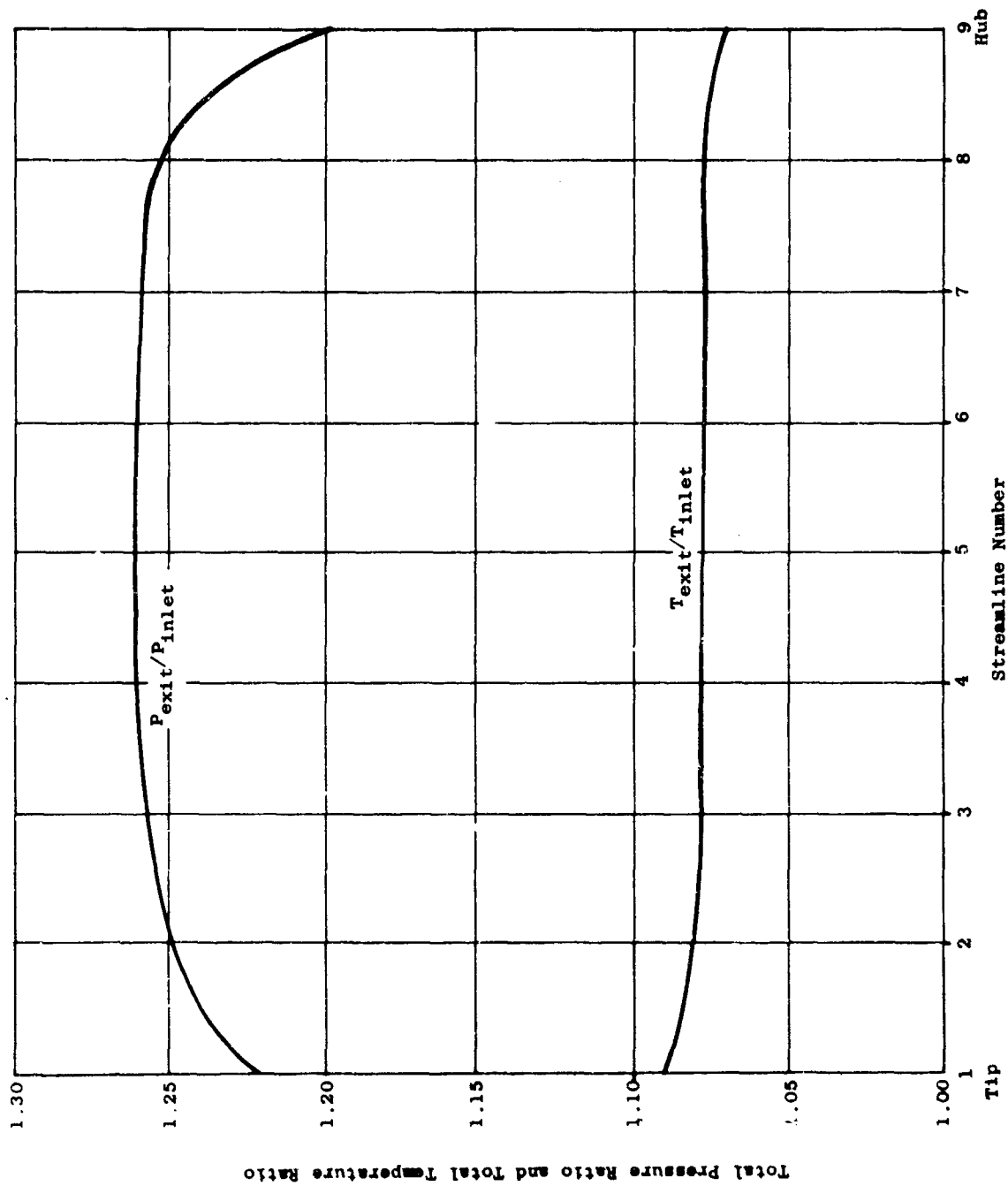


Figure 31. Total Pressure Rise Distribution.

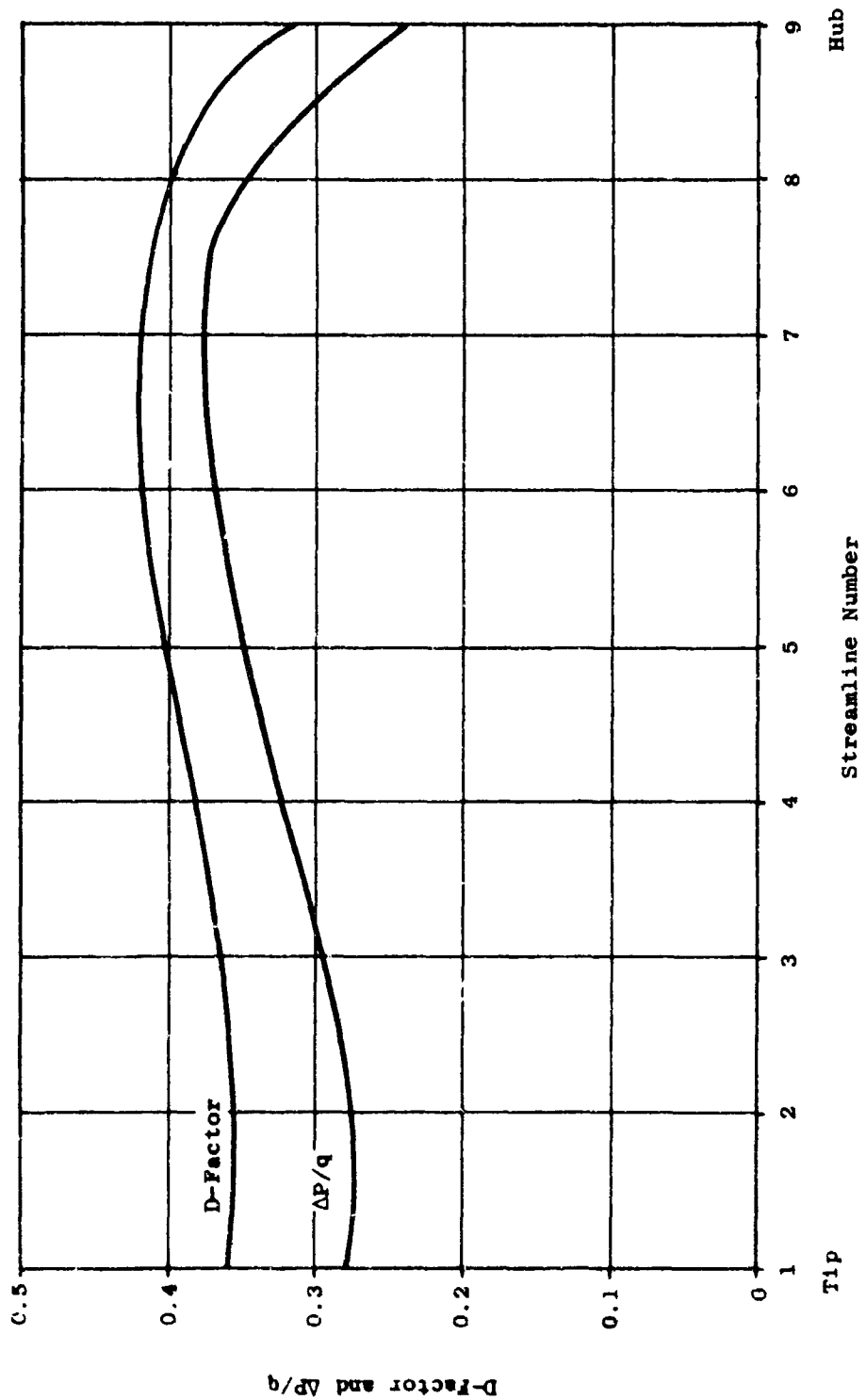


Figure 32. Rotor Loading Distribution.

value in avoiding choking, especially at the hub where the stream surface solidity is quite high. The deviation angles (Figure 33) were determined from a Carters' rule calculation with modification for radial shift and axial velocity change. Stator inlet Mach numbers (Figure 34) are not excessively high and both loading parameters are within a tolerable range. Airfoils of 65 series thickness distributions on circular arc mean lines were chosen because the positions of their maximum thicknesses would be well ahead of the throat regions where thickness might contribute to choking. Minimum loss considerations lead to the incidence angles chosen. The total pressure loss coefficients (Figure 35) are based upon measured performance reported in References 6 and 7. These figures were modified to reflect state-of-the-art difficulty in describing lift fan inlet flow. Resolution of this difficulty might result in loss coefficients approaching the dashed curves of Figure 35. Figures 39 through 44 describe other compressor aerodynamic characteristics.

Cross-Flow Performance Prediction

The effect of cross-flow velocities on fan performance and on the required computational techniques to establish design characteristics was the subject of a study performed in advancement of lift fan technology (Reference 9).

Using the calculation methods described in the reference, the LFX performance in a 135-knot cross flow was evaluated. Four sections, as shown in Figure 36, were used for the study.

At Section B, stall is indicated at the rotor tip. The incidence angles in this region were excessively high, as a result of crossflow. This problem is illustrated in Figure 37, in terms of a comparison of the design rotor inlet air angles and the computed rotor inlet air angles under cross-flow conditions. Two radial equilibrium calculations were performed at Section B. The first, A, established the presence of high incidence angles leading to the tip stall. A second calculation, B, was required in which the stalled tip was unloaded, enabling computation of the performance in the unstalled region (Figure 38). Section H, Figure 38, reflects the detrimental effects of the shadow. The computation indicates that a complete elimination of the lip separation would permit acceptable performance over the entire blade height. The X353-5 study has shown that the primary detriment of this tip stall is its lasting effects. Further effects of the tip stall are seen at Section F.

Design Technique Improvement

The state of the art of lift fan aerodynamic design technique will take two important steps forward as a result of currently programmed improvements. The timing of these improved techniques should make them available for use in the LFX detail aerodynamic design. The first of these

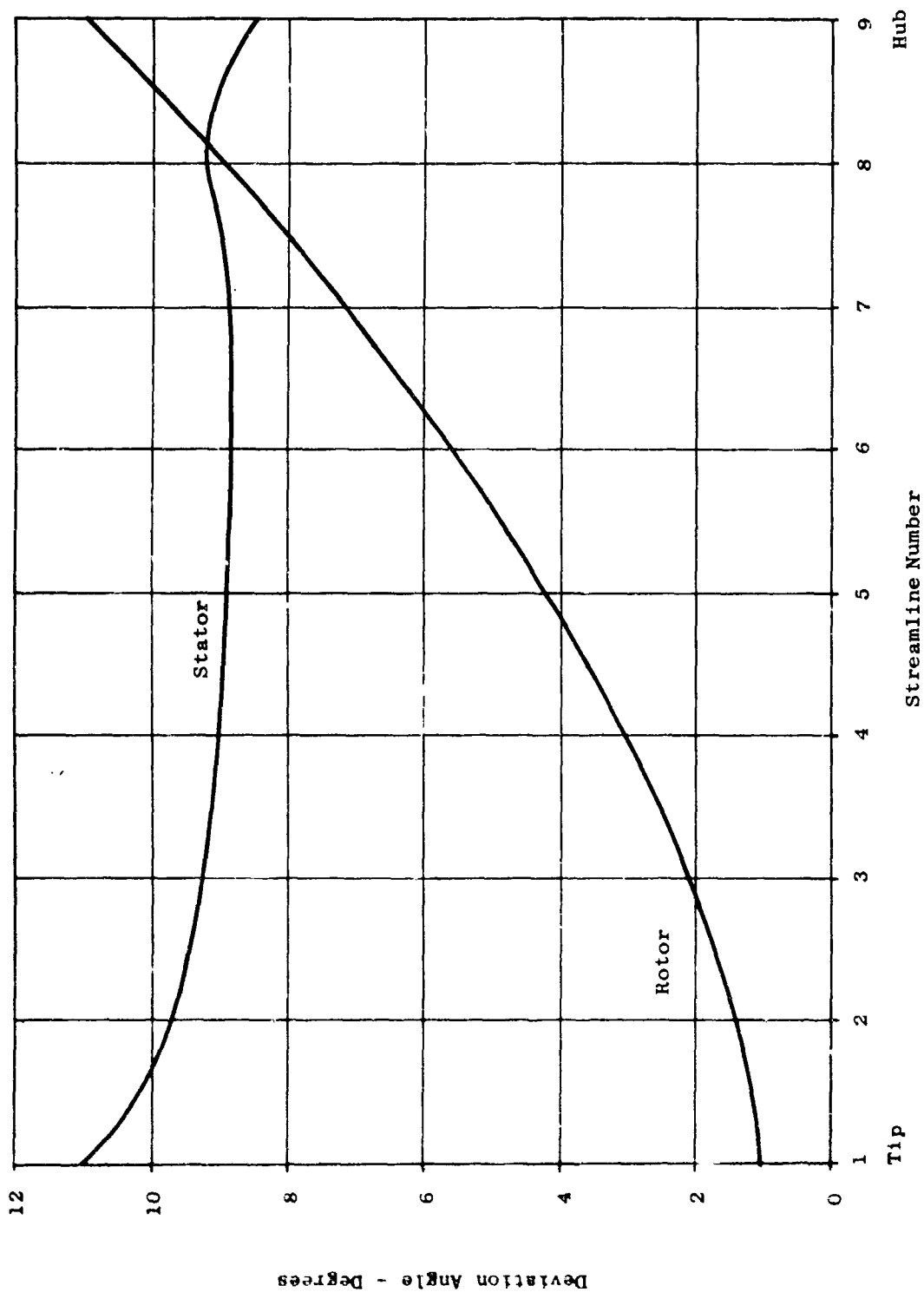


Figure 33. Deviation Angles.

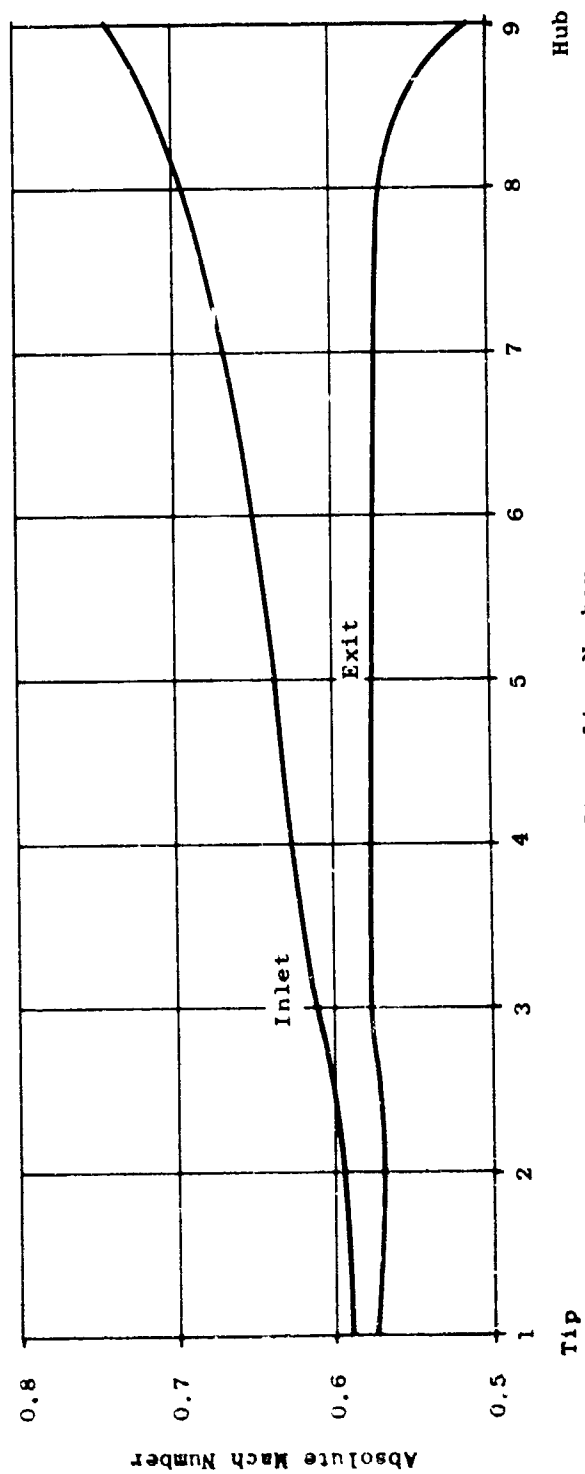


Figure 34. Stator Velocity Distribution.

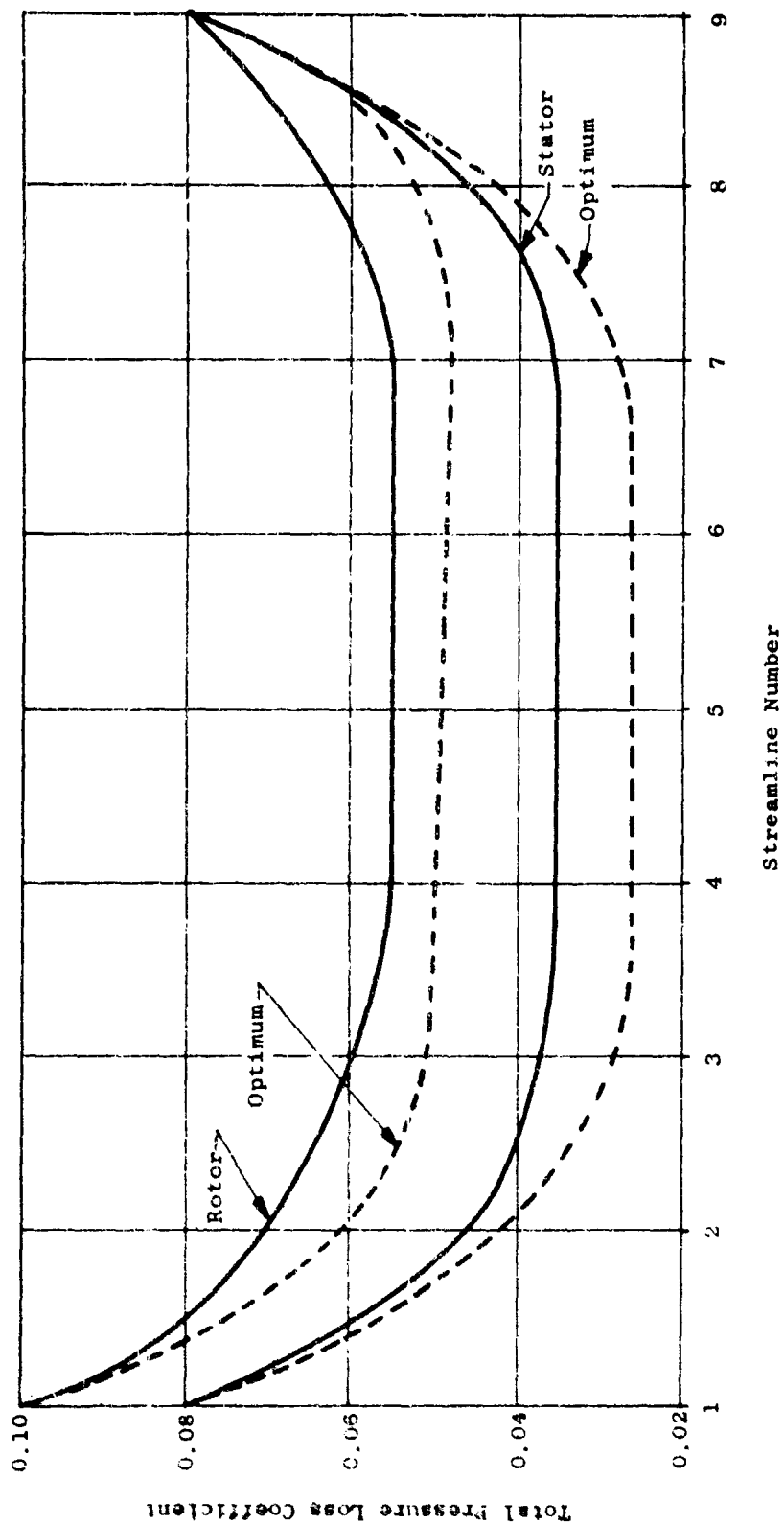


Figure 35. Total Pressure Loss Coefficient Distribution.

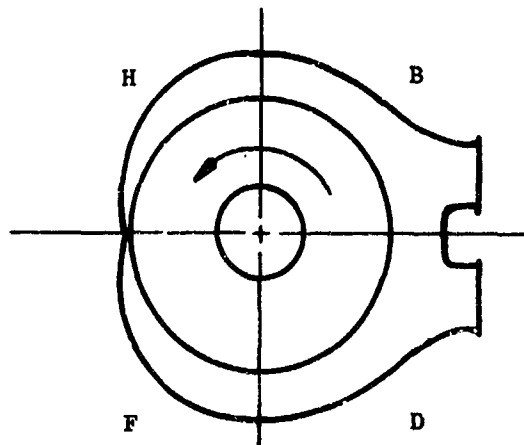


Figure 36. Schematic for Cross-Flow Performance.

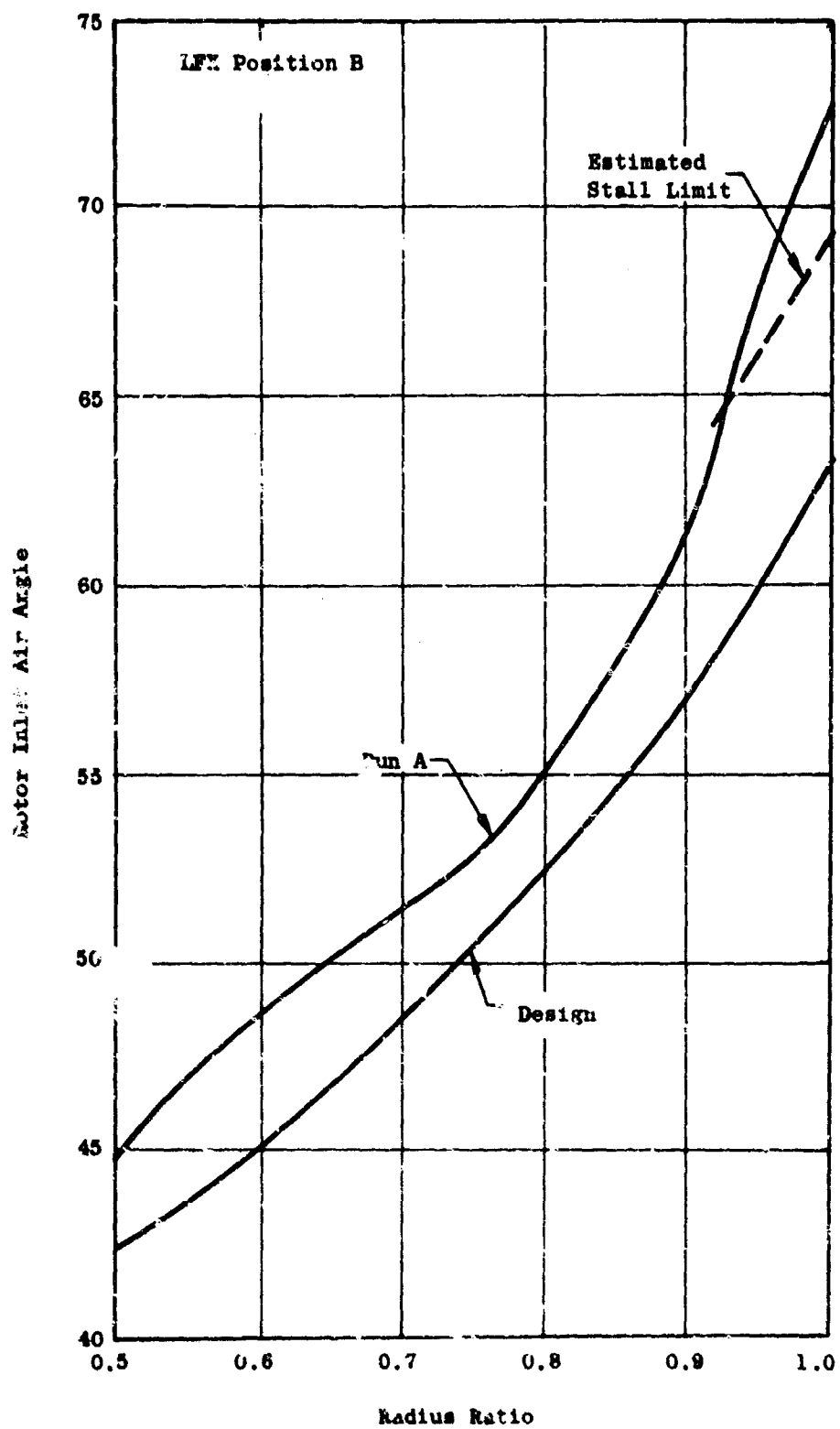


Figure 37. Rotor Inlet Air Angles - Cross-Flow.

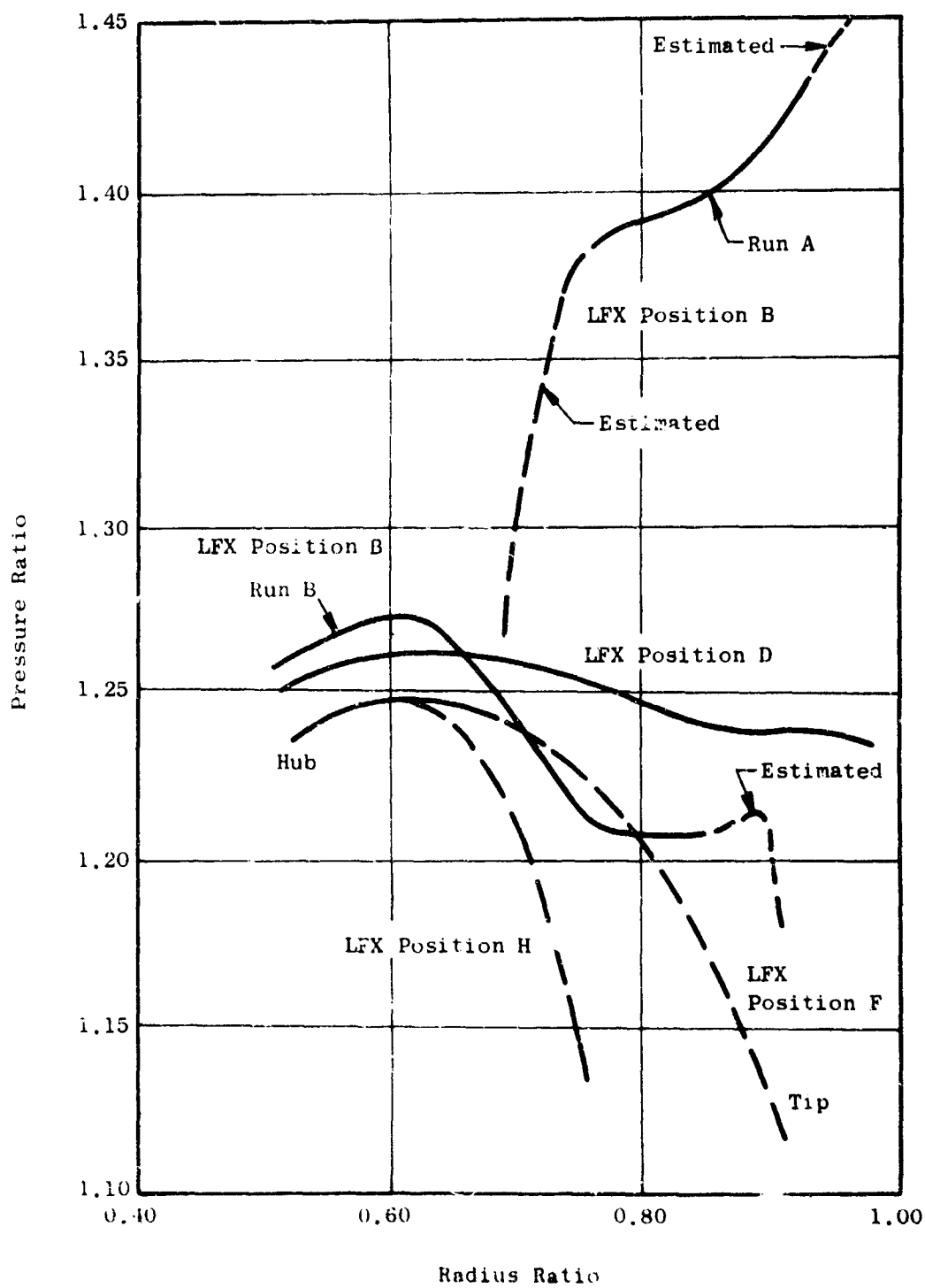


Figure 38. LFX Pressure Ratio Versus Radius Ratio.

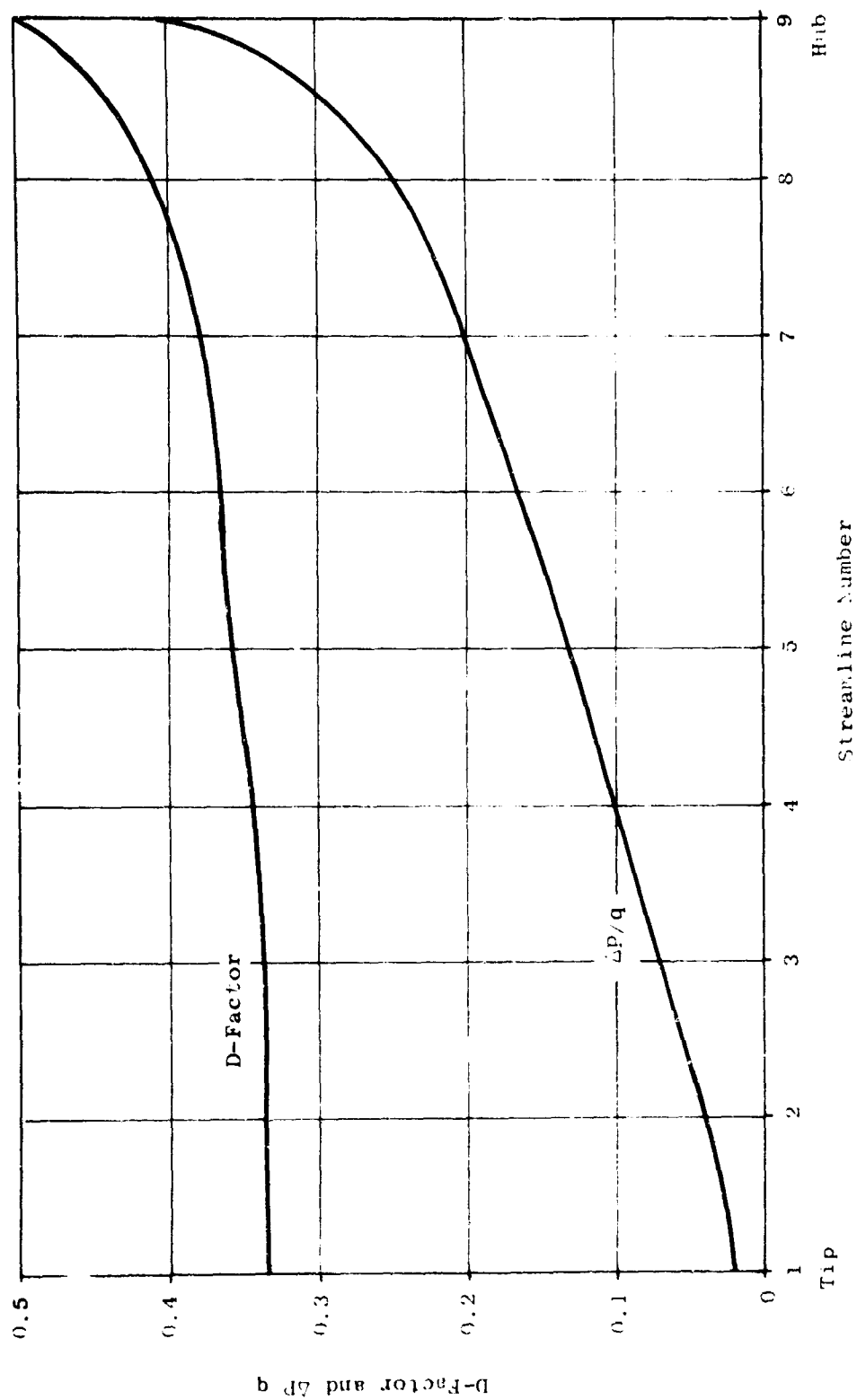
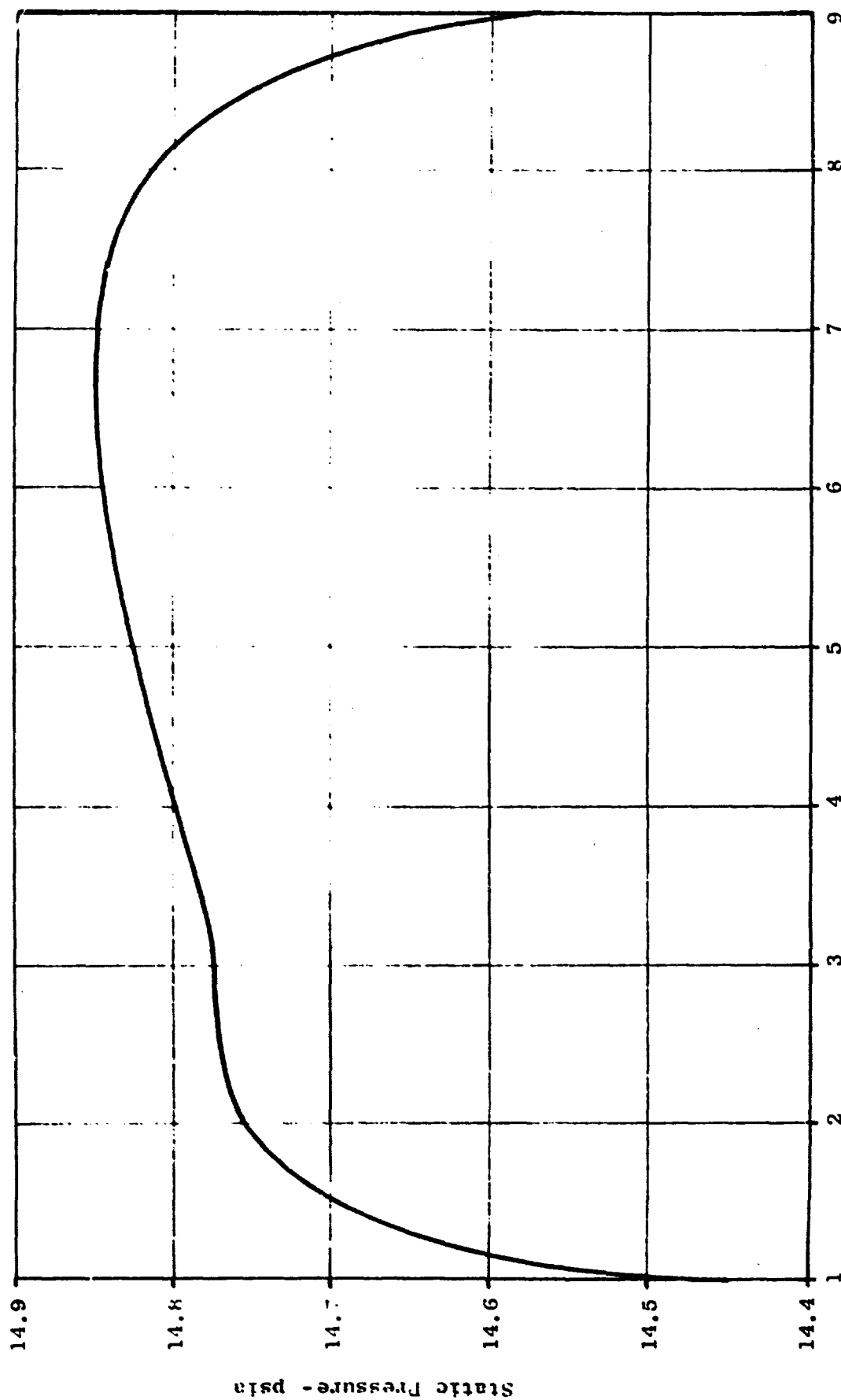


Figure 39. Diffusion Factor and Static Pressure Rise.



Streamline Number

Figure 40. Static Pressure Distribution.

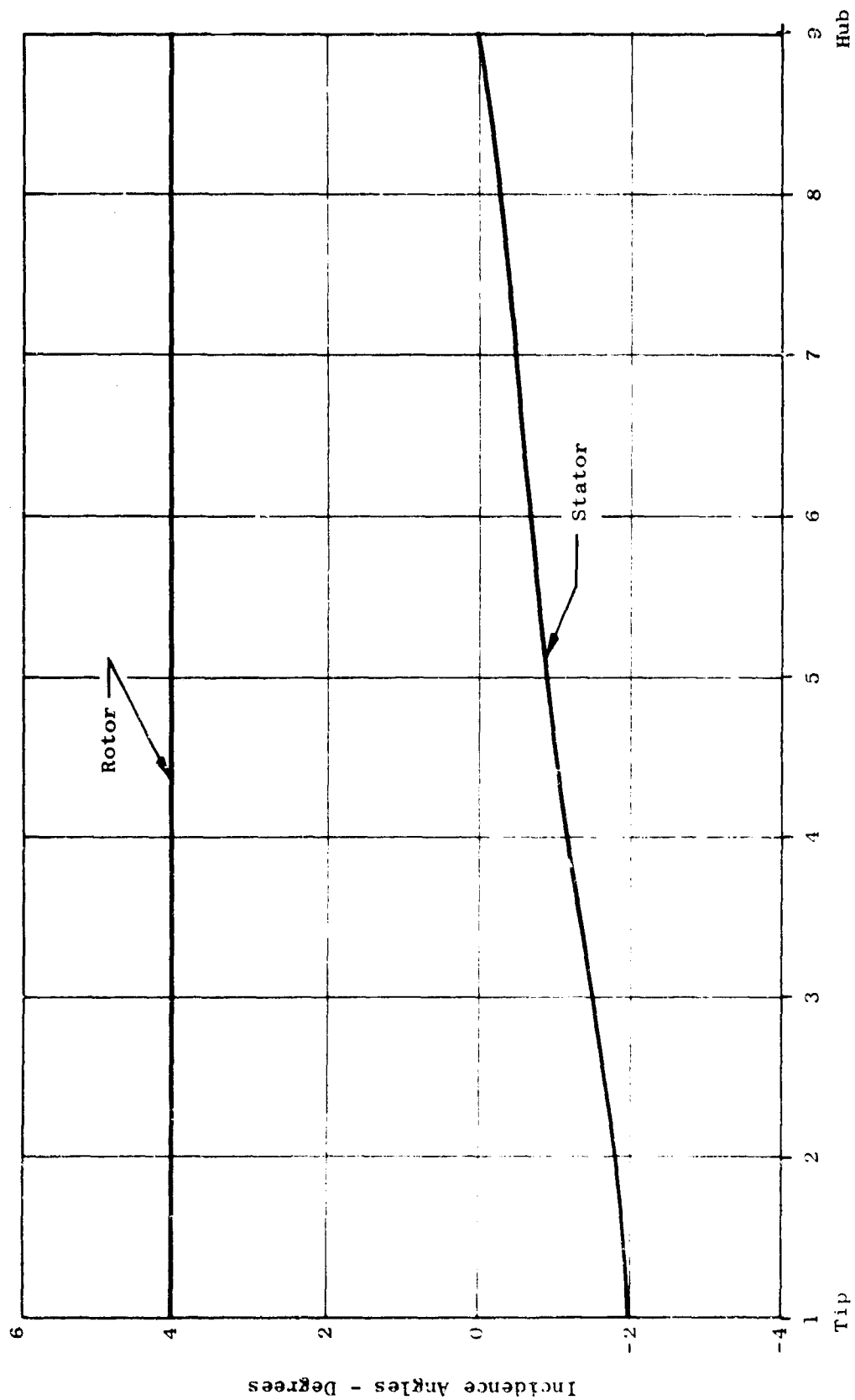


Figure 41. Incidence Angle Distribution.

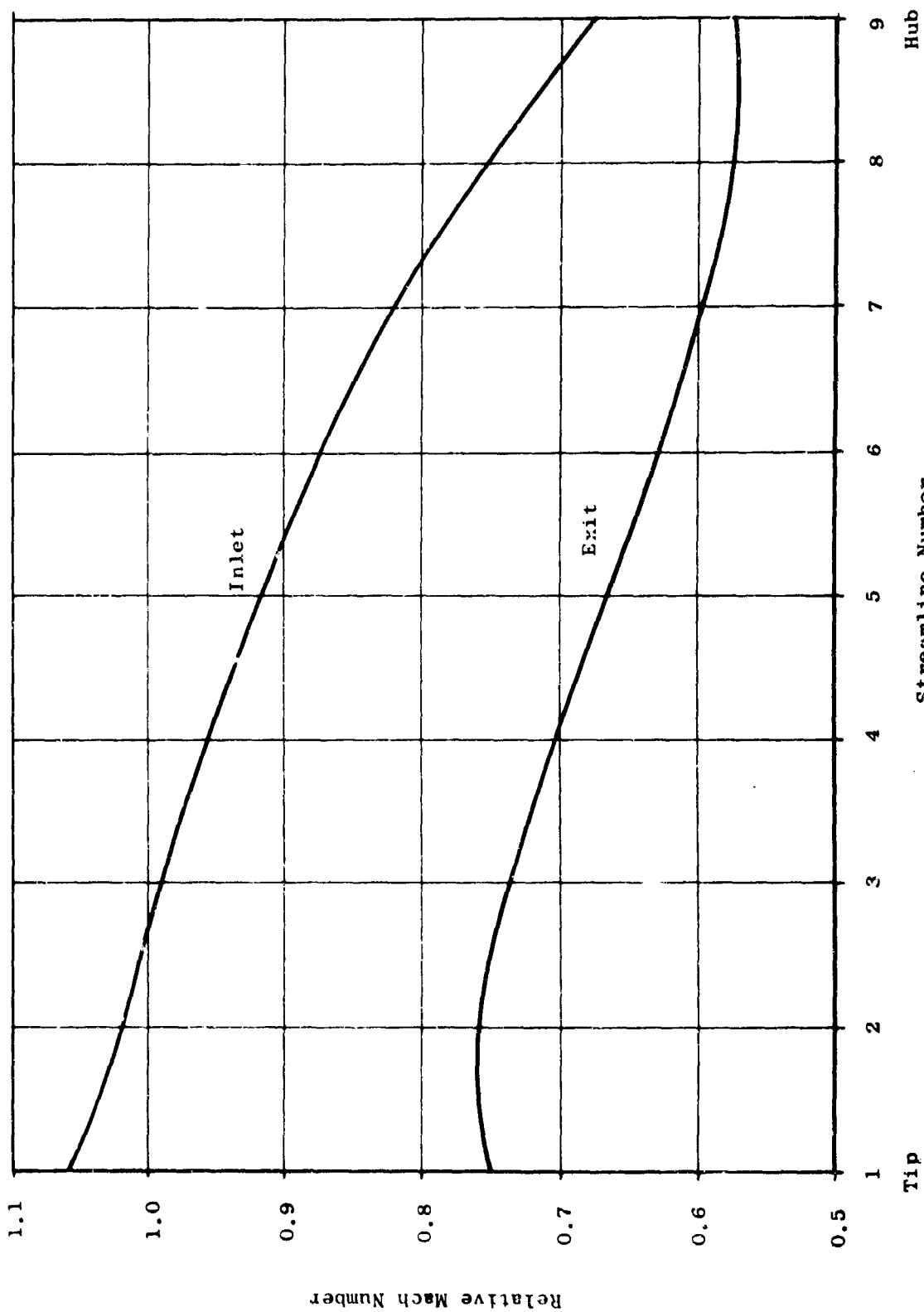


Figure 42. Relative Mach Number Distribution.

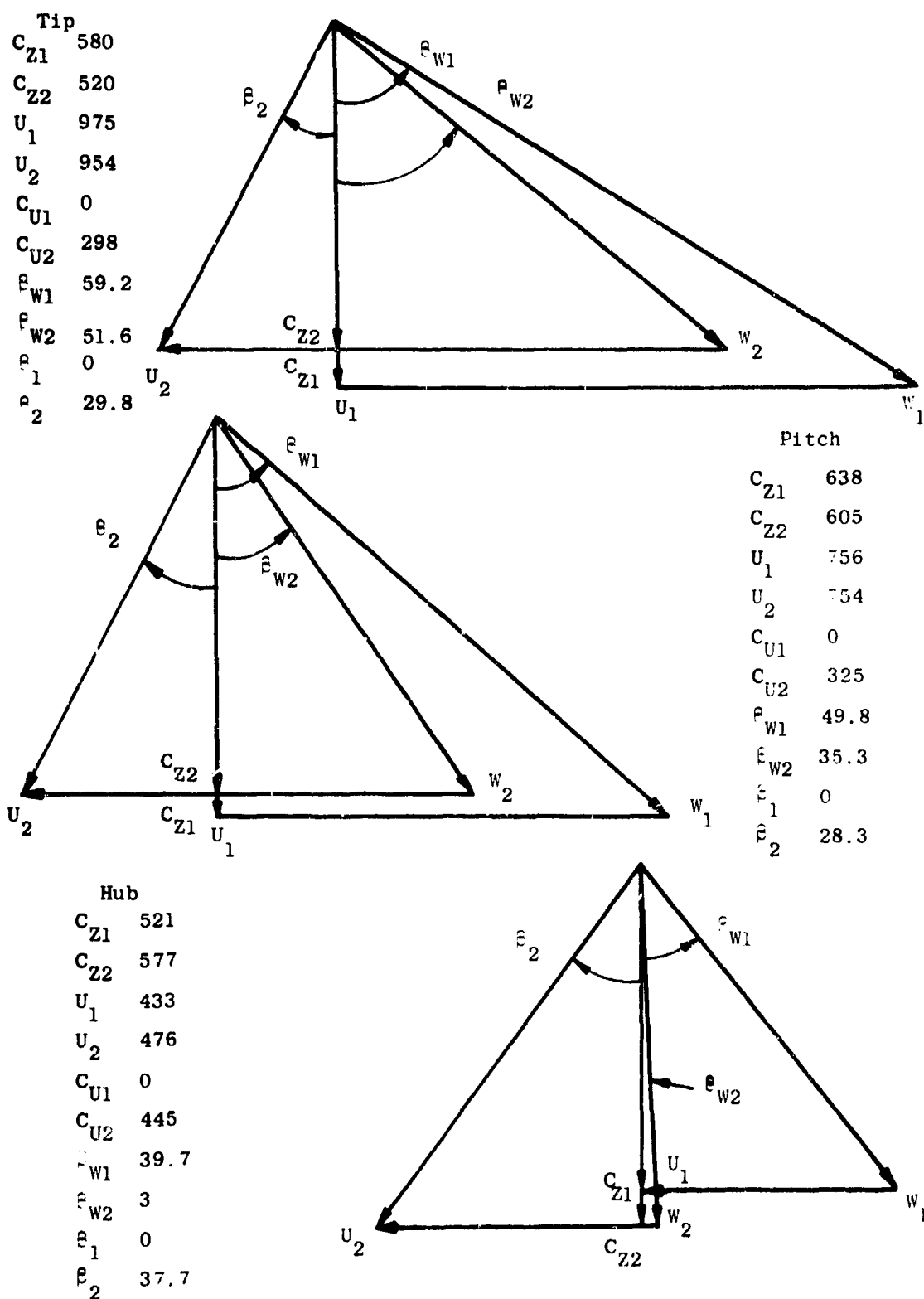
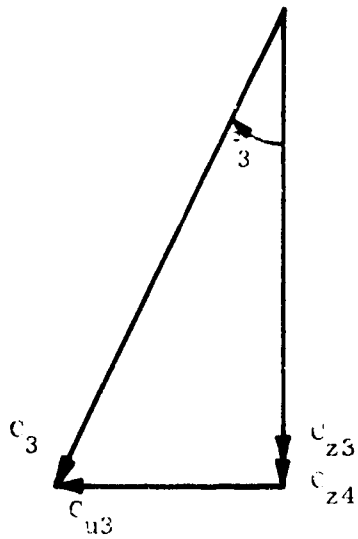
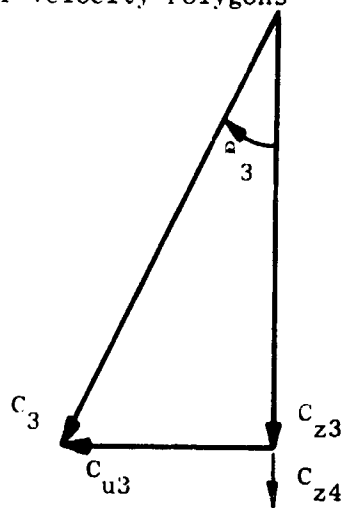


Figure 43. Rotor Velocity Diagram.

Stator Velocity Polygons

Tip	
C_{z3}	575
C_{z4}	647
C_{u3}	300
C_{u4}	0
C_3	564
C_4	647
β_3	27.5
β_4	0



Pitch

C_{z3}	629
C_{z4}	645
C_{u3}	326
C_{u4}	0
C_3	709
C_4	645
β_3	27.4
β_4	0

Hub	
C_{z3}	663
C_{z4}	573
C_{u3}	435
C_{u4}	0
C_3	815
C_4	573
β_3	33.2
β_4	0

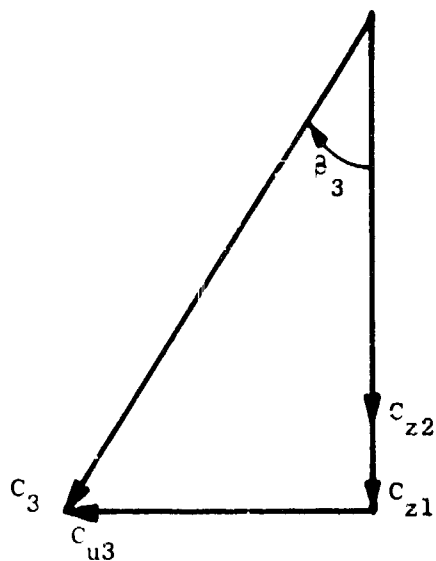


Figure 44. Stator Velocity Diagram.

is a new technique for calculation of the flow. Formerly, radial equilibrium, i.e., calculation along radial lines, was employed. Unfortunately this procedure is not suited to flows which are primarily radial, as experienced at the lift fan inlets. A procedure is now being developed which will enable computation along arbitrary lines called quasi-orthogonals. This method, based on the work of Theodore Katsanis (Reference 8), is being modified to fulfill more adequately lift fan analysis requirements. The flow will be described (Figure 45) from the beginning of the inlet to the stator exit. The wall boundary layers will be accounted for through a shift of the wall boundaries used for computation.

The second benefit should be derived from the results of a series of tests now being planned to determine the interaction of fan exit annuli and exit louvers. Increased thrust and improved stall margin during vectored operation may be expected.

Turbine Aerothermodynamic Design

General Description

The tip turbine is a single-stage, high-pressure-ratio impulse design. High energy gas is delivered to the turbine by means of a double-entry scroll running circumferentially about the fan outer diameter. The turbine exhaust gas enters a short, vaned annular passage which serves to remove any residual swirl velocity. The turbine flow-path walls are specially designed to eliminate static pressure gradients in the radial direction and to make possible the use of constant section, untwisted nozzles and buckets. Table VII lists a number of significant turbine design point parameters. The design point has been chosen at the nominal admission arc of 250° and with inlet gas conditions corresponding to 100-percent rated gas generator speed. Figure 46 shows a sketch of the turbine flow path and representative pressures and temperatures. Figure 47 shows the velocity diagram at the mean diameter. There is very little variation in the velocity diagram over the turbine annulus height.

A number of compromises have been made in the turbine aerodynamic design in order to achieve a proper balance between turbine efficiency and overall fan weight and size. The wheel speed is somewhat below optimum for peak turbine efficiency. It is estimated that about 1-percent increase in turbine efficiency would be obtained with a 5-to-10 percent increase in wheel speed. The axial clearance between the nozzles and buckets is quite large to permit design of more flexible and lighter weight frames and rotor. This creates large gaps in the flow path which generate losses. The turbine exhaust Mach number of 0.5 is higher than optimum for maximum net lift in order to minimize the turbine annulus height. This reduces both the rotor weight and overall tip diameter. Bucket solidity has been held to a minimum consistent with good performance. The cumulative effect of these compromises is estimated to be about 3 percent in turbine efficiency.

TABLE VII
LFX TURBINE DESIGN POINT

Inlet Total Temperature	1847°R
Inlet Total Pressure	48.42 psia
Inlet Gas Flow	49.01 lb/sec
Total to Static Pressure Ratio	3.26
Total to Total Pressure Ratio	2.77
Exit Static Pressure	14.86 psia
Exit Total Pressure	17.54 psia
Speed	4070 rpm
Pitch Wheel Velocity	1059 fps
Design power	6652 hp
Design specific energy	98.7 Btu/lb
Exit Mach Number	0.5
Efficiency	0.846%
Velocity Ratio	0.414 U/No

TABLE VIII
LFX TURBINE ENERGY SUMMARY

Shaft Power	0.7394
Exhaust Energy	0.1250
Nozzle Loss	0.0346
Bucket Loss	0.0776
Leakage	0.0106
Partial Admission Loss	0.0128
Swirl Loss	0.0000
	<u>1.0000</u>

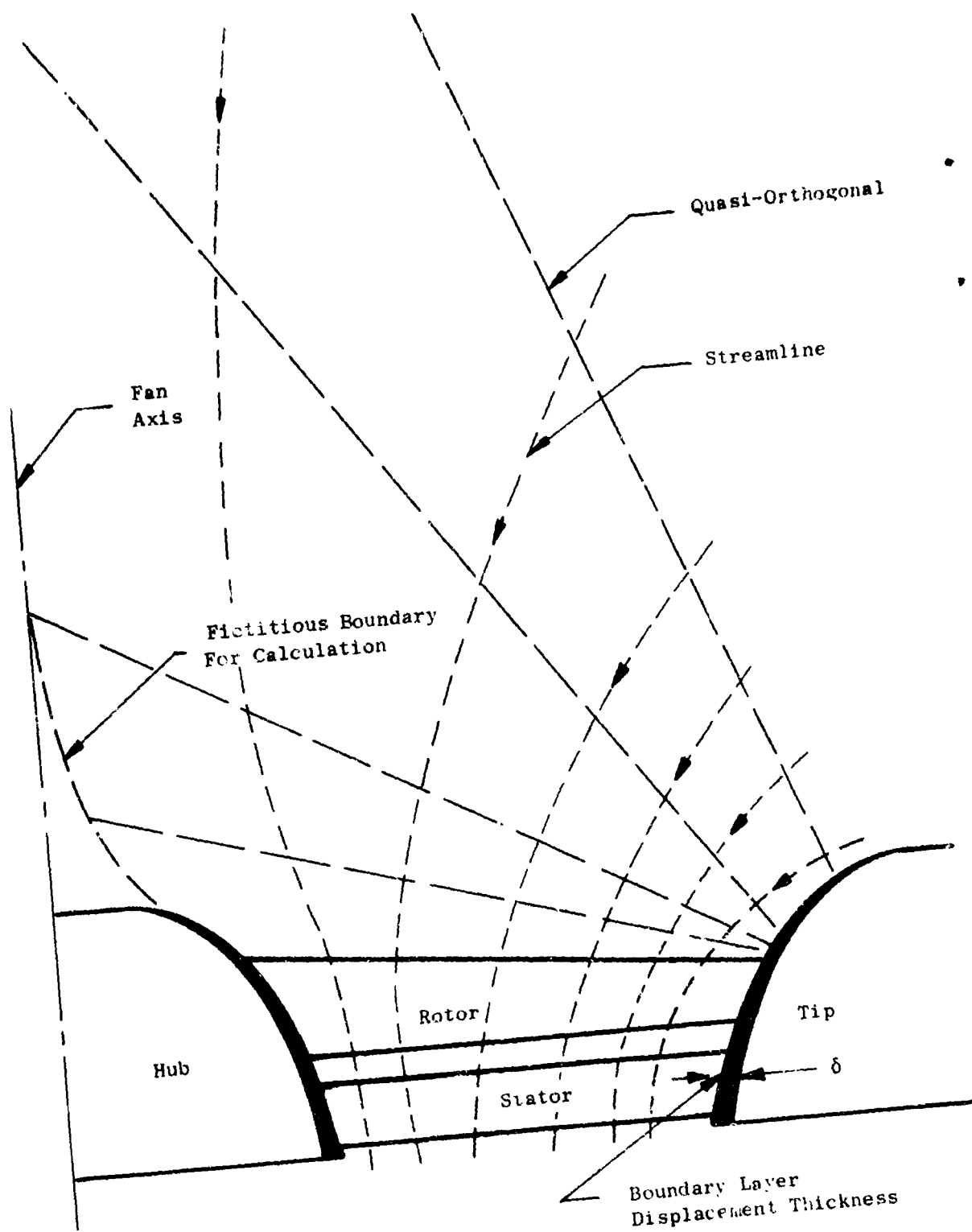


Figure 45. Quasi-Orthogonal Flow Schematic.

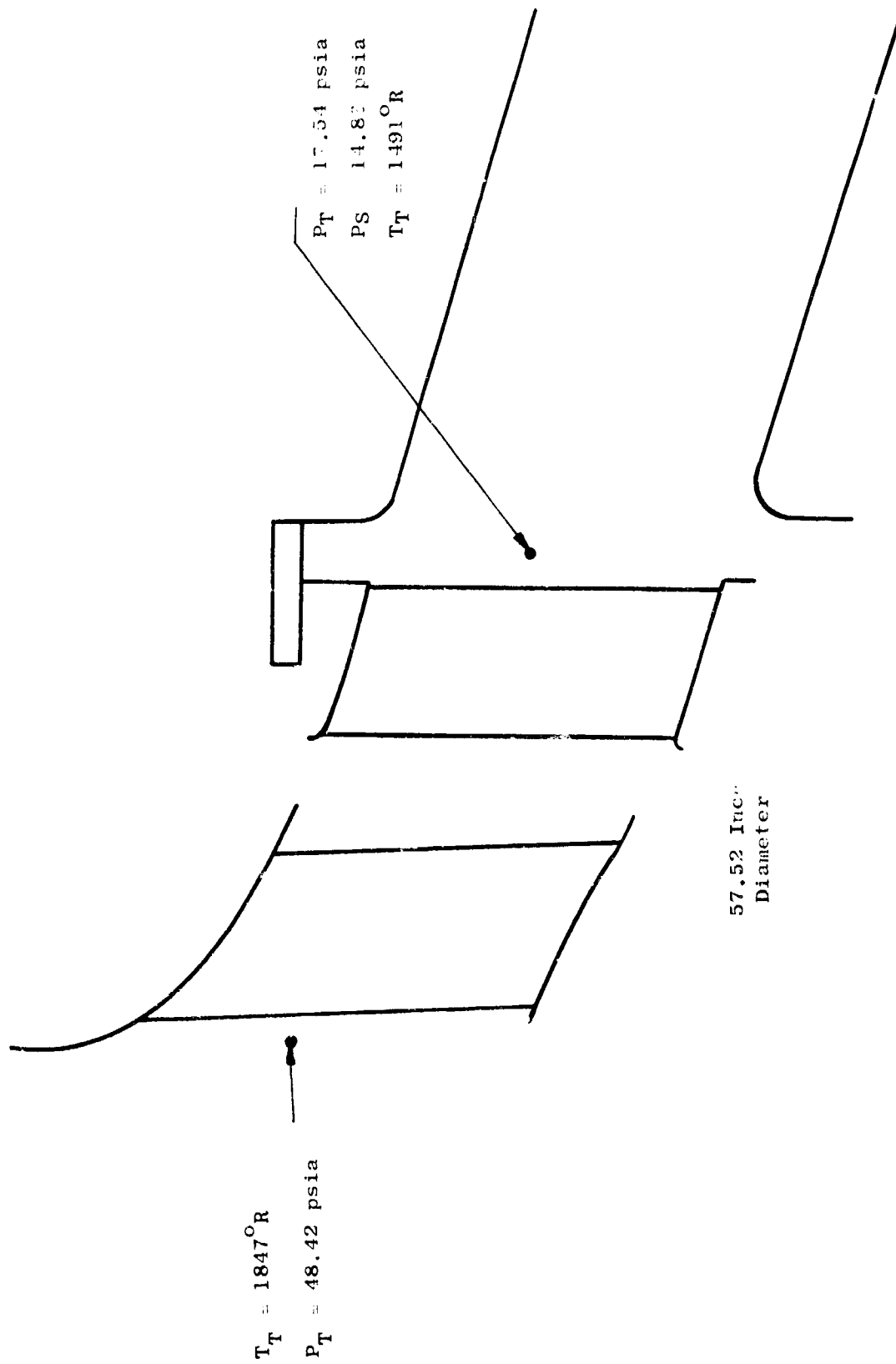


Figure 46. Turbine Flow Path.

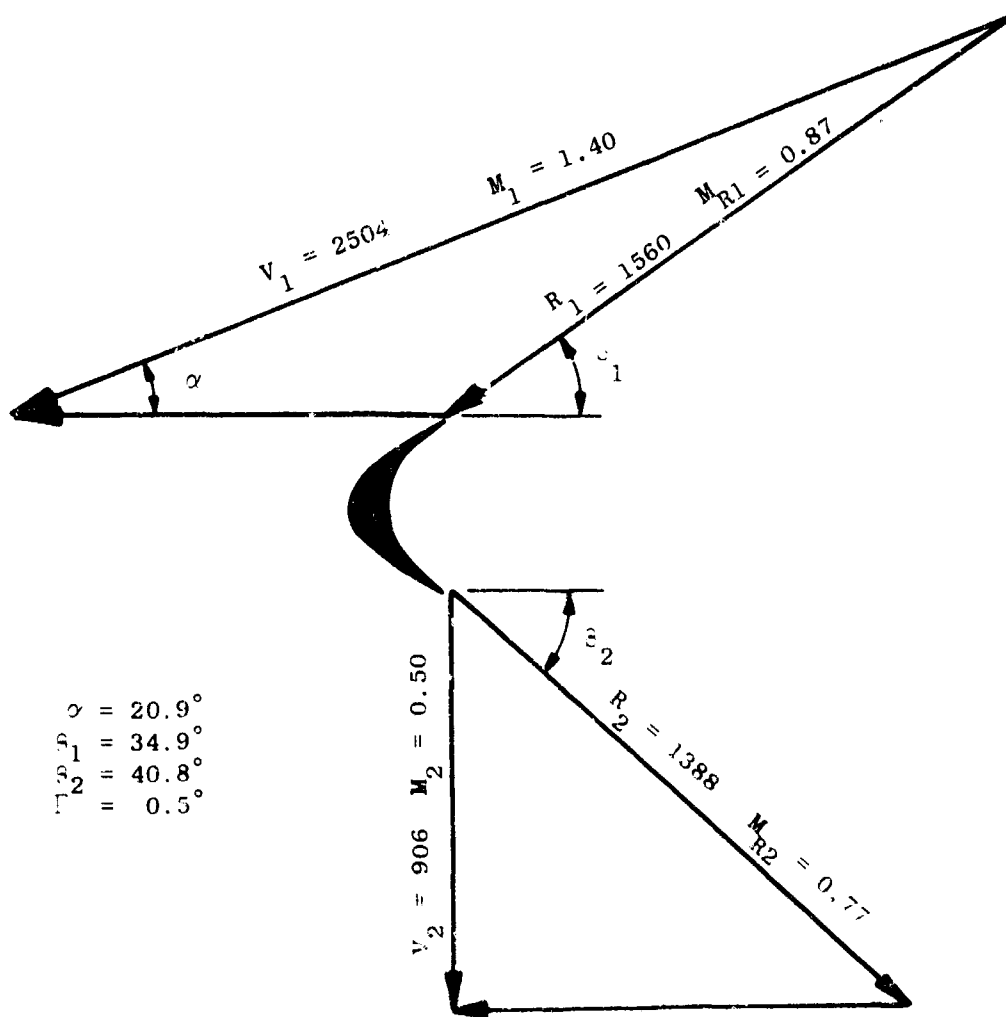


Figure 47. Turbine Velocity Diagram.

Design Point Performance

Table VIII gives a summary of how the total available energy at the nozzle entrance is distributed between net shaft power, exhaust energy and losses. The losses and efficiencies shown here and in Table VIII are those which should be attainable on a production fan. Prototype engine hardware is often of somewhat lower quality and may tend to reduce the turbine efficiency by as much as 4 or 5 points due to large seal clearances, flow-path misalignment, etc.

Incorporation of the variable admission arc feature into this turbine introduces losses into the system which have not been charged against the turbine design point efficiency but which have been accounted for in the turbine design.

At the nominal admission arc of 250° there will be about 1-pound-per-second flow leakage through imperfect sealing of the nozzle passages in the inactive arc. The active turbine arc has been designed for this reduced flow, but the quoted efficiency is based on the flow through the active arc only.

The presence of blocker vanes in the nozzle passages will cause some small loss in these passages. The magnitude of this loss will depend upon the final design of the vanes but should be quite small in any case.

Airfoil Design

From Figure 47 we see that the nozzle leaving velocity is well above sonic and that the entering bucket relative velocity is in the transonic range. This is a direct result of the high turbine total to static pressure ratio and the requirement that the turbine be single stage and impulse.

Test data on simple convergent nozzles show that they do not perform well for exit Mach numbers this high and that convergent-divergent nozzle passages are required. Figures 48 and 49 show nozzle airfoils designed with convergent-divergent passages. At least three different nozzle profiles will be required for use at various circumferential locations about the turbine. This is because of the wide variations in inlet angle at different locations in the scrolls. Figures 48 and 49 show the extremes to be expected; however, at least one additional intermediate design will be required. The several nozzle designs will have the same axial width and be geometrically similar downstream of the throat section. The divergent sections of the passages are designed to underexpand the flow slightly to obtain better part speed performance with no significant compromise in design speed performance.

The turbine bucket profile is shown in Figure 50. It is very similar in design to a series of profiles previously designed and tested in the transonic cascade wind tunnel. It differs mainly in that the edge

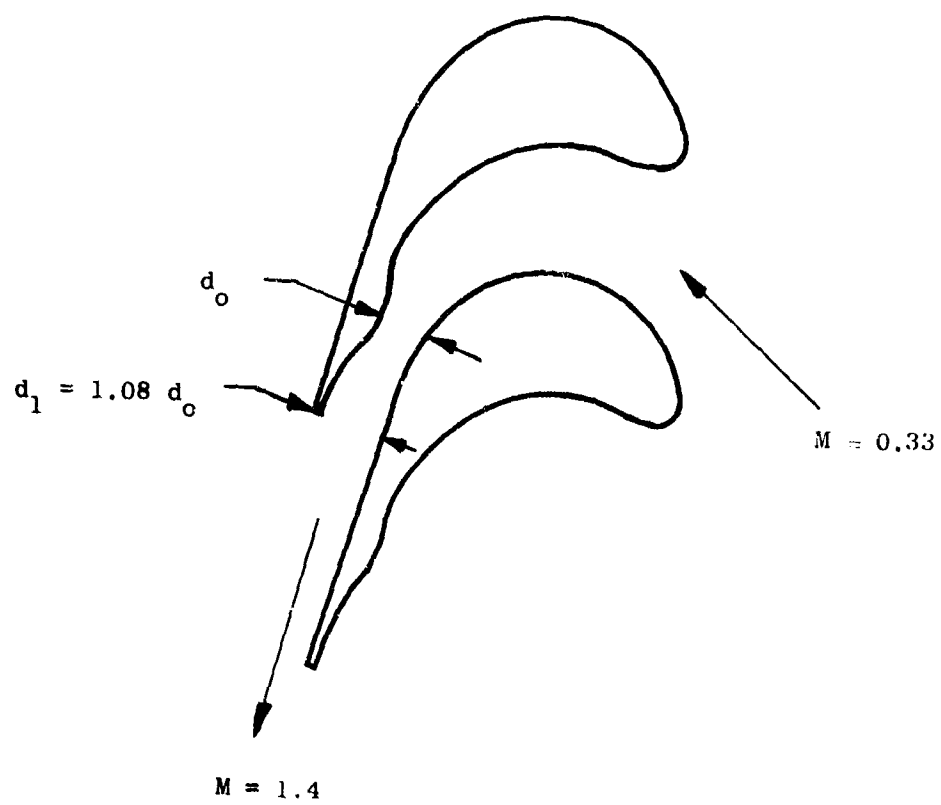


Figure 48. Turbine Nozzle Airfoils.

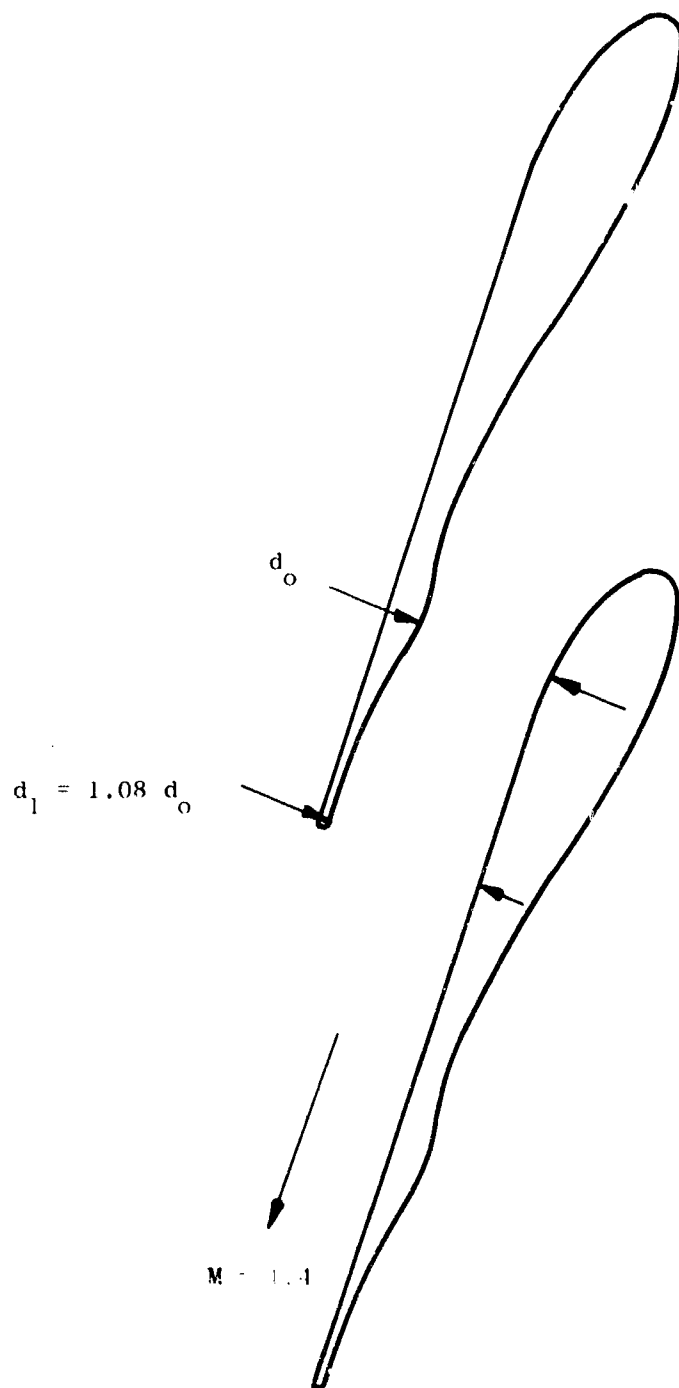


Figure 49. Turbine Nozzle Airfoils.

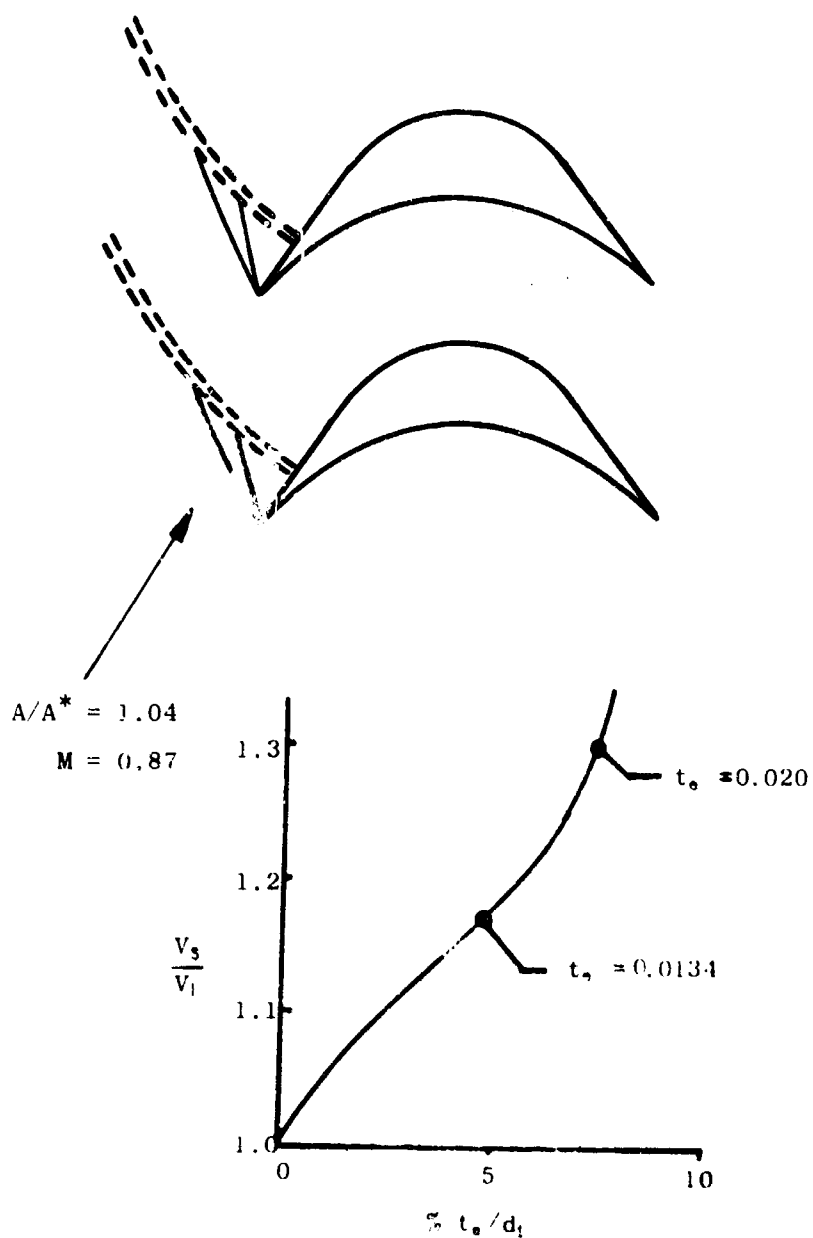


Figure 50. Turbine Bucket Profiles.

thickness has been increased from 5 percent of the throat width to 7 percent. It also has about 4 degrees less turning angle than the test profile. The results of this test showed that buckets designed by this procedure will have good performance up to an entering Mach number of about 1.1 with only slight performance penalty at very low Mach numbers. The bucket design is symmetrical fore and aft and has a solidity of 1.85 and an edge thickness of 0.020 inch.

The exit stator vanes in the turbine exhaust section are mainly structural in purpose, since the turbine exit swirl angle is nearly zero at the design point. At off-design conditions, however, these vanes will tend to recover some exit swirl energy. They have a chord length of 2.79 inches, a solidity of 0.626, and a maximum thickness of 15 percent of the chord. The airfoil shape is an NACA 64₂ A015 profile. The profile should have a good tolerance to off-design incidence angles and also provide a good structural section.

Scroll Design

The turbine inlet scroll has a double inlet as shown in the fan plan view of Figure 51. The forward inlet supplies the forward 180 degrees of admission arc while the rear inlet supplies the rear 180 degrees of admission arc. The scroll inlets are sized for an inlet Mach number of 0.3 with a nominal admission arc of 250 degrees. As the admission arc and turbine flow vary, the scroll inlet Mach number varies from a minimum of 0.19 to a maximum of 0.45. The area of the scroll arms is reduced progressively from the beginning of the nominal admission arc to the outboard side of the fans so as to maintain a constant scroll tangential Mach number of 0.3.

The geometry of this scroll is quite similar to that of the LF-1 scrolls. It differs in that its maximum admission arc is 360 degrees rather than 158 degrees. A scale model test was made of the LF-1 scroll configuration which included nozzle vanes and struts. The test was made on the scroll alone as well as on the scroll in combination with the entire upstream ducting system. The test conditions duplicated full-scale Mach numbers and Reynolds numbers. The results of this test gave a scroll total pressure loss coefficient of 0.53 based on inlet dynamic head. This loss did not depend greatly on whether the scroll was tested alone or with the rest of the ducting system. Analysis of the results indicated that most of the loss could be attributed to entrance losses, strut losses, and turbine nozzle entrance losses. Surface friction accounted for a rather small part of the loss.

Based on these facts it is not expected that the increased admission arc will greatly increase the scroll total pressure loss coefficient. A total pressure loss coefficient of 0.55 is therefore estimated for the LFX scrolls.

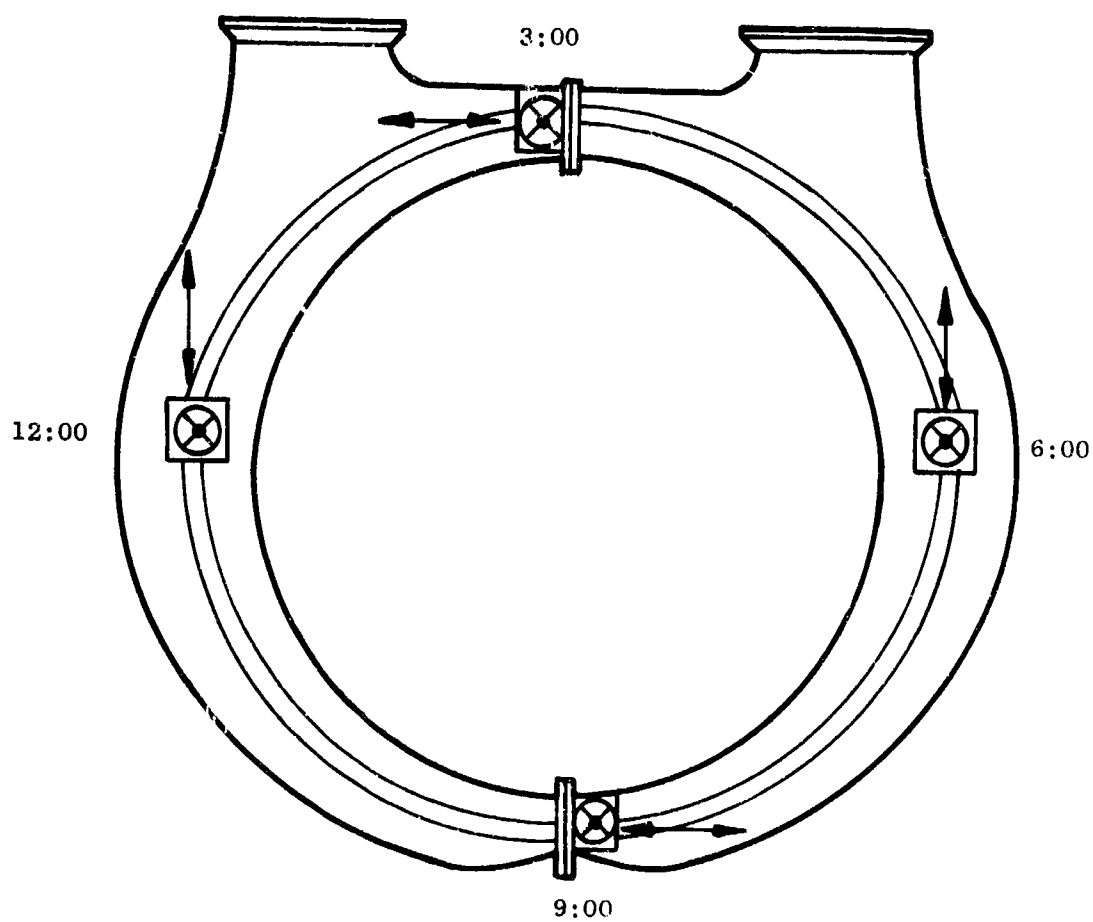


Figure 51. Scroll Planform.

LFX MECHANICAL DESIGN DEFINITION

The major emphasis in the preliminary design activity was on the wing fan. The design definition was completed in sufficient detail to permit definitive weight calculation. Major components were defined both by layout and by analysis. Layouts include a subassembly parts list, materials and stock thicknesses, assembly sequence, fasteners and special assembly tooling. Possible alternate design configurations have been identified where a potential exists for performance, weight, or cost improvement.

Major loads and associated stresses were calculated and load paths were identified.

MECHANICAL DESIGN REQUIREMENTS

Interface Requirements

Front Frame

The front frame major strut was designed with the capability of reacting door loads and door actuator loads for a split butterfly wing fan cover door. In addition, a weight estimate was made both with and without door mount capability.

Door loads used in design evaluation of the front frame are shown in Figure 52. Door load ratios are obtained from XV-5A calculated and measured loads.

The front frame has provisions for integral mounts at the major strut ends and as required at the minor struts. A bellmouth with a minimum radius of 6 inches is included in the front frame design. The bellmouth is tapered, as shown in Figure 26.

Scroll

The scroll is a 360-degree inlet design with a variable area power transfer mechanism. The variable area portion of the scroll is located at the inboard side of the fan. An actuation system for the scroll was identified and an estimate was made of the actuator force requirements.

Rear Frame

The rear frame basic design mounts the exit stators. In addition, weight changes were identified to provide the capability of mounting the exit louver actuating rod and of mounting the exit louvers. Exit louver design takes advantage of aerodynamic load balancing where feasible to reduce actuator loads. An estimate was made of exit louver actuator loads.

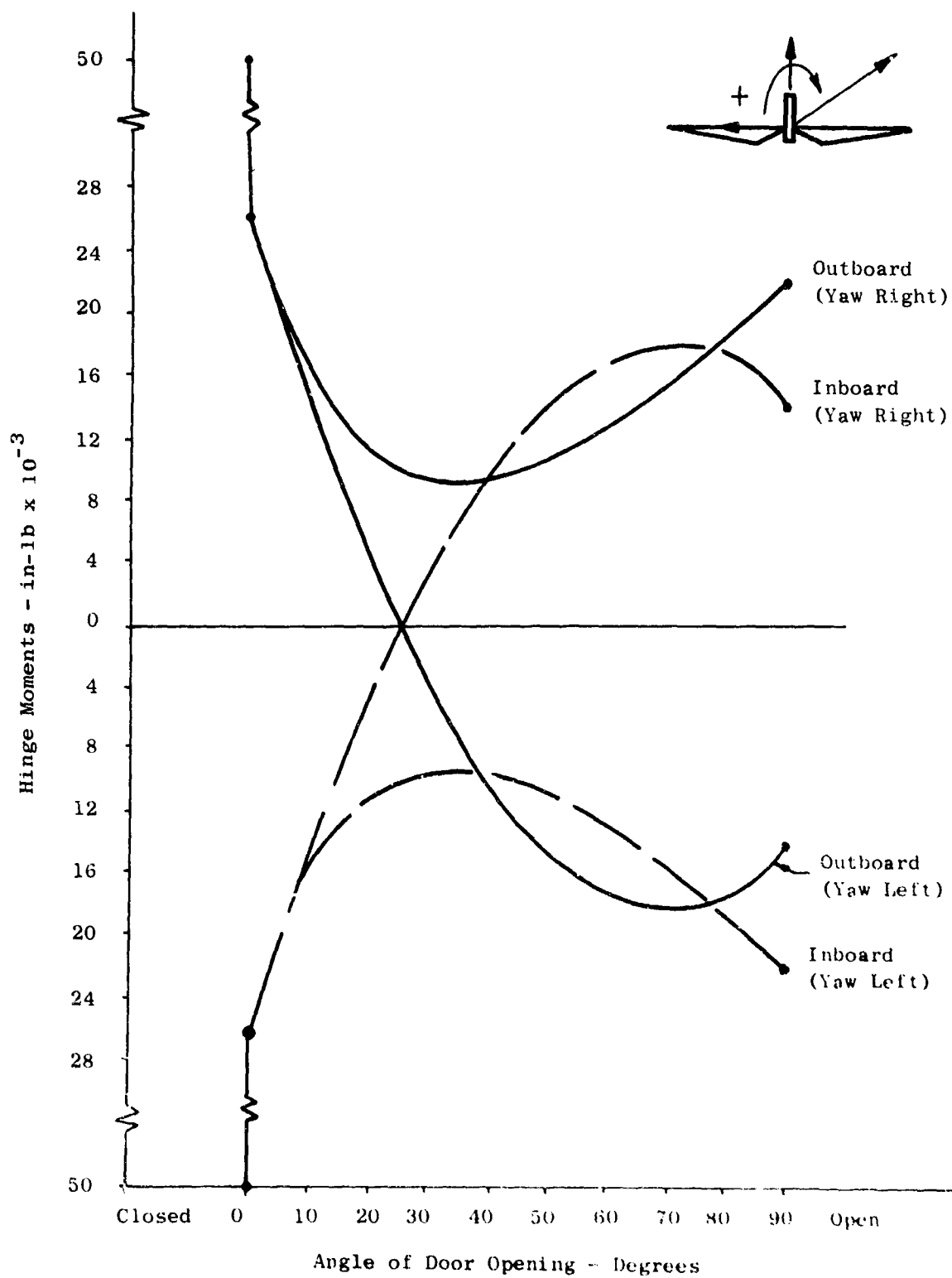


Figure 52. Wing Fan Door Loads.

Aerodynamic

A goal for fan purge flow pumping capability is $\frac{1}{2}$ percent of the total fan flow. Desired order of priority for introduction of the purge flow to the fan stream is: (1) aft of the rotor plane, (2) ahead of the rotor plane, and (3) in the rotor plane.

General - Integrated Structure

The basic design of the fan is an integral structure and includes the bellmouth, front frame, scroll, rotor, rear frame and exit louvers.

Mechanical Design Requirements

Rotor Speed

Rotor speed is 100-percent rpm at the nominal sea level static design point with 50.01-pound-per-second turbine gas flow. Physical rpm at 100 percent is 4070 rpm. The rotor is designed for continuous operation at 115-percent speed and is capable of short-time overspeed operation above 115 percent without structural failure.

Maneuver Loads

Maneuver loads are those due to the accelerations shown in Figure 53. The angular displacement rates are similar to those identified previously in design criteria.

Rotor Mechanical Design

The rotor blades and disc design material are titanium alloy. The number of blades is a maximum consistent with good rotor dynamic design practice.

The bearing arrangement is such that the rotor may be removed from its mounting without removing the frame from its installation.

The bearings are of the grease lubricated type of design.

Scroll Mechanical Design

The scroll is a power transfer design with a nominally active arc of 125 degrees per side. Maximum arc of admission is 180 degrees per side. The scroll design includes the power transfer actuation mechanism but not the actuator. An estimate has been made of the actuator load requirement.

The basic design of the scroll is based on a single skin of appropriate thickness for the wall.

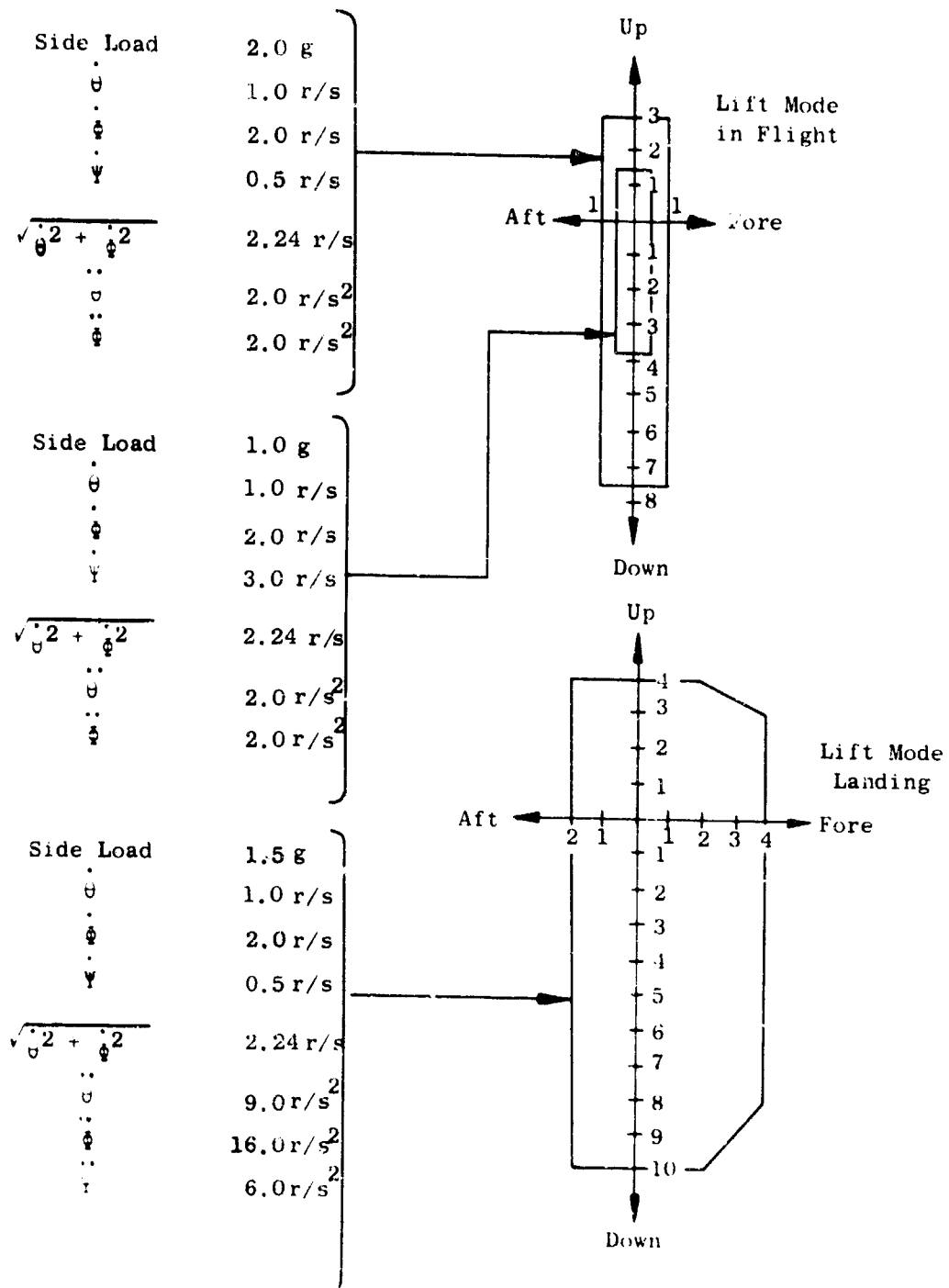


Figure 53. Maneuver Loads - Lift Mode.

The size of the scroll was established to provide a design flow Mach number of 0.3. The power transfer portion of the scroll arc is located between the two scroll inlets (inboard in an aircraft installation).

Rear frame loads are transmitted through the scroll structure. Self-centering type scroll mounts are utilized.

Scroll end seals and radial seal design have been identified, together with leakage estimates at operating conditions.

The scroll is designed so that thermal growth will permit the scroll turbine nozzles to match the turbine bucket height at the 100 percent rpm design operating point.

Front Frame Mechanical Design

The front frame is used to mount the fan in an installation. It includes a bellmouth, major strut, minor struts as required to react gyroscopic loads, fan hub, inlet bullet nose, scroll mounting provisions and aerodynamic seals.

The major strut includes representative hard points for mounting of the wing fan doors and the wing door actuators. The major strut material is steel. The strut protrudes above the wing skin in a typical aircraft installation. The design of the bullet nose and bellmouth is such that the wing fan doors may close over them with no bulges or lumps in the doors.

Rear Frame Mechanical Design

The rear frame basic design includes the compressor exit stators, turbine exit stators, dishpan and aerodynamic seals. In addition, weights have been estimated for the rear frame with exit louver actuation system mount capability and for the rear frame with capability to mount both the exit louvers and the exit louver actuation mechanism.

The exit louvers are aerodynamically counterbalanced to the extent feasible and compatible with a minimum thickness fan in a typical wing installation. Exit louver actuation loads have been estimated.

The exit louvers have been designed for an operating range of symmetrical vector angles from -25 degrees (aircraft rearward flight) to +45 degrees. No design requirement was established for differential movement (staggering) of the exit louvers.

Other Stress Considerations

In general, the following conditions were considered in the mechanical design of the LFX-6 components. These conditions were analyzed in as much depth as possible, and the design of the parts was adequate to sustain the design conditions.

Thermal Fatigue

Parts which frequently undergo temperature cycling were analyzed for the resulting thermal distortion. The design life of such parts must be at least a factor of 2.0 times the mission life. When such cycling is severe and/or very frequent, a Goodman diagram approach was used.

Thermal Transients

Thermal stresses occurring during starts, accelerations, decelerations and shutdowns were analyzed in the same manner as frequent maneuver loads. It was assumed that these stresses did not act concurrently with other maneuver loads.

Buckling

Structures were designed to withstand buckling loads wherever applicable. In general, the ratio of critical buckling loads to the maximum calculated loads was determined considering the risk associated with buckling, uncertainties of methods of calculations, etc.

Deformations

Some parts were designed to limit deflection, either elastic or plastic, such as to prevent interference between rotating and static parts under the specified operating conditions, maneuver loads, etc. For such parts, the design was based on the allowable deflection rather than the stress limits.

Stress Concentrations

For ductile material, stress concentrations are normally applied only to vibratory loads. For parts designed to long life requirements (30,000 hours), attention was given to the application of stress concentration factors to steady stress due to the cyclic nature of such stresses when subjected to many starts, stops, maneuver loads, etc., where a significant number of cycles can be accumulated.

OPERATIONAL REQUIREMENTS

Life Requirements

The LFX-6 fan was designed for 1,000 mission hours between overhauls. Life goal for life-limited parts was 10,000 mission hours. Replacement of rotor blades, turbine sectors, bearings and repair of other components was permitted to obtain the total life goals. Where the life objective causes a significant weight increase, the effect of reducing the total life was investigated.

<u>Mission Segment</u>	<u>Total Life</u>	<u>Gas Generator Power Setting</u>	<u>Fan Power Setting</u>
Takeoff	14%	100%	100%
Cruise	69%	95%	--
Landing	08%	100%	100%
Ground	09%	95%	80%

One percent of the total fan operating time was considered as being with single-engine inlet conditions.

Two percent of the total fan operating time was considered as being at the maximum fan rpm attainable with maximum scroll arc of admission.

Environmental Limits

Fan operating limits are from -30 knots EAS (rearward flight) to +150 knots EAS at altitudes from sea level to 10,000-foot density altitude and ambient temperatures from -30 degrees Fahrenheit to +115 degrees Fahrenheit. Side translation limit speed is 30 knots EAS right or left.

Maneuver Load Frequency

The fan is designed for continuous operation with 0.1 of the loads and accelerations shown in Figure 53 occurring once in each 0.1 fan operating hour. The maximum loads and accelerations shown in Figure 53 are considered to occur once in each 1.0 fan operating hour.

Instrumentation

Fan instrumentation for operational use has been identified. Instrumentation includes an rpm or fan speed indicator, bearing temperature indicator, vibration level indicator, and certain other indicators deemed necessary to indicate the safe operation of the fan.

Over-Temperature Tolerances

The possibility of over-temperature occurrences during the operating life of the fan was evaluated. The estimated material temperatures for steady-state operation of the fan should be determined during the detail design phase of the fan design cycle from cycle data and appropriate heat transfer analyses. To account for over-temperature possibilities, a temperature deviation is to be added in all cases to the calculated design temperature of the part. The exact temperature deviation for each part should be established during the detail design phase, but in any case should not be less than plus 50 degrees Fahrenheit. In the blade tip tang and surrounding region, this temperature deviation should be plus 100 degrees Fahrenheit. Additionally, parts which undergo frequent temperature cycling must be capable of meeting a design life equal to twice the given mission life. Parts which are subject to large thermal gradients (where the thermally induced stress approaches the yield stress) are designed to ratio of critical buckling load to calculated load equal to or greater than 3.

Accommodation for Specific Gas Horsepower Increases

The LFX-6 fan design is based on a gas generator with a specific gas horsepower equal to approximately 195 horsepower per second of turbojet exhaust gas flow. Much of the improvement in performance of the fan can be related to the increase in the specific gas horsepower. Future gas generator cycles with improved specific horsepower characteristics must be considered in the detailed design of the LFX-6 generation of fans. Within the weight limitations given in the detail design sections of this report, increases of specific gas horsepower can be tolerated, but with a commensurate reduction in design life. At even higher level of specific gas horsepower, a revised design concept to include cooling of critical static parts such as turbine nozzles, scroll struts and scroll walls will be required.

A possible engine cycle improvement of 10 percent in specific gas horsepower could be achieved through an increase in engine exhaust gas temperature of approximately 185 degrees Fahrenheit. A more reasonable criterion to include in the LFX-6 detail design would be the capability of accepting an increase in exhaust gas temperature of 56 degrees Fahrenheit or the equivalent of a 3 percent improvement through increased temperature.

Gas horsepower is relatively insensitive to changes in exhaust gas pressure while component weight is sensitive. Consequently, a reasonable criteria for LFX-6 detail design is the inclusion of capabilities for pressure not to exceed an increase of more than 6 pounds per square inch.

ROTOR MECHANICAL DESIGN

The LFX rotor design philosophy was established during the initial phase of the LFX studies and is as presented in Reference 1. The mechanical design of the rotor is based on the LFX design criteria, XV-5A experience, LF2 operating experience, and established rotor design practices. The rotor is a straddle-mounted single-stage design with concentrically mounted turbine segments attached to the blade tips. The LFX-6 fan blade is a comparatively high aspect ratio design, referred to as a "high-flex" blade. The straddle-mounted dual bearings, with the thrust and roller bearings similar to the LF2 configuration, are grease packed.

The rotor design shown by Table IX and the following description weighs 170 pounds, compared to 165 pounds reported in Reference 1. Table X shows the calculated rotor weights for the configuration shown on Figure 26.

The following outlines the rotor design criteria and operating conditions, describes the design and the results of the design analyses, and lists the areas requiring further study.

Rotor Design Requirements

The rotor is sized for maximum continuous speed equal to 115 percent of the 975-foot-per-second fan tip speed (nominal lift point). This provides an overspeed and tachometer readout error capacity of 3 percent over the thermodynamic design maximum speed of 112 percent. The design parameters for the LFX-6 rotor, defined by the aerodynamic design work, are:

TABLE IX
DESIGN PARAMETERS

Fan tip speed, ft/sec	975	
Fan tip radius, in.	27.45	
Radius ratio	0.442	
Outer fan flow-path slope, deg	15	
Hub flow-path slope, deg	26	
Number of blades	50	
Number of carriers	25	
Number of buckets	375	
Number of buckets/carrier	15	
	Tip	Hub
Solidity	0.9	1.74
Chord, in.	3.105	2.653
Stagger angle, deg	52.6	15.1
Camber angle, deg	14.8	45
tm/C	0.060	0.063
Number of blades	50	
Airfoil type	Bi-Convex	Circular Arc Mean Lines

TABLE X
ROTOR WEIGHT SUMMARY

Component	LF-2 (lb)	LFX-6 Objective Weight (lb)	LFX Preliminary Design (lb)	LFX-6 Design (lb)
Carrier System	50.4	27.6	38.0	31.4
Blades (solid)	77.0	53.5	58.2	71.1
Disc	67.2	39.1	50.7	48.6
Bearings	15.0	17.6	12.7	17.04
Miscellaneous	<u>8.4</u>	<u>3.2</u>	<u>5.4</u>	<u>1.72</u>
Total	218.0	141.0	165.0	169.86

The LFX-6 design criteria also specified that the fan blades should be of solid titanium construction, utilizing the proven "tip-tang" method of turbine sector attachment. These criteria were established to assure that compatible manufacturing technology would be available during the specified development time period.

Additional design criteria which pertain specifically to rotor components are discussed in the appropriate Design Analysis section on page 134.

Rotor Design Description

The mechanical design of the rotor, see Figure 54, is based on the LFX objectives and present lift fan rotor design state of the art. The rotor design consists of 375 turbine buckets, 25 turbine carriers, 50 fan blades, a disc, a ball thrust bearing, a roller bearing and the associated components and hardware. The turbine sectors span two fan blades and are attached by a single shear bolt at each blade tang. There are 15 buckets in each carrier which are shrouded to form the outer hot gas flow path. A fore and aft seal lip is provided to retard hot gas leakage into the fan flow stream. The center portion seal of the carrier serves dual purposes by sealing as well as providing the tip turbine torque transmission around the fan circumference for transmittal of tangential forces created by partial admission operation. This is accomplished by a tongue which overlaps the next carrier seal and is attached to it by a single 0.25-inch-diameter bolt. The blade tang is similar to other proven fan rotors and has a transition to the blade airfoil similar to that of the X376 Pitch Fan. This transition shape provides a smooth flow path at the blade tip and also provides a low stress concentration design.

Rotor components are identified in Figure 55.

Turbine Sector

The LFX-6 turbine sector design is similar to the successful LF-2 turbine sector. The LFX turbine sector is essentially a simply supported beam which is pinned to two fan blades. Fifteen integral shrouded turbine buckets are attached to the bucket carrier (Figure 56). A departure from the LF-2 design is the aerodynamic seals, which are angled to conform to the fan and turbine flow paths (Figure 56). Like its predecessors, the LFX-6 carrier is fabricated sheet metal. The turbine carrier system has two unique features: (1) an integral torque transmission system, and (2) tang cooling.

In an effort to reduce weight, an integral torque transmission system similar to the 80-inch tip turbine cruise fan has been incorporated in the LFX-6. This type of torque transmission device, while permitting thermal growth in the tangential direction, transmits torque by friction. It should be noted that the friction pad arrangement is designed to slip under thermal growth and not to slip under torque loads. The second feature includes internal bulkheads and external support pad shielding which provide cooler tang operating temperatures (Figure 57).

Air from the pressure side of the fan blade flows into the cavity formed by the bulkheads. Cooling air flows up and over the tang and out the low pressure side of the fan blades.

The individual turbine sector components and their function are described below.

The turbine bucket is an impulse type airfoil with three internal ribs used to reduce gas bending stresses at the root of the bucket. Tip shrouds are incorporated to damp vibratory motion and to maintain the bucket tip contour and form the outer flow path.

The bucket carrier is composed of four component parts: a box, two side rails, and the bottom plate. These four component parts when brazed together comprise a very efficient structure designed to resist the centrifugal and gas bending loads on the turbine buckets. These loads are in turn transmitted, through shear, to the rest of the carrier structure. The entire bucket carrier is constructed of Rene' 41.

The turbine bucket and bucket carrier centrifugal loads are transmitted to the fan blade tang by two bolts loaded in shear. The "bearing" support for these bolts is provided by the inner and outer support blocks which are brazed to the side rails.

Two one-tooth rotating seals integral with the bottom plate of the bucket carrier prevent leakage of turbine gases into the fan stream.

The internal bulkhead and side plate shield are designed to prevent hot turbine gases from impinging on the blade tang. The internal bulkhead also provides a cavity for the cooling air to flow around the tang. This internal bulkhead also reduces the shear stress in the side rail in that area where stresses are high due to high shear forces and small section properties.

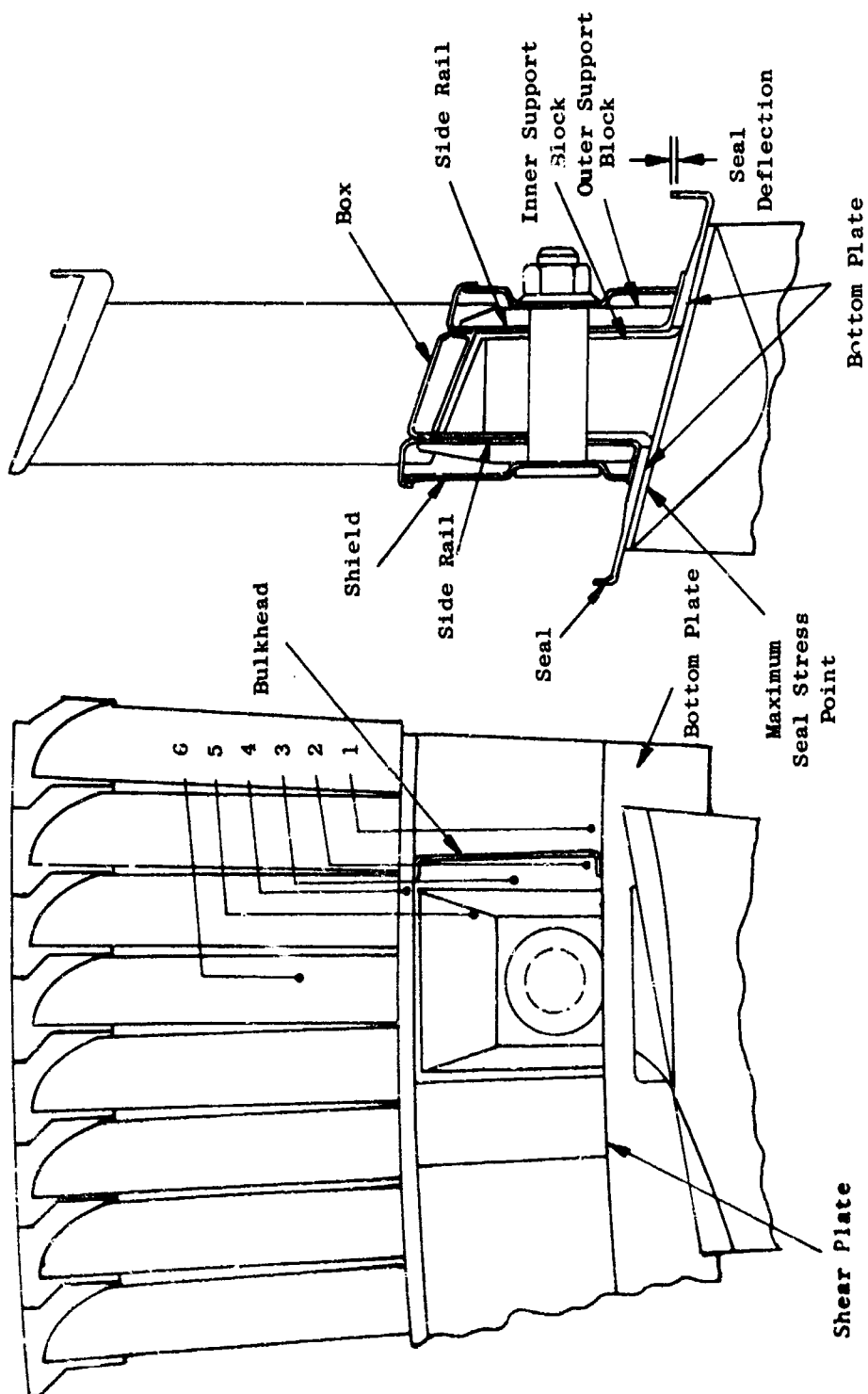


Figure 56. Bucket Carrier Section Identification.

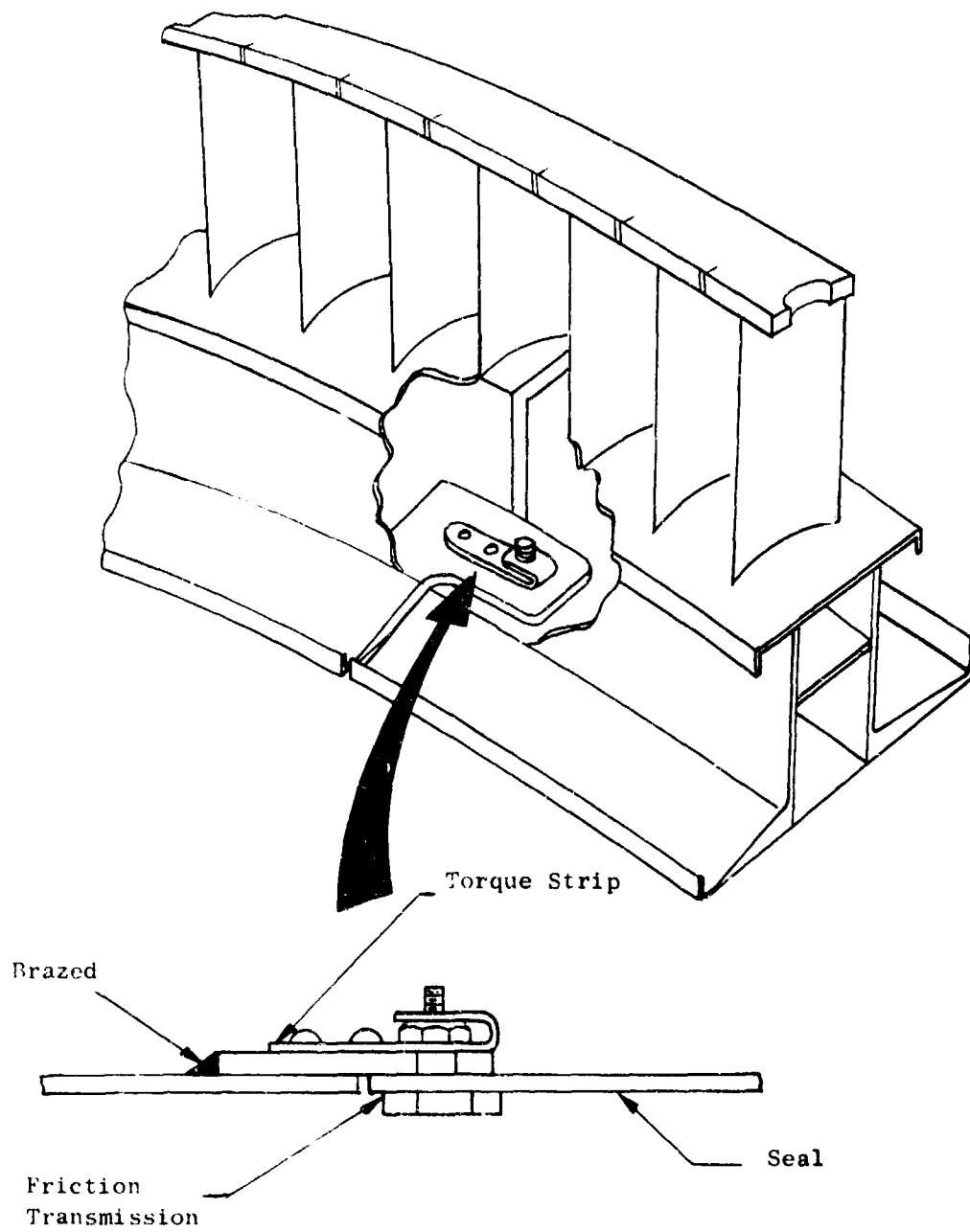


Figure 57. Turbine Sector Torque Transmission.

Two shear plates are brazed to the side rails adjacent to the support block to reduce shear stress in the side rails.

At the ends of the bucket carrier is a friction pad arrangement (integral torque band, Figure 57) which transmits torque from one turbine sector to another. Because of the partial admission arc arrangement resulting from power transfer, a required push-pull torque transmission system is provided by the friction pad arrangement.

Fan Blades

The fan blades are biconvex airfoils. The hub flow path is conical and slopes 26 degrees. The hub platform (inner flow path) is integral with the blade shank. The inner flow-path platform is an integral part of the blade. The dovetail broach angle is 15 degrees to conform to the blading stagger angle at blade hub. This is a necessity, since the radial distance between the inner flow path and the disc outer diameter is not sufficient to allow shank twist to change the dovetail angle. A straight single hooked dovetail is used to support the fan blades in the disc. The blade is retained in the disc by a tab located on the bottom aft end of the dovetail and a two-pronged blade retainer. The tab bears against a recess in the aft rim face and the retainer is both rabbeted and bolted to a scalloped flange by two bolts. The two bolts provide safety through redundancy, since one bolt has sufficient strength to carry the applied load.

Disc

The LFX-6 rotor disc is an integrated titanium structure made up of twin (identical) webs diffusion bonded together at the dovetail and sump areas; with axial slotted dovetails at the rim, and containing a press fit ball bearing and bolted roller bearing in the hub. The enclosed space between the webs is vented by six radial holes in the rim.

The disc material is Ti-6Al-6V-2Sn, which is one of the highest strength-to-weight ratio, moderate temperature materials considered available for manufacture of parts within projected program timing.

Overall disc axial thickness has been kept to a minimum in order to provide the maximum utilization of space for rotor supporting structure within a shallow wing installation. The disc hub thickness is 6.9 inches, compared to 8.0 inches for initial concepts.

The LFX-6 disc represents the lightest weight design yet obtained in the development of GE lift fans. It incorporates the best features of previous fans together with innovations that have significantly increased the effectiveness of the disc. This effectiveness can be shown by comparing fan disc weights in terms of the thrust/weight ratio and radial rim load/weight ratio as in Figure 58.

LFX-6 disc has excellent weight effectiveness, while still emphasizing maintainability, due to several design innovations.

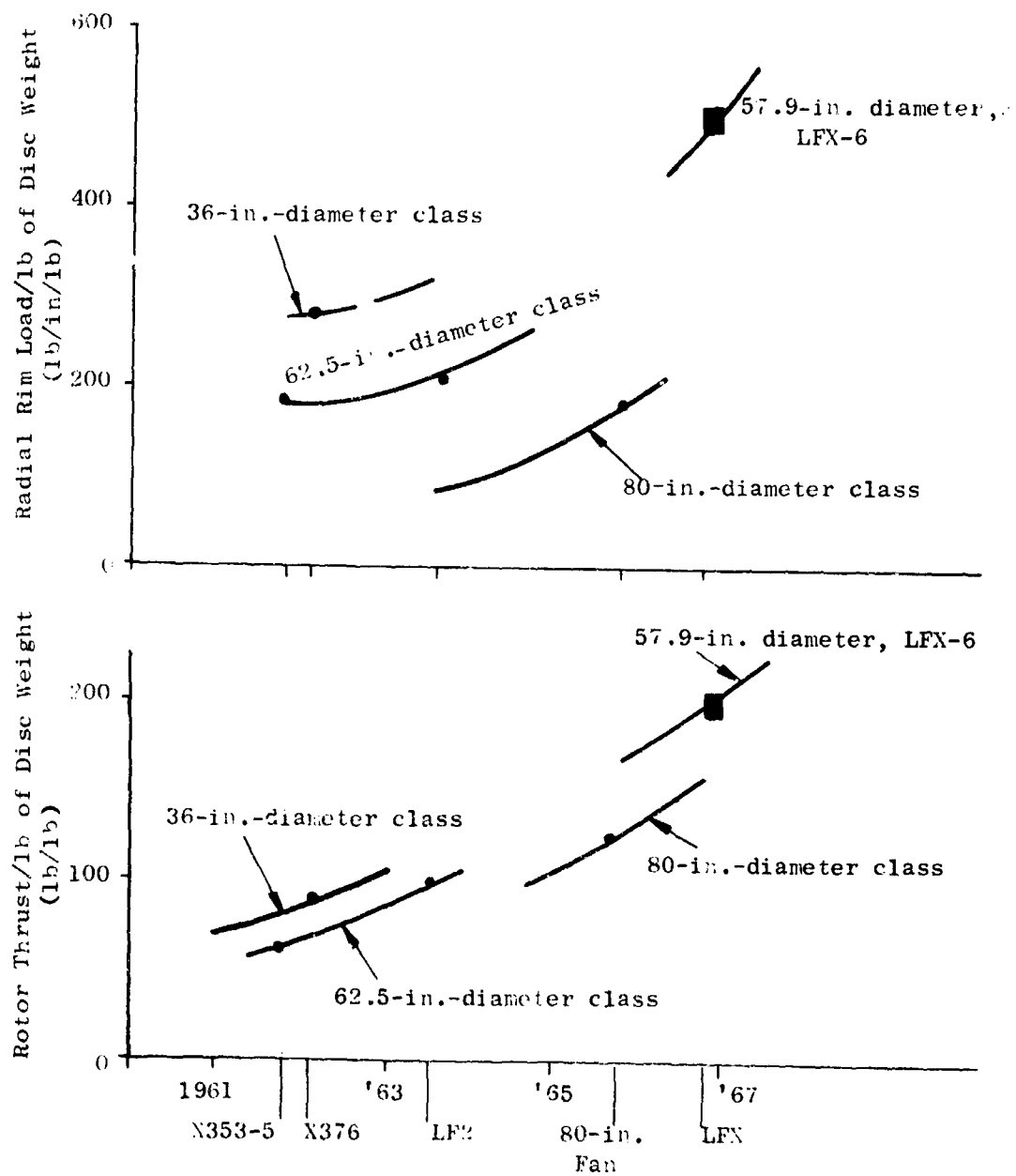


Figure 58. Rotor Disc Design Comparison.

The disc, although continuing to employ the twin web geometry proven in previous fans, avoids large bending stresses in the webs by forming the webs in catenary type shapes. This shape carries the disc rim load as pure tension and does not require the additional web thickness necessary to support added bending stresses. This design philosophy has also been recently applied to the design of NASA reentry bodies as pure tension shells with similar impressive results.

Reduction in the number of small parts has been accomplished. The outer seal and bearing retainer at each end of the disc sump have been combined into a double duty seal-retainer. The resulting advantages are fewer parts to control, inspect, and assemble, and better conduction of heat from rubbing seals.

Joining of the disc halves by diffusion bonding, instead of the bolted joints used in previous disc designs, offers major advantages. The joints are permanently fixed--insuring greater disc rigidity under maneuver loading and preventing possible dovetail mismatch that causes high loads on local surface faces. Weight is also reduced because of the elimination of the bolts at the rim and sump and because of a bolt flange at the sump. The cost reduction realized due to the elimination of the sump, flange and rim bolt holes will more than offset the close alignment tolerance requirements on disc half diffusion bonding joining surfaces.

Maximum advantage is made of fan axial space limitation by placing the bearings in a noncentered location with respect to the blade centerline, rather than centered as in previous fans. By shifting the bearings downward into the vacant area above the exit louvers, maximum space is provided above the disc for the structural front frame.

The ball thrust bearing is a press fit in the bore of the aft side of the disc. The thrust loading acts from the disc to the aft bearing retainer, to the ball outer race, through the balls to the forward half of the split inner race, and is supported by a shoulder on the shaft. The aft bearing retainer clamps the outer race of the bearing in the disc bore with a slight preload, 400 pounds on each of the 20 retaining bolts, to prevent bending the retainer at each start-stop cycle. The roller bearing is mounted to the forward side of the disc by a flanged bearing housing.

Piston-ring seals, similar to those used in the 80-inch cruise fan sump, are used on each side of the bearings to retain the grease packing. O-rings are used on each side of the bearing outer faces to prevent the loss of oil from the grease due to centrifugal forces. The roller bearing grease seal housings and inner race are held in position by a spacer which extends to the ball inner race forward surface. The inner race of the ball bearing is split to allow the installation of the maximum number of balls in order to obtain maximum load capacity. The ball bearing aft grease seal housing, used as an inner race retainer, is attached with a slight interference fit to assure a preload sufficient to withstand downward "g" forces.

In summary, the rotor geometric shape is basically similar to previous tip-turbine lift fan rotor designs, except for the following items:

1. The torque band is no longer a separate component part. In the LFX-6 design (Figure 57) the torque transmission system is integral with the turbine carrier bottom plate. This tangential force transmission from one carrier to another is required due to the loading created during partial scroll arc operation. A single bolt, through shear and friction loading, transfers this tangential force from one carrier to the next while providing differential thermal growth capability. This torque transmission system design provides low axial stiffness, thus helping to lower the 6 node wheel mode critical speed.
2. The turbine carrier has an external carrier support block, shielding, and internal cross-sectional baffling which prevent hot gas scrubbing of these external support blocks and provide a flow path for cooling the fan blade tangs. The tips of the fan blades are cooled by flow from the airfoil pressure side to the airfoil suction side, while blocking turbine gas from entering the carrier internal cavity. This method of tang cooling is incorporated in the LF-2 demonstrator test vehicle and is being further investigated.
3. The fan inner hub flow-path platform does not require separate component parts. In the LFX-6 design the platform is integral with the fan blade shank. This consolidation eliminates the need of platform attachment flanges and hardware, thus reducing weight.
4. The fan blade forward retainer, along with its hardware, is eliminated and blade retention in the disc is accomplished by an integral tab on the lower side of the blade dovetail and by separate retainer lugs, each of which secures two adjacent blades. Each lug is attached to the disc by two bolts and a rabbet providing a fail-safe feature.
5. Pin through bolts in the disc rim have been eliminated and diffusion bonding will be employed to join the two disc halves. This allows a larger number of blades to be inserted in the disc, which reduces the tip load per blade and thus reduces the individual blade-to-disc dovetail loading.

The one area which shows the largest weight reduction possibilities is the blading. This would require going to hollow titanium blading which is not considered feasible within program/material/process technology and timing objectives. A 12-pound saving could be realized through hollow titanium blading, but this would require a significant development effort. Of course, removal of weight above the disc (i.e., fan blades and turbine

sectors) would result in further weight reductions in the disc and the disc-to-blade attachment. A reduction in fan tip speed would also be a step toward lower objective weights. However, the rotor system appears to be stiffness limited rather than stress limited. This means that system vibratory criticals and deflection are dictating the rotor weight. The LFX-6 blade target weights were:

Tang (includes Transition)	4.648 pounds
Airfoil	34.675 pounds
Shank and Platform	5.759 pounds
Dovetail	<u>8.440 pounds</u>
Total	53.522 pounds

The calculated weights for the LFX-6 design are:

Tang	6.2 pounds
Airfoil	46.2 pounds
Shank and Platform	7.7 pounds
Dovetail	<u>11.2 pounds</u>
Total	71.3 pounds

The rotor polar moments of inertia for the various fan designs are:

LFX-6	12.2 lb-ft-sec ²
X376	1.2
X353B	28.4
LF-2	21.5

Sump

The sump layout (Figure 59) is grease packed with outer race rotation, as used on the LF-2, X376, and lift/cruise tip-turbine fans. It is composed of a ball bearing assembly and a roller bearing assembly spaced 4.5 inches apart.

The ball bearing assembly includes a grease shield, O-ring, ball bearing, O-ring, and a grease seal and retainer assembly. This subassembly is located and clamped in the aft side of the disc bore between the disc shoulder and the aft flange.

The shield is formed of 0.020-inch titanium sheet and provides a pocket for maintaining, or preventing loss of, grease on the forward side of this bearing.

The O-rings are located in grooves in each face of the outer race of the bearing. These O-rings prevent the loss due to centrifuging of the oil from the grease (between the mating surfaces of the shield, outer race and bearing retainer). The O-ring is 1/16-inch-diameter Buna-N rubber.

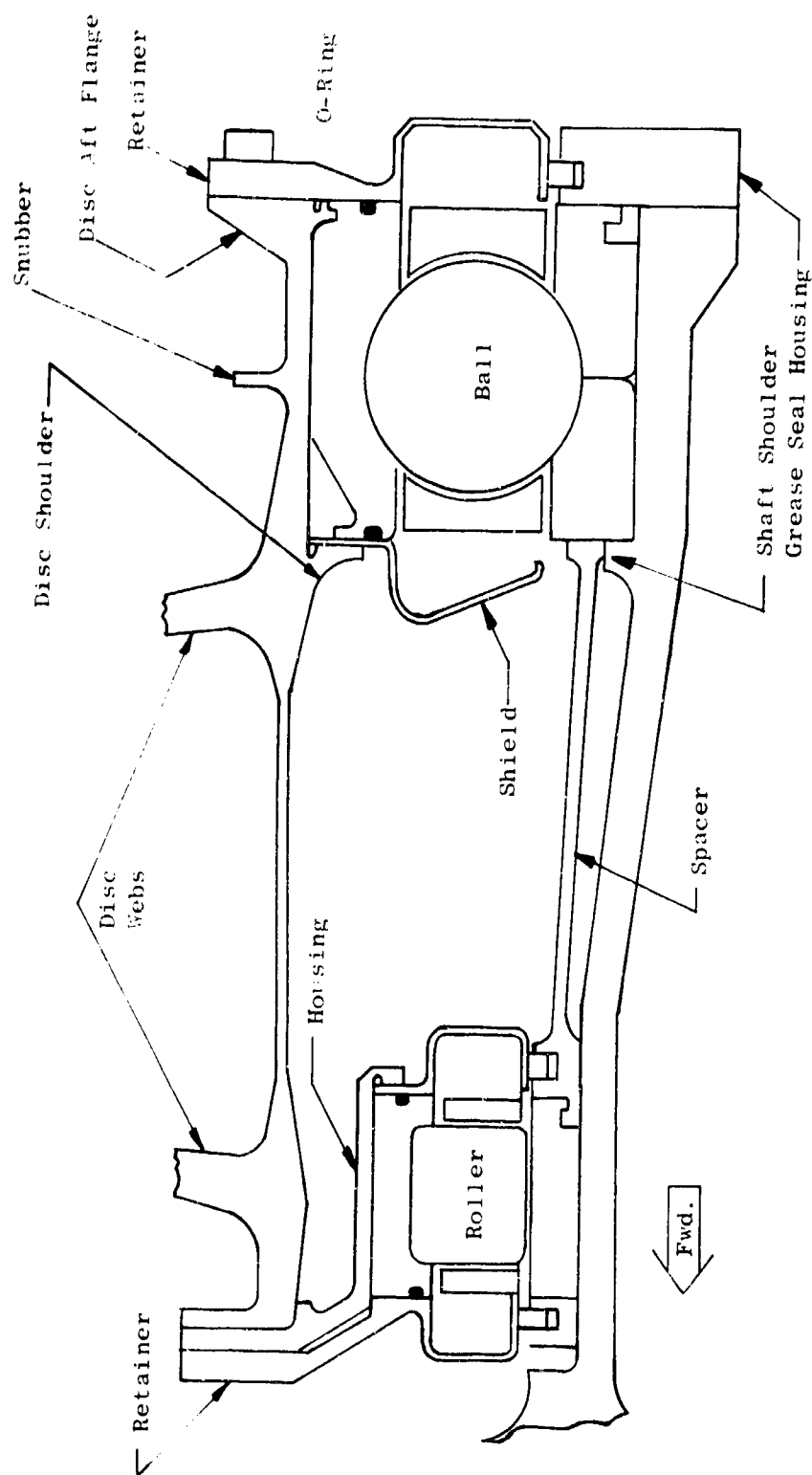


Figure 59. Sump Configuration.

The ball bearing, which has a deep groove and split inner race construction, transfers the rotor axial and radial loads to the rear frame shaft. Puller grooves are located in both the inner and outer race for bearing removal.

The ball bearing retainer has multiple functions. It retains the bearing in the disc, transfers rotor forward axial loads from the disc to the bearing outer race, forms the aft grease cup and provides a mating surface on which the grease seal piston ring seal slides and attaches. Twenty 10-32 size bolts and nuts secure the retainer to the disc aft flange. Each bolt supports a 400-pound load when the maximum forward axial load of 8000 pounds is acting. This 400-pound load produces a tensile stress of 24,000 psi in the bolts.

The piston-ring grease seal is similar to that used in the 80-inch tip-turbine lift cruise fan sump. It consists of a runner, a teflon-impregnated piston ring, a stainless steel expander ring, and a housing (Figures 59 and 60). The piston ring loads against the runner during operation and slides on one of the radial faces of the housing. A 0.025-inch radial clearance is provided between the runner and the housing for best operation. The housing also serves as the inner race retainer to the shaft, clamping it between a shoulder on the shaft and the shaft aft flange. A flush fit-up at the bearing outer race and runner assures a grease supply to the bearing by preventing trapping of the grease away from the bearing. This type seal has been tested more than 22 hours at temperatures to 180°F in the 80-inch cruise fan geometry size and at surface speeds of 6349 feet per minute with satisfactory results. In the LFX-6 design the surface speed is 5754 feet per minute or 9.4 percent less than that of the 80-inch lift cruise fan.

The roller bearing subassembly consists of a bearing retainer and forward grease seal, O-ring, roller bearing outer race, O-ring, aft grease seal and outer race housing. This subassembly is located at the forward side of the disc. Size 10-32 bolts secure the bearing housing and retainer to the disc forward flange. The retainer, O-rings, and grease seals are similar in geometry and function to the ball bearing assembly. The bearing housing rabbets on the inner radius of the disc flange. This arrangement of disc and bearing housing minimizes the bearing out-of-rotational plane deflections of the outer race. Minimum out-of-rotational plane deflections are required for best roller bearing operation. The inner race of the bearing is mounted on the shaft between the two grease seal housings and is positioned by the inner race spacer. Puller grooves are located in the inner and outer races for bearing disassembly.

Weight

The LFX-6 rotor weight is 169.86 pounds, 20 percent more than the objective weight of 141.0 pounds. The rotor weight objective is quite ambitious in that the preliminary design weight of 165 pounds (Reference 1) was reduced to an objective weight of 141 pounds. At the same time the fan tip diameter was decreased by 1 inch and the tip speed was increased from 950 to 975 feet per second. This diameter decrease, coupled with the tip velocity increase, increased the fan blade tip "g" field by 13 percent while decreasing

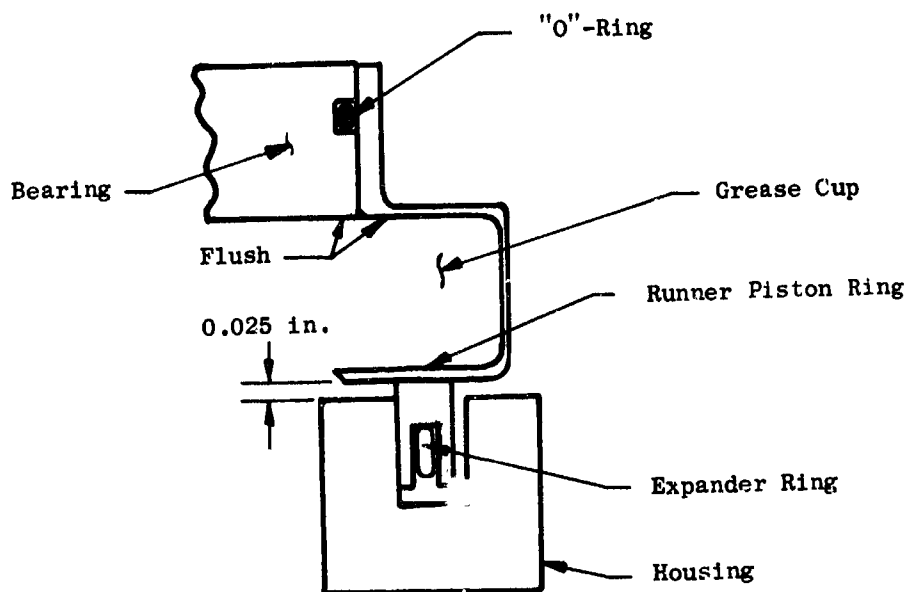


Figure 60. Grease Seal Configuration.

the tip mass by only 1.8 percent. This actually requires that the rotor become heavier in order to support the added loading induced by the larger "g" field. A breakdown and a comparison of the various rotor weights are given in Table X.

Design Analysis

Fan Blades

The LFX-6 fan parameters defined by the aerodynamic design work are given in Table IX. As noted previously, solid titanium blades and "tip-tang" turbine sector attachment were also part of the design criteria.

The LFX-6 blade geometry and the distribution of chord, t_m/C , t_e/C , stagger angle, and camber angle are shown in Figure 61.

The loading considered in the LFX-6 blade design included the centrifugal force, the blade air loads, and the gyroscopic maneuver loading. Figure 62 shows the "g" field as a function of radius for the 115-percent rated speed (4681 rpm). The preliminary tangential and axial air loads acting on the rotor blades are shown in Figure 63. These air loads are given for the rotor as a disc and must be distributed equally among the rotor blades.

A Twisted Blade Program analysis of the LFX-6 blade was made for the steady-state case which included the centrifugal effect as well as the air loading. During these analyses, the boundary conditions at the blade root were assumed fixed while the blade tip was assumed pinned. The sketch in Figure 64 shows the assumptions made for blade length. The centrifugal force applied to the fan blade by the tip turbine mass was included in the Twisted Blade analysis. This tip load (at 115-percent N_f) is 12,868 pounds (based on a turbine sector design weight of 0.7338 pound). The tip load would be 9112 pounds for the turbine sector objective weight of 0.5196 pound. The steady-state stresses, deflections, and loading distributions are shown in Figures 65 through 68 for the 100-percent fan speed point.

A dynamic analysis using the Twisted Blade Program determined the blade natural frequencies for the fundamental modes of blade vibration. The preliminary Campbell diagram is shown in Figure 69. In addition, Figures 70 through 75 show the stress and deflection distributions for the first flexural, first torsional, and second flexural modes of the blades. The reduced velocity parameter for the 115-percent N_f is 2.31 (2.06 at 100 percent N_f). Gyroscopic analysis of the LFX-6 rotor was made for a precession rate of 1 radian per second at 115-percent N_f . Figures 76 through 79 show the gyroscopically induced stresses and deflection of the blades. The wheel critical speeds for cosine 2θ and cosine 3θ using this blade design are approximately 96.5-percent N_f (unsatisfactory) and 60-percent N_f respectively.

The tang dimensions were selected to carry the maximum tip load without exceeding the 0.02-percent yield strength at points of local stress concentrations. The sketch in Figure 80 shows the dimensional ratios which were

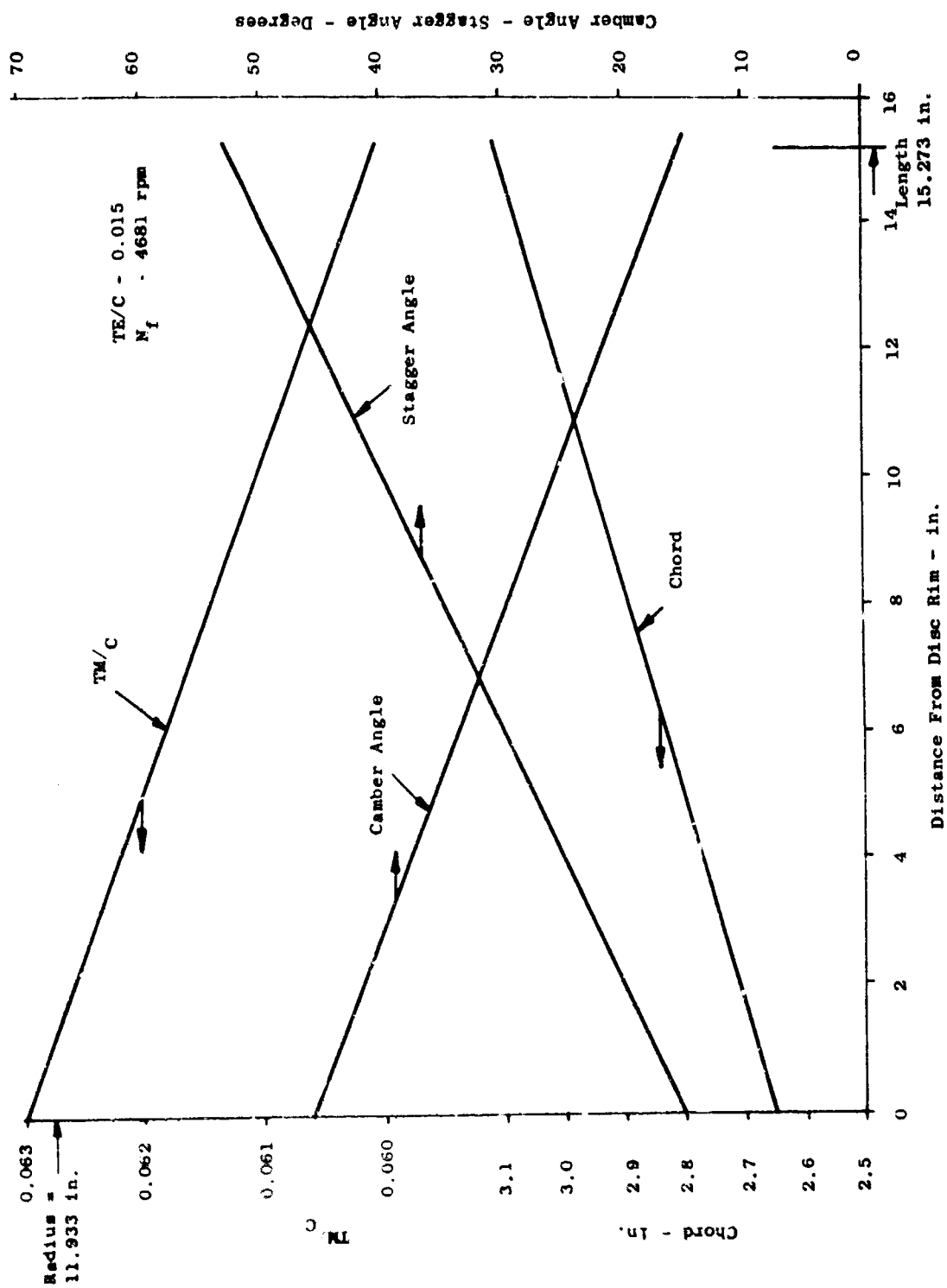


Figure 61. Blade Geometry.

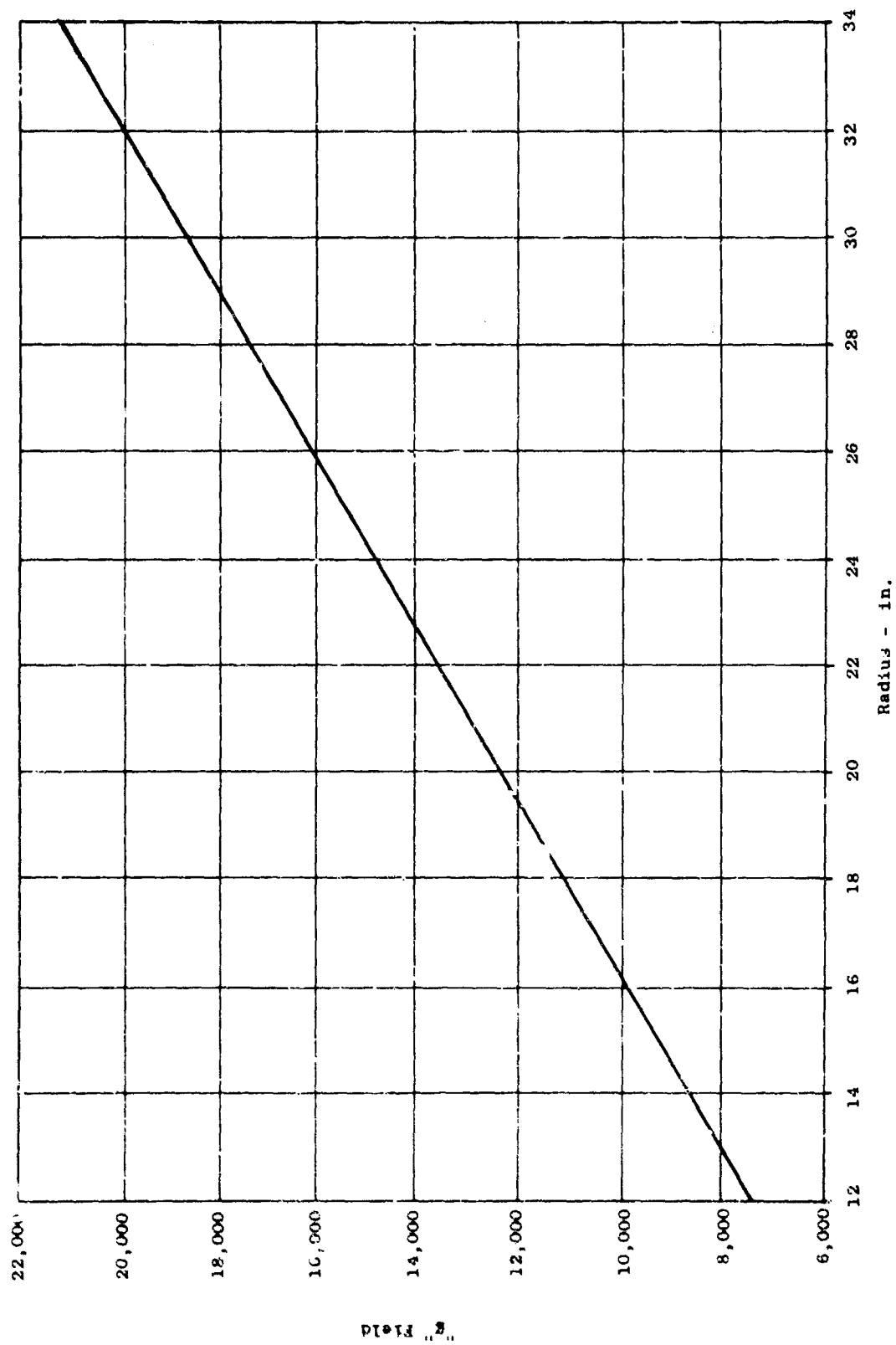


Figure 62. Rotor "g" Field Versus Radius.

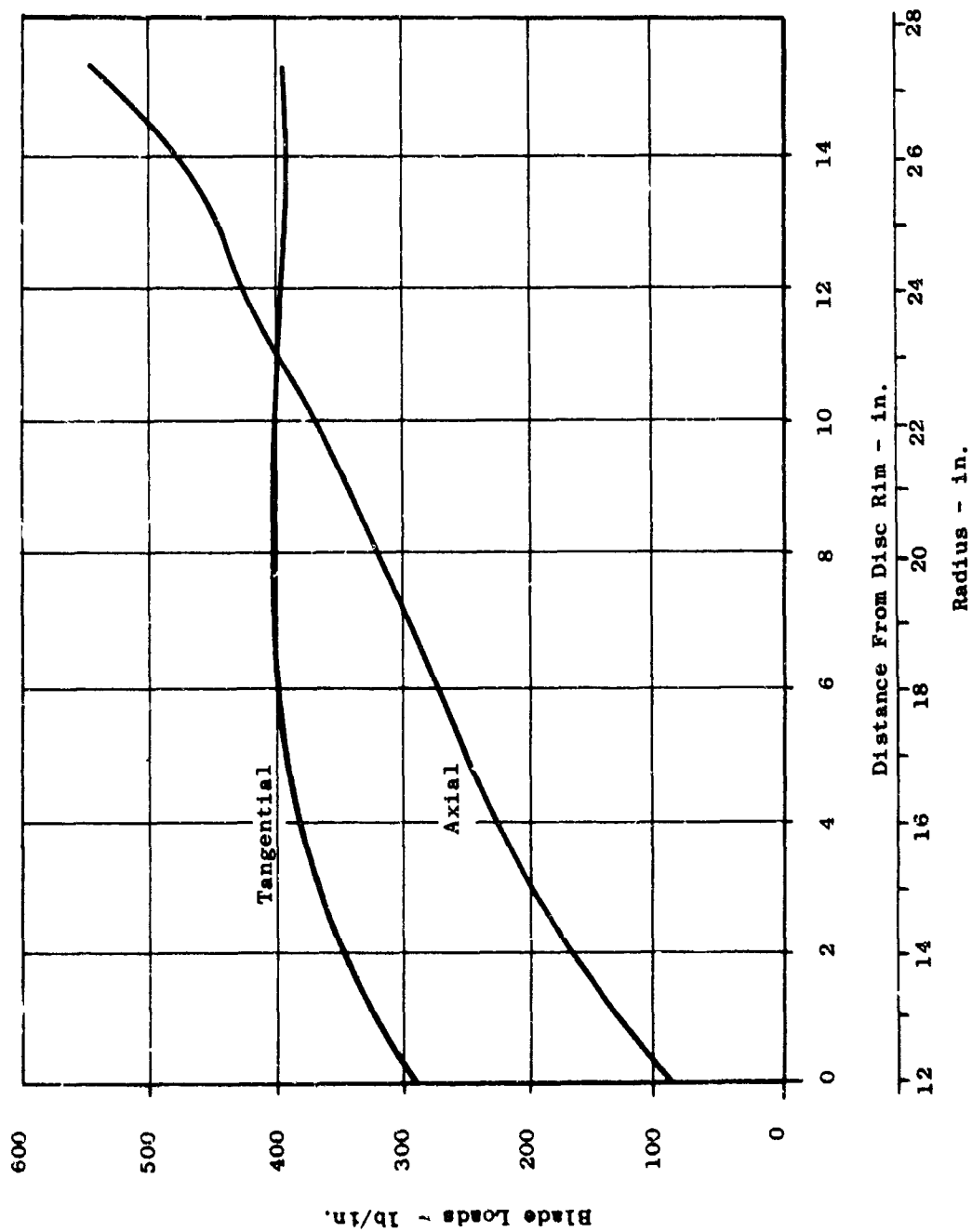
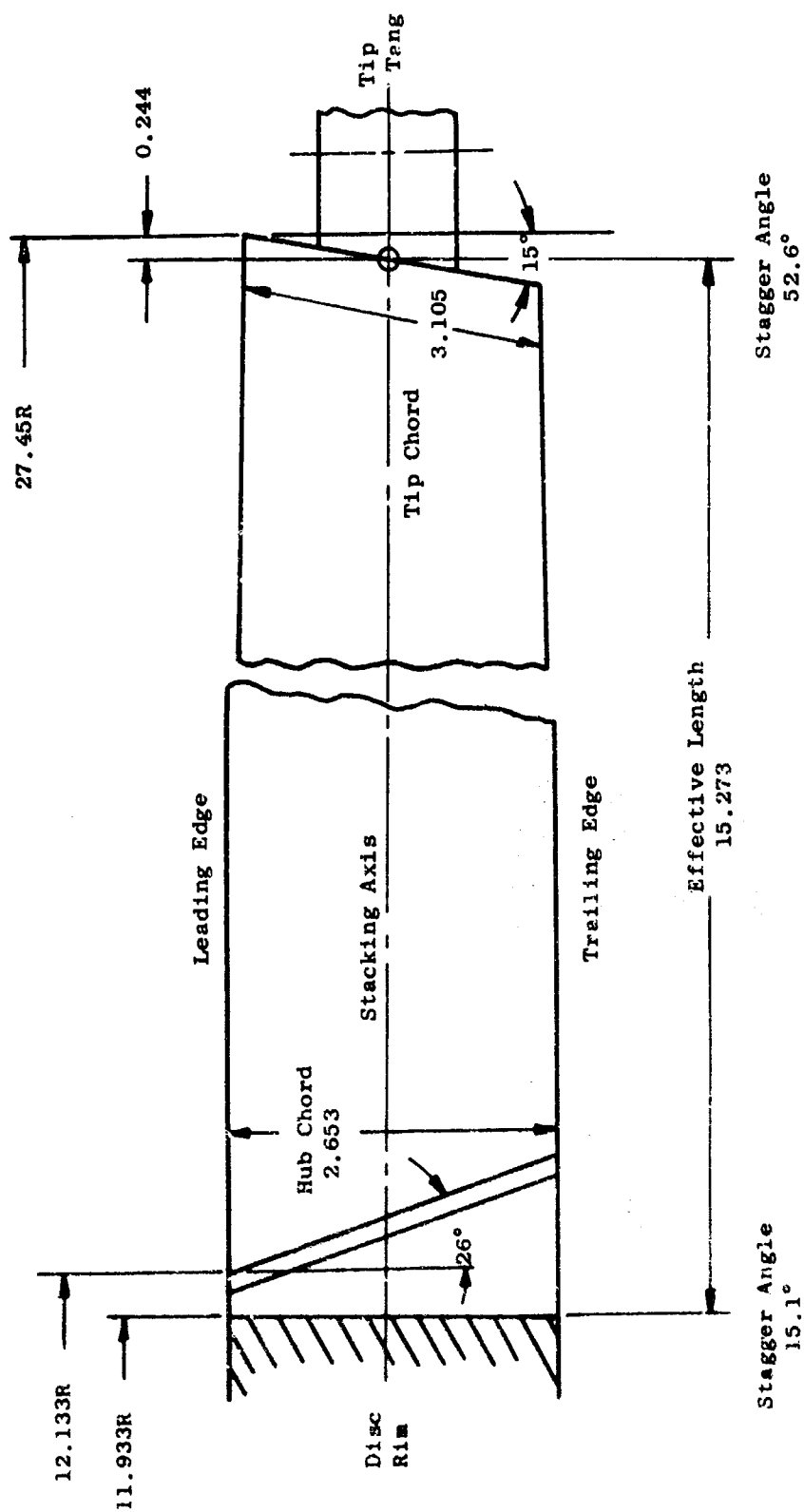


Figure 63. Blade Air Loads.



(All Dimensions in Inches)

Figure 64. Blade Geometry.

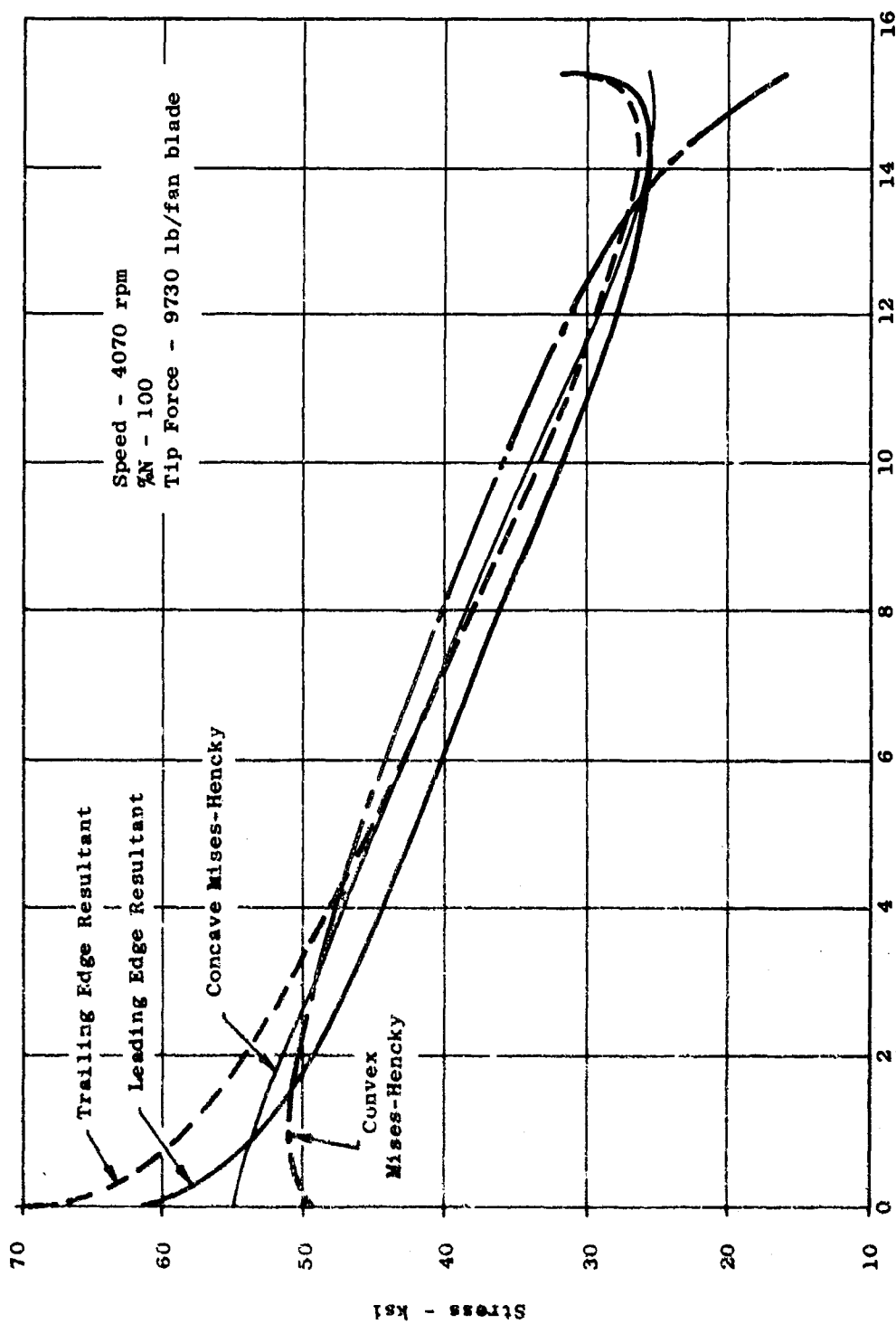


Figure 65. 100-Percent N_f Blade Stress.

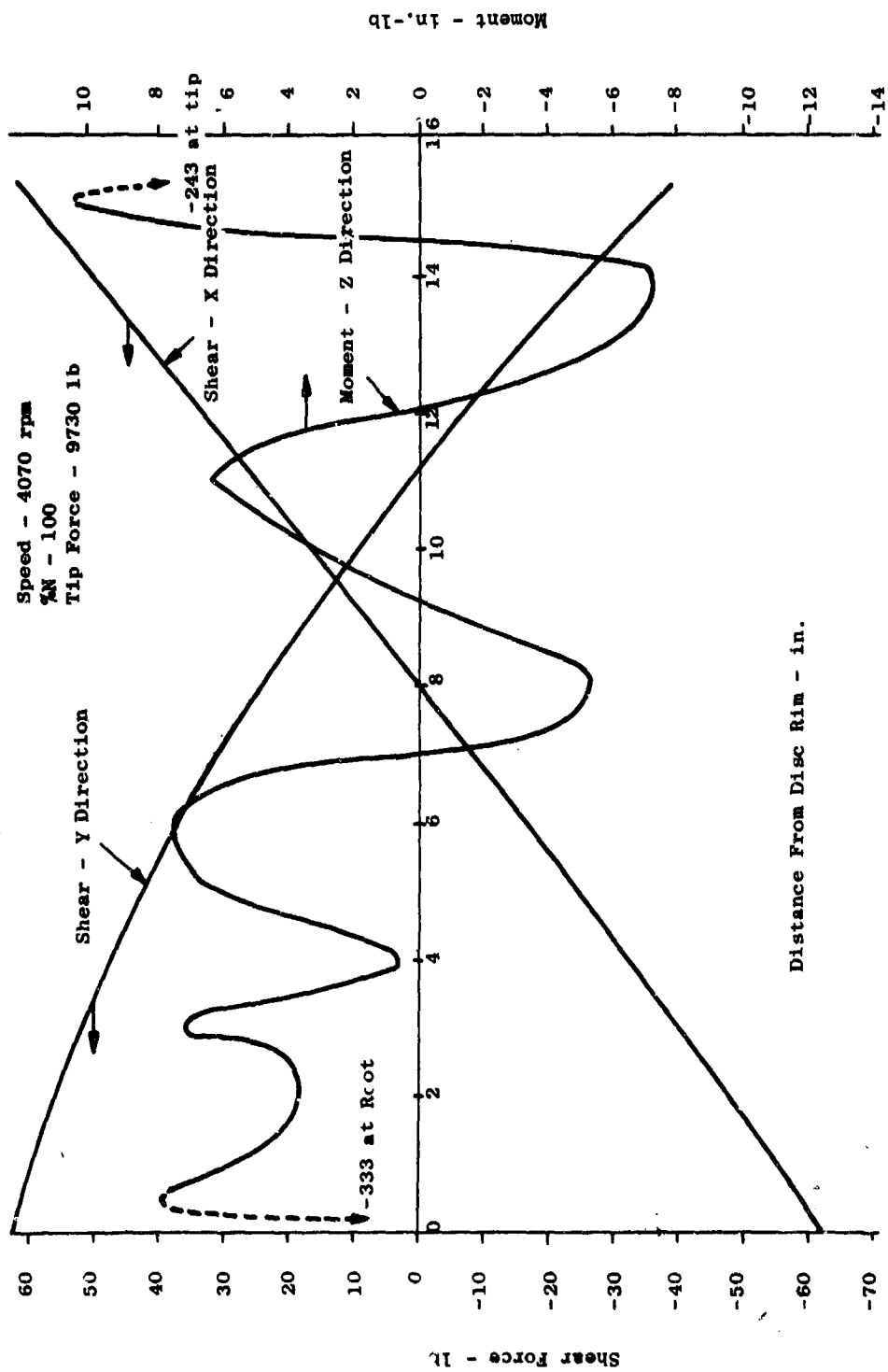


Figure 66. 100-Percent N_f Blade Shear.

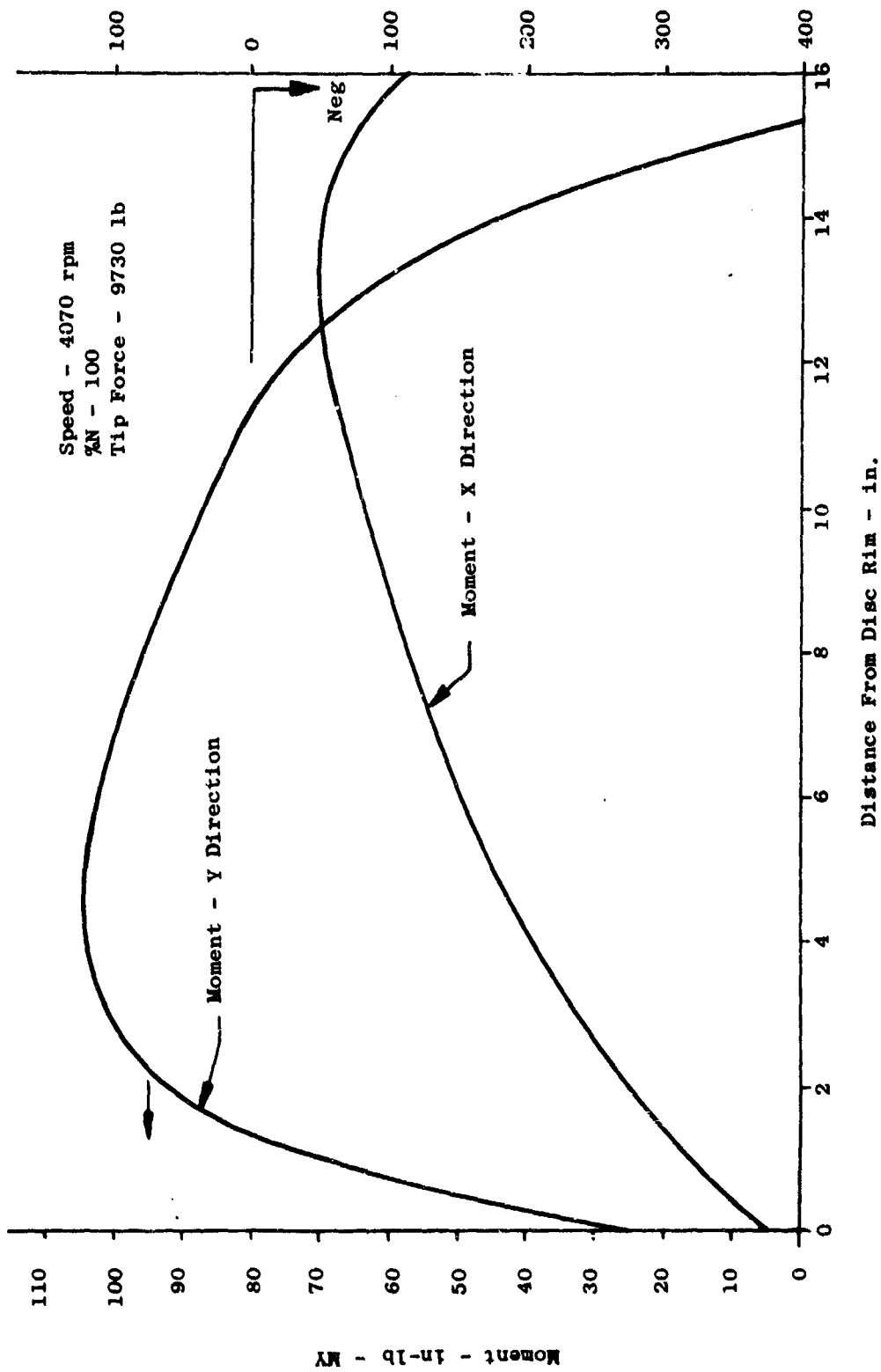


Figure 67. 100-Percent N_f Blade Moment.

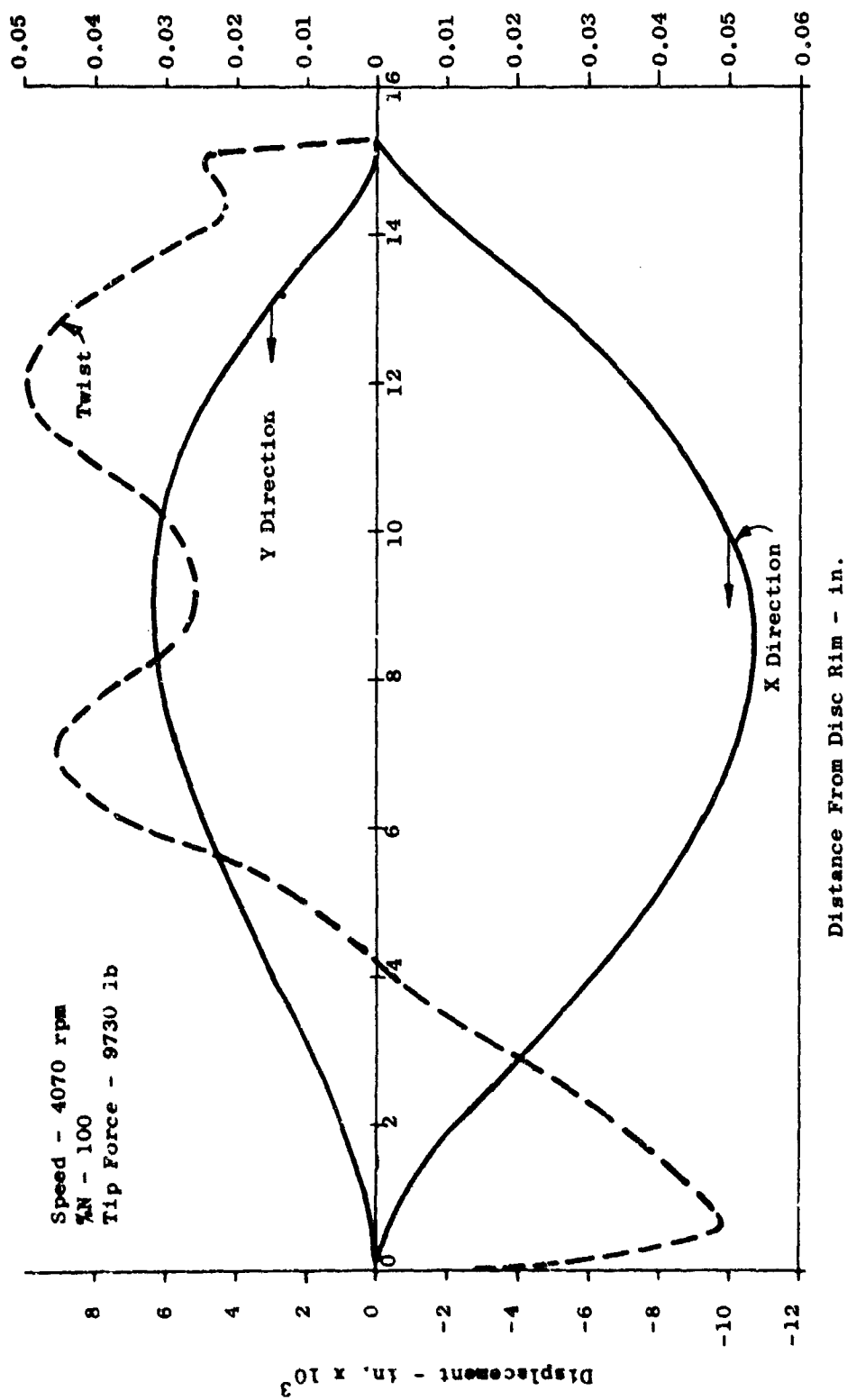


Figure 68. 100-Percent N_f Blade Displacement.

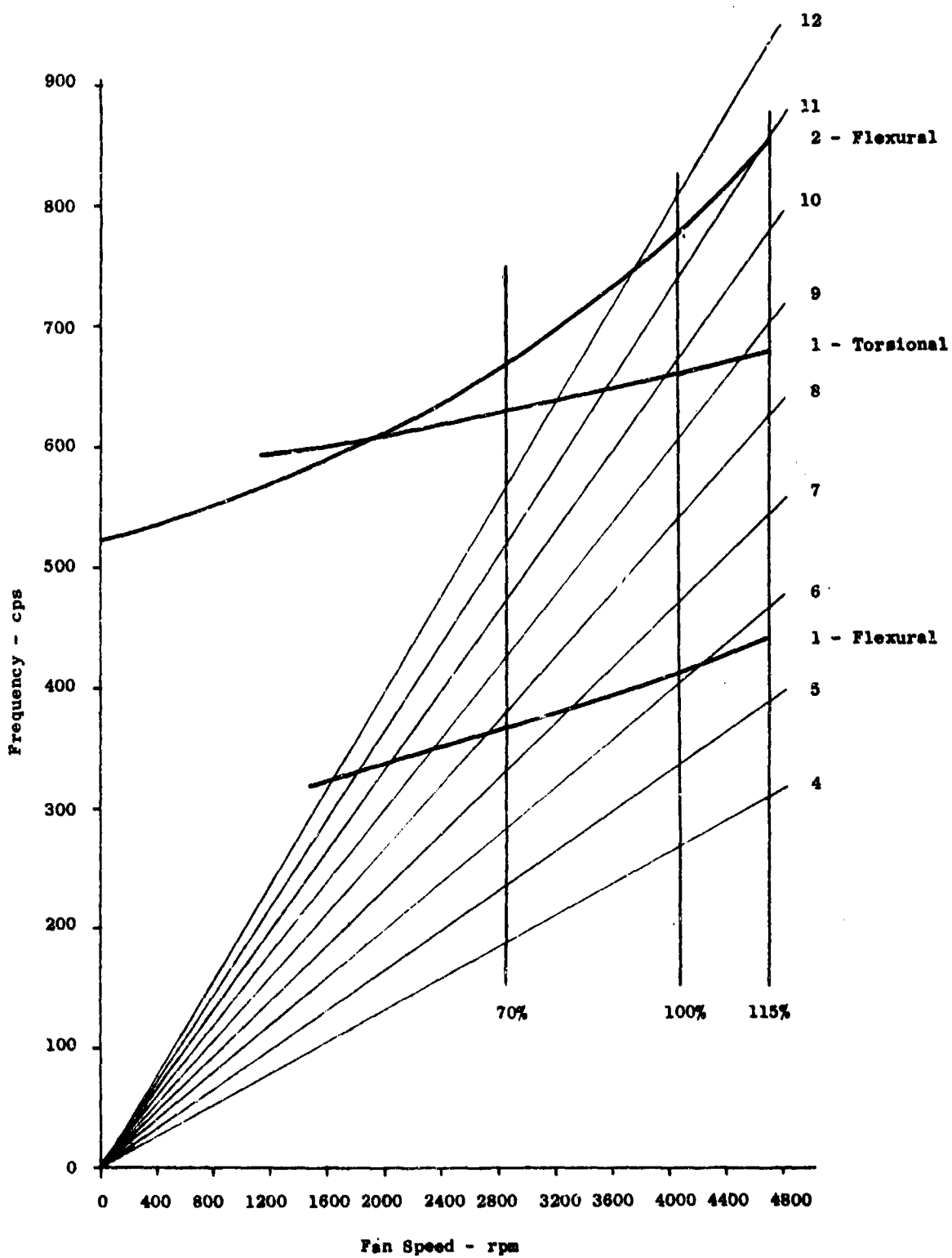


Figure 69. Blade Campbell Diagram.

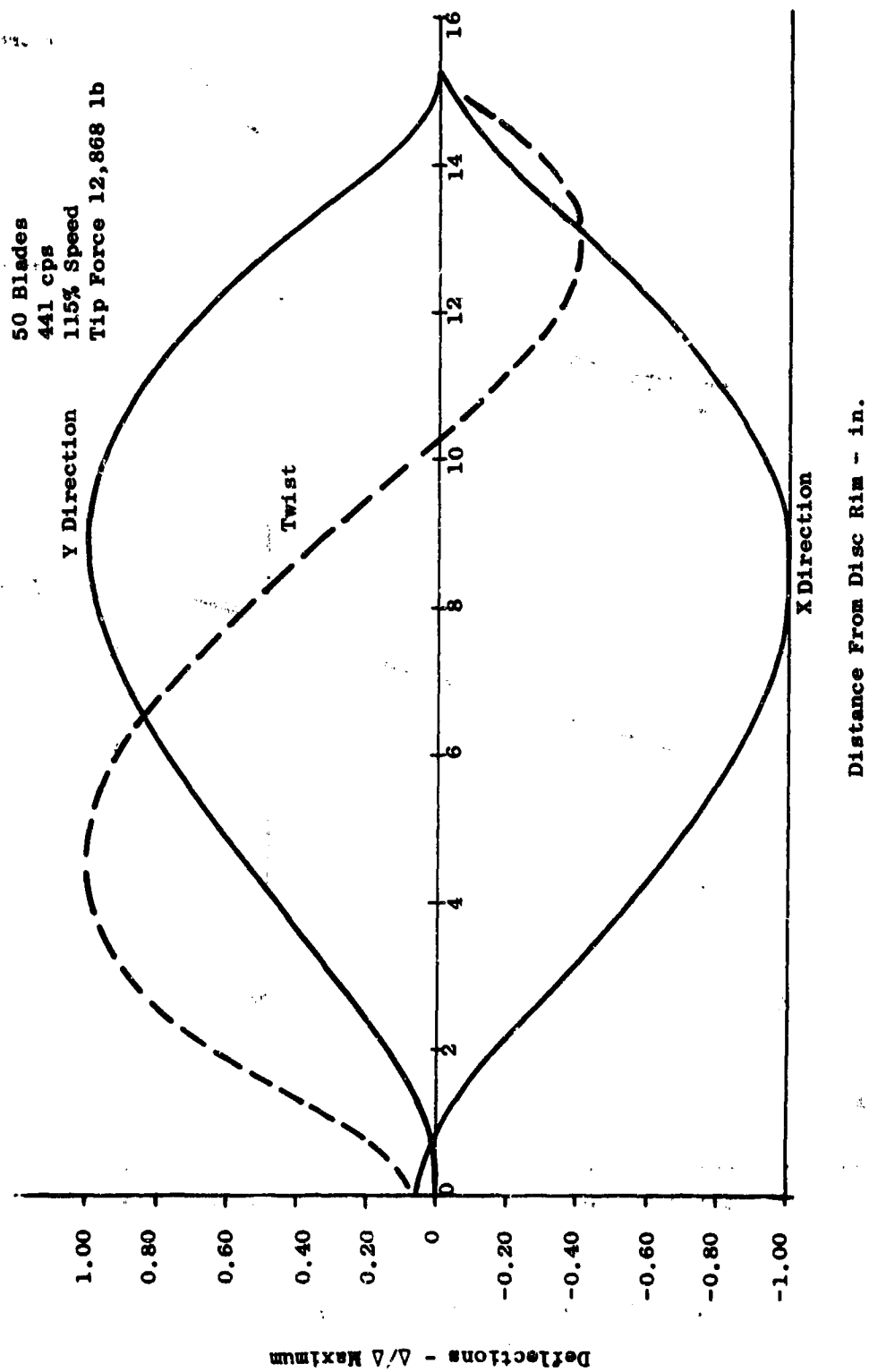
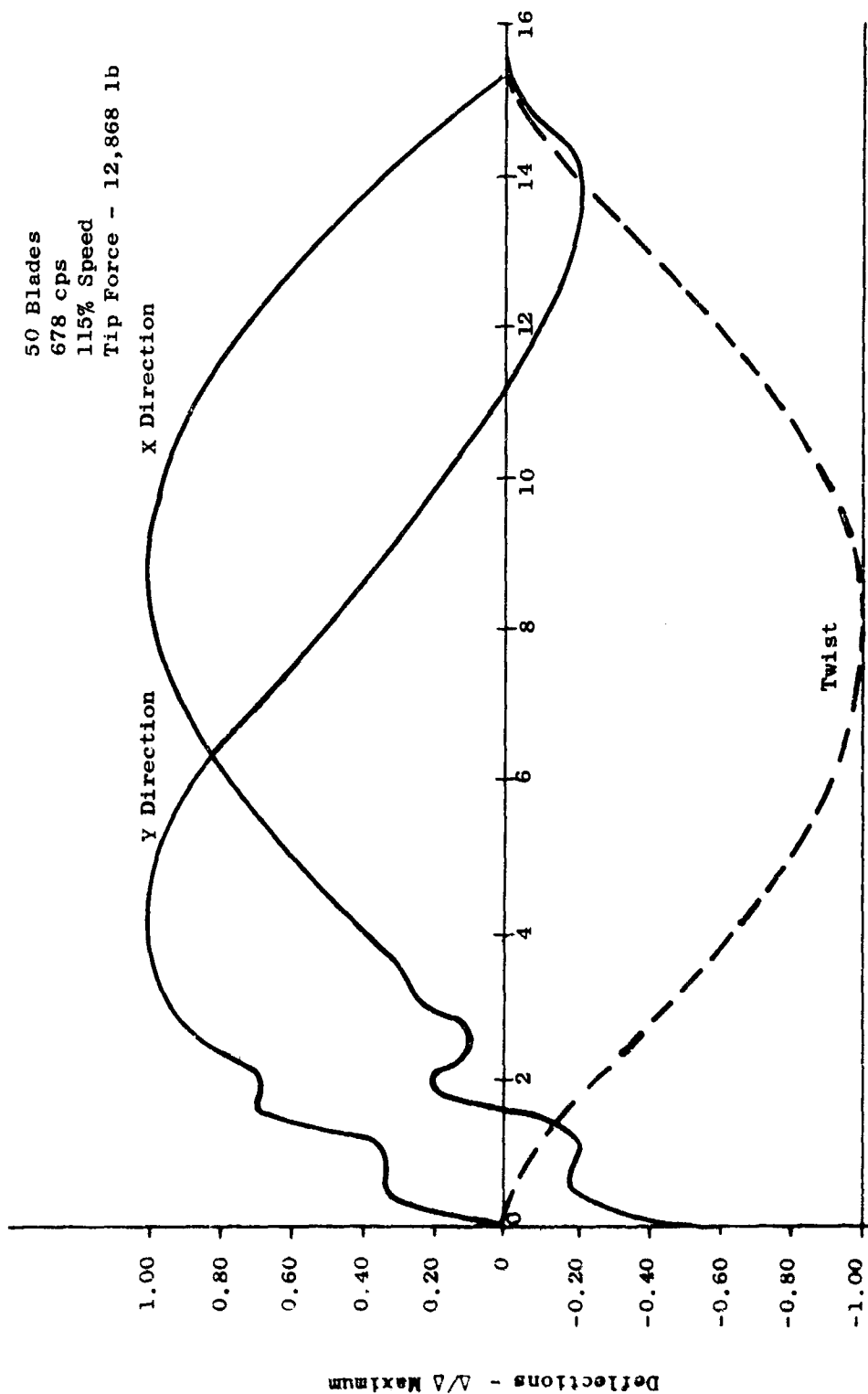


Figure 70. First Flexural Mode Blade Deflection.



Distance From Disc Rim - in.

Figure 71. First Torsional Mode Blade Deflection.

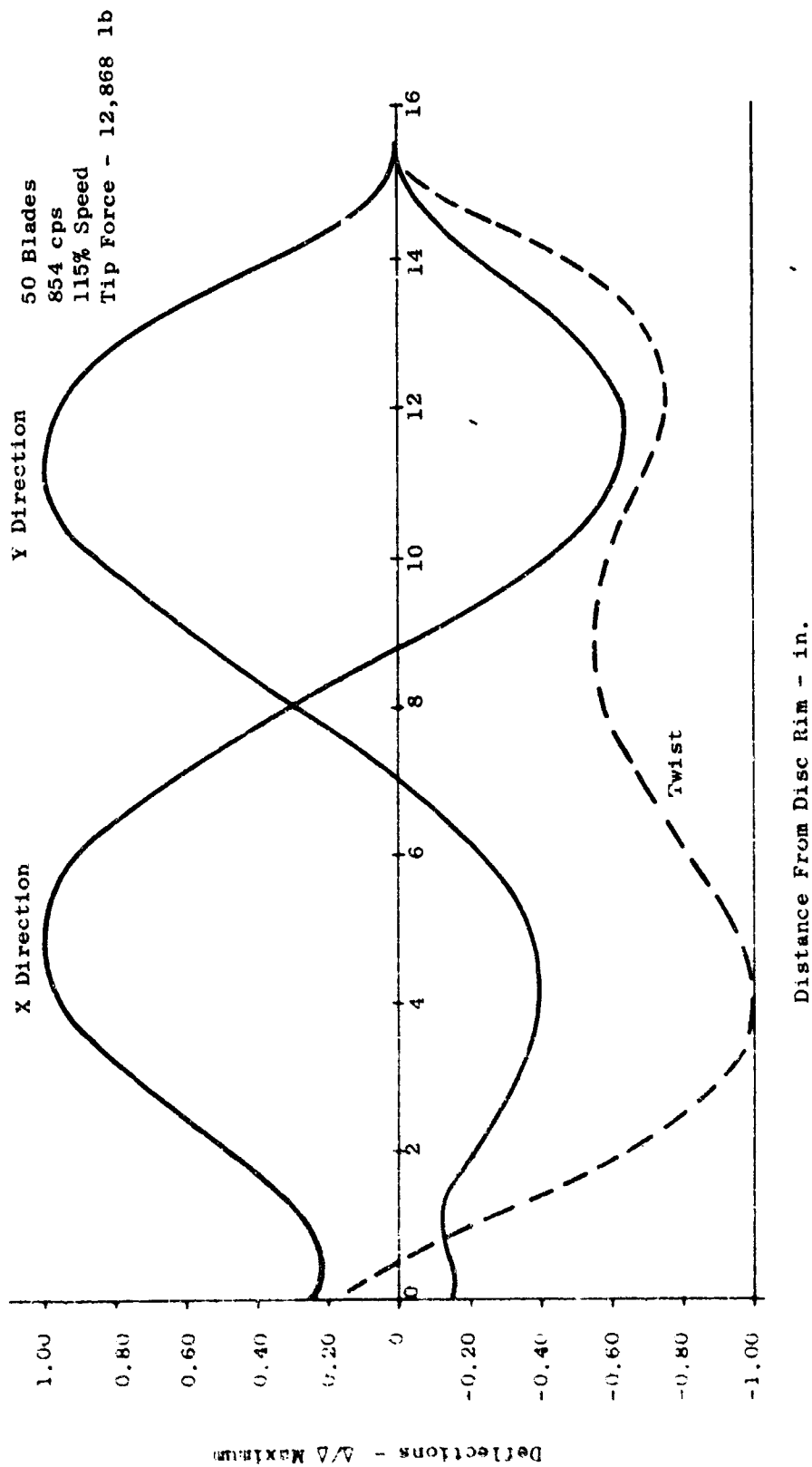


Figure 72. Second Flexural Mode Blade Deflection.

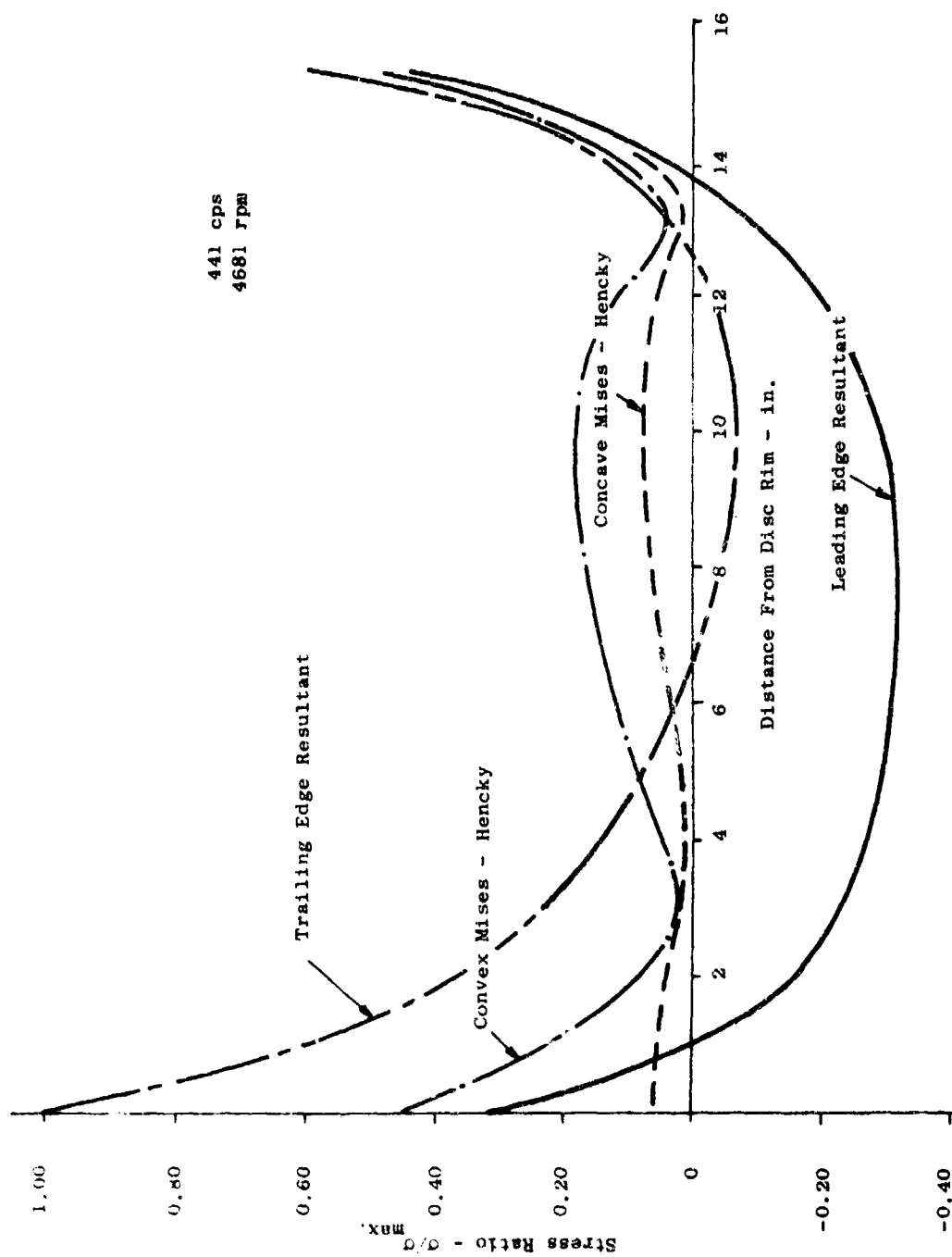


Figure 73. First Flexural Mode Blade Stress Ratio.

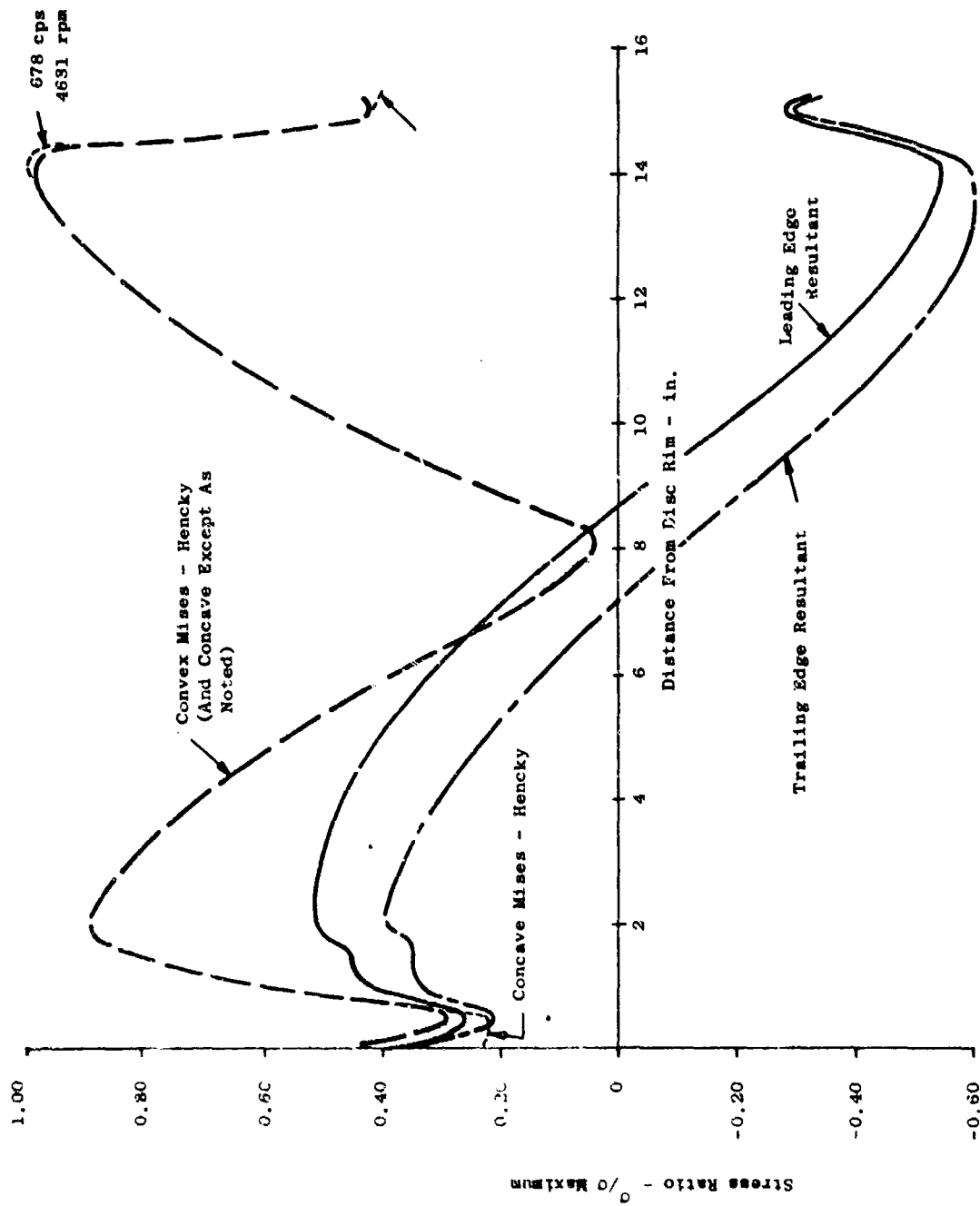


Figure 74. First Torsional Mode Blade Stress Ratio.

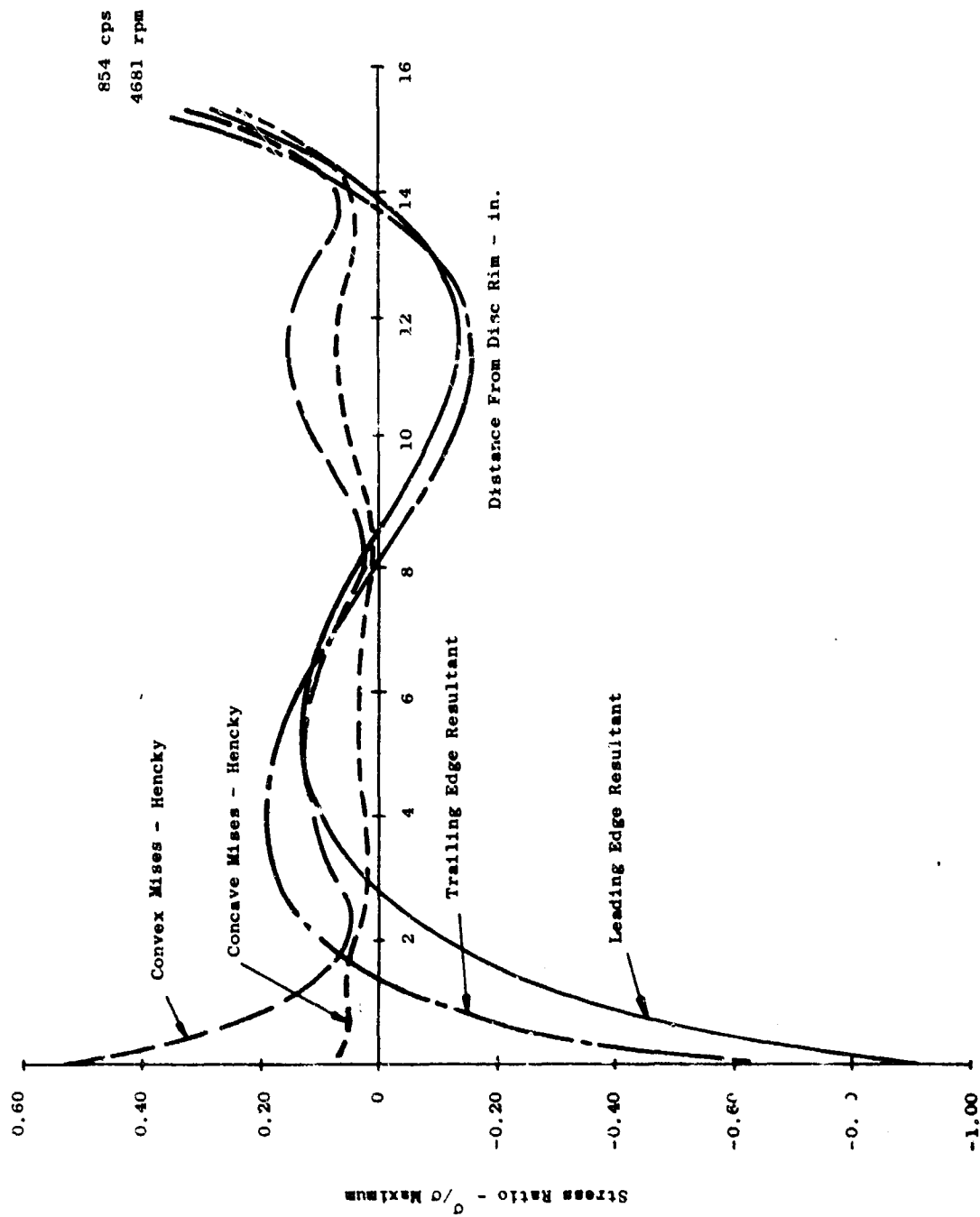
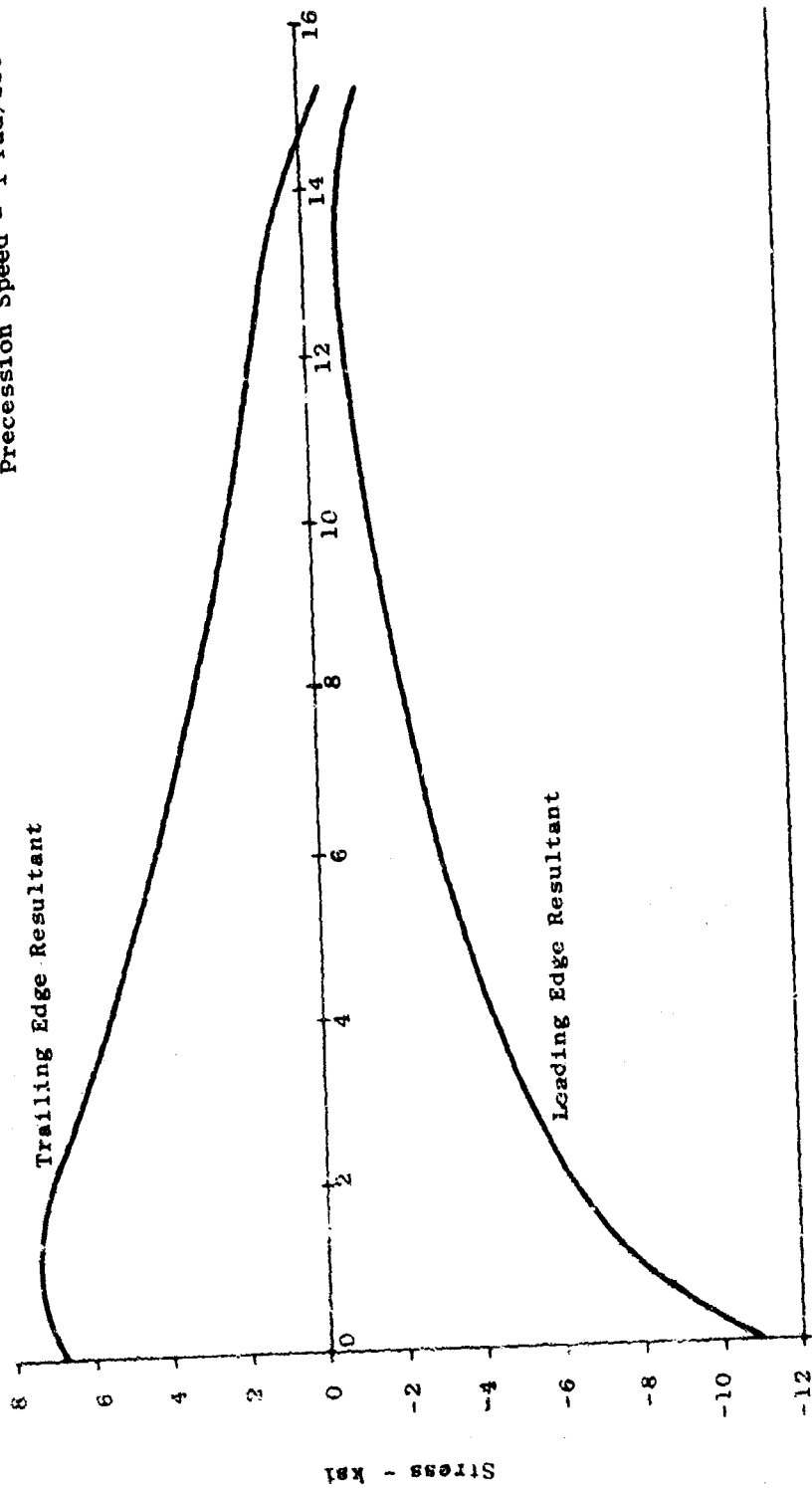


Figure 75. Second Flexural Mode Blade Stress Ratio.

Rotor Speed - 4681 rpm
 Blade Freq - 78 cps
 Precession Speed - 1 rad/sec



Distance From Disc Rim - in.

Figure 76. Gyroscopic Blade Stress.

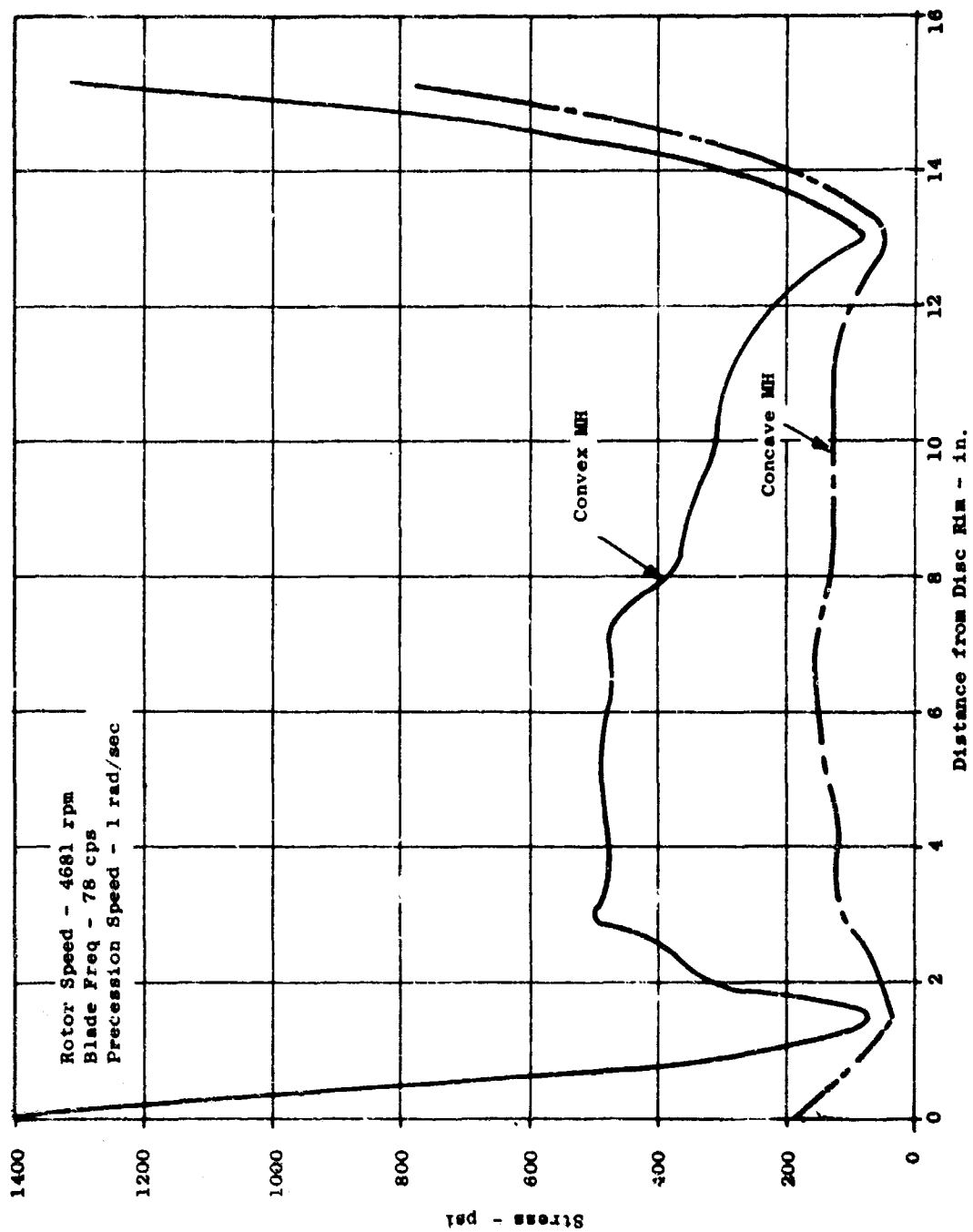


Figure 77. Gyroscopic Blade Stress.

LFX-6 Blade Gyroscopic Axial Deflection

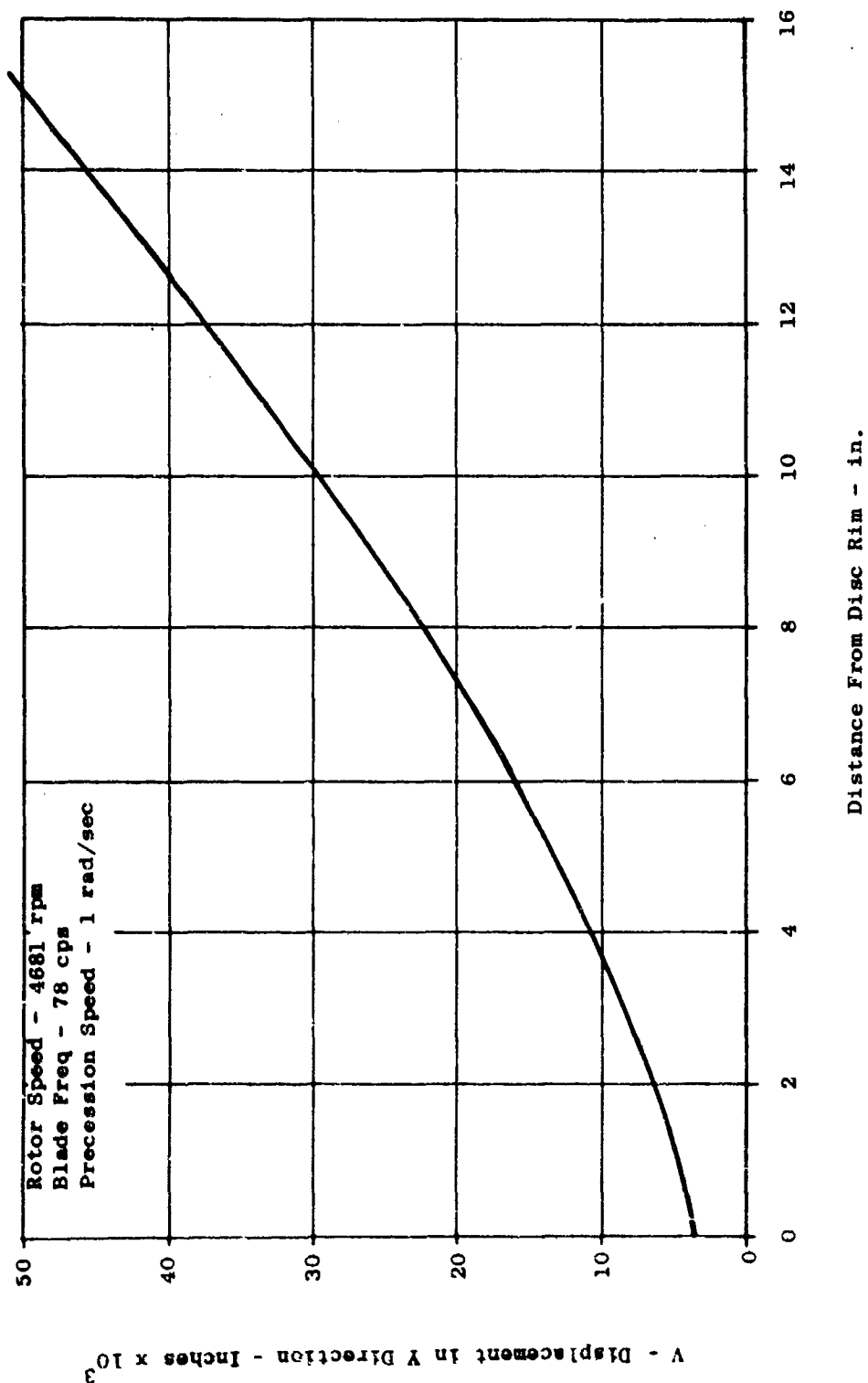


Figure 78. Gyroscopic Blade Deflection.

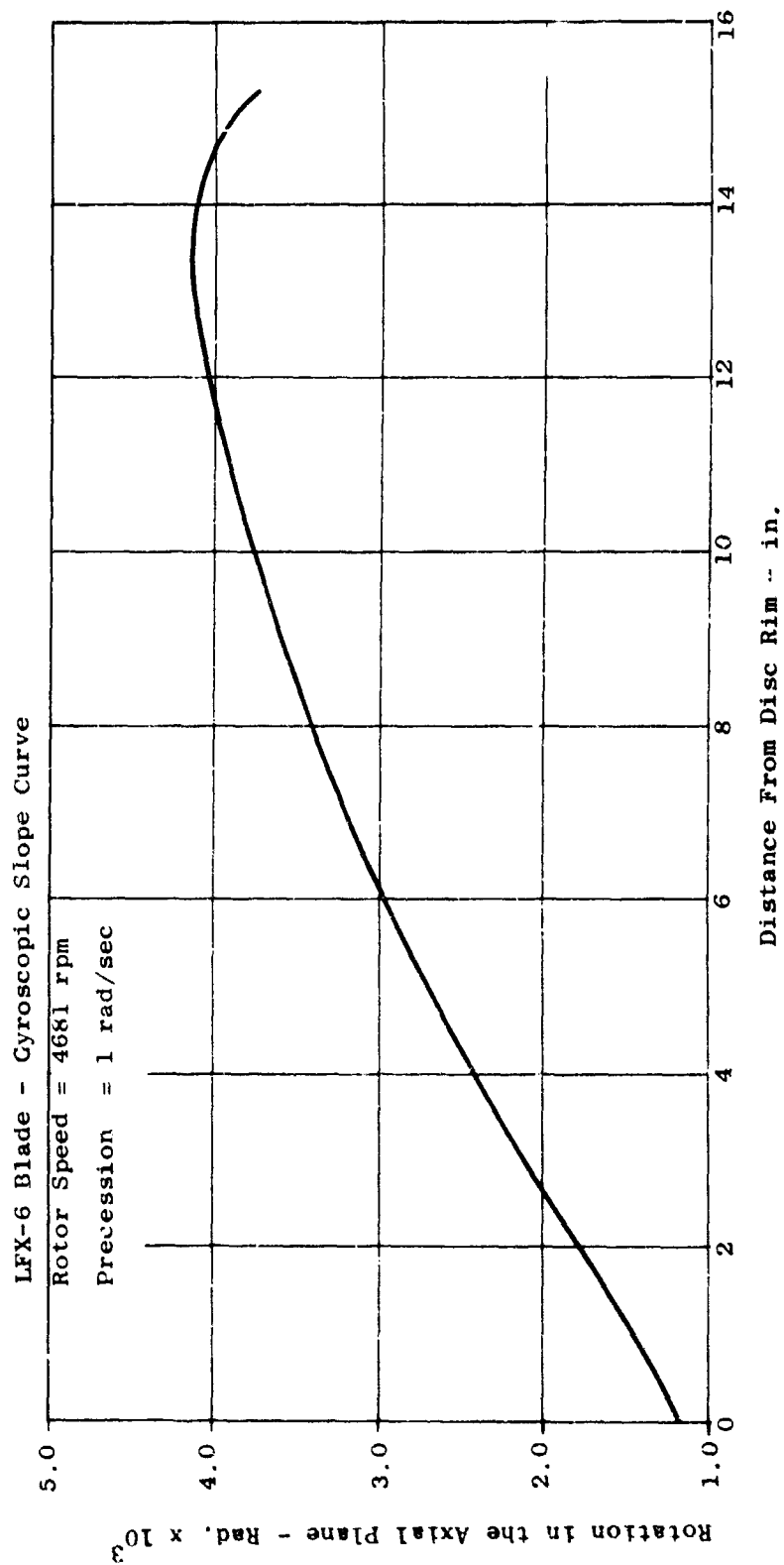


Figure 79. Gyroscopic Blade Slope.

used and lists the limiting values normally used in tip-tang design. The transition from the tang to the airfoil section is similar to the X376 fan blade.

The LFX-6 has a single hook straight dovetail to attach the blades to the disc. Figure 81 shows two views of the dovetail portion of blade and disc (approximately true size). The lip on the aft edge of the blade dovetail fits into a notch in the aft face of the disc to prevent the blade from sliding forward in the disc slot. Retainers bolted to the aft face of the disc rim complete the positive location of the blades in the disc. The inner flow path is formed by the platform which is integral with the fan blade.

The criteria used for sizing of the dovetail were based on dovetail design techniques used successfully in previous fans and compressors. They included:

Single tang

55 degrees face angle

40 ksi average blade shank centrifugal stress

25 ksi average disc neck centrifugal stress

30 ksi average tang crushing stress

H.J. Macke's Single Tang Dovetail Analysis (Reference 12)

Figure 82 shows the steady-state stresses in the blade and disc dovetails due to aerodynamic and centrifugal loads on the blades and dovetails. This figure defines the locations at which these stresses occur. The material selected for both the disc and the blade is 6AL6V2SN titanium. Figure 83 shows a Goodman diagram for this material with the steady-state and permissible vibratory stresses in the blade, the blade dovetail and the disc dovetail when the blade is vibrating in the first flexural mode. These stresses were calculated by scaling the vibratory loads in the blade so the blade stresses are at the allowable material limit. These loads are then put into the Single Tang Dovetail Analysis Program along with the steady-state blade loads. The worst resulting dovetail stresses are shown in the figure. The disc dovetail is stronger than the blade dovetail, which in turn is stronger than the blade itself. This ensures that any vibratory failure will occur in the blade where less mass is involved, rather than in the dovetail.

The LFX-6 fan rotor was analyzed for gyroscopic forces, for the two-wave axial mode (cosine 2θ), and for the three-wave axial mode (cosine 3θ) critical speed.

The parameters used for these analyses were:

Disc

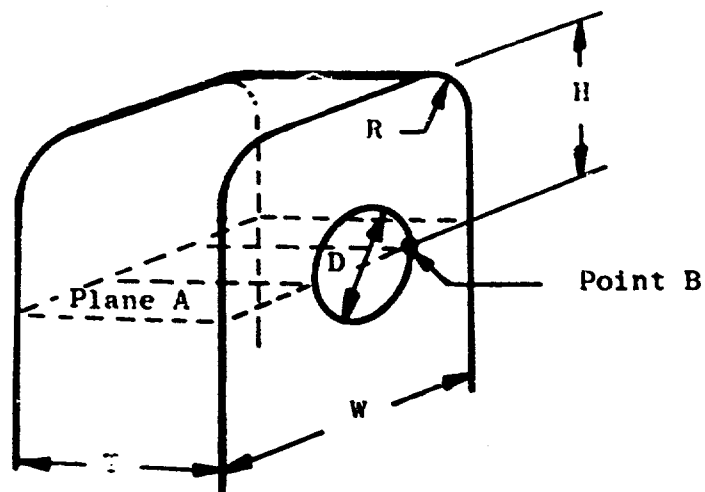
Web root radius = 4.2 inches

Web tip radius = 11.933 inches

Web root thickness = 0.169 inch

Web tip thickness = 0.145 inch

Web tip spacing = 1.33 inches



Criteria:

Net Tensile Stress - Plane A	25,000 psi
Bearing Stress in Hole	\leq 50,000 psi
Theoretical K_T at Point B	$=$ 1.5
Length to Diameter Ratio - Bolt	$\frac{T}{D} \leq$ 1.65

Resulting Size:

$D = 0.350$ in.
$T = 0.551$ in.
$H = 1.050 D$
$W = 3.330 D$
$R = 0.500 D$

Figure 80. Tang Schematic.

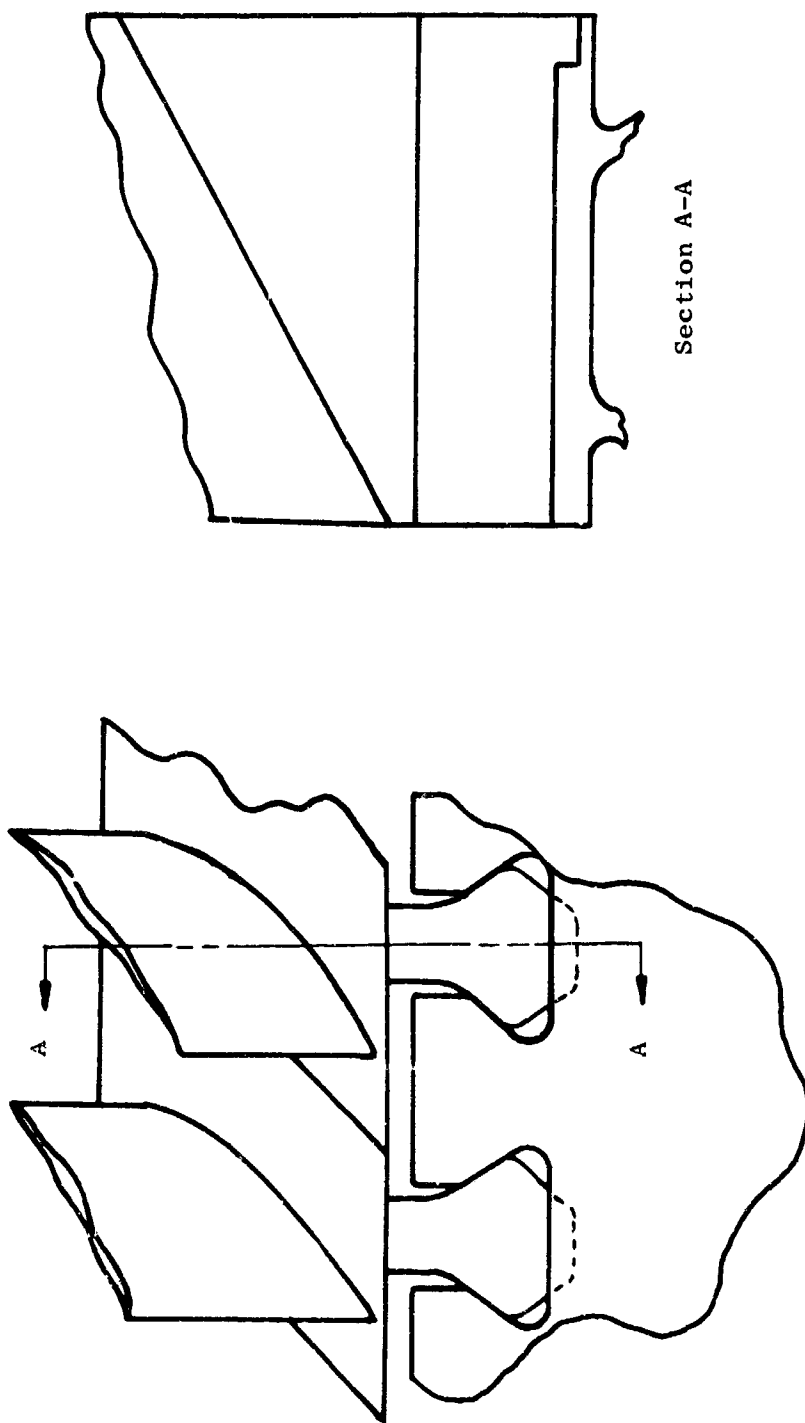
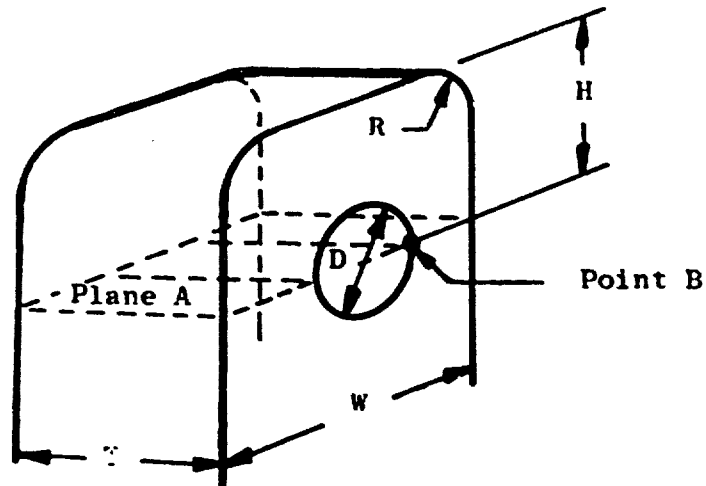


Figure 81. Dovetail Configuration.



Criteria:

Net Tensile Stress - Plane A		25,000 psi
Bearing Stress in Hole	\leq	50,000 psi
Theoretical K_T at Point B	$=$	1.5
Length to Diameter Ratio - Bolt	\leq	1.65

Resulting Size:

$$D = 0.350 \text{ in.}$$

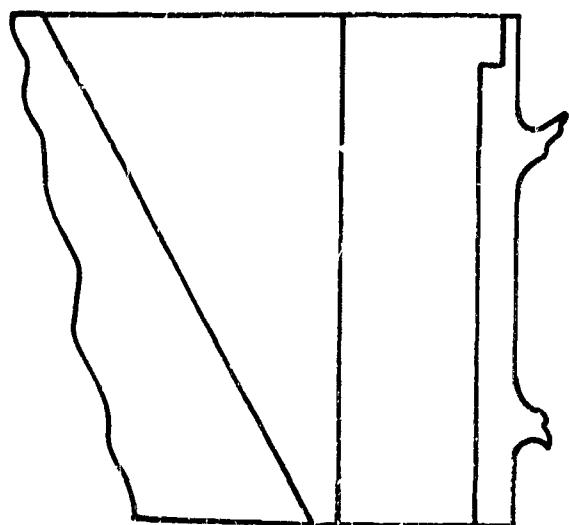
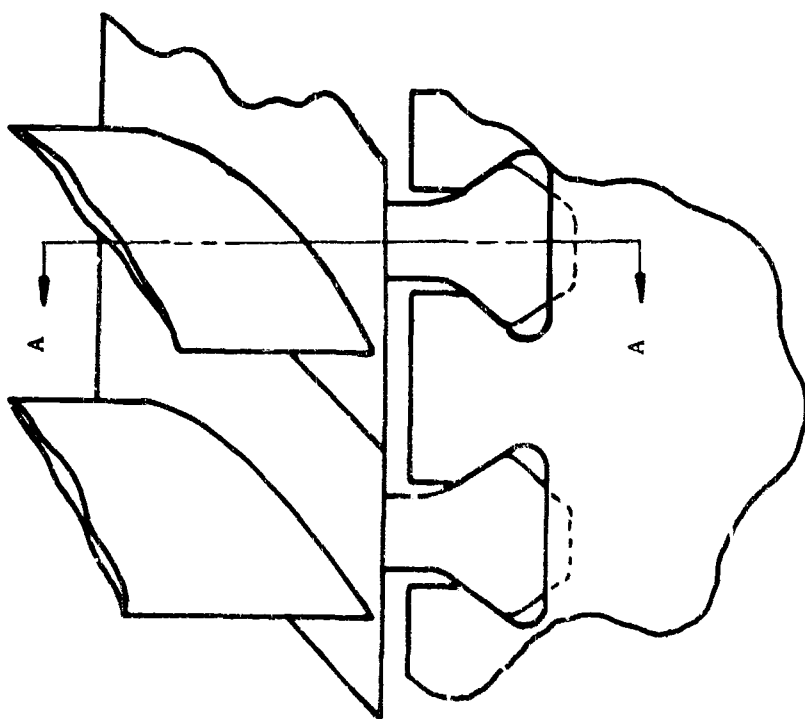
$$T = 0.551 \text{ in.}$$

$$H = 1.050 D$$

$$W = 3.330 D$$

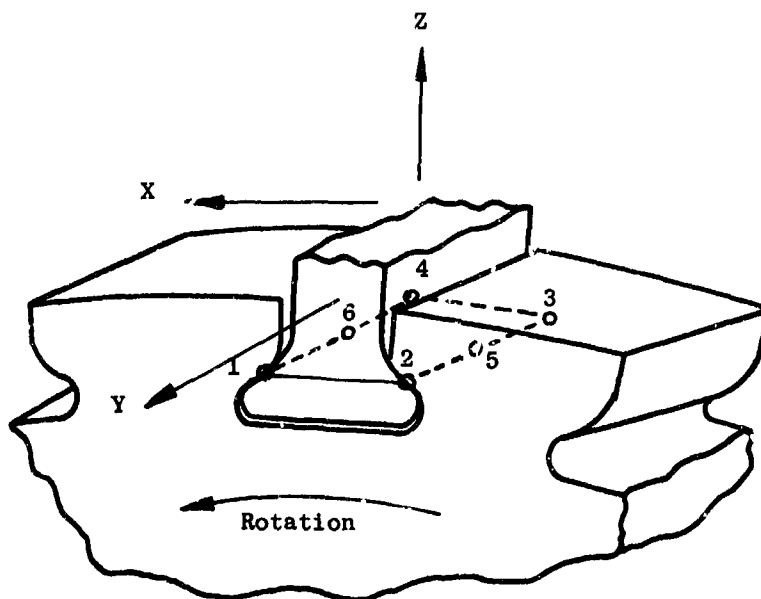
$$R = 0.500 D$$

Figure 80. Tang Schematic.



Section A-A

Figure 81. Dovetail Configuration.



Steady Stresses - ksi

<u>Blade Dovetail</u>						
1	2	3	4	5	6	Corner
21.2	37.3	21.5	42.7	29.7	32.2	Combined
10.4	20.8	9.8	24.5	15.3	17.5	Neck Tensile
11.1	17.2	12.0	19.0	14.6	15.0	Tang Bending
5.6	8.7	6.1	9.6	7.4	7.6	Tang Shear
9.8	15.2	10.7	16.8	12.9	13.3	Tang Crush

<u>Disc Dovetail</u>						
1	2	3	4	5	6	Corner
17.5	31.8	17.4	36.6	31.8	33.7	Combined
10.0	20.6	9.1	24.4	14.9	17.2	Neck Tensile
8.5	13.2	9.3	14.6	11.2	11.6	Tang Bending
4.8	7.5	5.2	8.3	6.4	6.5	Tang Shear
9.8	15.2	10.7	16.8	12.9	13.3	Tang Crush

Figure 82. Blade and Disc Dovetail Stresses.

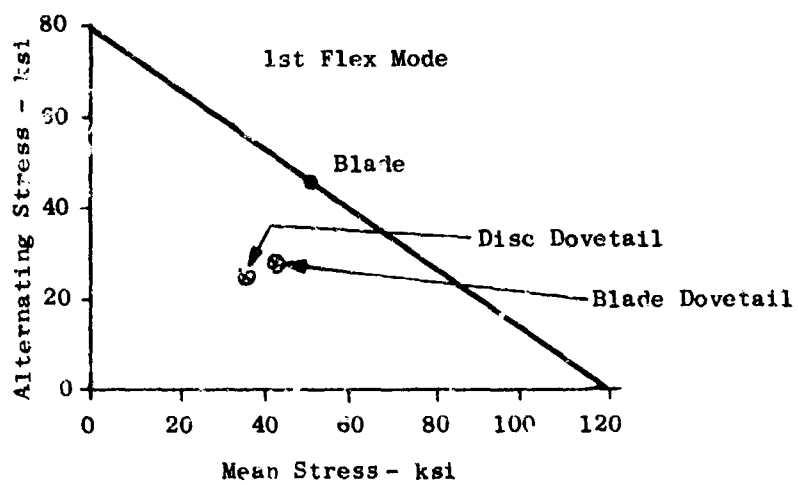


Figure 83. Goodman Diagram.

Web angle = 8 degrees
Rim width = 2.66 inches
Rim thickness = 0.966 inch
Modulus of elasticity = 15.5×10^6 psi
Mass density = 4.25×10^{-4} lb-sec²/in.⁴

Blade

Blade length = 15.273 inches
Mass density = 4.17×10^{-4} lb-sec²/in.⁴
Modulus of elasticity = 16×10^6 psi

Mass at Blade Tip

Tip mass = 0.00202 lb-sec² per inch per blade
Radius at center of gravity of tip mass = 27.77 inches

The gyroscopic analysis was made at 115-percent speed (4681 rpm) and with a precession rate of 1 radian per second.

The blade responses to the gyroscopic forces in terms of deflections, slopes and stresses are given in Figures 76, 77, 78 and 79.

The disc effective spring constant for the cosine 2 θ mode is 2784 pounds per inch. Figure 84 shows spring constant versus speed.

The two-wave mode (cosine 2 θ) critical speed occurs at 96.5-percent N_f (3928 rpm).

The disc effective spring constant for the cosine 3 θ mode is 3961 pounds per inch. Figure 85 shows blade spring constant.

The three-wave (cosine 3 θ) mode critical speed occurs at 61.4-percent N_f (2499 rpm).

Rotor design presented in this report is not satisfactory with the cosine 2 θ axial mode at 96.5-percent speed. All fan experience and designs to date are based on criteria that 2 θ and 3 θ modes be eliminated from the normal fan operating range. To meet acceptable design objectives, the cosine 2 θ critical speed must be raised to a minimum of 120-percent speed without raising the cosine 3 θ critical speed above 70-percent speed, or the cosine 2 θ critical speed must be reduced below 70-percent speed. Experience, rotor axial stiffness (gyroscopic displacement) and blade normal vibratory characteristics suggest that the most practical final design approach will be a high cosine 2 θ critical speed configuration. Accordingly, preliminary analysis shows that this may be accomplished by increasing the disc web spacing (by 0.50 inch) and by increasing the blade effective axial bending stiffness inertia by 0.10 in⁴. Attendant weight changes will require a reevaluation of blade airfoil construction and might require that hollow blades be used to maintain a reasonable rotor weight.

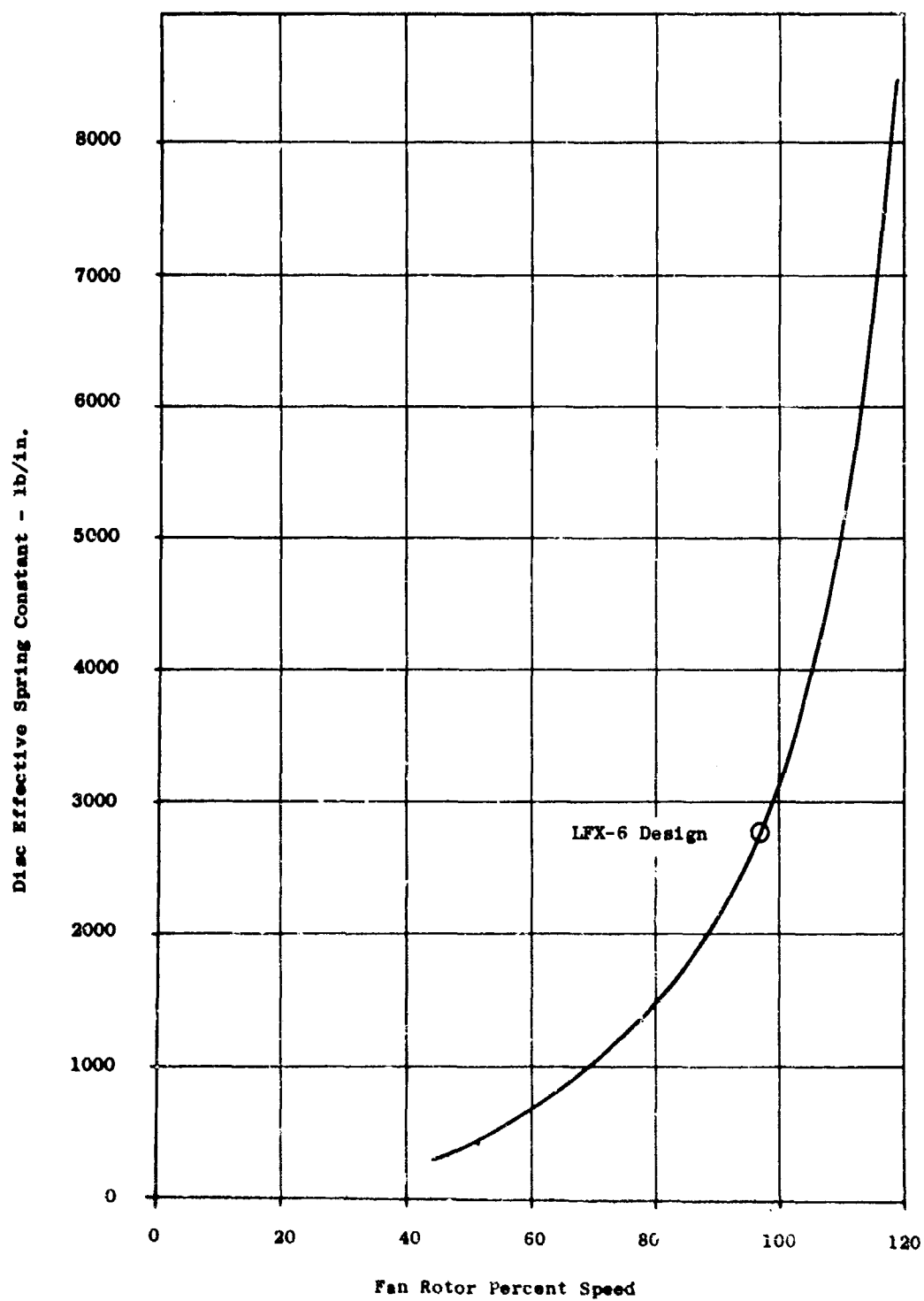


Figure 84. Disc Effective Spring Constant.

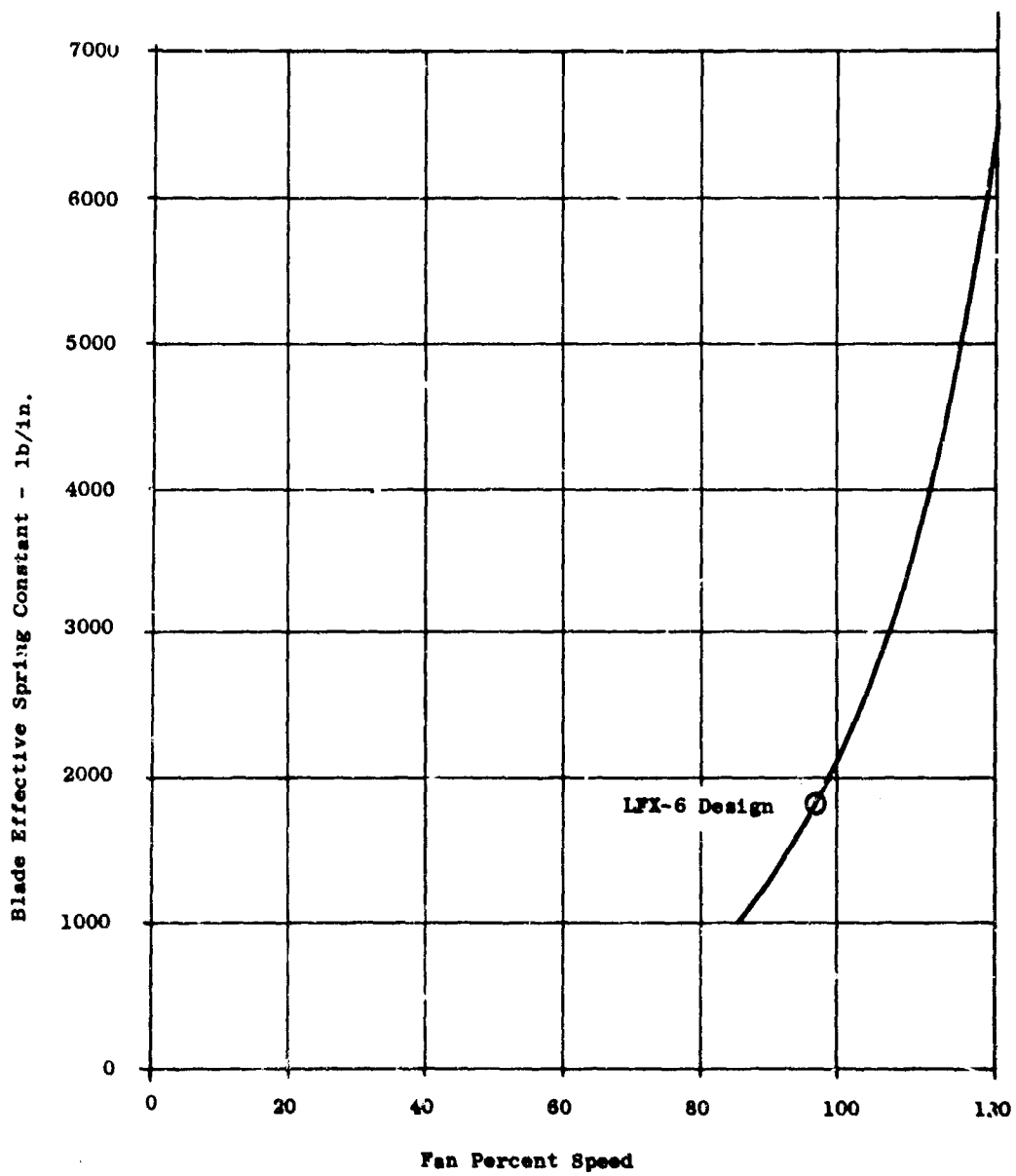


Figure 85. Blade Effective Spring Constant.

Disc

The disc was designed to remain within the allowable limits of stress throughout and within the maximum allowable deflections at the bearing-sump and at the rim. From the overall LFX-6 load spectrum the worst load conditions on the disc are:

1. Maximum developed stress

In landing mode - centrifugal load at 115-percent N_f ,
fan gas load at 115-percent N_f

4	G	up
4	G	forward
1.5	G	side
2.24	rad/sec	gyro
45,500	in-lb	cross-flow moment
12,500	in-lb	off center 1.0 ft moment

2. Maximum rim deflection

In landing mode - centrifugal load at 115-percent N_f ,
fan gas load at 115-percent N_f

4	G	up
1.414	rad/sec	gyro
45,000	in-lb	cross-flow moment
12,000	in-lb	off center lift moment

3. Maximum allowable sump deflections over the bearing centers are:

Ball bearing: radial deflection ≤ 0.003 inch
angular rotation ≤ 0.8 degree

Roller bearing: radial deflection ≤ 0.003 inch
angular rotation ≤ 0.15 degree

Maximum rim allowable deflection is such that

the resultant disc deflection at the rim shall contribute no more than 0.100 inch to blade tip axial deflection.

Internal heat is generated by the bearings and their seals. The LFX-6 bearing seals are similar to the successful 80-inch cruise fan seals where approximately half of the heat is generated by the seals and half by the bearings. A comparison of the overall heat generation rates of these fans (LFX-6 and 80-inch cruise fan) shows little difference, since the higher LFX-6 rotational speed is offset by its smaller bearing and seal sizes. Thus, under worst conditions (120°F hot day) LFX-6 disc temperatures should approximate those of the 80-inch fan (300°F maximum in the sump area, decreasing to approximately 150°F at the rim).

The guidelines for estimating usable material strengths have been developed from experience with several generations of General Electric jet engines, as well as from test experience on present lift fans. Of particular interest are material property levels being used on the latest jet engine compressors composed of new high-strength alpha-beta titanium alloys, similar to the Ti-6Al-6V-2SN of the LFX-6 disc. Out of the range of limiting levels, those that limit the LFX-6 disc properties are:

Web bore stress < 120 percent x 0.2-percent yield strength

Effective local stress < 80 percent x ultimate strength

Average tangential stress < 70 percent x ultimate strength

Correcting average Ti-6Al-6V-2SN properties to minimum values by subtracting three standard deviations gives working stress values of

Web bore stress = 130,000 psi at 300°F

Effective local stress = 100,000 psi at 300°F
120,000 psi at 150°F

Average tangential stress = 102,000 psi at 225°F

A detailed analysis of the disc through the use of computer shell programs has given a very complete picture of disc response to steady-state and maneuver load conditions. A summary of the stresses and deflections at vital areas of the disc is given in Figure 86.

A comparison of these calculated values with allowable stress and deflection values listed earlier shows that all criteria are met.

Two bolts fasten each fan blade retainer to the retainer flange on the disc rim. This prevents twisting of the retainer and also prevents loss of the blades in the event of a single bolt failure.

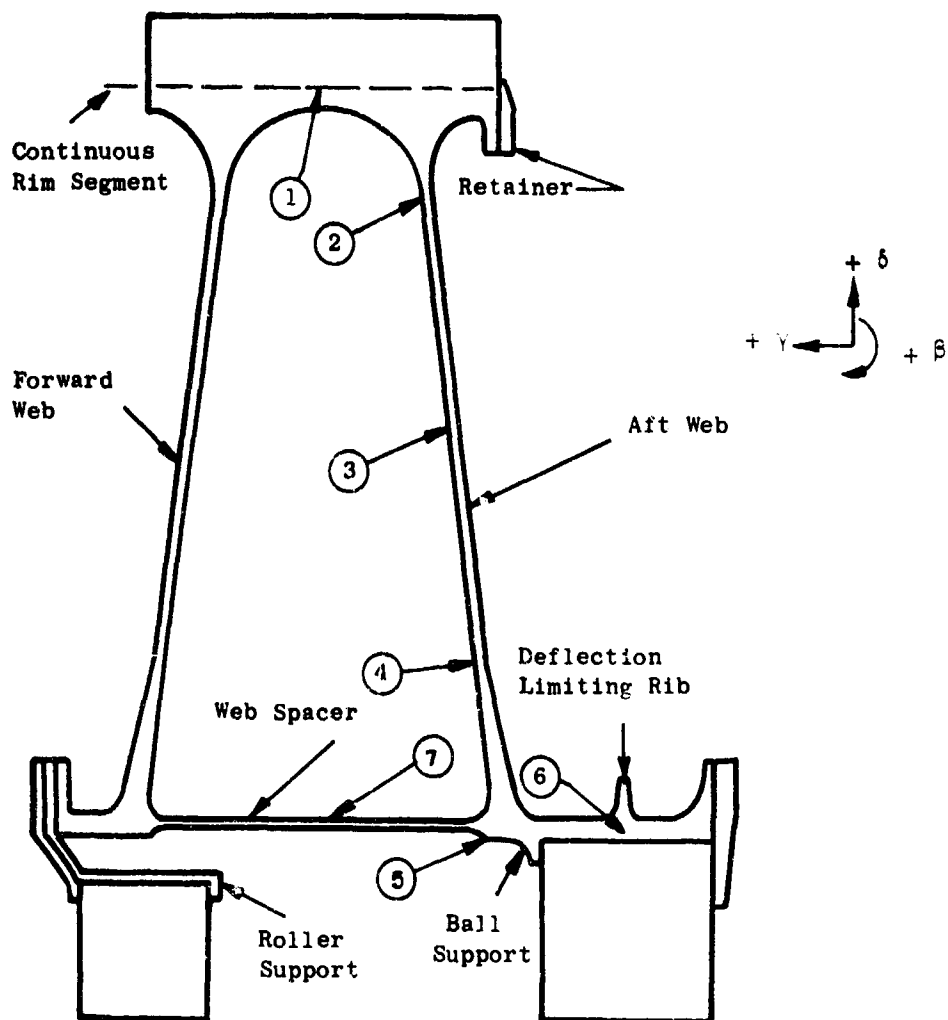
Rotor blade retainer material is Ti-6Al-6V-2SN with properties equivalent to those of the disc. The maximum bending stress is 130,000 psi caused by a blade force due to 1.5 load factor at 2.25 radian/second gyroscopic maneuver.

Motion of the blade as it loads the retainer (and resultant dovetail fretting) is minimized by deflecting the retainer as it is bolted on, thus preloading the blade. This preload will be half the maximum design load, limiting axial blade motion to approximately 0.012 inch under maximum load.

Figure 87 shows the retainer configuration with applied loads, bolt locations, and point of maximum stress.

Bearings

The spacing of 4.5 inches between the two bearings is based on the gyroscopic loading of 1 radian per second at 115-percent N_1 . The roller



Location	Load	σ_r (ksi)	σ_θ (ksi)	σ_{eff} (ksi)	Location	Load	δ_r (in.)	γ_x (in.)	ρ (°)
2	S.S.	70	77	100	1	S.S.	0.043	-0.011	-0.25
	Gyro			115		-Gyro	~0	+0.005	-0.10
3		71	67	86					
				120					
4		73	78	107	Location	Load	σ_x (ksi)	σ_θ (ksi)	σ_{eff} (ksi)
				118	7		-33	2	68
5		26	86	88					68
				130					

Gyro: 1.414 rad/sec for values at position 1
 2.24 rad/sec for values at all other positions

Figure 86. Disc Stress and Deflection Summary.

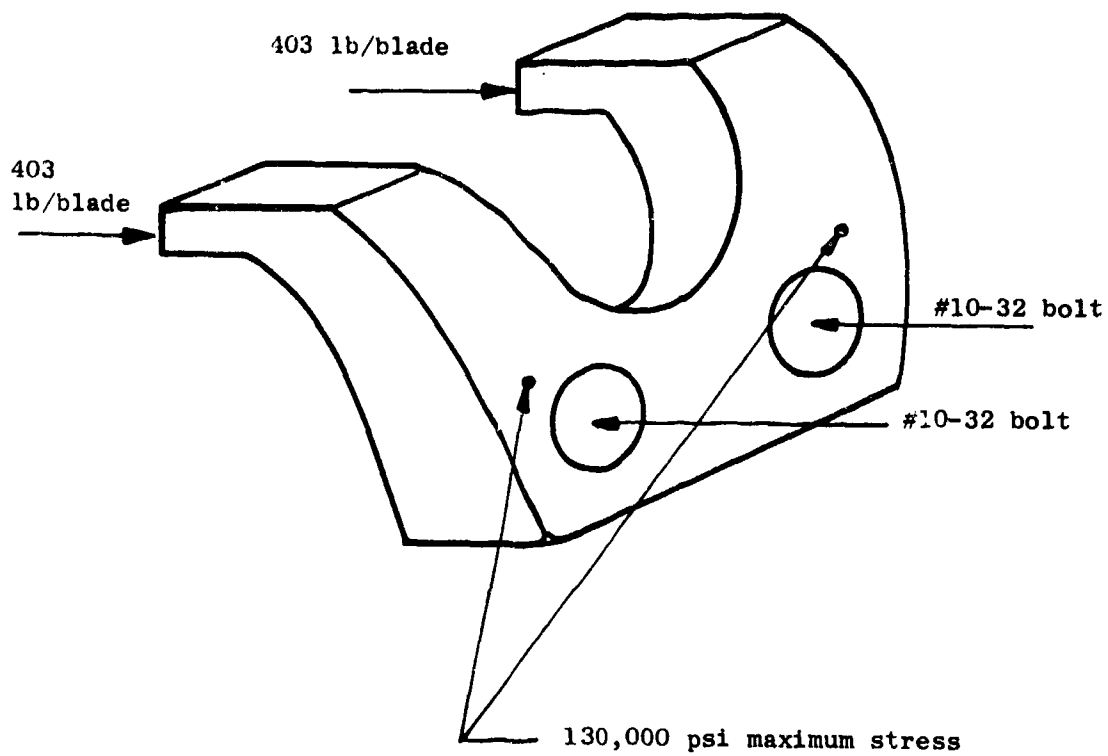


Figure 87. Blade Retainer.

bearing, acting in conjunction with the ball bearing, supports and stabilizes the rotor by transferring all rotor moment and acceleration ("g") loads to the stationary shaft/front frame. With this spacing the resulting radial load does not exceed the dynamic capacity of the bearings. For gyroscopic precession rates greater than 1 radian per second, a brinelling of the race will result. However, this brinelling will not preclude further short-time operation. In order for the ball to support the resulting radial load, a decrease of contact angle takes place. At this decreased angle, loading will exceed the dynamic capacity of the bearing and brinelling will occur out of the normal ball path (Figure 88). Therefore, the balls should not be over-running the damaged race area in normal operation, and the bearing can be safely operated until return to the ground.

In order to meet the bearing life objectives of 1000 hours between overhauls and yet meet bearing weight objectives, a material factor of 2.86 is applied to the calculated B10 life based on AFEMA Standards. In industry use, factors as high as five times that calculated in accordance with AFEMA Standards have been obtained for consumable electrode vacuum melt high purity alloys. The load table used in the life calculations is shown in Table XII.

Bearing lubricant will be Uni-temp 500 grease. This grease has been successfully used in all previous General Electric tip-turbine fans to date with more than 80 continuous hours of trouble-free operation. The amount of grease in each bearing is intended to provide 30-percent filling.

Material stabilization temperature for the bearings is 400°F, in order to assure temperature induced distortion-free operation at the bearing maximum operating temperature of 350°F.

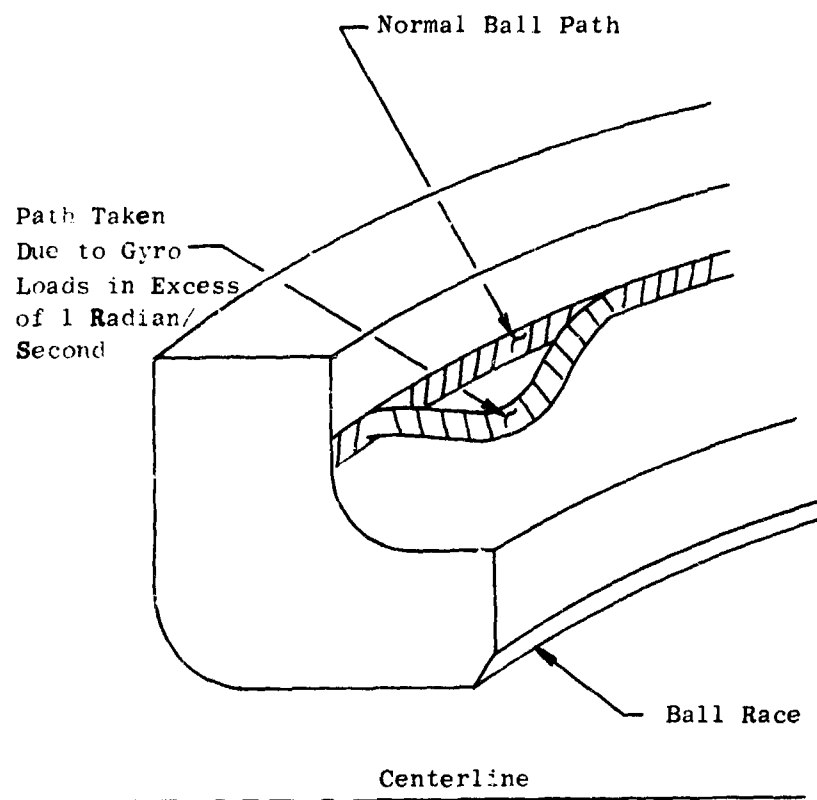
The DN value (based on the bearing mean diameter) is higher than the present state of the art. It is 52 percent higher than that of the X353B rotor based on the ball bearings. A comparison of DN values for various fan rotors is as follows:

	<u>Ball</u>	<u>Roller</u>
LFX-6	*0.621	0.611
X376	0.316	0.312
X353B	0.409	0.273
80-Inch Cruise Fan	0.584	0.655

*DN value is given in millions and based on bearing mean diameter

Turbine Sector

The turbine sector mechanical design criteria and results of the analyses are outlined as follows:



Normal Path Loads Due to Gyro ≤ 1 Radian/Second
 Brinelling Acceptable for Gyro Induced Loads > 1 Radian/Second

Figure 88. Bearing Deflection Path.

Design Criteria

1. Seals

Maximum allowable radial deflection - 0.35 inch

Maximum allowable bending stress - 70 percent of 0.2-percent yield stress

2. Turbine Buckets

Maximum allowable uncorrected gas bending stress - 10,000 psi

3. Bucket Carrier

Maximum allowable shear stress tensile equivalent not to exceed 70 percent of 0.2-percent yield stress

4. Support Blocks

Maximum allowable bearing stress 90,000 psi at design speed

5. Side Rails

Shear tensile equivalent ($\frac{\text{shear stress}}{0.6}$) not to exceed 0.02-percent yield stress minimum

6. Mechanical Design Speed

115-percent N_f shall be used to size all rotor geometry

Design Objectives

1. Design the turbine sector to be as light as possible.
2. Fabricate the turbine bucket out of sheet metal.

Design Requirements

1. Use current state-of-the-art technology.
2. Internal bulkheads shall be employed to seal between blade tangs and at each end of the carrier to prevent hot gas from circulating through the carrier and to form a flow path over the tip of the blade to provide tang cooling.
3. Shields shall be employed to cover the support blocks to prevent scrubbing by the hot gas.
4. Braze construction shall be used in turbine carrier design.

Turbine Sector Operating Temperatures

Estimated operating temperatures for the various parts of the turbine sector are shown in Figure 89.

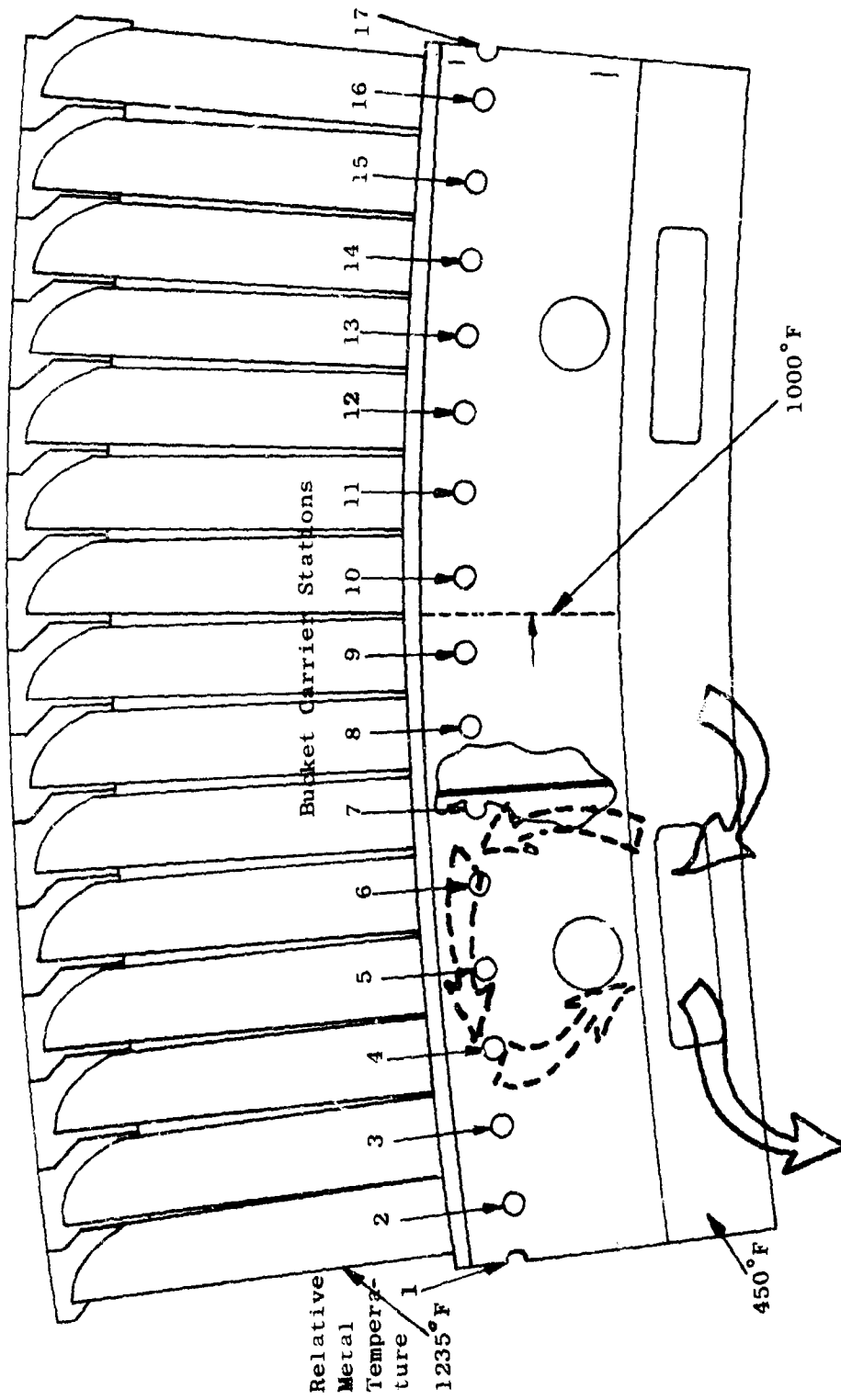


Figure 89. Turbine Sector Stations.

LFX-6 Design Analyses Results

Turbine Bucket

Section Properties and Stress Functions

Cross-section area - 0.02903 in^2

Minimum moment of inertia - 0.0003135 in^4

Maximum moment of inertia - 0.0019528 in^4

Bending stress functions

Leading edge - 527 psi/lb

Trailing edge - 527 psi/lb

Convex side, maximum thickness - 529 psi/lb

Loads

- a. Gas resultant force per inch of active arc length shown in Figure 90
- b. Tangential force - shown in Figure 91
- c. Centrifugal "g" field - shown in Figure 92

Turbine Bucket Stresses

Maximum uncorrected gas bending - 8,650 psi
(at 82.5-percent N_f and 156-degree arc)

Maximum tensile centrifugal - 16,300 psi
(at 115-percent N_f)

Maximum gas bending, locked rotor - 15,000 psi

Turbine Bucket First Flexural Natural Frequency - shown in Figure 93

Campbell diagram

First flexural - 1,749 cps

Section Properties

The cross section geometric properties are given in Table XI; Figures 56 and 89 show the location of the sections.

Loads - Carrier

- a. Shear diagram - Figure 94
- b. Moment diagram - Figure 95
- c. Torque transmission - the most adverse condition for the torque transmission system occurs when the core engine is at 100-percent N_f power setting and the turbine scroll position is at 156 degrees (reference Figure 98)
- d. Shear and bending moment stresses - Figures 96 and 97

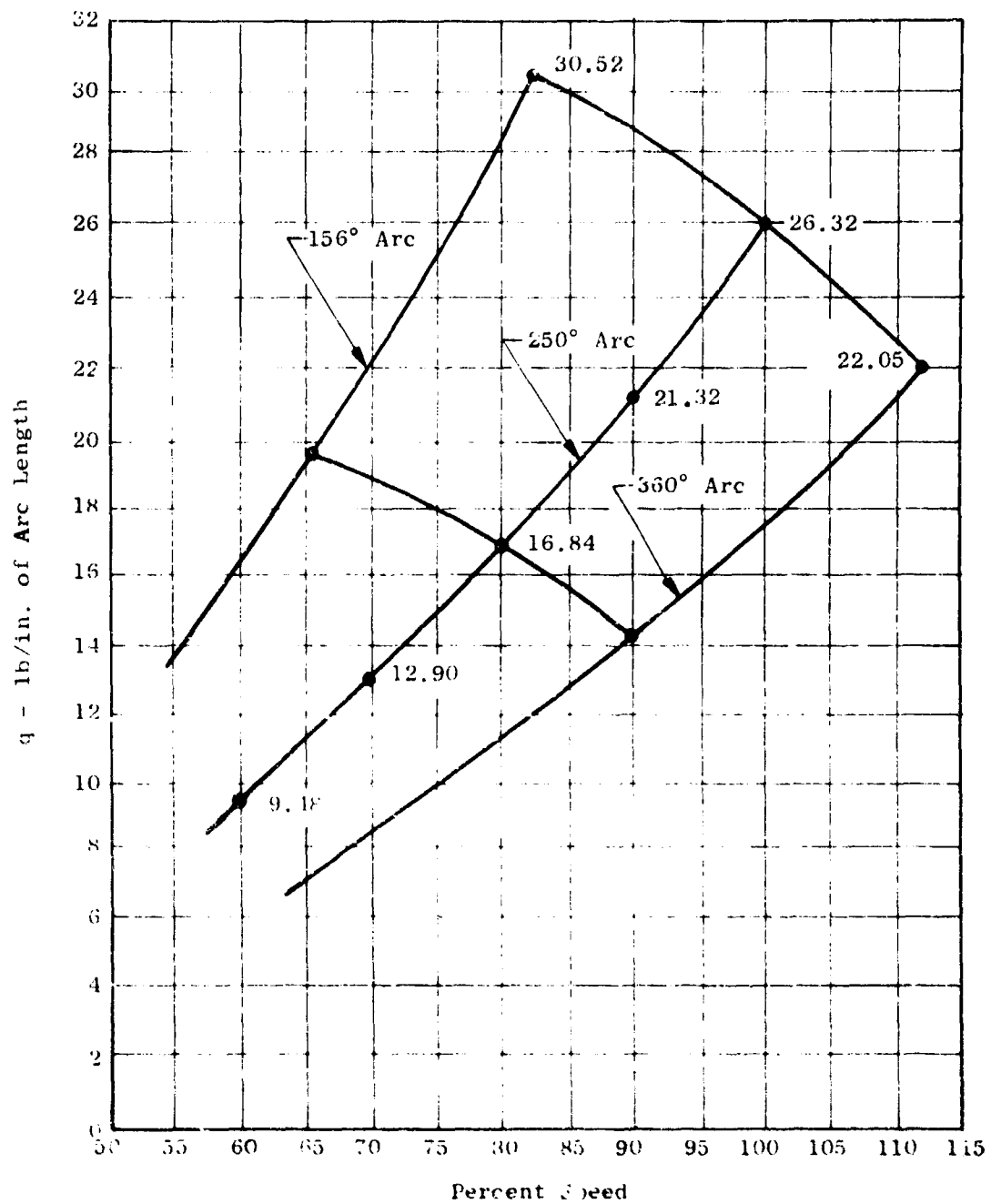


Figure 90. Turbine Bucket Gas Load.

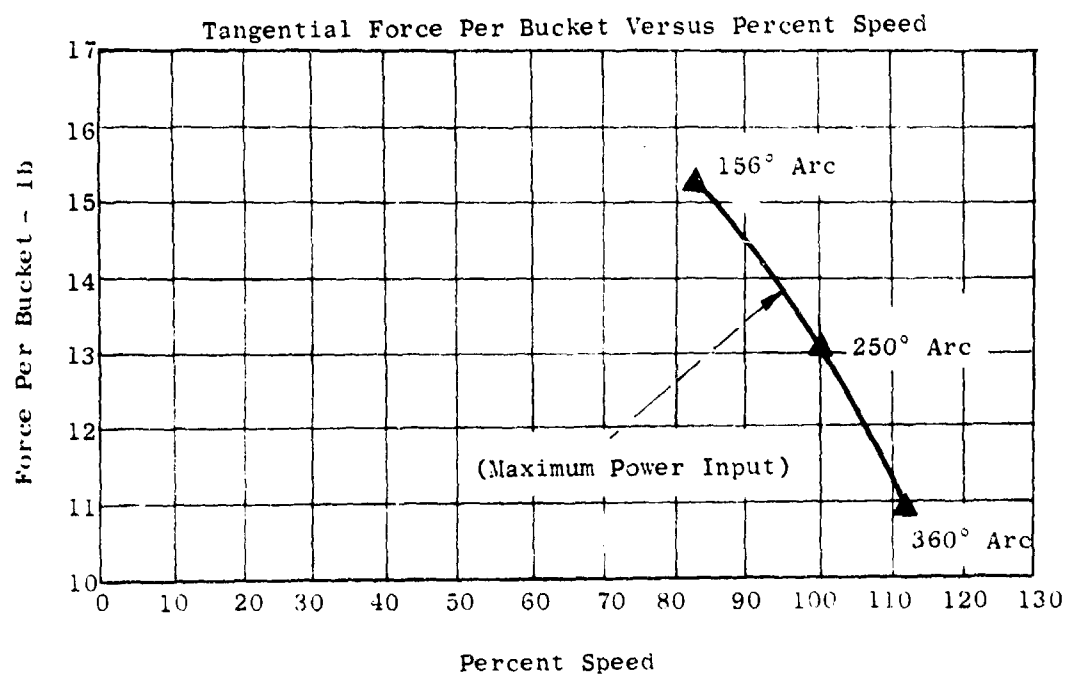


Figure 91. Turbine Bucket Tangential Force.

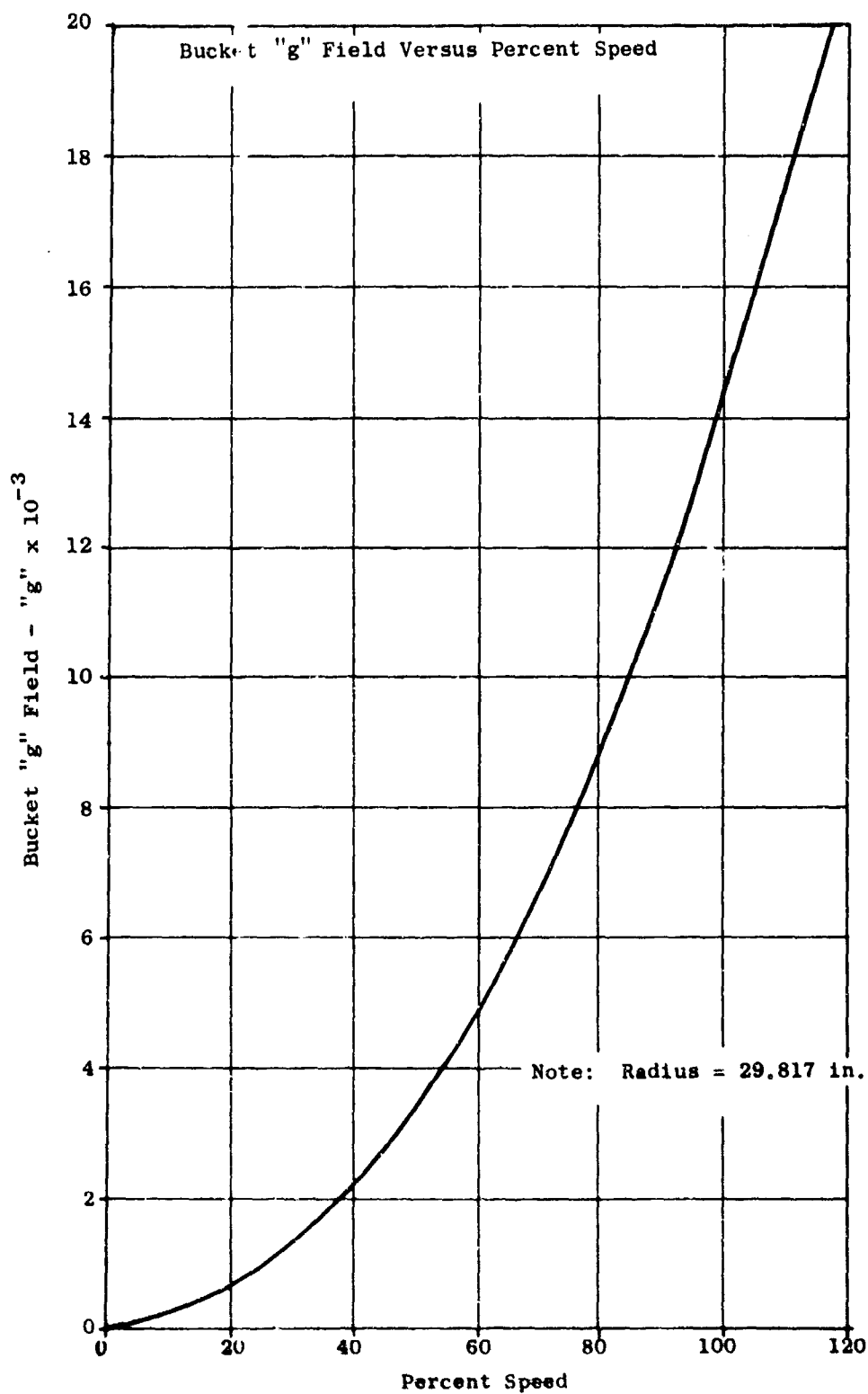


Figure 92. Turbine Bucket "g" Field.

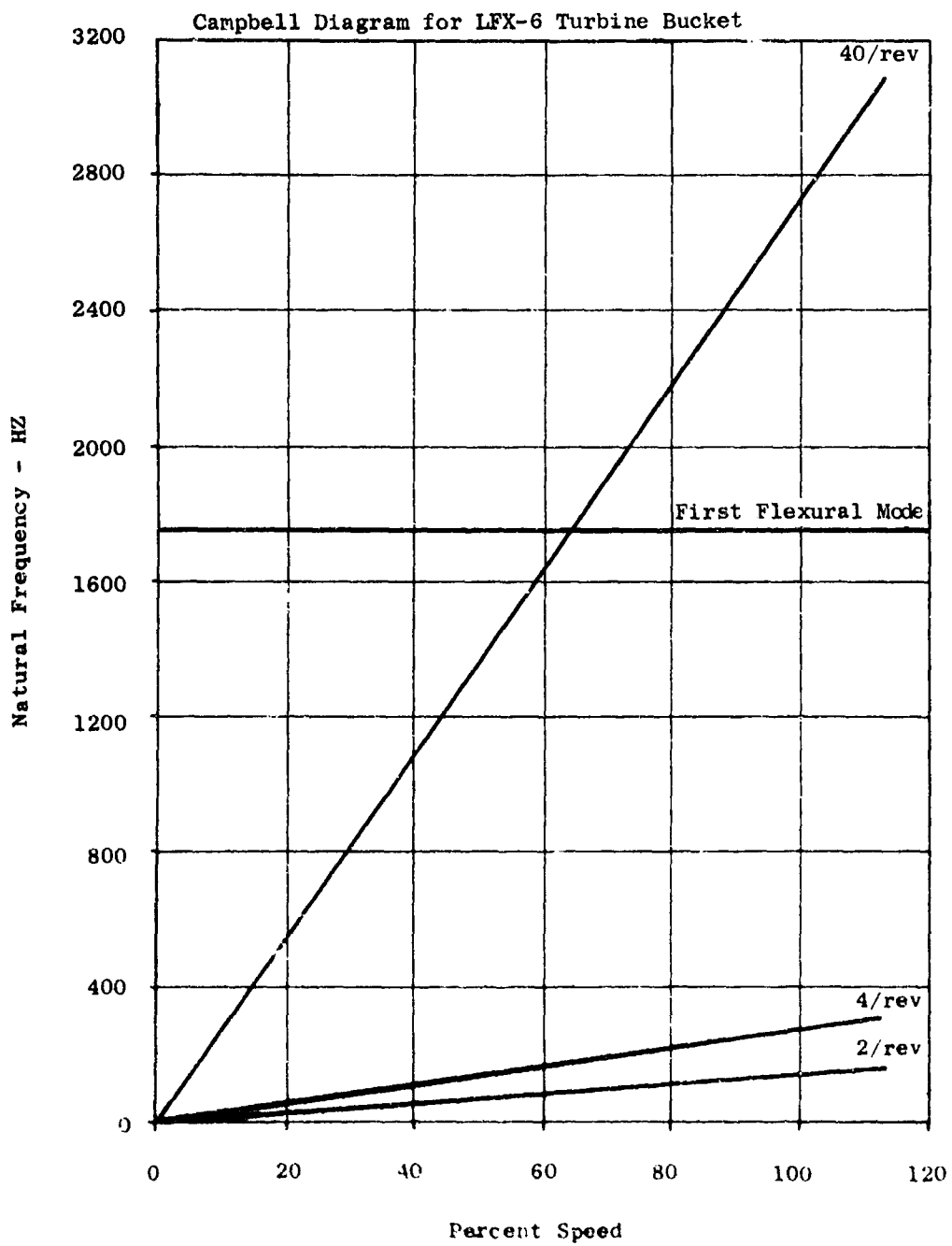


Figure 93. Turbine Bucket Campbell Diagram.

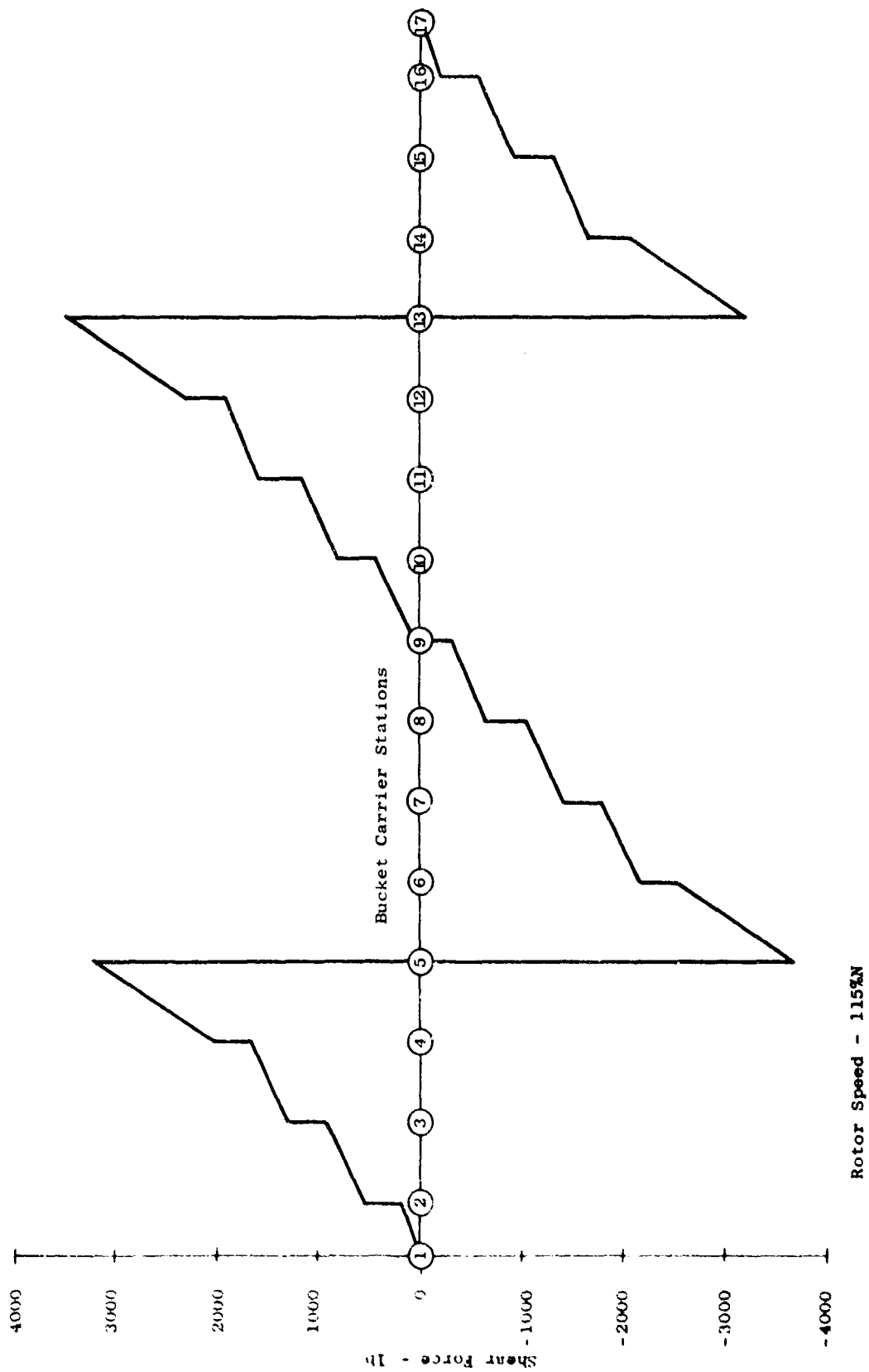


Figure 94. Bucket Carrier Shear Diagram.

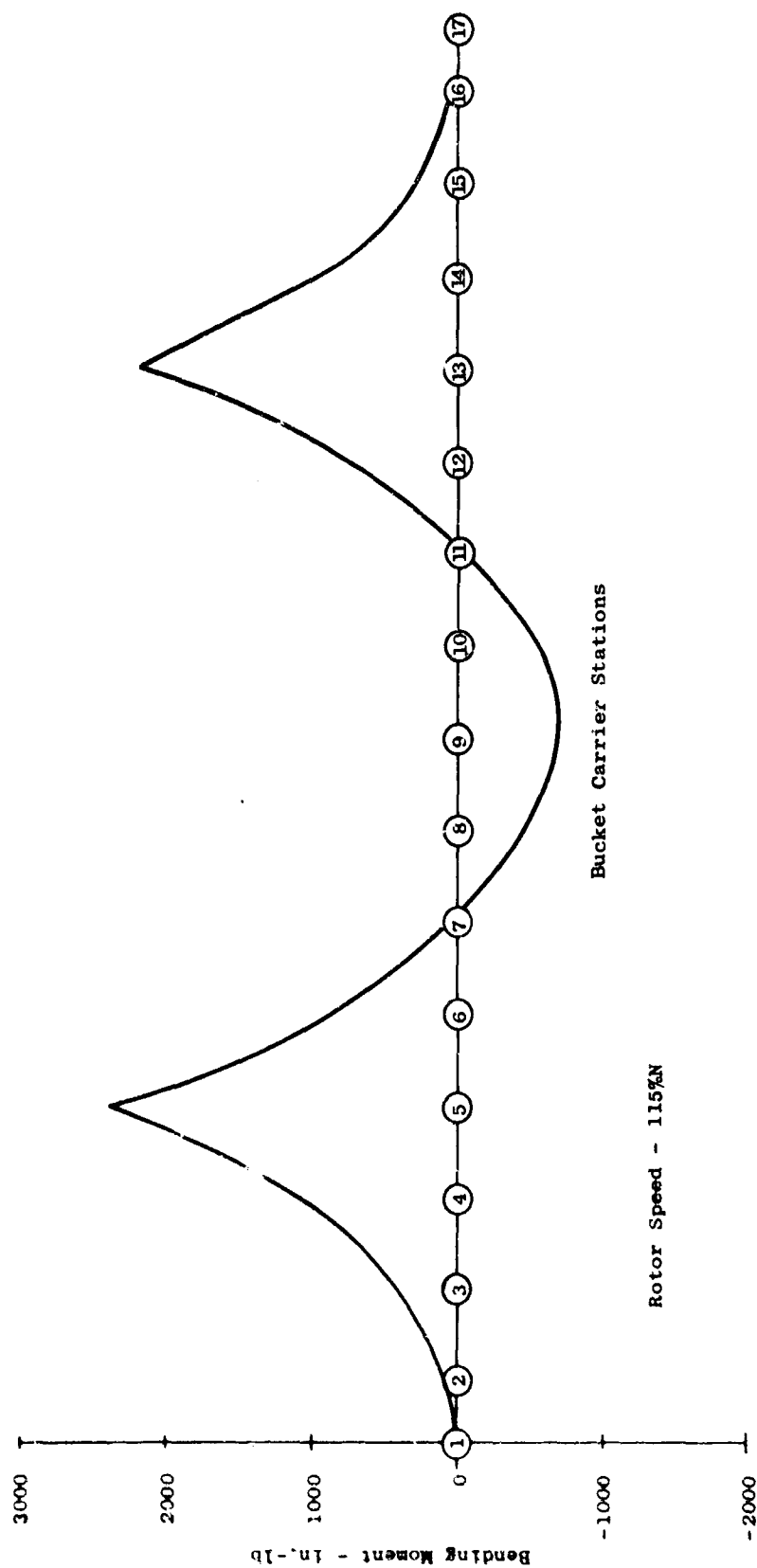


Figure 95. Bucket Carrier Moment Diagram.

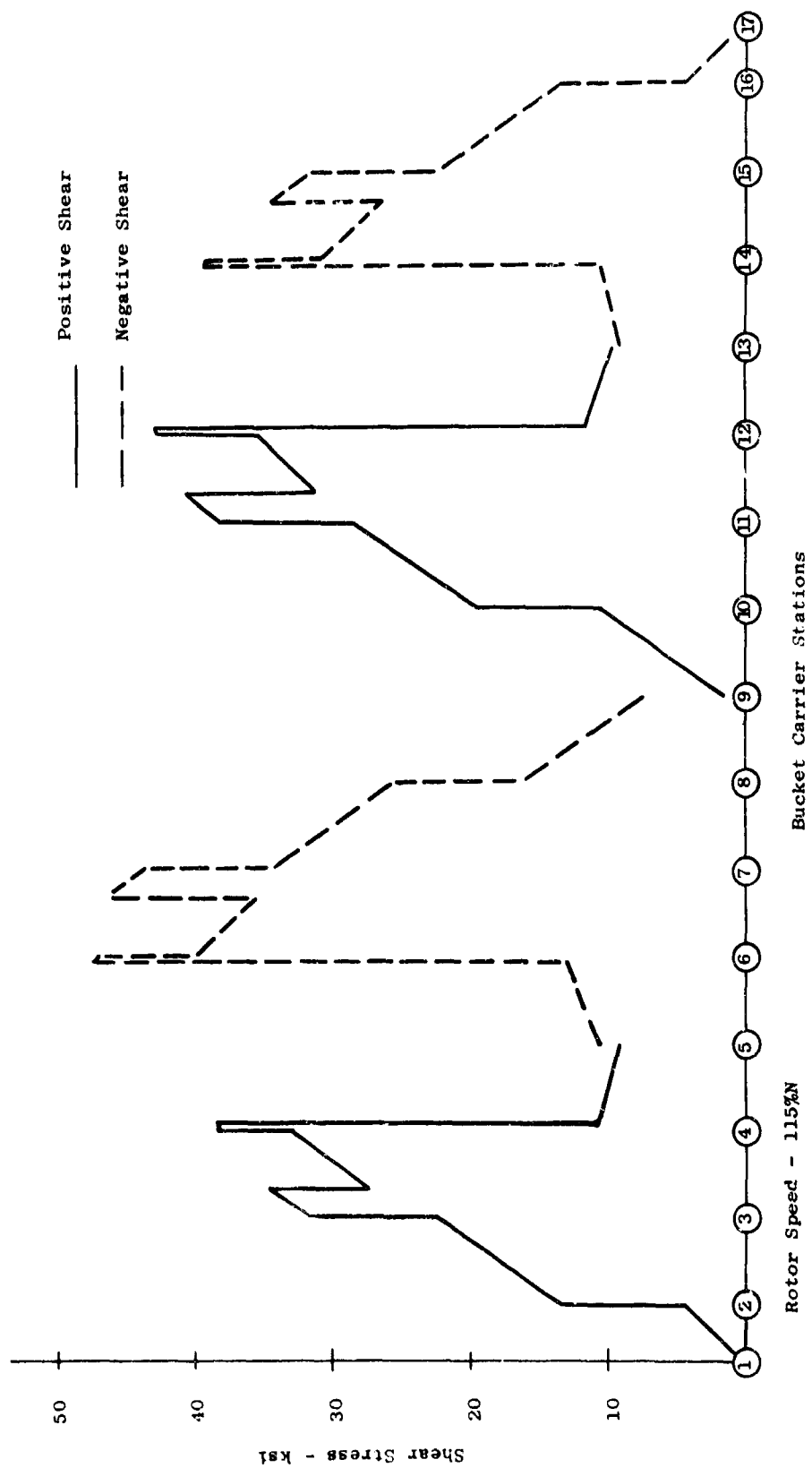


Figure 96. Bucket Carrier Shear Stress.

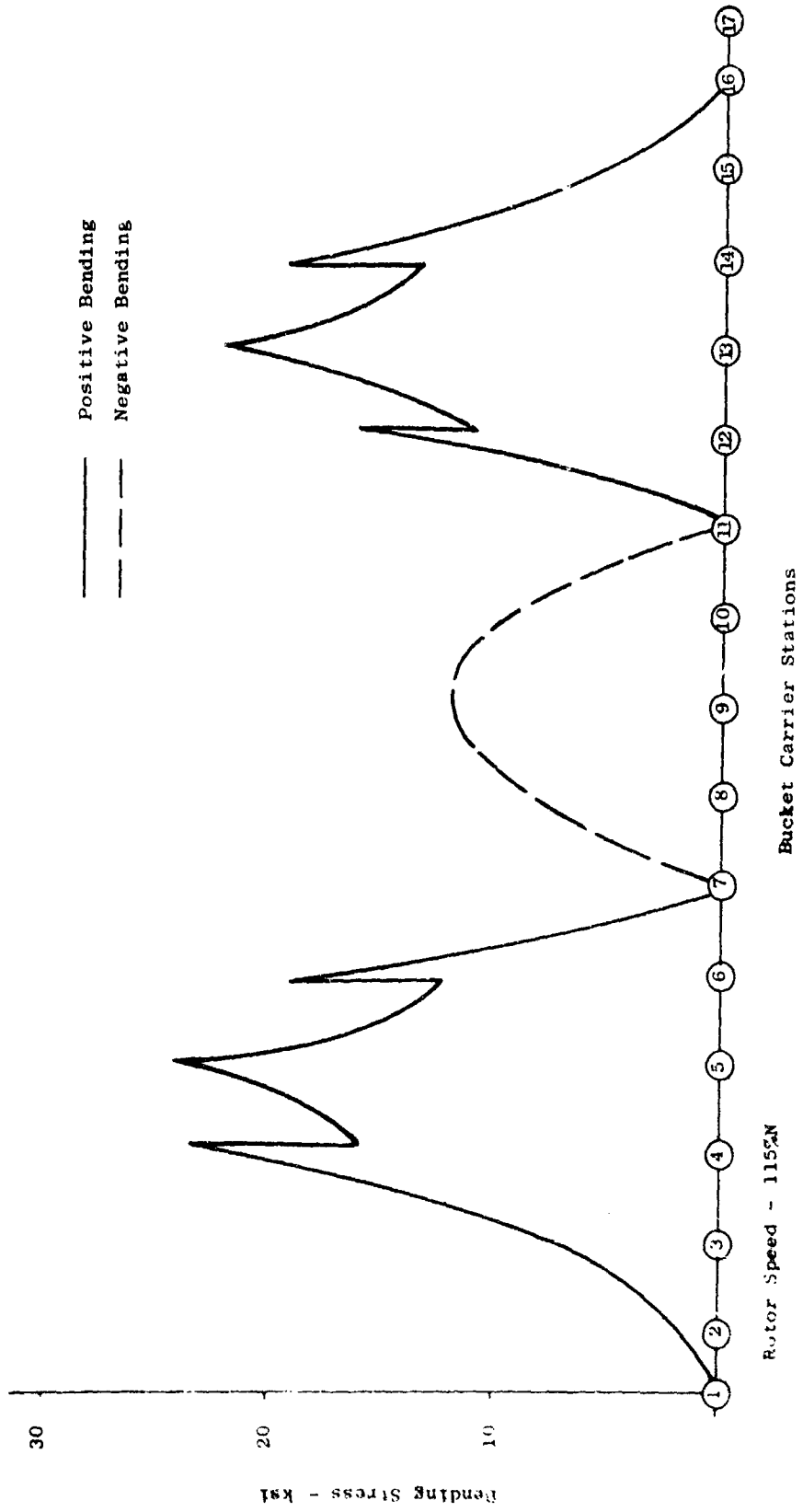
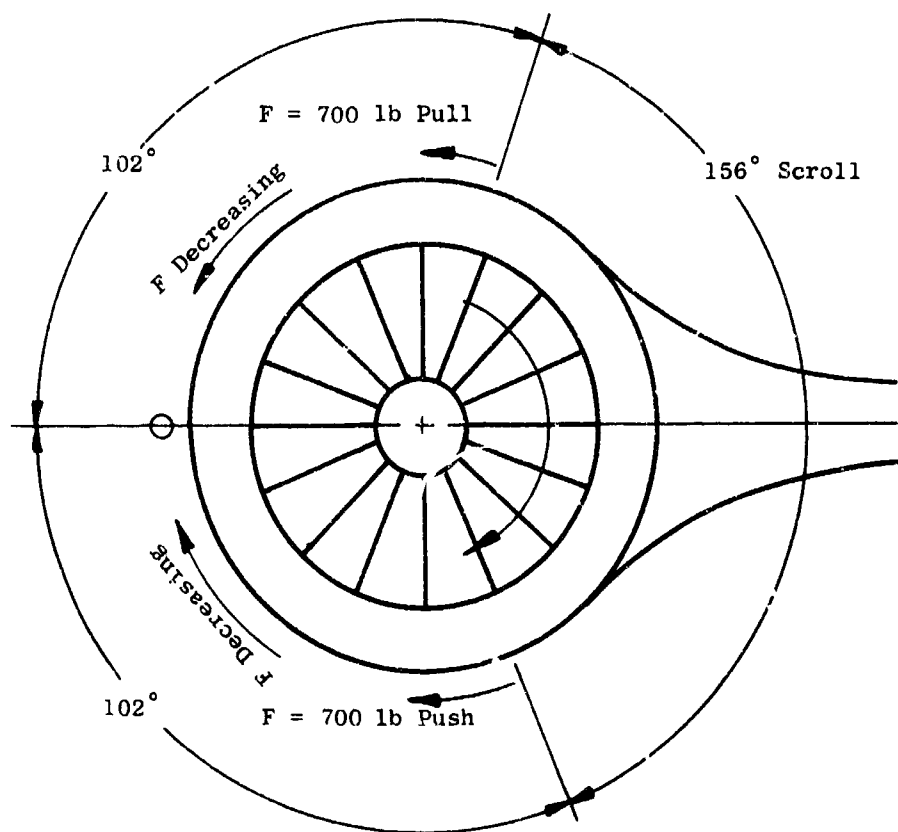


Figure 97. Bucket Carrier Bending Stress.



Note: F is the magnitude of the tangential force which the friction pads must transmit from bucket carrier to bucket carrier.

Figure 96. Torque Transmission System Schematic.

TABLE XI
BUCKET SECTION PROPERTIES

Cross- Section Location Number	Area in. ²	I _{Max} in. ⁴	I _{Min} in. ⁴	Shear Stress Function (lb/in. ² -lb)
1	0.1483	0.05624	0.02716	24.481
2	0.1601	0.05794	0.02813	18.698
3	0.1377	0.05116	0.02752	18.603
4	0.2955	0.07271	0.04389	5.195
5	0.4865	0.09872	0.07435	2.856
6	0.3704	0.09625	0.07330	2.693

TABLE XII
BEARING LOADS

Flight Cond.	Percent Total Time	Percent Percent N Time				g's Up	g's Fwd	g's Side	Gyro Rad/Sec	Rotor Lift Total lb	Radial Part. Add. lb	Cross- Flow Moment in.-lb	Resulting Bearing Load	
		Each Point	Each Point	Each Point	Each Point								Lift lb	Radial lb
Idle	2	65	2	0.5	0	0.5	0	0.5	0.1	2760	225	2K	2595	752
Taxi	5	66	1	0.5	0.5	0.5	0.5	0.5	0.1	2760	558	2K	2595	1226
		80	2	0.5	0.5	0.5	0.5	0.5	0.1	4200	338	2K	4035	1028
		90	1	0.5	0.5	0.5	0.5	0.5	0.1	5220	0	2K	5055	706
		100	1	0.5	0.5	0.5	0.5	0.5	0.1	6450	328	2K	6285	1050
Check Out	10	80	3	0.5	1.5	1.5	1.5	1.5	0.1	4200	338	8K	4035	2595
		90	5	0.5	1.5	1.5	1.5	1.5	0.1	5430	426	16K	5265	4476
		100	2	0.5	1.5	1.5	1.5	1.5	0.1	6450	528	24K	6285	6373
Hover	63	82	3.15	3	0.5	0.5	0.5	0.5	0.4	4452	874	10K	4290	3744
		90	9.45	3	0.5	0.5	0.5	0.5	0.2	5451	546	15K	5289	4286
		100	37.80	3	0.5	0.5	0.5	0.5	0	6450	528	20K	6288	5089
		106	9.45	3	0.5	0.5	0.5	0.5	0.2	7050	156	20K	6288	5058
		112	3.15	3	0.5	0.5	0.5	0.5	0.4	7650	0	20K	7488	5282
Transition	20	100	8	1	1	1	1	1	0.3	6450	528	40K	6286	10134
		105	6	1	1	1	1	1	0.3	6450	498	40K	6286	10127
		110	4	1	1	1	1	1	0.3	6450	462	40K	6286	10115
		115	2	1	1	1	1	1	0.3	6450	426	40K	6286	10103

Outer Fan Flow-Path Seals

Maximum seal lip deflection - 0.0195 inch

Maximum bending stress of 88,600 psi is located in the forward and aft seal lip portions as shown in Figure 56.

Material

The material selected for the turbine carrier is Rene '41 because of its satisfactory properties at 1400°F.

Areas Requiring Further Study

The design work and analyses described above have revealed certain areas which require further detail study to assure mechanical design integrity or to provide design improvements.

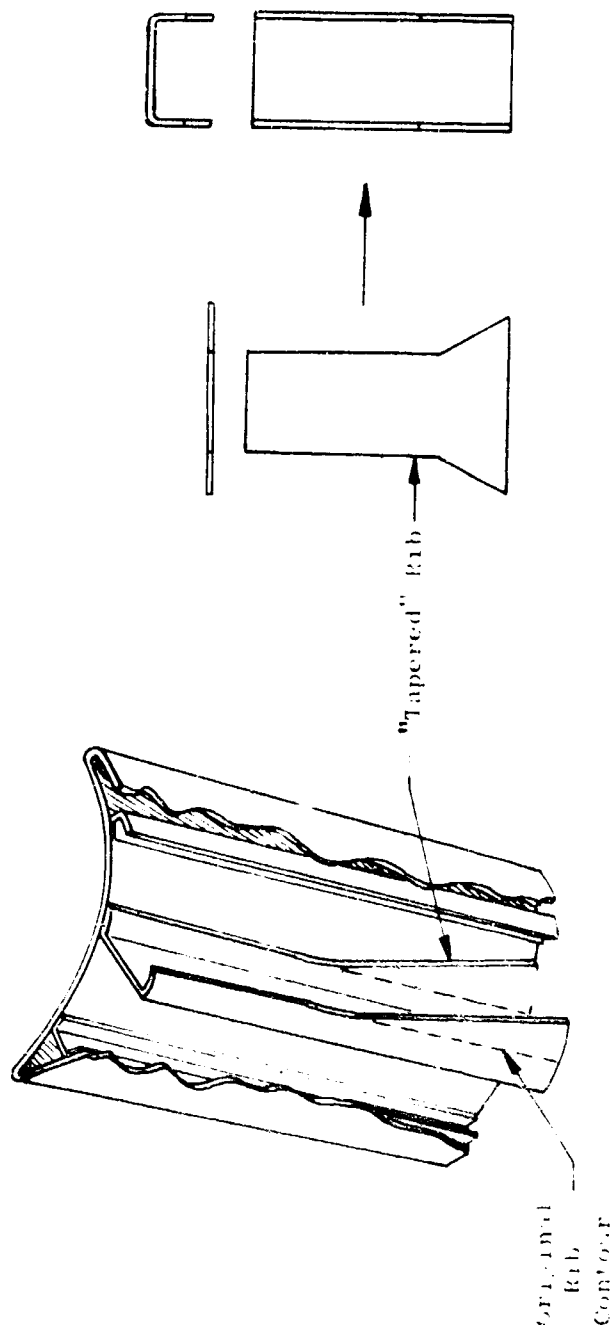
In general, the manufacturing procedures established for the LF-2 turbine carrier sectors provide the techniques necessary to produce the LFX-6 turbine sectors. However, it may be necessary to taper the turbine bucket wall thickness from the root to the tip in order to provide the desired bucket vibratory characteristics. Further study is required to minimize the possibility of undesirable bucket vibratory characteristics and to explore the techniques required to produce tapered wall thickness buckets, if it should become necessary. Figure 99 shows a possible alternate design.

Model tests should be planned to study the final tip-tang-to-fan blade transition design before the design is released to manufacturing.

Although the disc is significantly more efficient and lighter than previous fan designs, it does have areas where further weight reductions may be possible. Both webs are now symmetric in order to minimize manufacturing cost. As a result, the forward web is less highly stressed because of the rotor thrust loading. Accordingly, the forward web thickness could be reduced to produce the same stress level as exists in the aft web. Titanium 200K offers 10 percent greater strength than Ti6Al5V2SN, and its use would reduce weight. However, Ti 200K ductilities comparable to Ti 6-6-2 have not yet been demonstrated.

The LFX-6 disc rim with blended web ends constitutes 10 to 20 percent of the disc weight. A thinner rim with only local web blend reinforcement under the dovetail posts would be more efficient. Additional detail analyses are required before it can be determined whether such a configuration is mechanically acceptable.

Several changes are required to improve the LFX-6 blade to a point where it can be considered an acceptable design. Included among the present relatively undesirable design characteristics are:



Alternate Bucket Fabrication

Figure 99. Alternate Bucket Configuration.

Fundamental vibratory modes are low (Figure 69).

First flexural mode crosses the 6-nodes-per-revolution line at 100-percent N_f .

First torsional mode crosses the 10-nodes-per-revolution line at 95-percent N_f .

Second flexural mode crosses the 12-nodes-per-revolution line at 90-percent N_f .

The reduced velocity parameter is greater than 2.0

Cosine 2 θ system mode critical frequency occurs at an operational speed point (96.5 percent N_f).

Steady-state stress at the blade root is slightly high.

Rotor weight is more than target value.

It is desirable to have the blade fundamental mode frequencies above the second harmonic of known excitation sources. For the four-strut front frame design, an 8-nodes-per-revolution second harmonic can be a primary source of excitation. One of the more effective ways to increase blade frequencies is to reduce the effective blade length (i.e., increase radius ratio, add blade restraint at the platform, add midspan shroud restraint, or reduce fan tip diameter). Changing blade section properties by increasing chord, t_m/C , or both will increase the natural frequencies. Reducing the number of blades while holding design solidities constant will increase flexural frequencies by changing blade section properties. A change in material properties or in tip boundary conditions can increase the blade frequency. However, presently available materials are not effective in this regard and past attempts to change tip boundary conditions have not been successful. Consideration can also be given to changing the front frame design to use nonradial struts or to increase the number of struts.

Most of the available means for raising the natural frequency result in an increased blade weight. For this reason, more detailed analysis is needed to effect the necessary frequency shifts with a minimum weight penalty. The reduced velocity parameter or flutter criteria can be helped by increasing chord and/or t_m/C . As noted above, these changes could cause a potential increase in blade weight.

System mode critical speeds can be changed by alterations in several rotor components. A change in blade stiffness, I_{max} , or in blade length will help change the critical speed. Increased stiffness and reduced length raise the blade critical speed, while reduced stiffness and increased length lower the critical speeds.

The steady-state stress level at the root, where rapid transitions are made to the blade shank, should be reduced somewhat. This can be accomplished with local increases in t_m/C with little overall weight change, provided reductions in t_m/C are made in other areas of the blade.

From foregoing discussion, it is recognized that considerable difficulty was encountered in attempting to meet the very stringent target weight set for the LFX blades. Potential weight savings through the use of hollow titanium flages are limited because of the anticipated manufacturing timing. The most critical challenge, however, is to design the lightweight fan blade with sufficient stiffness to meet desired rotor dynamic characteristics. For the LFX-6 blade design, the stiffness rather than the stress is the limiting factor currently preventing further weight reductions.

FRONT FRAME MECHANICAL DESIGN

The front frame provides the sole structural support of the fan in the airframe. All rotor, rear frame, and scroll maneuver and aerodynamic loads are taken by the front frame and transferred to the airframe. The front frame to airframe mounting method, described below, is designed to transfer the fan loads to the airframe without imposing airframe loads on the fan structure. The front frame also maintains internal fan static to rotating component concentricity and forms the fan inlet flow path.

The prime objective of the LFX front frame mechanical design effort was the definition of the lightest possible frame, consistent with the fabrication and materials technology defined for the LFX. Accordingly, the intent of the design effort was to define a frame configuration and frame materials which reached shear stress, buckling and deflection limiting values at the same loading condition. This condition of multiple design limits should produce optimum utilization of structural material.

The front frame design described in this report weighs 101.7 pounds, compared to the weight of 127 pounds given in Reference 1. The front frame includes the major and minor struts, the hub dome section and rotor shaft, and the bellmouth assembly.

Essentially the same concept as defined in Reference 1 has been retained. However, there are two significant differences necessitated by the weight reduction effort and the magnitude of the fan loads. The major strut material was changed from aluminum to steel, and the front frame/nub section is an integral assembly.

The following outlines the front frame design criteria and operating conditions, describes the resultant design and the results of the design analyses, and lists the areas requiring additional detail study.

Design Requirements

The loads used for front frame mechanical design analysis were determined at the maximum power transfer condition (i.e., 115 percent fan speed).

The major loads to which the LFX front frame is subjected come from six sources:

1. Moments produced by the aerodynamic loads on the fan doors
2. Moment due to cross flow effects
3. Moment due to rotor gyroscopic forces during maneuvers
(Figure 53)

4. Maneuver ("g") loads (Figure 53)
5. Scroll loads (lift and piston loads)
6. Rear frame lift loads (transmitted to the front frame through the scroll)

A tabulation of these loads is given in Table XIII. These values are the maximum which the front frame design must accommodate. Figure 100 shows schematically where the applied loads act on the front frame and the restraints on the frame provided by the fan mounts. Figure 101 shows the major load paths within the fan which produce the applied loads on the front frame.

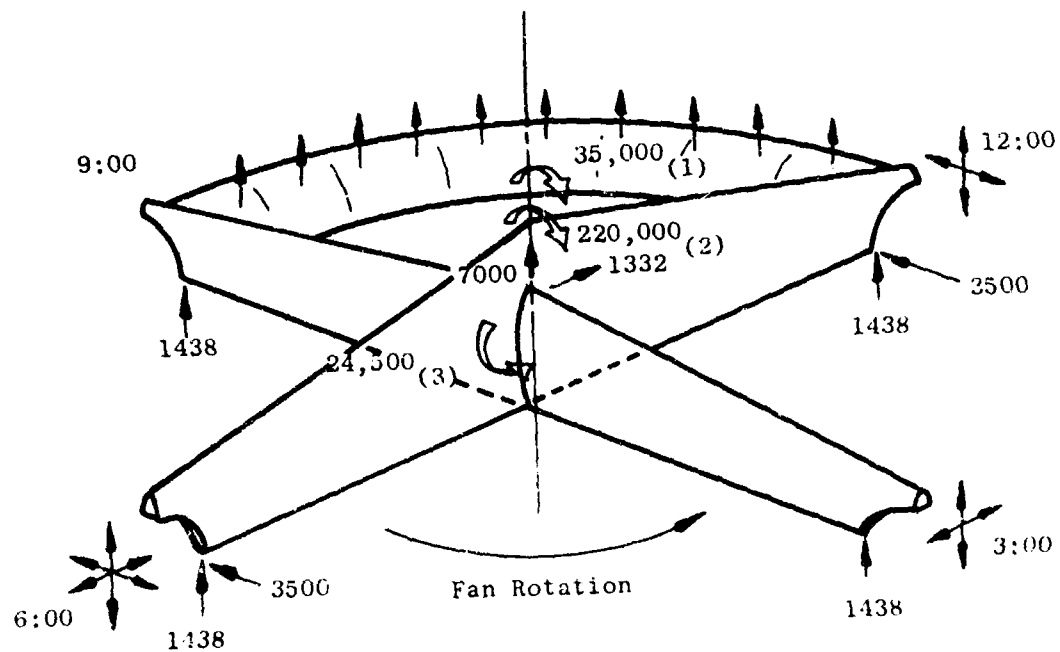
The material properties and fan operational life and environmental requirements were discussed previously in this report.

The front frame mechanical design described below does not provide hard points for mounting the fan door hinges or actuators. However, the front frame design is sized to withstand the forces associated with mounting the fan doors on the major strut.

Figure 52 shows the door moments calculated for the LFX fan and used in the front frame design analysis. These values were obtained by ratio from those calculated or measured for the XV-5A aircraft.

Figure 102 shows a representative position (for XV-5A type hinges and hydraulic actuators) of the hard points welded into the major strut for fan door hinge mounting. The hard points shown would increase the front frame weight by 18.5 pounds. However, the specific fan door installation has not been defined and the hard points shown are only representative. This particular aspect of the frame design will require further definition when the specific fan/airframe interface is established. (It should be noted, however, that the mechanical design of the front frame does include the fan door loads.)

Another detail which must await definition of the fan/airframe interface is the method of locking the fan doors in the closed position. Should it be necessary to penetrate the bellmouth with locking devices, appropriate openings can be provided and the areas around the openings suitably reinforced with doubler plates.



- (1) Door Moment
 - (2) Gyroscopic Moment
 - (3) Cross-Flow Moment Plus Moment Due 4"g" On Rotor
- All Forces - Pounds

Figure 100. Front Frame Load Schematic.

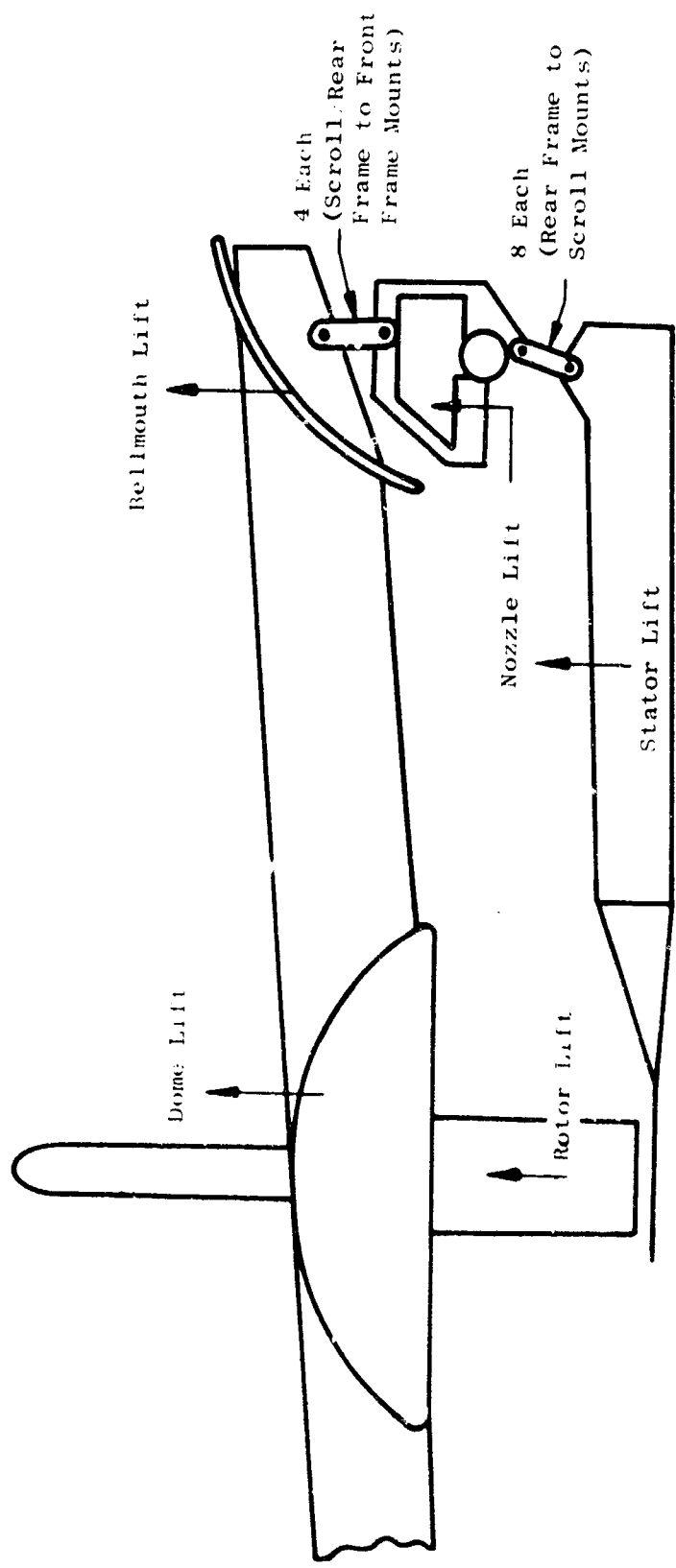


Figure 101. Front Frame Load Paths.

TABLE XIII
FRONT FRAME LOADS

<u>Source</u>	<u>Forces, lb</u>
Rotor Lift	5218
Rotor Disc Lift	783
Bellmouth Lift	1886
Hub Section Lift	996
Fan Stator Lift	1554
Turbine Nozzle Lift	1649
Lower Shroud Lift	664
Total Lift	12,750

Design Description

The LFX front frame is a composite integral structure of 17-4 stainless steel, titanium, aluminum, and honeycomb. The calculated weight (Table XIV) is 101.7 pounds, compared to an objective weight of 105 pounds. The major load-carrying members are the major and minor struts, with overall structural rigidity enhanced by the bellmouth assembly. The major and minor struts are integral with the hub and rotor shaft in order to transmit most efficiently the rotor loads to the mounting points. The front frame is supported in the wing at 3 locations. Figure 102 shows the overall configuration of the front frame, and the fan mounting method. The 6 o'clock and 12 o'clock mounts support the main lift and thrust loads, while the 3 o'clock mount supports the gyroscopic and cross flow induced loads. The 9 o'clock minor strut maintains bellmouth concentricity and rotor tip seal clearance. Figures 103 and 104 show component details.

Major Strut

The major strut, Figure 105, is a composite structure of 17-4 stainless steel and aluminum honeycomb. Minimum strut weight was obtained at the expense of an increase in overall strut height. Since the major strut is subjected to a large bending moment, a relatively large moment of inertia is required. By increasing the height of the major strut it was possible to obtain a satisfactory moment of inertia with the minimum amount of material (weight). A smaller strut height would require more material to obtain the same moment of inertia and would move the strut away from the optimum condition of being shear stress limited as well as deflection limited. Even though the major strut projects above the wing surface, it should present a minimum amount of drag due to the fact that it is narrow in the chordwise direction.

TABLE XIV
FRONT FRAME WEIGHTS

	Weight (lb)	Total
<u>Major Strut</u>		
Upper Cap Strips	11.49	
Lower Cap Strips	9.24	
Side Skins	7.79	
Shear Webs	4.06	
Central Post	.94	
Honeycomb Core	4.71	
End Sections	<u>10.38</u>	
		48.61
<u>Minor Strut</u>		
Upper Cap Strips	5.68	
Lower Cap Strips	3.68	
Side Skins	1.19	
Honeycomb Core	0.52	
End Sections	5.00	
Ribs	<u>0.23</u>	
		16.30
<u>Rotor Tip Seals</u>		
Honeycomb	0.20	
Backing Strip	1.96	
Scroll Cavity Seal	<u>1.72</u>	
		3.88
<u>Bellmouth</u>		
Flanges	4.27	
Honeycomb Core	0.57	
Skins	<u>5.00</u>	
		9.84
<u>Center Section</u>		
Shaft	10.92	
Dome Spider	9.56	
Dome Cap	<u>0.60</u>	
		21.08
<u>Fasteners</u>		
	<u>2.00</u>	
		<u>2.00</u>
		101.71

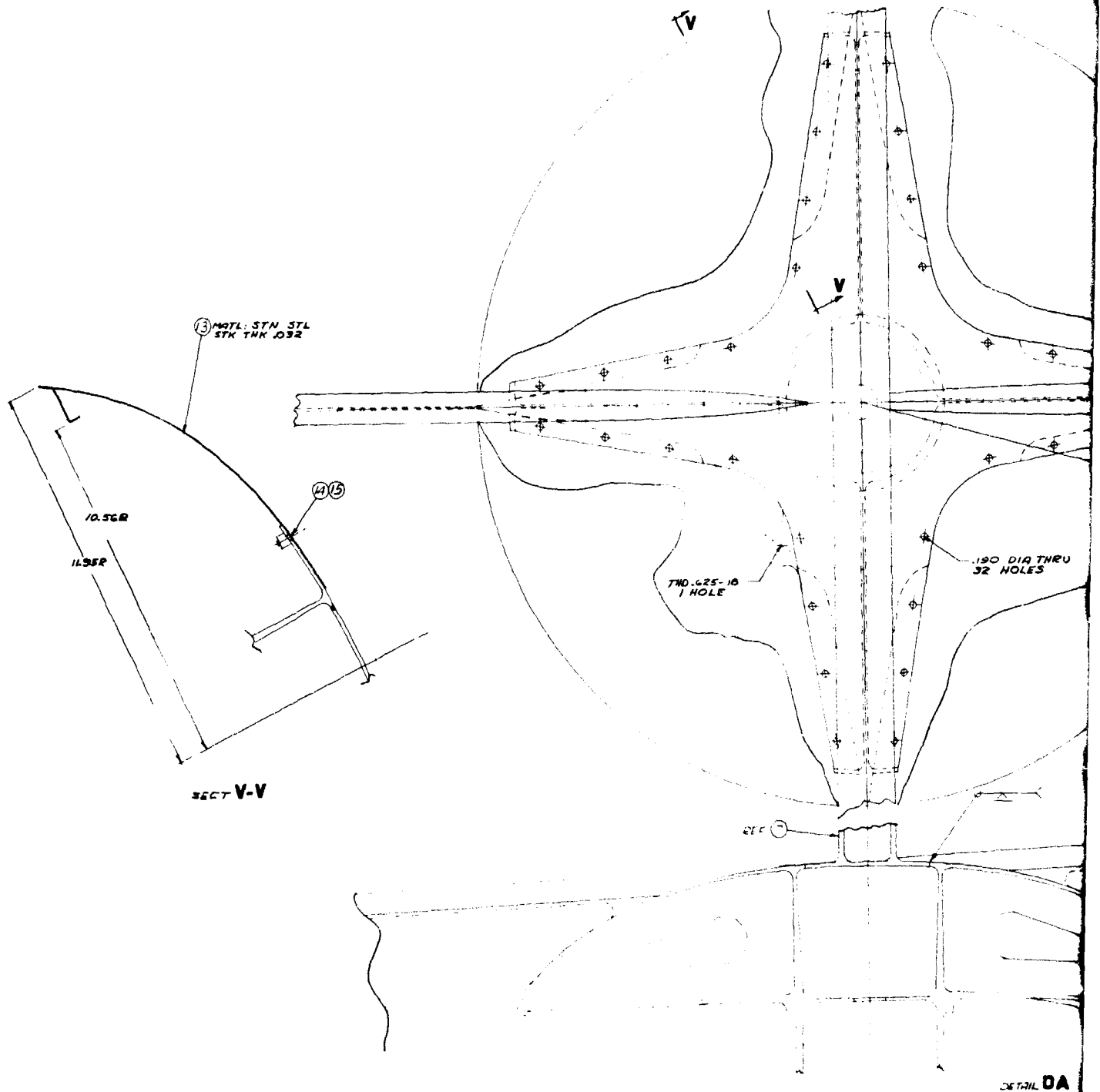
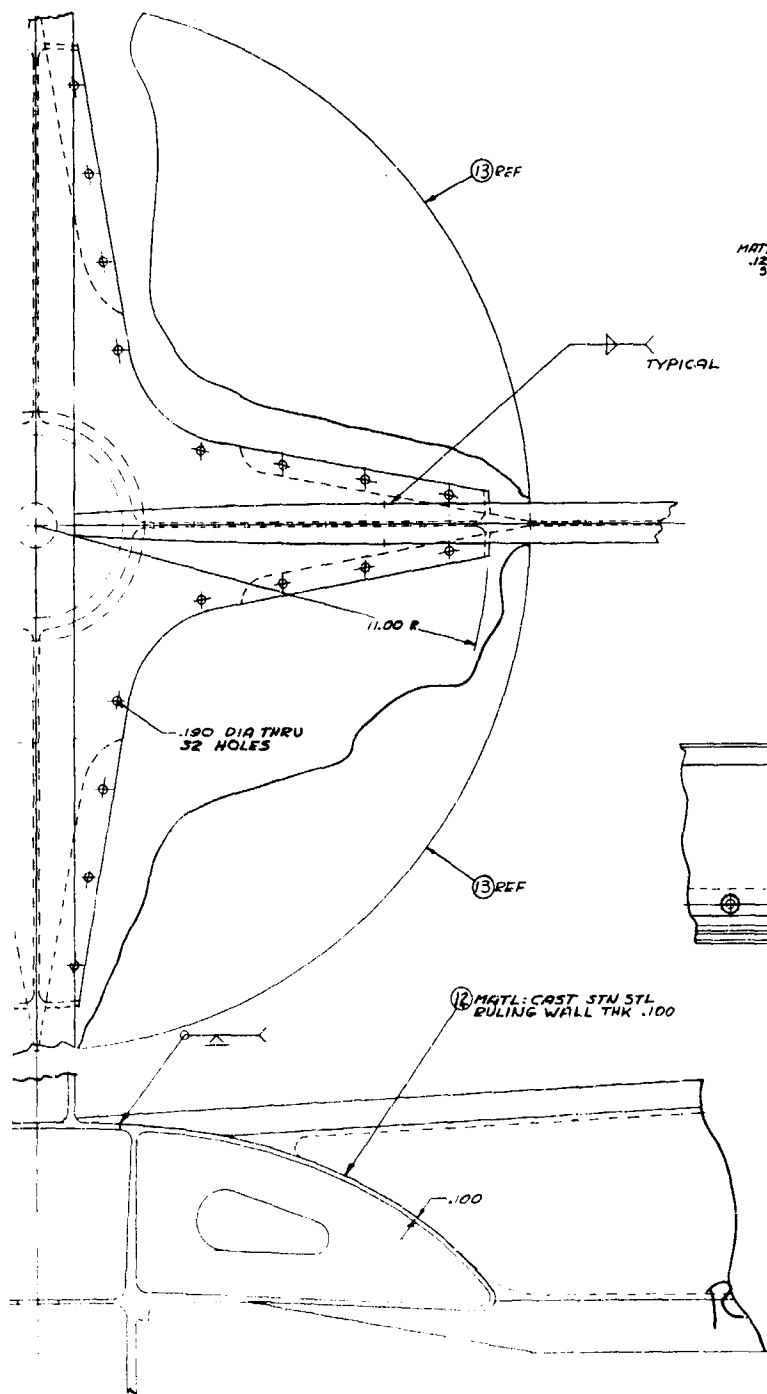
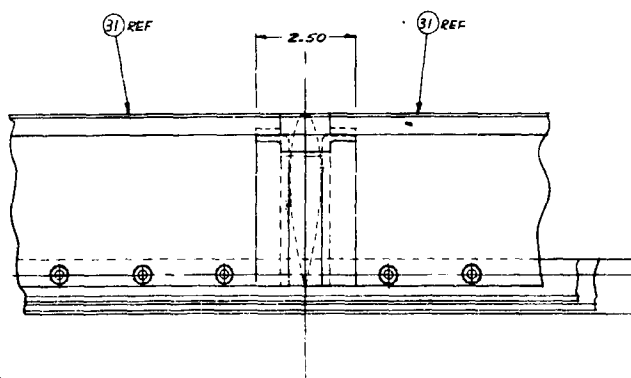
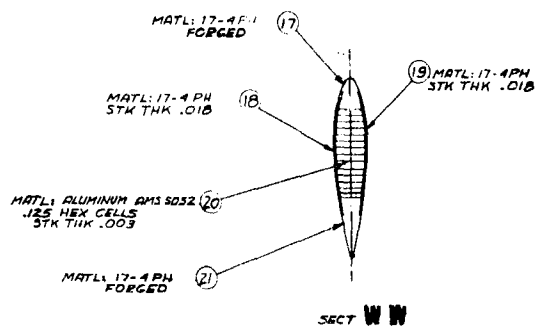


Figure 103. Front Frame Components.



DETAIL DA



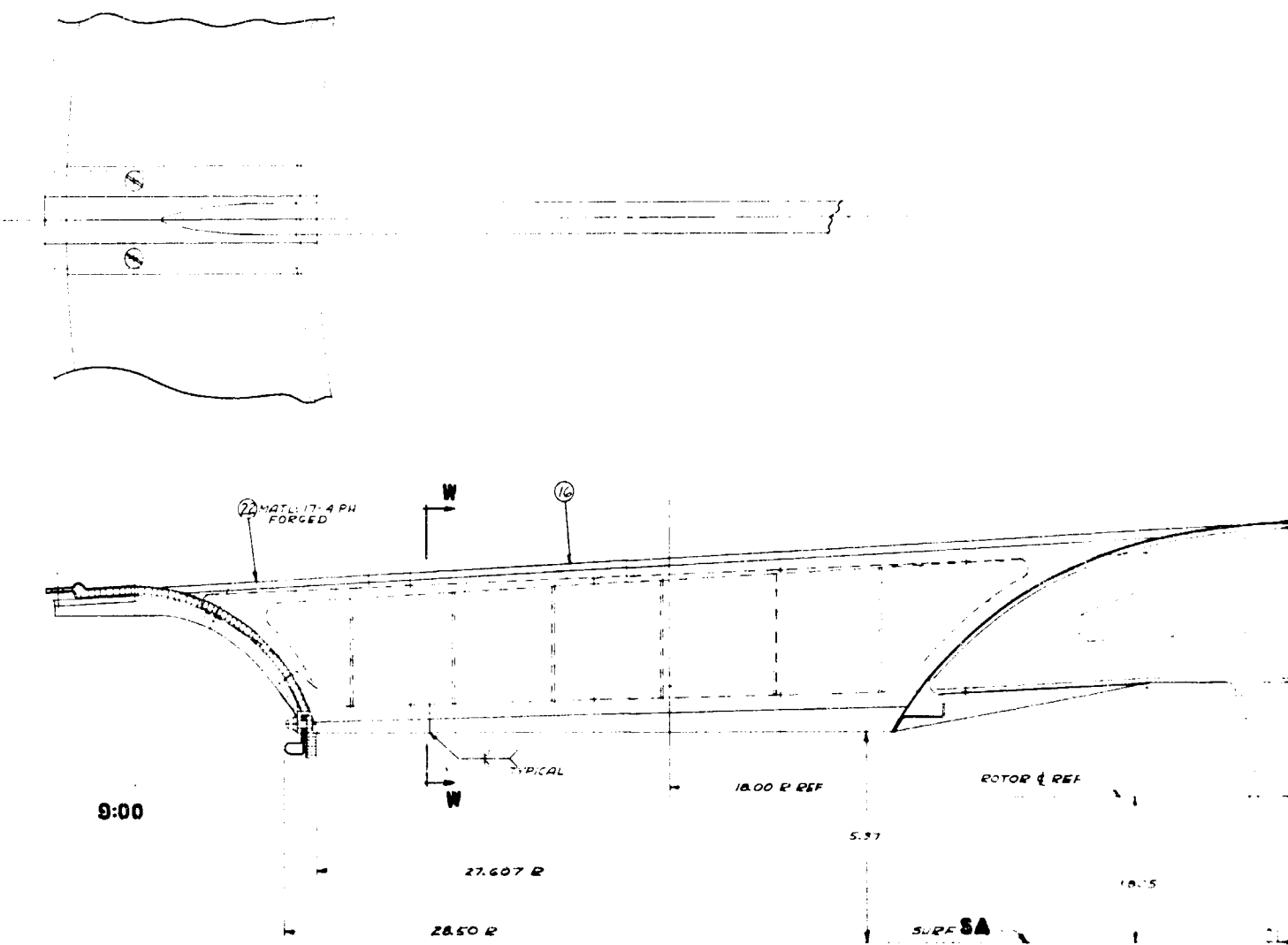
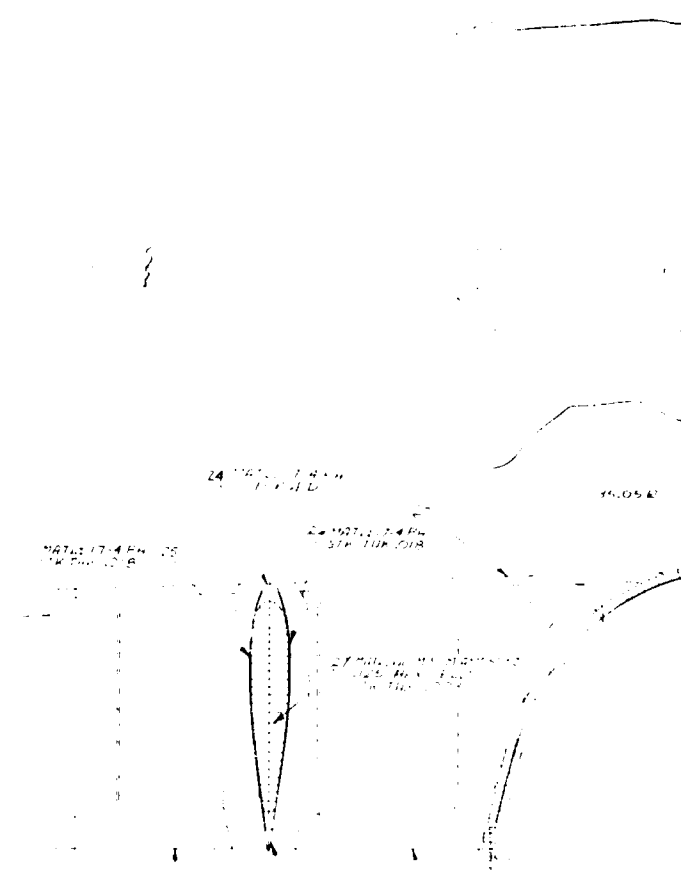
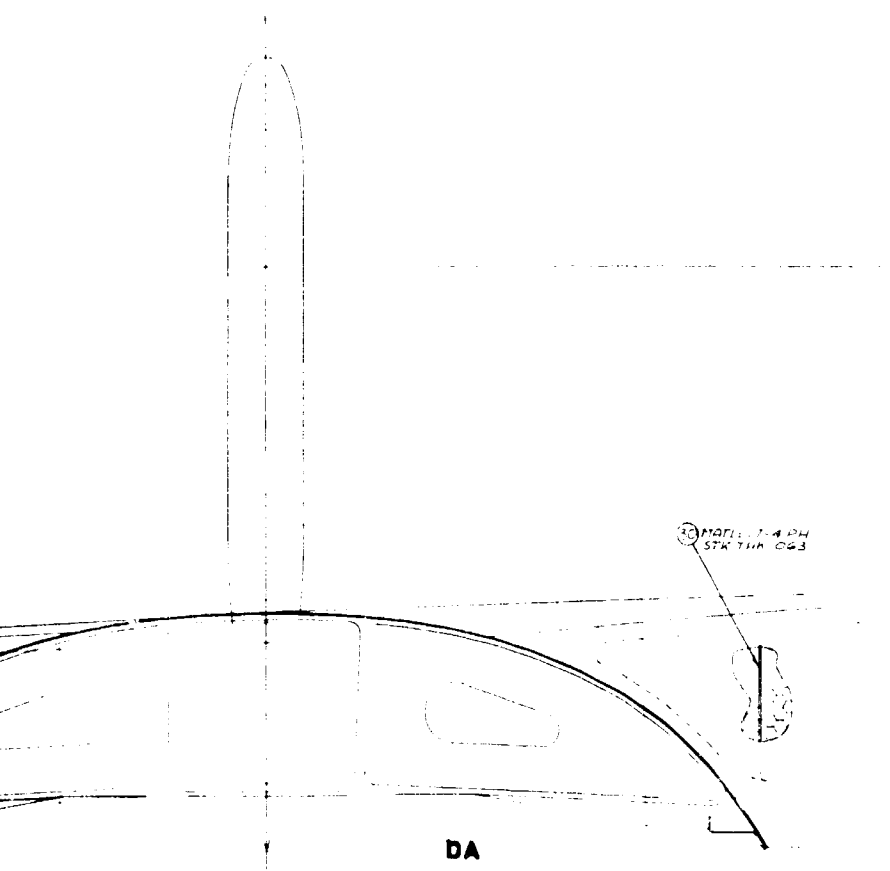


Figure 103. (Cont'd.)



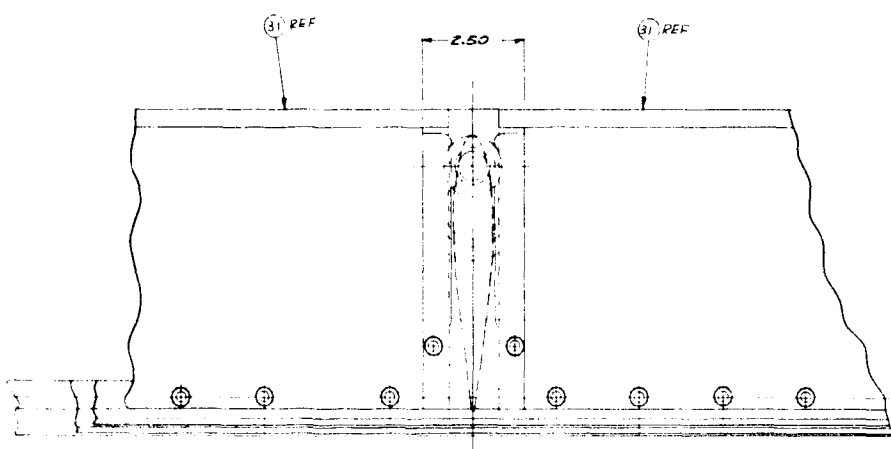
1 2 3 4 5 6 7 8 9 10 11 12 13 14 15 16 17 18 19 20 21 22 23 24 25 26 27 28 29 30 31 32 33 34 35 36 37 38 39 40 41 42 43 44 45 46 47 48 49 50 51 52 53 54 55 56 57 58 59 60 61 62 63 64 65 66 67 68 69 70 71 72 73 74 75 76 77 78 79 80 81 82 83 84 85 86 87 88 89 90 91 92 93 94 95 96 97 98 99 100

1 2 3 4 5 6 7 8 9 10 11 12 13 14 15 16 17 18 19 20 21 22 23 24 25 26 27 28 29 30 31 32 33 34 35 36 37 38 39 40 41 42 43 44 45 46 47 48 49 50 51 52 53 54 55 56 57 58 59 60 61 62 63 64 65 66 67 68 69 70 71 72 73 74 75 76 77 78 79 80 81 82 83 84 85 86 87 88 89 90 91 92 93 94 95 96 97 98 99 100

3:00

18.00 K

15.05 R



3:00

16.00 70 1/2

LAYOUT		CHECKED	
ALL DIMENSIONS IN INCHES ✓		FRONT FRAME LFX 6	
07482 4013007-734		07482 4013007-734	

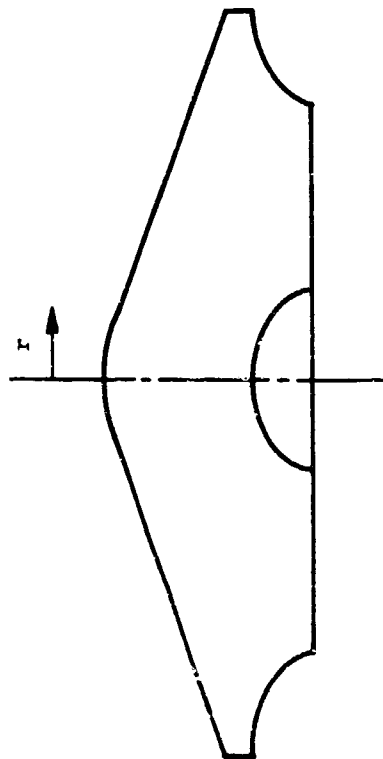
U

PARTS LIST CODES				REVISION CODES										
1 ASSY - SEE SEPARATE PARTS LIST		4 SEE DWG FOR CASTING OF FORGING DWG		1 ITEM OR ASSY ADDED		2 ITEM OR ASSY DELETED		3 QUANTITY CHANGED		4 ZONE OR SHEET CHANGED		7 ITEM NO. CHANGED		
2 VENDOR ITEM - SEE SPEC CONTROL DWG		5 VENDOR ITEM - SEE SOURCE CON. NO. DWG		P/E		COR		P/E		5 ZONE OR SHEET CHANGED		8 ITEM NO. CHANGED		
3 SELECTIVE FIT ITEM - SEE DWG		IDENTIFICATION		NOMENCLATURE		FL		COR		6 NOMENCLATURE CHANGED		9 CODE IDENT CHANGE		
ITEM NO.	DWG ZONE	DWG SHEET NO.	IDENTIFICATION	NOMENCLATURE	FL CODE	P/E	G	J	2	3	4	5	21 COR	27
8500010001	B-13	1	4013007-734G01	FF ASSY				X						
20002	H-5	1	G02	MAJOR STRUT ASSY				1	X					
30003	H-13	1	P03	CAP STRIP L.E.					1					
30004	F-8	1	P04	STRUT END 6:00					1					
30005	F-23	1	P05	STRUT END 12:00					1					
30006	C-20	1	P06	CAP STRIP T.E.					2					
30007	H-11	1	P07	RIB					1					
30008	H-9	1	P08	SHIELD					1					
30008	J-11	1	P08	SHIELD					1					
30009	J-9	1	P09	SHIELD					1					
30009	H-11	1	P09	SHIELD					1					
30010	H-11	1	P10	INSERT					1					
30010	H-12	1	P10	INSERT					1					
20011	D-14	1	G03	DOME ASSY				1		X				
30012	C-24	2	P12	SPIDER						1				
30013	F-30	2	P13	COVER, DOME						4				
30014	E-29	2	R1473P005	BOLT						32				
30015	E-29	2	R409P1B	NUT						32				
20016	E-18	2	4013007-734G04	STRUT ASSY 9:00				1			X			
30017	J-22	2	P17	CAP STRIP L.E.							1			
30018	J-22	2	P18	SHIELD							1			
30019	J-22	2	P19	SHIELD							1			
30020	H-22	2	P20	INSERT							1			
30021	H-22	2	P21	CAP STRIP T.E.							1			
30022	E-20	2	P22	STRUT END 9:00							1			
20023	E-9	2	G05	STRUT ASSY 3:00				1				X		
30024	E10	2	P24	CAP STRIP L.E.								1		
30025	E-10	2	P25	SHIELD								1		
30026	E-10	2	P26	SHIELD								1		
30027	D-10	2	P27	INSERT								1		

Figure 104. Front Frame Parts List (4013007-734).

PARTS LIST CODES				REVISION CODES																	
1 ASSY - SEE SEPARATE PARTS LIST				4 SEE DWG FOR CASTING OR FORGING DWG				1 ITEM OR ASSY ADDED				4 ZONE OR SHEET CHANGED				7 ITEM NO. CHANGED					
2 VENDOR ITEM - SEE SPEC CONTROL DWG				5 VENDOR ITEM - SEE SOURCE CONTROL DWG				2 ITEM OR ASSY DELETED				5 IDENT NO. CHANGED				8 GENERAL CHANGE					
3 SELECTIVE FIT ITEM - SEE DWG								3 QUANTITY CHANGED				6 NOMENCLATURE CHANGED				9 CODE IDENT CHANGE					
ITEM NO.	DWG 75%	DATE 5-415	NO.	IDENTIFICATION	NOMENCLATURE	K (CMM)	CMM UNIT	PC SUFFIX NO. AND QUANTITY REQUIRED						RY (CMM)	RY						
								G	1	2	3	4	5			6					
8500030028	C10	2		4013007-734P28	CAP STRIP T.F.																
30029	C09	2		P29	STRUT END																
30030	E12	2		P30	RIB																
20031	D22	1		G06	BELLMOUTH				1												
30032	J22	1		P32	BELLMOUTH 12:00-3:00															X	
30033	E5	1		P33	BELLMOUTH 3:00-6:00															1	
30034	E7	1		P34	BELLMOUTH 6:00-9:00															1	
30035	F22	1		P35	BELLMOUTH 9:00-12:00															1	
30036	F22	1		R1474P012	BOLT															24	
30037	F22	1		R406P2B	NUT															24	
30038	C10	1		4013007-734P38	COMP SEAL ASSY															1	
30039	C10	1		P39	SCROLL SEAL ASSY															1	
30040	C11	1		R543P16	BOLT															58	
30041	C7	1		R1182P003	NUT															58	

FINAL SHEET



Radius (in.)	Section Area (in. ²)	Chord Length (in.)	Applied Moment X10 ⁻³ (in.-lb)	I _{Max} (in. ⁴)	I _{Min} (in. ⁴)	Torsional Constant	Flexural Stress Major Axis X10 ⁻³ (psi)	Shear τ Max Stress X10 ⁻³ (psi)
5	1.65	17.5	271.0	71.2	0.439	1.795	34.78	14.574
10	1.59	16.8	237.0	59.3	0.392	1.595	33.57	15.181
15	1.53	15.3	203.0	48.5	0.343	1.392	32.07	16.670
20	1.47	13.9	169.0	38.8	0.294	1.190	30.18	18.349
25	1.41	12.4	135.0	30.2	0.249	0.990	27.71	20.569
27.607	1.38	11.6	117.3	25.1	0.223	0.883	25.49	21.987

Figure 105. Front Frame Major Strut.

The strut is fabricated by welding the upper and lower caps strips to the end sections and to the central hub section. Central shear webs, of 17-4, are welded into position at the inner and outer ends of the cap strips to provide a more gradual load transition into the hub and end sections. The primary function of the 17-4 side skins is to withstand the vertical shear loads on the strut. Buckling of these side skins is prevented through the use of a lightweight honeycomb core bonded into the strut assembly and to the side skins. Internal vertical ribs are also welded into the strut and adhesively bonded to the honeycomb to provide additional required shear strength.

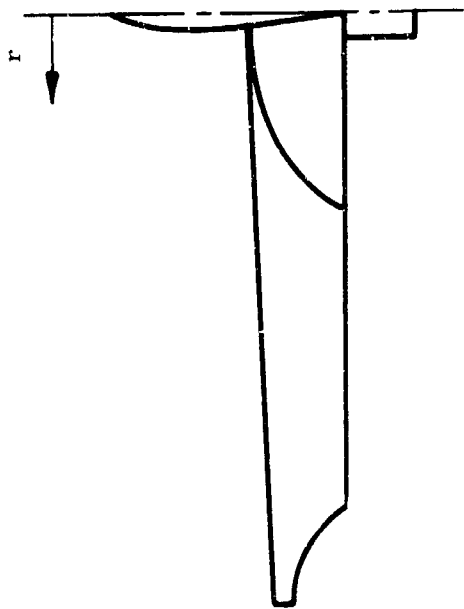
The major strut cross section is airfoil shaped to provide as little disturbance as possible to the flow entering the fan. The airfoil cross section is based on an 18-percent-maximum-thickness, 10-inch-chord NACA 0018 type airfoil modified with a constant thickness center section insert.

The major strut is tapered in the chordwise (12:00-6:00) direction to provide a moment of inertia distribution which closely matches the applied moment distribution. Both ends of the strut are flared horizontally, beneath the wing surface, to provide sufficient lateral strength to carry the horizontally acting pressure differential induced scroll loads (scroll piston force). The scroll/rear frame structure is mounted to the front frame at four points, one at each end of the major and minor struts. These mounts are designed to transmit the scroll/rear frame loads into the front frame and also to allow radial differential thermal expansion between the scroll/rear frame and the front frame.

Minor Strut

The configuration of the minor strut, Figures 106 and 108, is similar to that of the major strut. There is a difference, however. While the major strut is narrow (chordwise) and can project above the wing surface without a significant aircraft drag effect, the minor strut runs chordwise and would expose its entire profile to the flow over the wing if it projected above the wing. Accordingly, the minor strut must be designed to provide the necessary strength and yet remain below the wing surface. Since the wing contour does not allow the minor strut depth to be as highly tapered as that of the major strut, radial variation of the minor strut section properties is obtained by reducing the cross-sectional area of each cap strip from the hub to the strut end. In this manner, the moment of inertia distribution can be made to match closely the applied moment distribution, thus providing an efficient utilization of material.

Fabrication is similar to that of the major strut: 17-4 cap strips welded into the strut ends and the hub section, central shear webs to provide gradual load transitions, aluminum honeycomb core bonded into the strut, and side skins bonded to the strut and the honeycomb core.



Radius (in.)	Section Area (in. ²)	Chord Length (in.)	Applied Moment X10 ⁻³ (in.-lb)	I ^{Max} (in. ⁴)	I ^{Min} (in. ⁴)	Torsional Constant	Flexural Stress Major Axis X10 ⁻³ (psi)	Shear τ Max Stress X10 ⁻³ (psi)
5	0.656	5.15	87.4	2.13	0.023	0.038	105.8	32.5
10	0.586	4.90	71.9	1.76	0.019	0.035	100.3	34.9
15	0.517	4.65	56.5	1.38	0.017	0.031	94.9	36.2
20	0.449	4.40	41.0	1.01	0.016	0.028	89.1	37.4
25	0.351	4.15	25.6	0.64	0.013	0.025	83.1	37.5

Figure 106. Front Frame Minor Strut - 9:00 O'Clock.

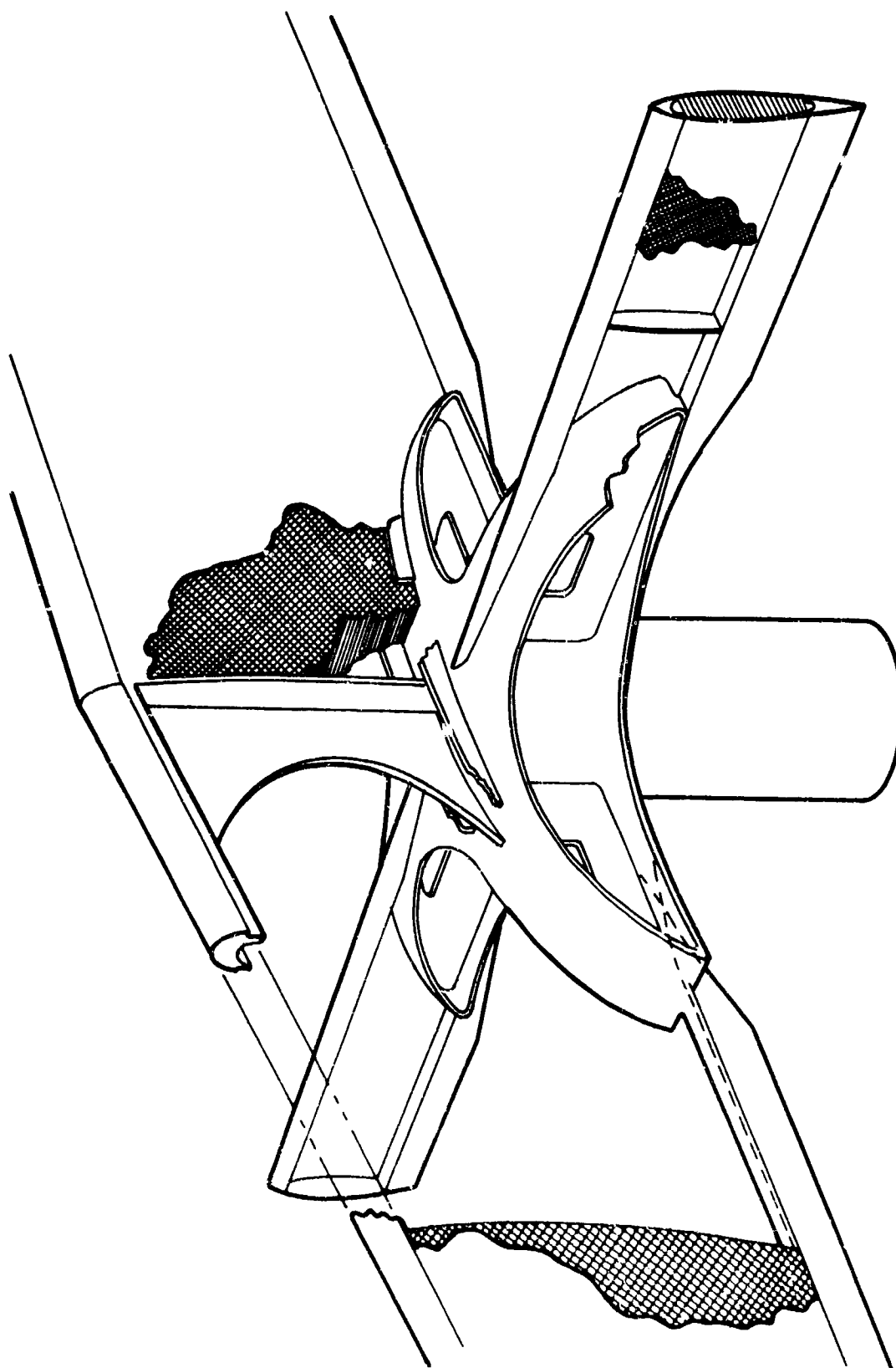
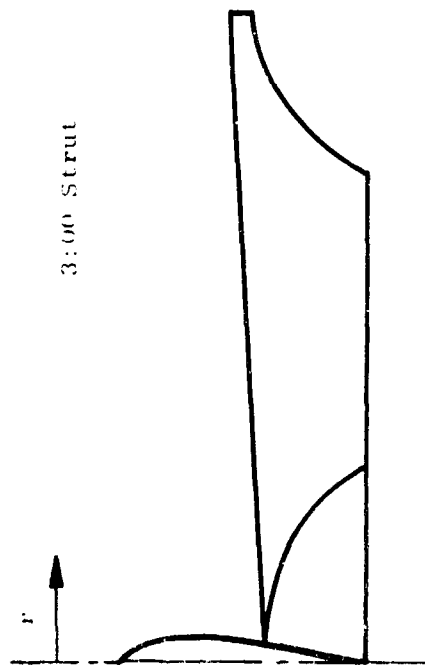


Figure 107. Front Frame Hub.



3:00 Strut

Radius (in.)	Section Area (in. ²)	Chord Length (in.)	Applied Moment $\times 10^{-3}$ (in.-lb)	I_{Max} (in. ⁴)	I_{Min} (in. ⁴)	Torsional Constant	Flexural Stress Major Axis $\times 10^{-3}$ (psi)	Shear τ Max Stress $\times 10^{-3}$ (psi)
10	0.583	5.69	153.97	4.64	0.123	0.067	94.46	43.50
15	0.362	5.836	120.96	3.79	0.047	0.073	93.04	42.43
20	0.233	5.980	87.94	2.87	0.045	0.079	91.60	41.40
25	0.128	6.124	54.93	1.87	0.038	0.086	90.04	40.43
30	0.085	6.268	21.91	0.85	0.037	0.092	81.14	39.50

Figure 108. Front Frame Minor Strut - 3:00 O'Clock.

The strut cross section is a 15-percent-maximum-thickness, varying-chord NACA 0015 airfoil modified with a constant thickness center section insert. The ends of the minor strut (Figure 106) have mounting provisions for the scroll/rear frame assembly and are designed to accommodate the resultant loads. The 3 o'clock end of the minor strut is designed to accept a ball mount to transmit fan loads into the airframe structure.

Both ends of the minor strut have a ledge, Figure 103, to mount the bellmouth assembly.

Hub Section

The primary function of the hub section is to support the rotor shaft and effectively transmit the rotor loads into the major and minor struts. It also serves as a structural member to provide continuity of the major and minor struts across the fan center. This integral hub section/shaft/strut arrangement provides the most efficient (lightest) means of transmitting the rotor lift and gyroscopic forces into the struts.

The hub structure, Figure 107, is a welded 17-4 assembly consisting of upper and lower dome shaped load distribution members, four radial webs (90° apart) between the load distribution members, and the rotor shaft. The major and minor struts weld directly to the upper and lower load distribution members to accept all rotor load. The hub section flow path bullet nose is 0.030-inch aluminum (made in detachable quadrants to provide access to the speed sensor).

The major and minor strut cap strips are welded to the hub section as shown in Figure 107.

Bellmouth

The bellmouth structure is an adhesively bonded titanium sheet and aluminum honeycomb composite assembly, fabricated in quadrants. Each quadrant consists of a 0.25-inch-thick aluminum honeycomb core, shaped to the bellmouth contour, with titanium sheet bonded to the inner and outer surfaces. The end flanges are titanium, as are the edge flanges where the bellmouth bolts to the major and minor strut ledges.

The bellmouth lower edge flange contains provisions for mounting the stationary rotor tip honeycomb seal and the scroll cavity seal.

Design Analysis

Analyses conducted to establish the design of the front frame included:

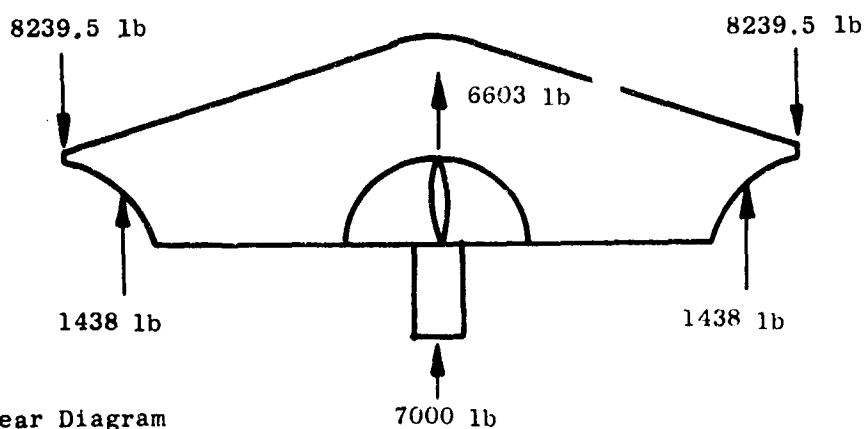
1. Definition of applied loads and moments
2. Preliminary definition of front frame mounting to the airframe
3. Determination of major loads and load paths within the front frame
4. Preliminary definition of front frame component configuration and section properties
5. Calculation of structure deflections and loads at key locations
6. Determination of required properties at critical locations (stress, buckling, or deflection limited locations)
7. Iteration of 4, 5, and 6 to optimize structure weight/required strength

The applied loads to establish the front frame design are shown in Figures 100 and 109 through 112. The vertical (downward) maneuver load was not included in the analyses, since it acts in the opposite direction to the fan lift. The gyroscopic induced moment due to maneuver (roll, pitch, or a combination) was applied, alternately, to load the major strut or the minor strut, and the resultant deflections were calculated.

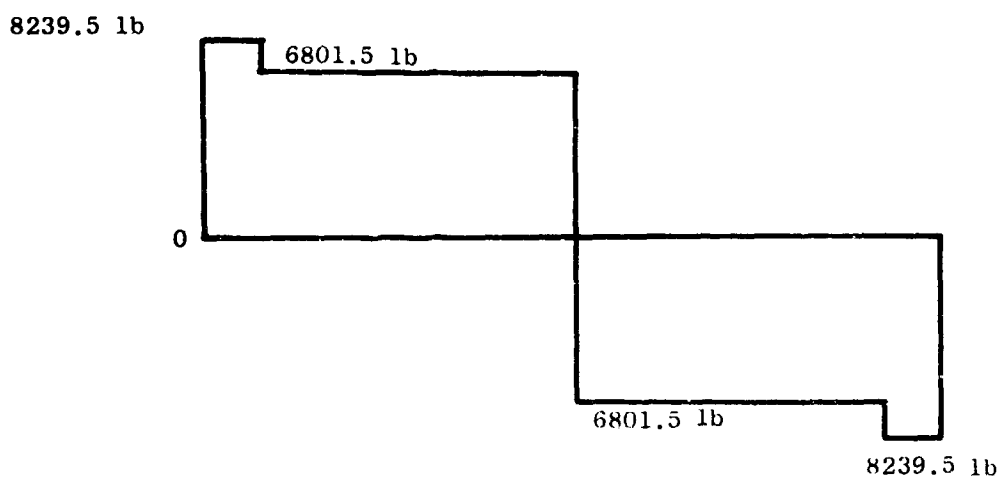
Front frame deflections were calculated using a program capable of analyzing three-dimensional structures consisting of straight and curved members of varying properties. For purposes of clarity, the structure deflections were calculated in two cases and the results superimposed. Specifically, the front frame deflections due to the lift forces only were determined. Additional calculations then determined the deflections due to the gyroscopically induced moment (one case where the moment loads the minor strut and one case where the moment loads the major strut). Calculation of the deflections due to lift and due to gyroscopic moment separately allowed an assessment of the relative effect of each on the structure. This, in turn, permitted a determination of the best manner to accommodate the applied loads and resultant deflections.

From the front frame loading shown schematically in Figure 100, the load, shear and bending moment diagrams for the major and minor struts were derived. This information is given in Figures 109 and 110 for the major strut, in Figure 111 for the 9 o'clock strut and in Figure 112 for the 3 o'clock strut.

(a) Load Diagram



(b) Shear Diagram



(c) Moment Diagram

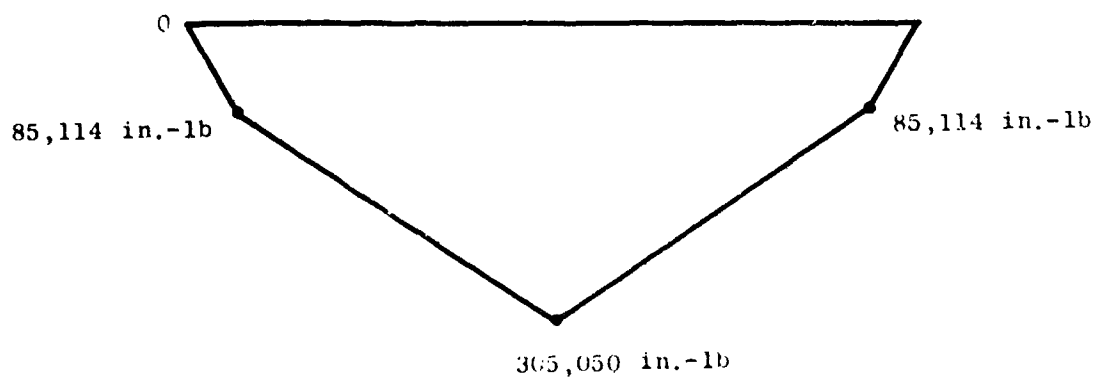
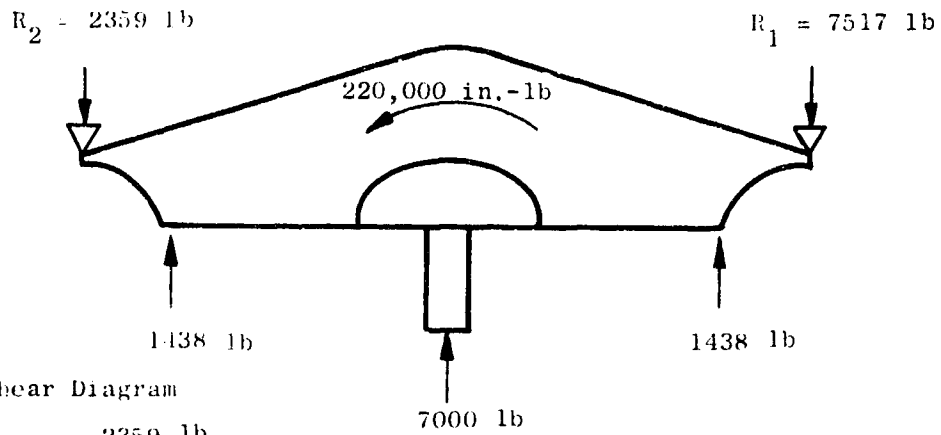
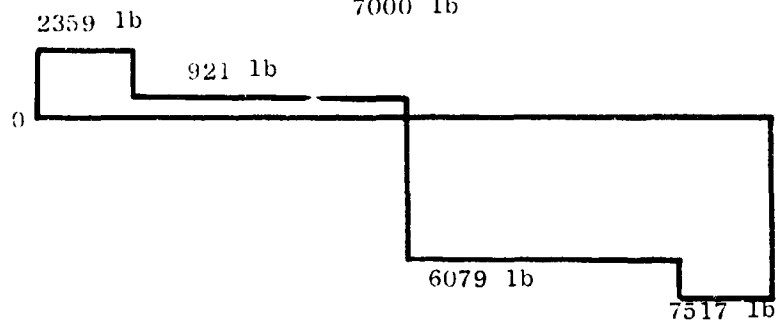


Figure 109. Major Strut Loads, Shear and Moment.

(a) Load Diagram



(b) Shear Diagram



(c) Bending Moment Diagram

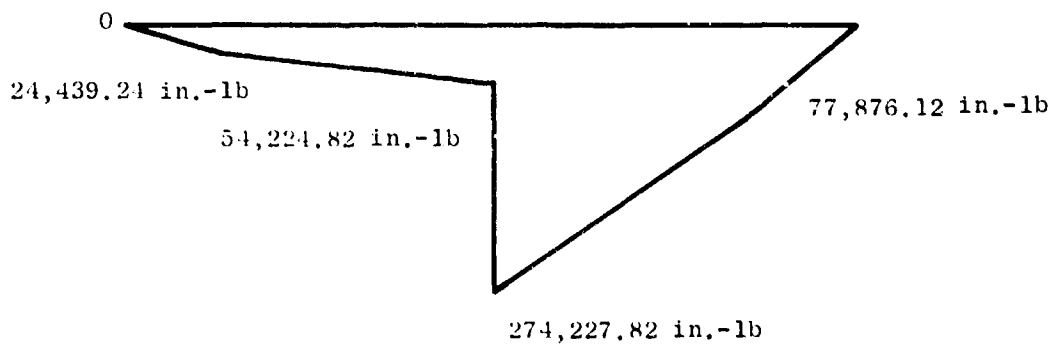
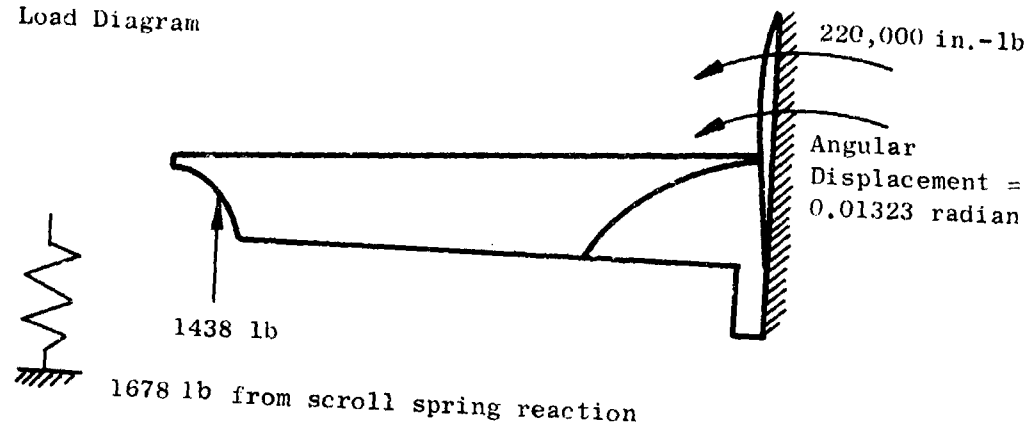
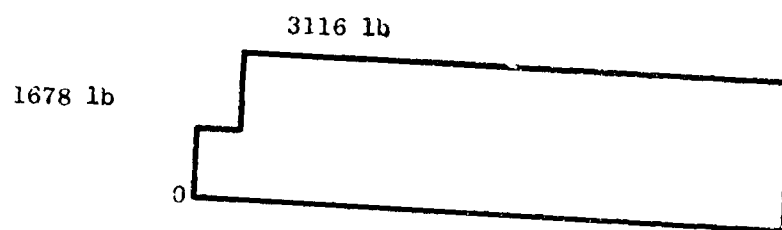


Figure 110. Major Strut Loads, Shear and Moment.

(a) Load Diagram



(b) Shear Diagram

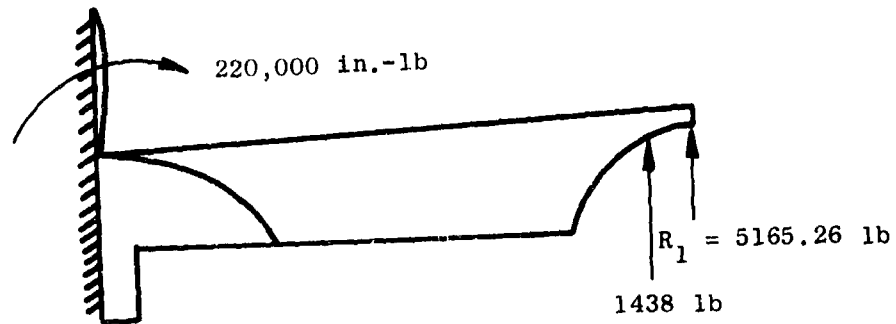


(c) Moment Diagram

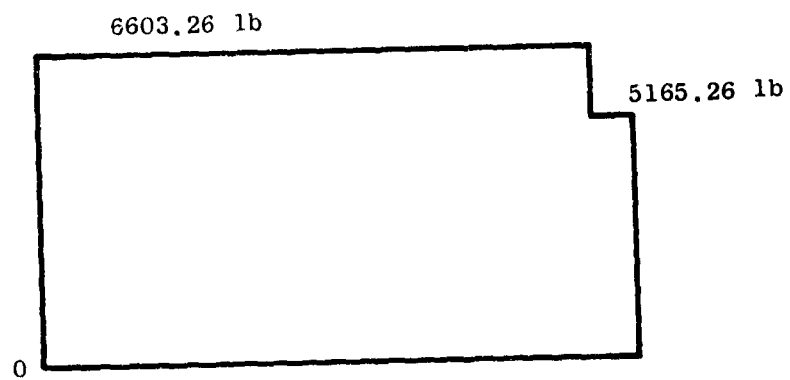


Figure 111. Minor Strut Loads, Shear and Moment.

(a) Load Diagram



(b) Shear Diagram



(c) Moment Diagram

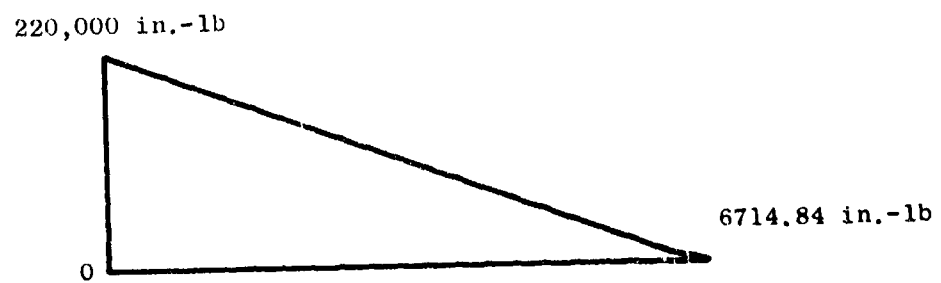


Figure 112. Minor Strut Loads, Shear and Moment.

Based on this information, the front frame configuration and section properties were preliminarily defined and iterated with the deflection calculations to arrive at section and material properties which produced acceptable deflections. The resulting design was described in the previous section and the section properties are shown in Figures 105, 106 and 108. The calculated deflections for this frame configuration are shown schematically in Figures 113, 114 and 115. The specific loading conditions used to calculate the deflections are noted on the respective figures.

Shear and buckling criteria were used to design the strut core sections and side skin material and thickness. While these components do have an effect on the strut moment of inertia, the effects are relatively much smaller than the effects of strut cap strip size and chordwise spacing. Thus, the major considerations in core and skin design were shear and buckling. The strut side skins carry 75 percent of the shear on the strut, the remainder being carried by the strut cap strips and honeycomb core. Strut and skin buckling is prevented by the light, rigid honeycomb core. The shear stresses are summarized on Figures 105 and 106.

The analysis discussed above was sufficient to define detail frame configuration, strut section properties, size of components (and resultant frame weight), and general suitability of the design. However, there are specific areas requiring further detail analysis and refinement. A more detailed evaluation of the strut ends is warranted, both to further assure design integrity and to attempt additional weight reduction.

It would be desirable to move the rear frame/scroll mounts outboard on the major strut (closer to the fan mounts) to reduce the transverse moment on the front frame major strut. This moment could be essentially eliminated by proper design of the major strut/airframe mounts. Figure 101 shows the desired restraints on the front frame mounts. However, further definition of the fan/airframe interface is necessary before the most efficient mounting method can be designed.

Also, to assure design integrity and to attempt further weight reduction, the bellmouth design and hub section design should be investigated in more detail.

Even though additional detail analysis is required, sufficient work has been done to assure that the front frame design, as defined above, represents a major advancement in lightweight, current material and process technology, lift fan structures.

Alternate Concept

In an effort to reduce the overall lift fan system installed weight and to improve the installation aspects of the fan system, alternate frame design concepts were considered. One concept which shows promise is the combination of the fan door structure and the major strut. The fan would

Gyroscopic Load on Major Strut
plus Bellmouth Load

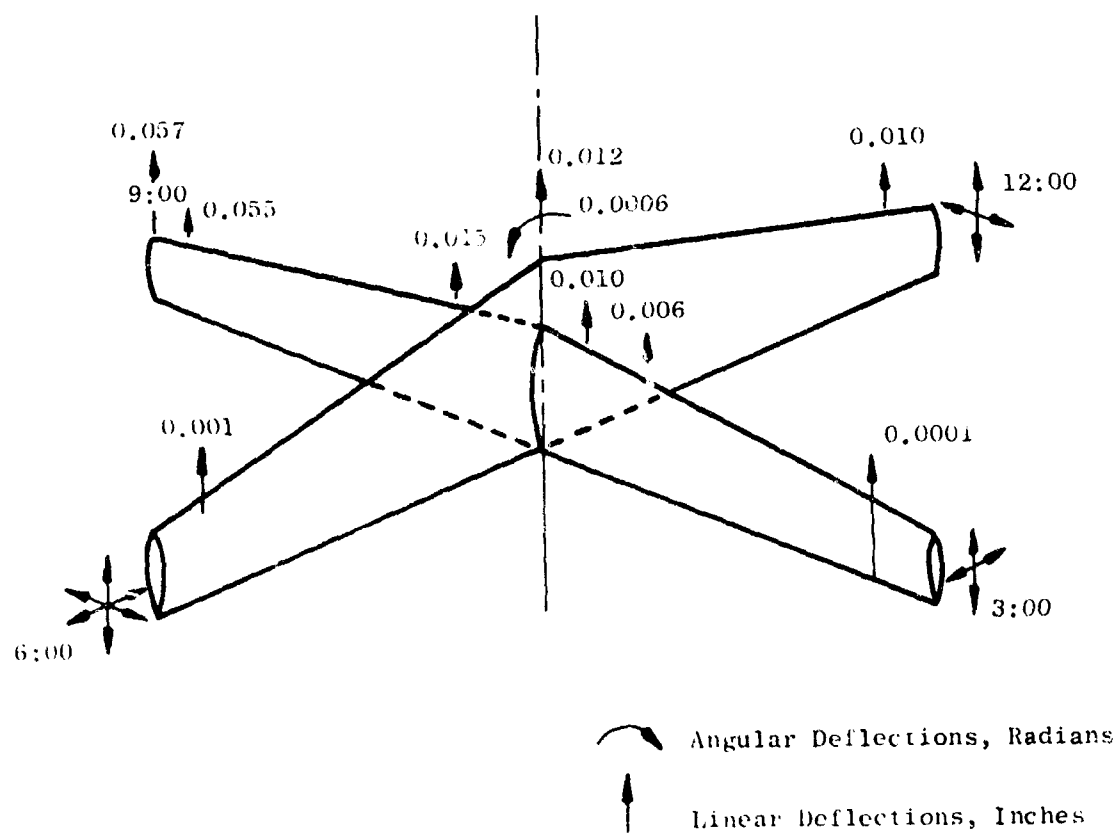


Figure 113. Front Frame Deflections.

Lift Forces combined with
4 "g" Forward

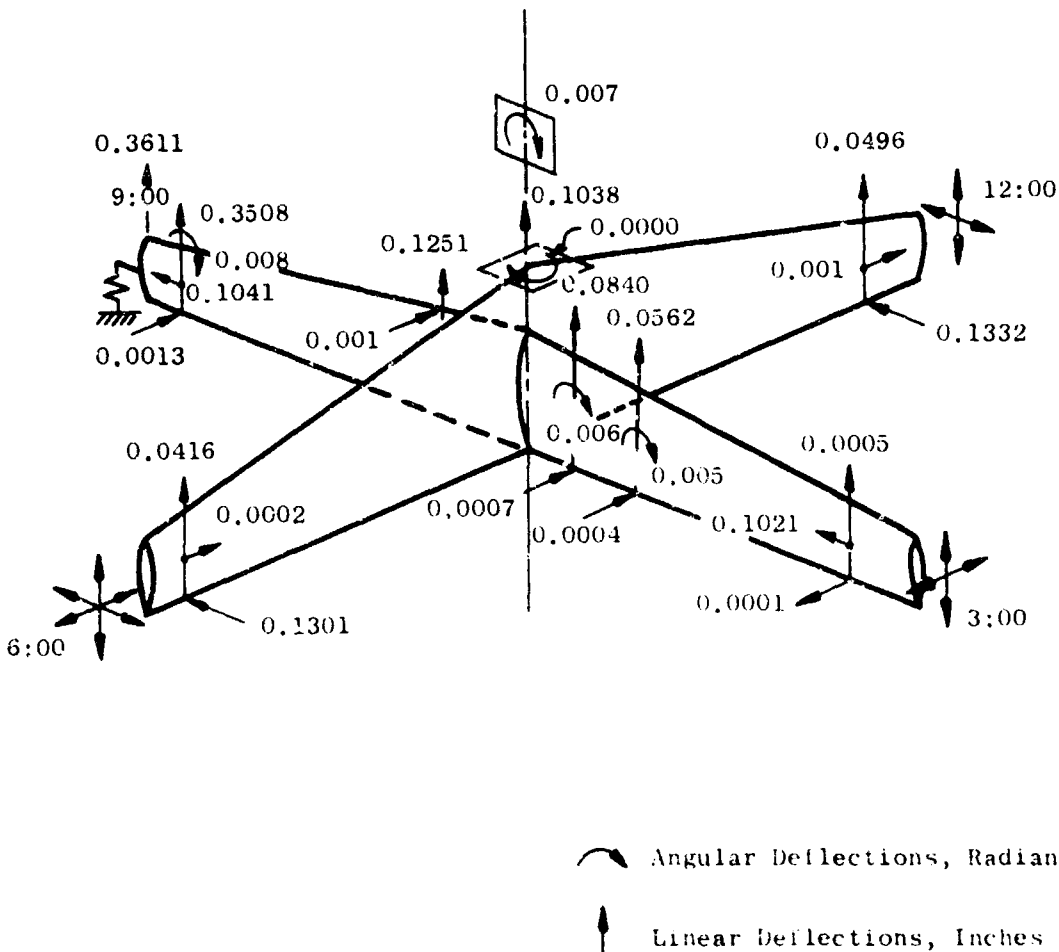


Figure 11-4. Front Frame Deflections - Lift Forces.

Gyroscopic Loading on Minor Strut
 100,000 Inch-Pounds Induced Moment
 Acting on Minor Strut

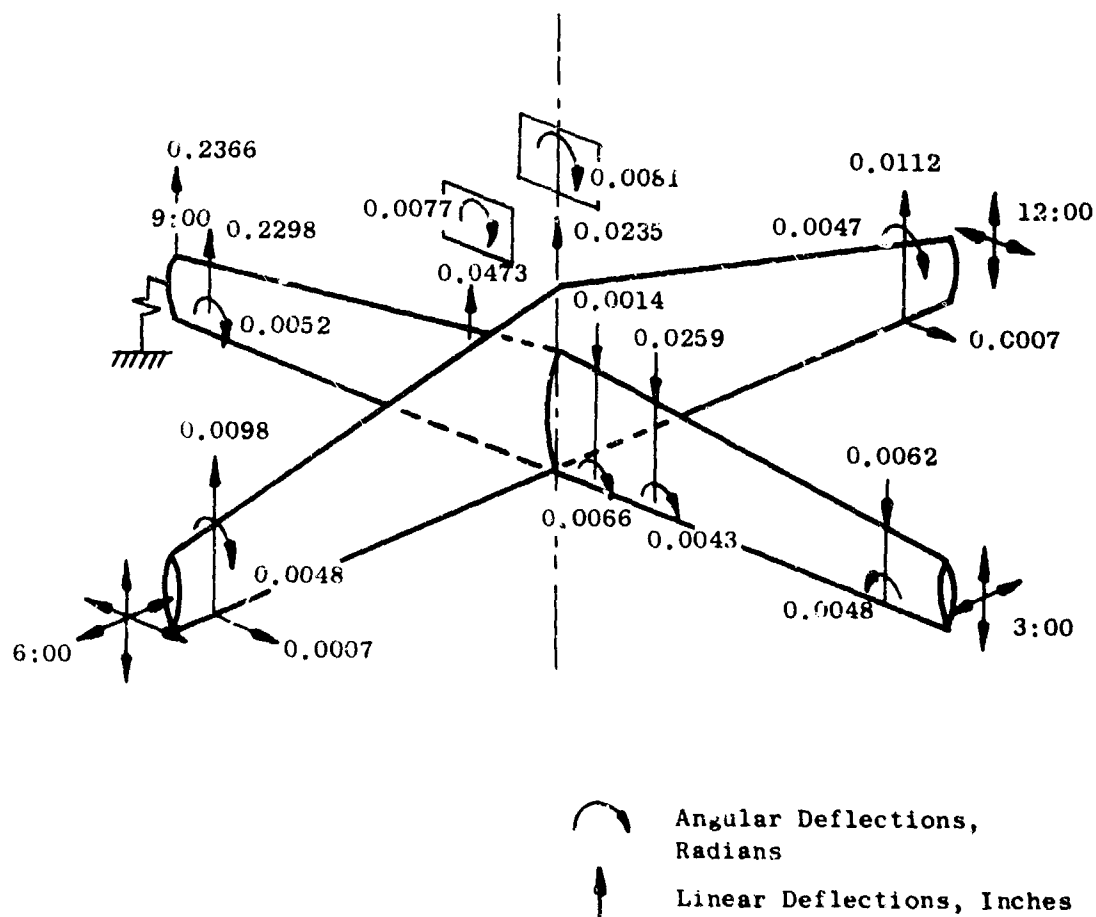


Figure 115. Front Frame Deflections.

be supported in the airframe, when not operating, by what are essentially the present lower elements of the major and minor struts. When the fan is to be operated in the lift mode, the fan cover doors are opened and in turn erect transverse (spanwise) links. These spanwise links serve to stabilize the door panels and are sized to act as the upper elements of the minor struts.

As shown in Figures 116 through 118, this arrangement would allow the door actuators to be placed forward and aft of the fan itself, thus providing essentially the entire depth of the wing for actuation action (rather than attempting to place the actuation system within the central hub section). Whether a worm and sector or a hydraulic cylinder and bellcrank actuation system were to be used, the increased depth available would reduce the forces required to actuate the fan doors.

Utilization of the deep (in the open position) door for major strut beam strength would provide the required moment of inertia with minimum weight. Buckling would undoubtedly become the major design criteria. However, use of the stabilizing struts (upper elements of the minor struts) would reduce the buckling tendency.

The main advantages of this concept are: (1) it essentially eliminates the major strut upper structural elements and thus reduces the projection above the wing surface (fan doors closed) to that required to cover the door hinge, and (2) it allows the minor strut upper elements to perform double duty, stabilizing the open door and providing the required minor strut moment of inertia. As in the case of the door/major strut, moving the upper elements of the minor strut outward decreases the weight required to provide an equivalent moment of inertia.

An approximate comparison of the potential system weight reduction for this concept is given in Table XV. The weights shown for the LFX-6 are for a system similar to the XV-5A, ratioed to the LFX-6 size and loads. The alternate concept weights are preliminary estimates. The weights of actuators, door-closed locks, etc., were assumed to be comparable for both concepts.

A preliminary evaluation of this concept indicates that it is feasible. Additional study is necessary to define the actuation system and hinge arrangement in more detail. One specific area to be explored in more detail is the transfer of the gyroscopically induced moment from the hub section into the door/major strut. It appears that an appropriate combination door locking/moment transfer arrangement is possible.

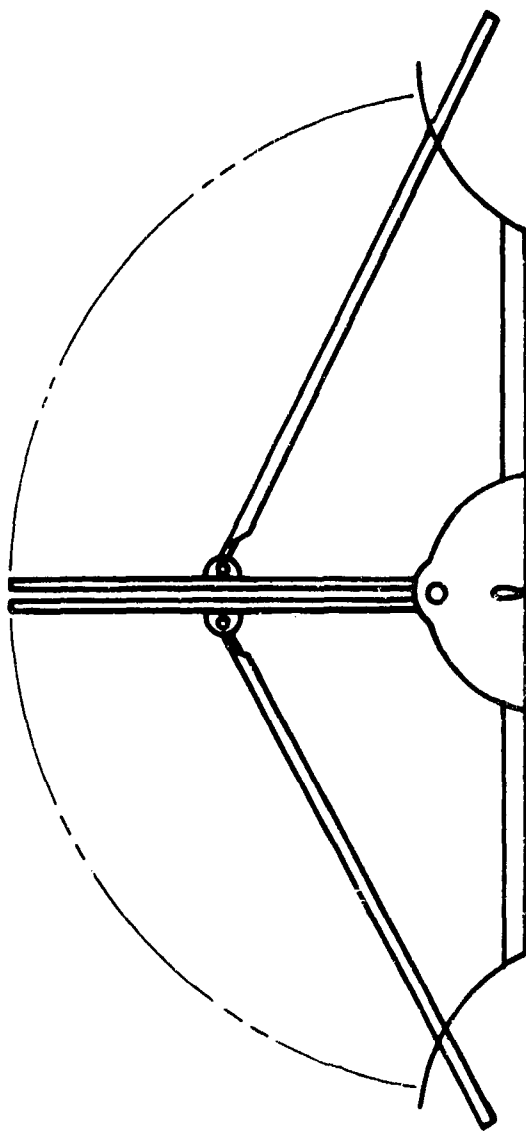


Figure 116. Door-Strut Combination Concept.

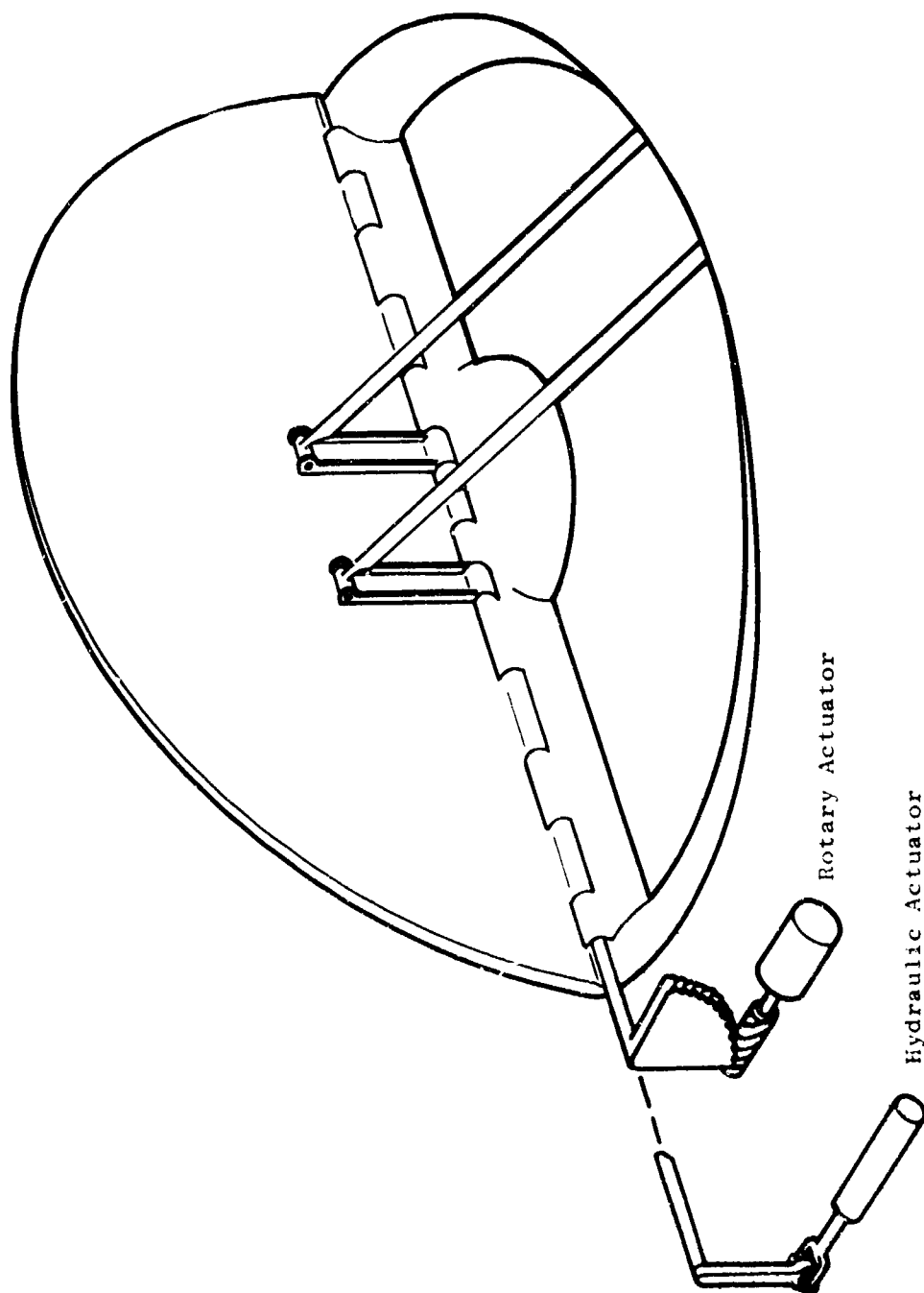
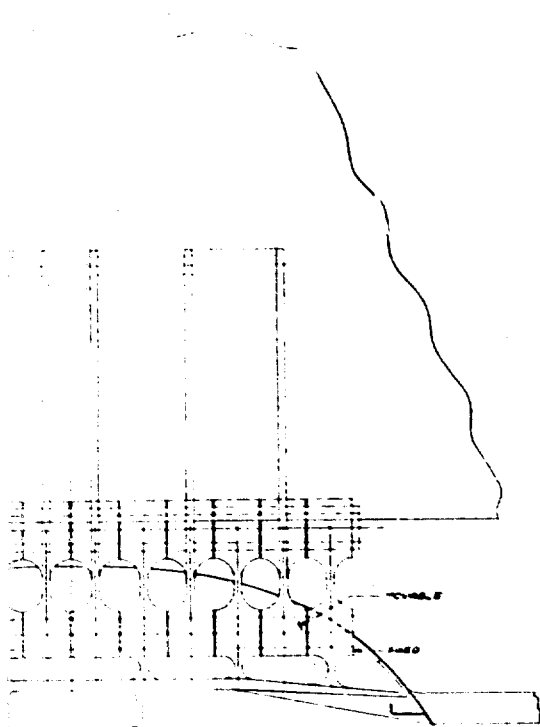
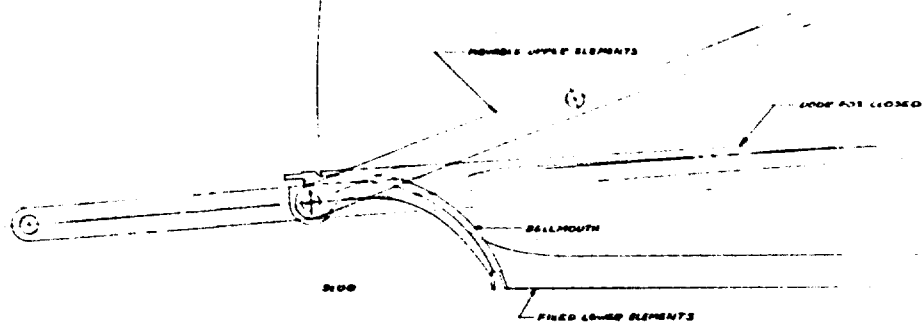


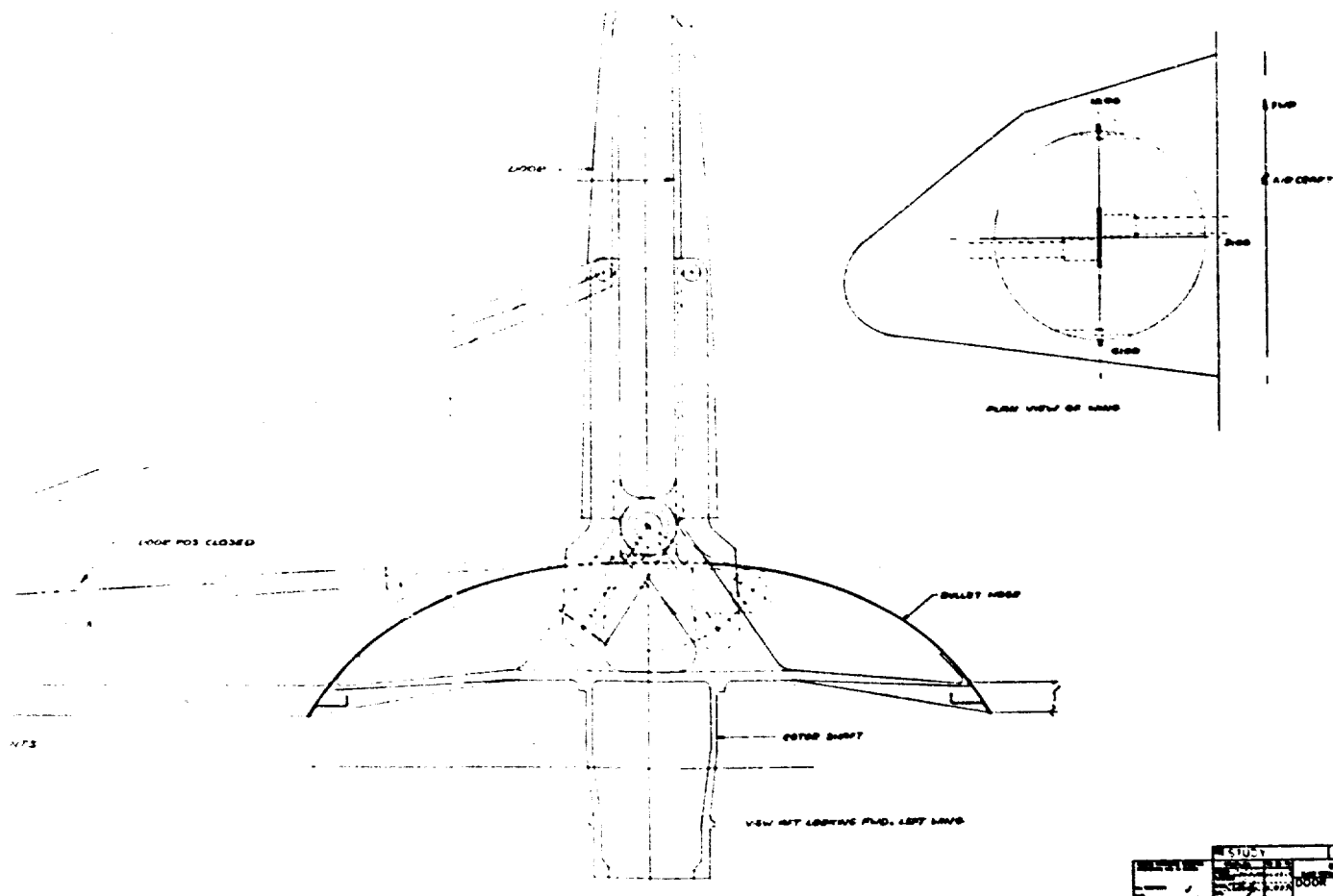
Figure 117. Door-Strut Combination Concept.



... IN C. 7. 100000 IN. 100000



B



STUDY		CONTROL
DATE	10/10/70	10/10/70
BY	J. D. H. G.	J. D. H. G.
DOOR STUDY CONTINUED		STUDY
J. D. H. G. 10/10/70		10/10/70

C

REAR FRAME MECHANICAL DESIGN

The rear frame provides the aerodynamic flow straightening required to remove rotor swirl aft of the fan. For this design the exit louver system will be directly attached to the airframe; no rear frame strut has been used in the fan structure. This approach is considered to result in the lowest overall system weight. The rear frame design described below weighs 96.9 pounds, compared to the weight of 138 pounds reported in Reference 1. Table XVI shows the calculated rear frame weights for the configuration shown on Figures 119 and 120.

The only attachment to the rear frame is at the periphery of the casing to a 360-degree circular flange extending aft (downstream) from the scroll. The rear frame was designed so that it can be taken apart in order to allow the use of low temperature materials across the cool fan portion while retaining high temperature material requirements through the 1000-degree-Fahrenheit turbine exhaust.

Essentially, the design concept reported in Reference 1 has been retained. The only basic change is the provision of the 360-degree circular flange to mount the rear frame to the scroll (instead of the four A-frame type mounts reported in Reference 1).

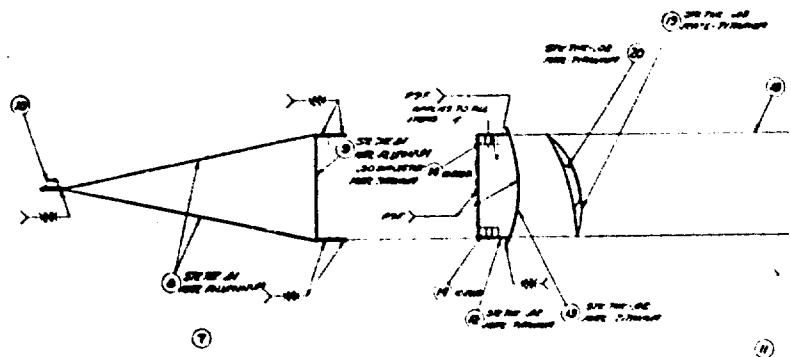
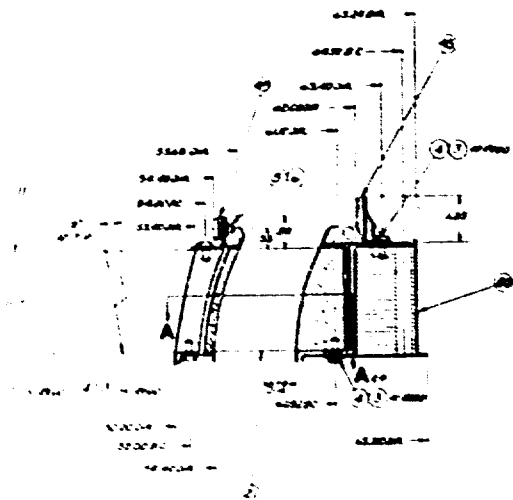
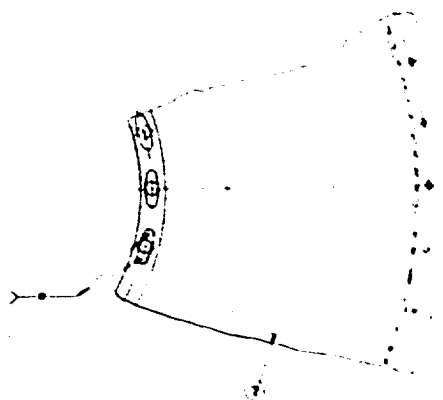
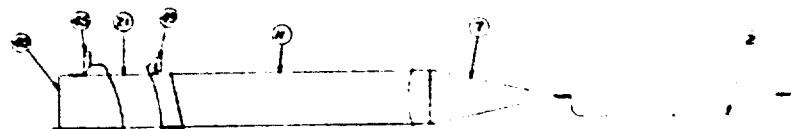
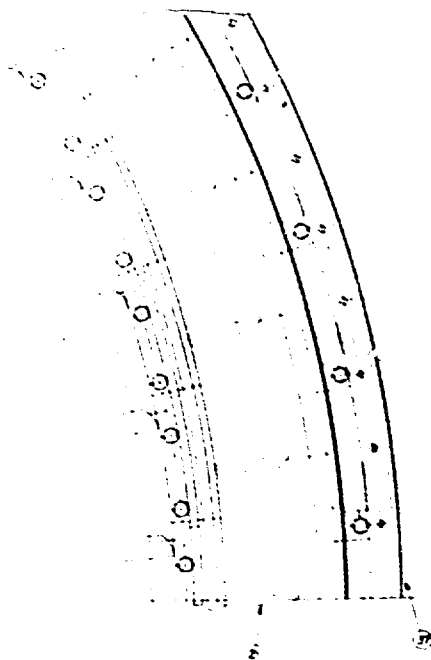
The following outlines the rear frame design criteria and operating conditions, describes the design and the results of the design analyses, and lists the areas requiring further study.

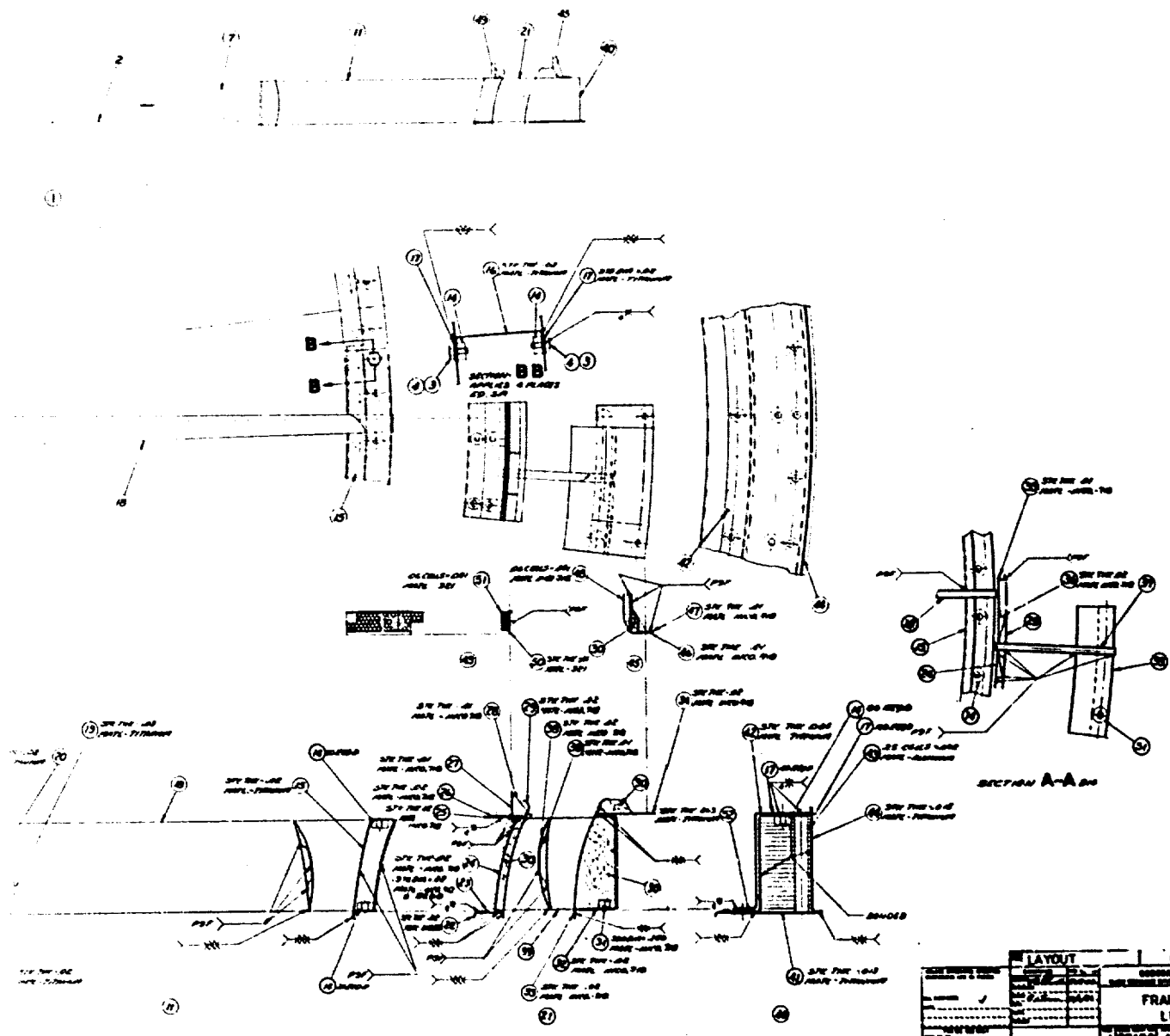
Design Requirements

The loading and operating conditions used for rear frame mechanical design analysis were determined at the maximum power transfer condition (i.e., 115-percent fan speed).

The loadings on the rear frame components are:

1. Fan stator torque - 123,000 inch-pounds, acting as an in-plane, distributed load of 13.65 pounds per circumferential inch of fan stators. This torque is uniformly accepted by the scroll skirt.
2. Fan stator axial load - 1554 pounds, acting forward (lift) as a distributed load of 3 pounds per inch on the fan stators.
3. Rear frame hub axial load - 664 pounds, acting forward (lift).
4. Turbine stator aerodynamic loading is assumed to be negligible.
5. Aft honeycomb air seal loads are assumed negligible.





LAYOUT		REVISIONS	
NO.	DATE	NO.	DATE
1	10/1/55	1	10/1/55
2	10/1/55	2	10/1/55
3	10/1/55	3	10/1/55
4	10/1/55	4	10/1/55
5	10/1/55	5	10/1/55
6	10/1/55	6	10/1/55
7	10/1/55	7	10/1/55
8	10/1/55	8	10/1/55
9	10/1/55	9	10/1/55
10	10/1/55	10	10/1/55
11	10/1/55	11	10/1/55
12	10/1/55	12	10/1/55
13	10/1/55	13	10/1/55
14	10/1/55	14	10/1/55
15	10/1/55	15	10/1/55
16	10/1/55	16	10/1/55
17	10/1/55	17	10/1/55
18	10/1/55	18	10/1/55
19	10/1/55	19	10/1/55
20	10/1/55	20	10/1/55
21	10/1/55	21	10/1/55
22	10/1/55	22	10/1/55
23	10/1/55	23	10/1/55
24	10/1/55	24	10/1/55
25	10/1/55	25	10/1/55
26	10/1/55	26	10/1/55
27	10/1/55	27	10/1/55
28	10/1/55	28	10/1/55
29	10/1/55	29	10/1/55
30	10/1/55	30	10/1/55
31	10/1/55	31	10/1/55
32	10/1/55	32	10/1/55
33	10/1/55	33	10/1/55
34	10/1/55	34	10/1/55
35	10/1/55	35	10/1/55
36	10/1/55	36	10/1/55
37	10/1/55	37	10/1/55
38	10/1/55	38	10/1/55
39	10/1/55	39	10/1/55
40	10/1/55	40	10/1/55
41	10/1/55	41	10/1/55
42	10/1/55	42	10/1/55
43	10/1/55	43	10/1/55
44	10/1/55	44	10/1/55
45	10/1/55	45	10/1/55
46	10/1/55	46	10/1/55
47	10/1/55	47	10/1/55
48	10/1/55	48	10/1/55
49	10/1/55	49	10/1/55
50	10/1/55	50	10/1/55
51	10/1/55	51	10/1/55
52	10/1/55	52	10/1/55
53	10/1/55	53	10/1/55
54	10/1/55	54	10/1/55
55	10/1/55	55	10/1/55
56	10/1/55	56	10/1/55
57	10/1/55	57	10/1/55
58	10/1/55	58	10/1/55
59	10/1/55	59	10/1/55
60	10/1/55	60	10/1/55
61	10/1/55	61	10/1/55
62	10/1/55	62	10/1/55
63	10/1/55	63	10/1/55
64	10/1/55	64	10/1/55
65	10/1/55	65	10/1/55
66	10/1/55	66	10/1/55
67	10/1/55	67	10/1/55
68	10/1/55	68	10/1/55
69	10/1/55	69	10/1/55
70	10/1/55	70	10/1/55
71	10/1/55	71	10/1/55
72	10/1/55	72	10/1/55
73	10/1/55	73	10/1/55
74	10/1/55	74	10/1/55
75	10/1/55	75	10/1/55
76	10/1/55	76	10/1/55
77	10/1/55	77	10/1/55
78	10/1/55	78	10/1/55
79	10/1/55	79	10/1/55
80	10/1/55	80	10/1/55
81	10/1/55	81	10/1/55
82	10/1/55	82	10/1/55
83	10/1/55	83	10/1/55
84	10/1/55	84	10/1/55
85	10/1/55	85	10/1/55
86	10/1/55	86	10/1/55
87	10/1/55	87	10/1/55
88	10/1/55	88	10/1/55
89	10/1/55	89	10/1/55
90	10/1/55	90	10/1/55
91	10/1/55	91	10/1/55
92	10/1/55	92	10/1/55
93	10/1/55	93	10/1/55
94	10/1/55	94	10/1/55
95	10/1/55	95	10/1/55
96	10/1/55	96	10/1/55
97	10/1/55	97	10/1/55
98	10/1/55	98	10/1/55
99	10/1/55	99	10/1/55
100	10/1/55	100	10/1/55

C

PARTS LIST COBES				REVISION COBES														
1 ASST - SEE SUP. RATE PARTS LIST		4 SEE DNG FOR CASTING OR FORGING DNG		1 ITEM OR ASSY ADDED		4 ZONE OR SHEET CHANGED		7 ITEM NO. CHANGED		8 GENERAL CHANGE		9 CODE IDENT CHANGE						
2 VENDOR ITEM - SEE SPEC CONTROL DNG		5 VENDOR ITEM - SEE SPEC CONTROL DNG		2 ITEM OR ASSY DELETED		5 NOMENCLATURE CHANGED		6 CODE IDENT CHANGE										
3 SELECTIVE ITEM - SEE DNG				3 QUANTITY CHANGED														
ITEM NO.	DWG NO.	DWG SHEET NO.	IDENTIFICATION	NOMENCLATURE	QTY	CM DWT	1/6	SUFFIX NO.	1	2	3	4	5	6	7	8	REV	
3850010001	H10	1	4013007-736P02	FRAME ASSY, REAR					X									
20002	B21		MS20033-4	COVER, HUB					1									
20003	B20		MS20995C20	BOLT #10-32 HEX. HD					352									
20004	B19		EWSB922-3-5	LOCKWIRE					AR									
20005	C15		LA3858-02	BOLT #10-32 12 POINT					40									
20006	C15		4013007-736G02	NUT #10-32					40									
20007	A12		4013007-736G02	SUPPORT, VANE ASSY					1	X								
30008	A12		4013007-736P08	CONE						2								
30009	B11		4013007-736P09	SPACER						2								
30010	B13		LHTA521-2860P-02	NUT, FLG.					4	24								
20011	A9		4013007-736G03	VANE ASSY, STATOR							X							
30012	A11		4013007-736P12	SHIELD, INNER						1								
30013	A10		4013007-736P13	SHIELD, INNER						1								
30014	B11		4013007-736P14	BLOCK						62					80			
30015	C3		4013007-736P15	SHIELD, INNER						1								
30016	F7		4013007-736P16	SPACER						1								
30017	F7		4013007-736P17	PAD						1								
30018	C9		4013007-736G04	VANE ASSY						2		X			148			
40019	C10		4013007-736P19	SHIELD						10								
40020	C10		4013007-736P20	STIFFENER								1						
20021	A7		4013007-736G05	VANE ASSY, TURBINE									X					
30022	B5		4013007-736P22	RING, SECTOR					40					1				
30023	B8		4013007-736P23	PAD										2				
30024	B8		4013007-736P24	SHIELD										1				
30025	B8		4013007-736P25	PAD										2				
30026	C8		4013007-736P26	RING, SECTOR										1				
30027	C8		4013007-736P27	PLATE										1				
30028	C7		4013007-736P28	GUSSET										2				
30029	C7		4013007-736P29	SHIELD										1				
30030			4013007-736P30	INSULATION												AR		

Figure 120. Rear Frame Parts List (4013007-736).

TABLE XV
ALTERNATE FRONT FRAME CONCEPT WEIGHT

<u>LFX-6 (As Designed)</u>		<u>Alternate Concept</u>	
Front Frame	102	Front Frame	70
Major Strut, 48.6 lb		Fan Door/Strut	90
Minor Strut, 16.3 lb		(with links which	
		act as minor strut	
Fan Doors	<u>126</u>	upper elements)	<u> </u>
	228		160

TABLE XVI
REAR FRAME WEIGHTS

<u>Component</u>	<u>Calculated Weight (lb)</u>
Hub	1.76
Fan Stator Assembly (40 vanes)	28.80
Turbine Stator Assembly (40 vanes)	32.95
Casing	12.50
Insulation	4.00
Aft Inner Air Seals	3.70
Aft Outer Air Seals	4.95
Bolts	8.10
Nuts	<u>0.20</u>
Total	96.96

The estimated operating temperatures of the rear frame components are:

Hub and stator sectors, excluding stator outer box	100°F
Stator sector outer box	200-300°F
Turbine sector assembly	1050°F
Casing	300°F

Design Description of Rear Frame

Hub

The two-piece dishpan, Figure 119, has a 0.030-inch-thick removable aluminum cup which provides access to the rotor sump area and provides access for the attachment of a rotor slip ring during test evaluation. The other part of the hub is fabricated from two conical, 0.010-inch-thick aluminum sheets bonded together at their inner diameter and held apart at their outer diameter by a 0.010-inch-thick aluminum circular "U" channel. This channel provides the inner structural support for attachment of the inner box of the fan stator vane assembly. Although this part is not highly stressed, the 0.010-inch thickness was deemed a minimum for good fabrication practice and is considered to be a practical lower limit to preclude handling damage.

Fan Stator

The four fan stator sectors (Figure 119) are titanium, fabricated in 90-degree sections to facilitate assembly to the hub section. Each 90-degree section has 10 radially positioned aerodynamic turning vanes brazed into a structural box at each end. The vanes, having 2.75-inch chords with 10-percent maximum thickness, are fabricated from 0.030-inch-thick skins with a 0.020-inch-thick stiffener hat brazed within the vane. Both inner and outer structural boxes are fabricated from 0.020-inch-thick titanium. The inner box has a flanged "U" channel attached to the curved panel which forms the inner fan flow path aft of the rotor. The outer box is of one-piece stretch-formed construction and its inner surface forms the outer fan flow path aft of the rotor.

The fan aft blade tip air seals have been attached to the cool middle box and casing to preclude excessive differential radial thermal growth. Each ring of the seals is fabricated from 40 individual mating pieces to allow circumferential thermal growth. Every effort will be made during detail design to eliminate the outer seal (over the bucket tip) because of the difficulty which might be anticipated from the long extension required on the rotating part of the rotor turbine shroud.

Both the outer box of the fan stator sectors and the rear frame casing (Figure 121) require cooling during fan operation to preclude adverse differential thermal expansion. Figure 122 shows the path of the cooling flow.

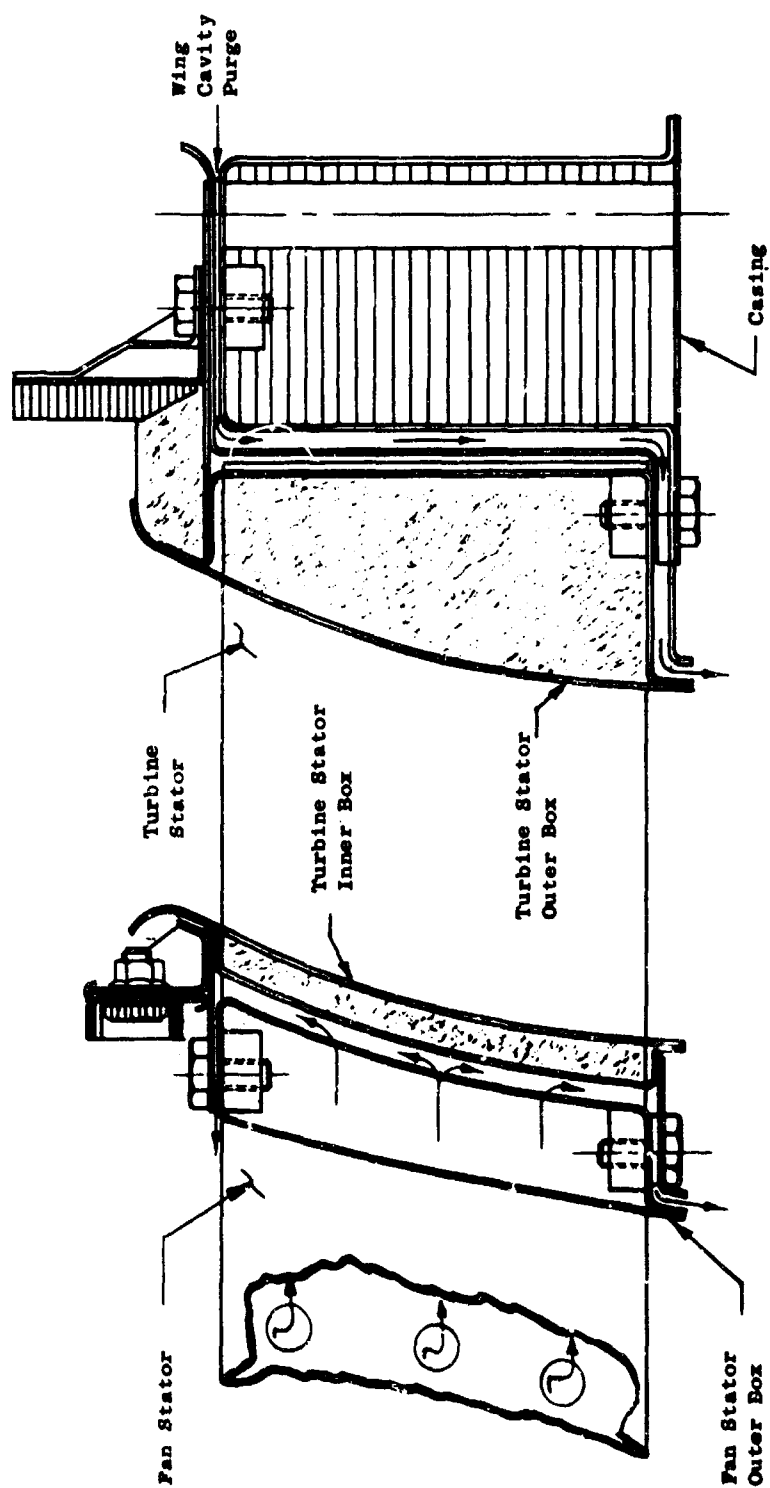


Figure 121. Rear Frame Cooling.

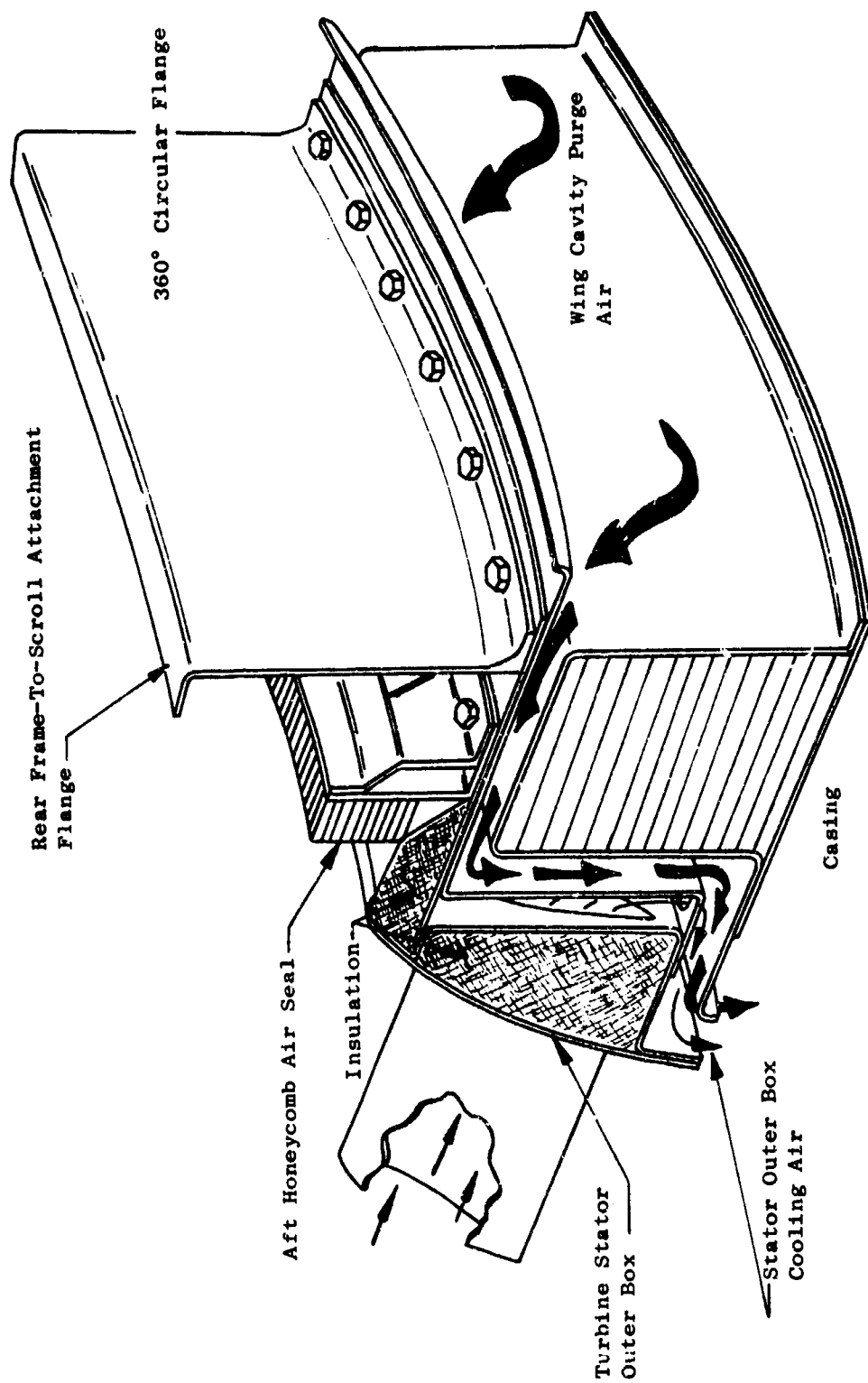


Figure 122. Rear Frame Outer Box.

Three holes in the pressure side skin of each fan stator vane receive cool fan air and discharge it into an annular cavity between the fan stator outer box and the turbine stator inner box. This air then flows over the forward, aft, and outer surfaces of the fan outer box and is then ejected (by fan flow ejector pumping action) into the fan stream between the fan outer box and the forward and aft attachment flanges on the turbine vane sectors.

Additional cooling air is drawn between the turbine stator outer box and the casing and thus purges the wing cavity. Both of these cooling systems will require extensive evaluation to assure extended trouble-free operation.

Turbine Stators

Forty individual turbine stators, using a brazed fabrication of Inconel 718 material, form the turbine stator section of the rear frame. Each turbine stator vane is positioned radially half-way between each fan stator vane with two circumferential bolts on the forward and aft side of the fan outer box. Bolting is at the 1/4 points between stator vanes to reduce in-plane deformation of the fan outer box due to stator vane torque. Each stator has an integral inner and outer box structure for load transmission. Flanges on the forward and aft edges of both boxes provide attachment to the fan stator outer box and the casing.

Attached to the forward flange of the inner box is a braced 0.010-inch-thick attachment for the aft honeycomb air seal. The inner box structure, with a 0.010-inch-thick flanged "U" channel, attaches to the 0.020-inch-thick curved outer sheet which forms the inner turbine flow path aft of the rotor. Within this box at the turbine vane attachment is a formed 0.020-inch stock thickness stiffener, which transfers the in-plane fan torque accepted by the forward and aft flanges from the outer fan box structure into the inner end of the turbine vane. A 0.010-inch space between the outer fan box and the inner turbine box is provided for a cooling air passage to cool the outer fan box.

The outer turbine box has a 0.020-inch-thick flanged "U" channel attached to the 0.020-inch-thick formed sheet which forms the outer turbine flow path aft of the rotor. Again, forward and aft flanges transfer the turbine torque loads to the outer casing. The turbine stator vanes, with 2.75-inch chords of 18-percent maximum thickness, are fabricated from 0.020-inch-thick skins with a 0.010-inch-thick stiffener hat section brazed within the vane.

Insulation within the inner and outer turbine boxes is required to prevent excessive heat transmission from the turbine sectors to their attachment at the casing and outer box of the fan stator sectors. In addition, airflow through the cooling cavity described previously provides additional protection against heat transmission from the turbine sectors.

Casing

The casing is a 360-degree honeycomb-filled structural ring which accepts all rear frame loads and transfers them to the skirt of the scroll. The

structural portion of the casing is fabricated from three pieces of 0.015-inch-thick titanium to facilitate the fit-up requirements for bonding to the aluminum honeycomb.

A 0.005-inch-thick shield over the top and inside surface of the casing provides a 0.100-inch airflow passage for cooling the structural ring and providing a hot gas purge for the wing cavity. This shield is separated from the casing with 0.060-inch-thick doublers.

Air from the wing cavity is admitted between the scroll skirt and the casing and flows around the casing to isolate it from the hot turbine parts and is drawn out near the outer edge of the high velocity turbine exhaust stream by an annular discharge ejector type pumping action.

Design Analysis

The results of the design analyses are outlined below in the form of stress levels in key components. The stresses calculated for the components of the rear frame are the two maximum stresses based on the above gas and thermal loads at the design condition (maximum power transfer). No exit louver loads have been included.

1. Outer Casing

- a. 33,500 psi - bending stress due to stator torque
- b. 4,100 psi - shear stress due to stator torque

2. Turbine Stators

- a. 49,500 psi - bending stress due to stator torque
- b. 8,630 psi - bending stress due to lift loading

3. Fan Stator Outer Box

- a. 27,430 psi - bending stress due to stator torque
- b. 6,000 psi - shear stress due to stator torque

4. Fan Stator

- a. 42,900 psi - bending stress due to stator torque
- b. 7,075 psi - bending stress due to lift loading

5. Hub and Fan Stator Inner Box

- a. 10,120 psi - bending stress due to lift load
- b. 7,500 psi - shear stress due to tension in stator vanes

SCROLL MECHANICAL DESIGN

The scroll carries the gas generator discharge gas to the fan tip turbine. The scroll nozzle diaphragm is used to vary the energy input to the fan turbine through variation of the turbine admission area.

Basically, the scroll design defined below is very similar to the design reported in Reference 1. The major difference is the elimination of the scroll flanges in the present design in order to reduce weights. A more detailed design mechanical analysis has resulted in a scroll weight of 150.1 pounds (Table XVII); the scroll weight reported in Reference 1 on a comparable basis was 132.7 pounds.

The scroll assembly is mounted to the front frame at each of the four front frame struts. Since the rear frame is supported solely by the scroll, these four front frame mounts also support the rear frame external loads as well as the scroll external loads. The four mounts are designed to provide the necessary scroll/rear frame constraint and still allow unrestrained scroll thermal growth.

The following outlines the scroll design criteria and operating conditions, describes the design and design analyses results, and lists the areas requiring further study or definition.

Design Requirements

The following design criteria were used to design the LFX scroll:

1. Nominal gas flow Mach number not to exceed 0.30 (scroll arms)
2. Maximum operating temperature - 1400° Fahrenheit (includes 1-percent deviation)
Maximum operating pressure - 49 psia
3. Material operating life at maximum temperature - 1000 hours
4. Variable admission arc
Minimum arc - 78 degrees per scroll half
Maximum arc - 180 degrees per scroll half
5. Dual inlet system - required for single-engine operation
6. Scroll will support the rear frame (loads discussed in analysis section)
7. Weight objective - 130 pounds (including insulation and variable area control system, less actuator)

TABLE XVII
SCROLL WEIGHTS - POUNDS

Nozzle Partitions (I)	9.3
Nozzle Partitions (II)	8.2
Inner Band Hat Section	3.0
Torque Tube	12.2
Top Hat Section	7.5
Spout and Bubble	22.0
Struts	6.6
Inlet Flanges and Transition	6.9
Baffle	5.4
Separating Flanges and Structure	8.0
Inner Band Seals	4.0
Hat Sections (Inlets)	12.0
Skirt	5.2
Braze and Weld	7.8
	<hr/> 118.1
Insulation Blanket	7.0
Variable Area Control	25.0
	<hr/> 150.1

The following external forces act on the scroll during normal operation:

- Nozzle Torque - 123,000 inch-pounds uniformly distributed around the scroll periphery during full admission. This can be further reduced to a running load of 21.3 pounds per inch in the plane of the nozzles.
- Nozzle Lift - 1,600 pounds uniformly distributed around the scroll periphery during full admission. This can be further reduced to a running load of 8.4 pounds per inch acting normal to the plane of the nozzles.
- Rear Frame Torque - This is equal in magnitude and opposite in direction to the scroll nozzle torque.
- Rear Frame Lift - 2,210 pounds uniformly distributed around the scroll periphery during full admission.
- Inlet Piston Force - 3,810 pounds. This includes the additional area for bellows having a 0.75 inch convolution height. This load acts on the projected area of the inlet flanges.

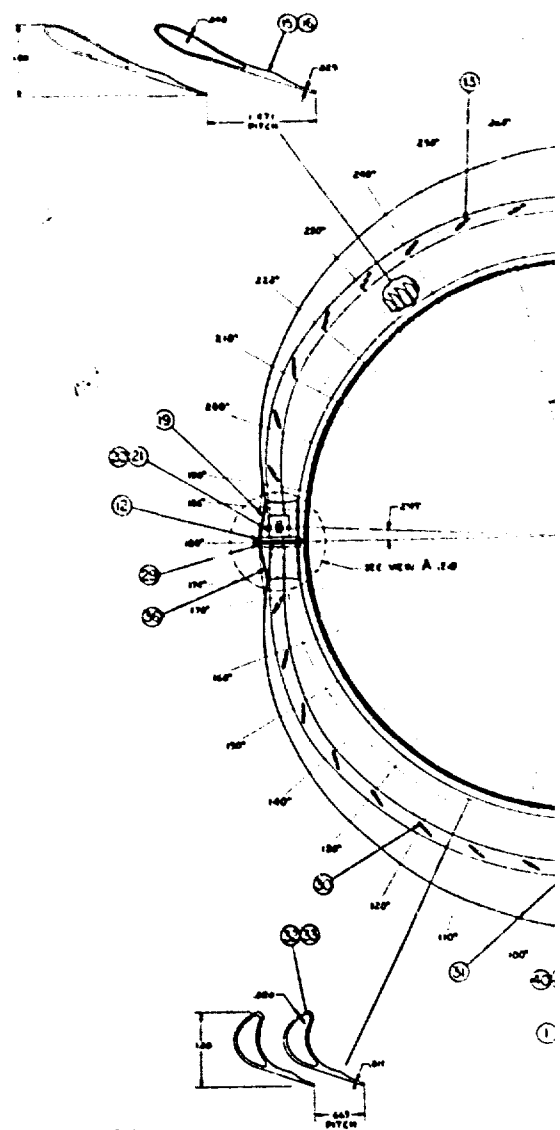
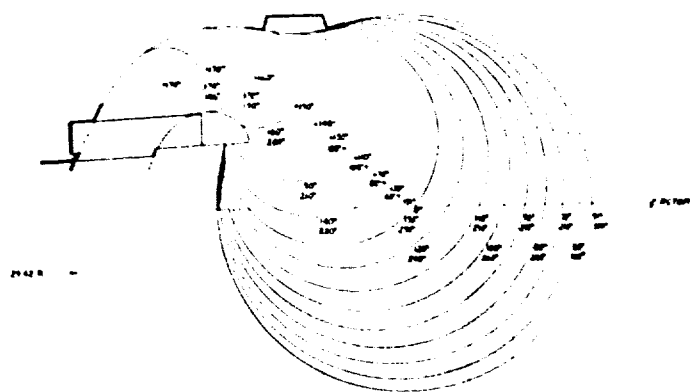
Design Description

Scroll Inlet Geometry

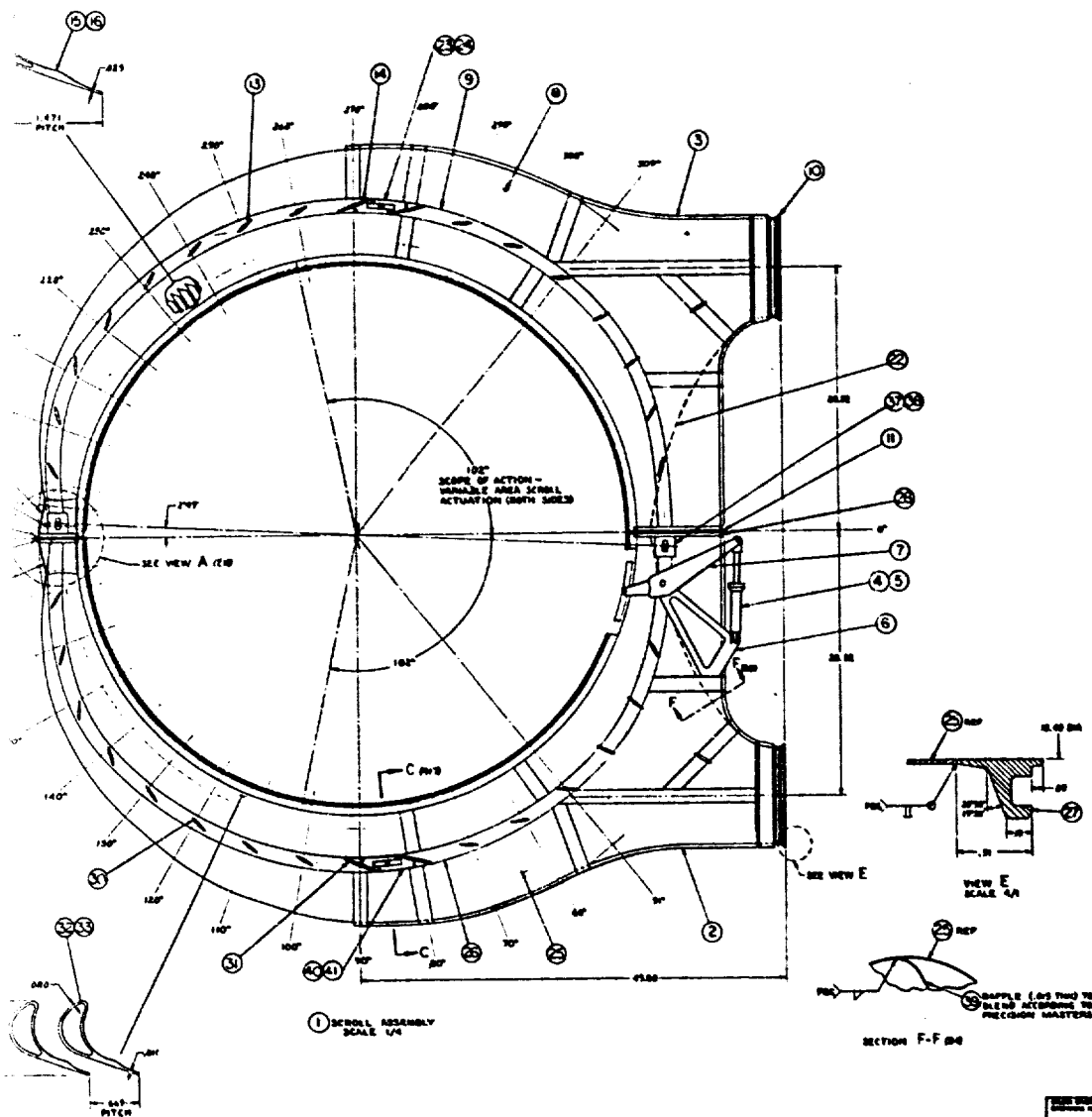
The centerline locations of the scroll inlets were not arranged to meet a specific installation configuration. The inlet geometry shown on Figures 123 and 124 was selected for both structural and performance optimization. The scroll assembly is mounted to the front frame at each of the four front frame struts. Each mount consists of a set of clevises and a 0.50 inch diameter pin. The pin longitudinal axis is oriented radially and thus allows unrestrained scroll thermal growth as shown in Figure 123.

Since the rear frame is supported solely by the scroll, these mounts must support the rear frame external forces as well as the scroll external forces. This mounting scheme was designed to control the scroll thermal growth to maintain the alignment of the hot gas seal (between the scroll and front frame).

Since bellows will likely be utilized to connect the scroll to the gas supply ducts it was desirable to position the inlets to minimize piston force induced bending stresses in the scroll structure (by aligning the applied piston load with the scroll mounts). However, the selection of this position also considered the taper of the hypothetical wing envelope toward the leading and trailing edges. From a performance viewpoint the inlets were aligned with the nominal scroll admission arc to minimize the gas turning angle and attendant aerodynamic losses.



6



MUST CONFORM TO:
MTR CL-A (INTERPRETATION OF DME)

LAYOUT		ORIGINAL & REVISIONS	
NO.	1	DATE	12/1/62
BY	JDM	DESIGNED BY	JDM
CHECKED BY	JDM	DATE	12/1/62
APPROVED BY	JDM	DATE	12/1/62
REVISION		REASON FOR CHANGE	
SCROLL ASSEMBLY		LFX-6	
JDM		4013007-737	

C

PARTS LIST CODES				REVISION CODES									
1	2	3	4	5	6	7	8	9	10	11	12	13	14
1. ASBY - SEE SEPARATE PARTS LIST	2. YENDOR ITEM - SEE SPEC CONTROL DWG	3. SELECTIVE ITEM - SEE DWG	4. SEE DWG FOR CASTING OR FORGING DWG	5. VENDOR ITEM - SEE SOURCE CONTROL DWG	6. ITEM OR ASSY ADDED	7. ITEM NO CHANGED	8. GENERAL CHANGE	9. CODE IDENT CHANGE	10. ZONE OR SHEET CHANGED	11. IDENT NO. CHANGED	12. MONUMENTALURE CHANGED	13. SUFFIX NO. AND QUANTITY REQUIRED	14. REV
ITEM NO	REV	REV	REV	REV	REV	REV	REV	REV	REV	REV	REV	REV	REV
1	2	3	4	5	6	7	8	9	10	11	12	13	14
8700010001	B6			4013007-737G01	SCROLL ASSY								
20002	BA			G02	" RH								
20003	B3			G03	" LH								
20004	E3			G04	" VA								
30005	E3			P01	ACTUATOR								
6	D3			P02	BRACKET								
7	E3			P03	LEVER								
8	J5			P04	SHIELD								
9	J5			P05	STIFFENER, HAT								
10	H4			P06	FLANGE, INLET								
11	E3			P07	" , COUPLING								
12	E3			P08	" , "								
13	J6			P09	STRUCT								
14	J6			P10	STRUCT								
15	J7			P11	NOZZLE, TYPE I								
16	J7			P12	" , II								
17	F19			P13	" , ARTICULATED								
18	H19			P14	" , SPLITTER								
19	F8			P15	STIFFENER, BOX								
20	E8			P16	PAD, MTG								
21	E8			P17	BRACKET, MTG								
22	F3			P18	BAFFLE								
23	F3			P19	PAD, MTG								
24	F5			P20	BRACKET, MTG.								
25	B5			P21	SHIELD								
26	B5			P22	STIFFENER, HAT								
27	E2			P23	FLANGE, INLET								
28	E3			P24	" , COUPLING								
29	E3			P25	" , "								
30	(7			P26	STRUTS								

Figure 124. Scroll Assembly Parts List (4013007-737).

The arrangement of the scroll inlet geometry required that a baffle, or liner, be installed between the inlets. The baffle serves the function of reducing the gas flow area toward zero at the center of the inboard portion of the scroll. Because of its complex curvature the baffle will be vented to the surrounding shell structure and, consequently, will not function as a structural member. Along with the area reducing function, the baffle is also a necessary part if the propulsion system is to be capable of efficient operation with only one of the two core engines running.

To reduce manufacturing complexity, handling difficulties, and storage space, the scroll assembly will be made in two 180-degree sectors. Figure 123 shows a configuration with the split lines at 3:00 and 9:00. This configuration was selected because it provided the best design from a weight standpoint. Several other split line configurations are also possible, as shown in Figures 125 and 126. The final selection of the split lines will be governed primarily by the inlet configuration needed to satisfy the particular installation and the variable area control system hard points.

Machined Marman flanges on the scroll inlets are shown in Zone C3 of Figure 123; bolted flanges are not desirable because of potential alignment problems with the engine ducting, and increased weight.

Nozzle Partitions

The primary function of the nozzle partitions is to accelerate the hot gases in a given direction. Because it is important to minimize the scroll height (and weight) for fan-in-wing installations, the nozzle partitions must also function as structural members to support the two-part shell structure.

The two extreme types of nozzle partition contours which were analyzed in depth are shown in Figures 127 and 128. The actual hardware will have a third nozzle partition contour which will provide the transition between Type I and Type IV. All four types will be required in the scroll assembly.

The trailing edge portion of the LFX nozzle partitions forms a convergent-divergent (supersonic) nozzle. This represents a departure from the design of previous scroll nozzle partitions in that they were designed only for sonic flow velocities.

Struts

The strut supports the scroll spout and bubble at their "point" of intersection. The struts, in conjunction with the top circumferential hat section and torque tube, form the primary scroll "beam" structure.

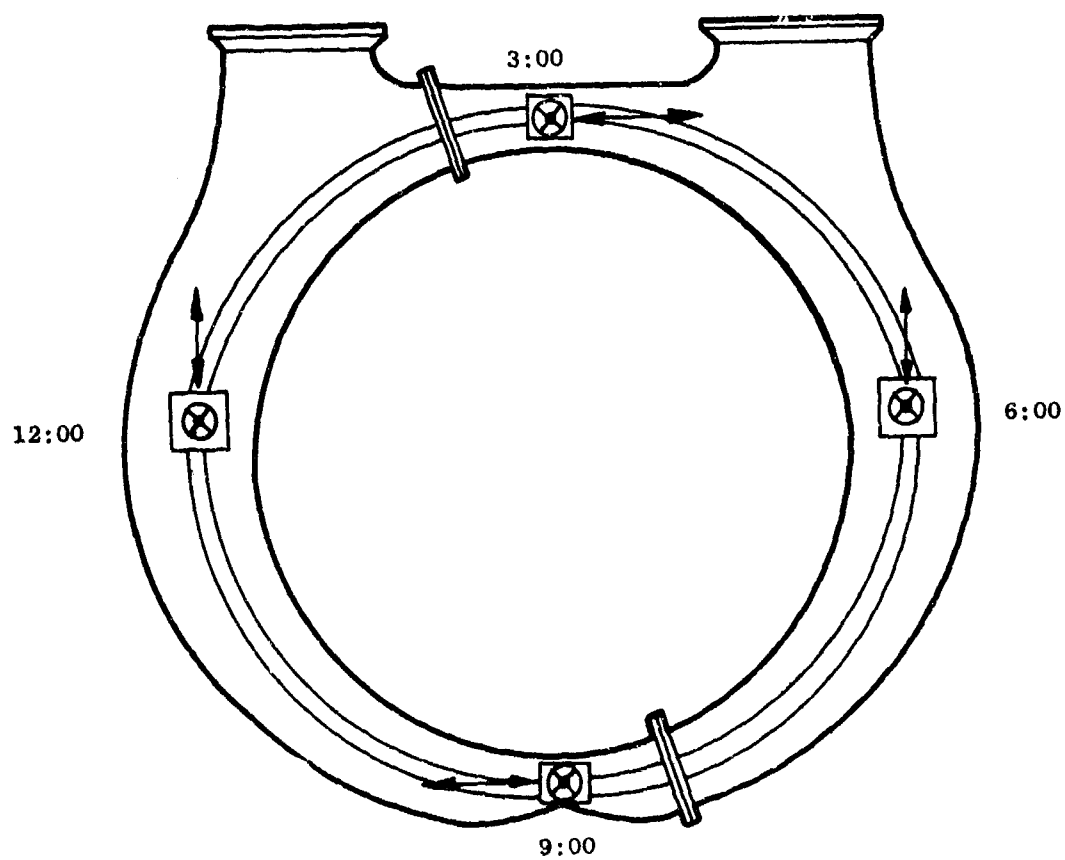


Figure 125. Alternate Scroll Split-Line Concept.

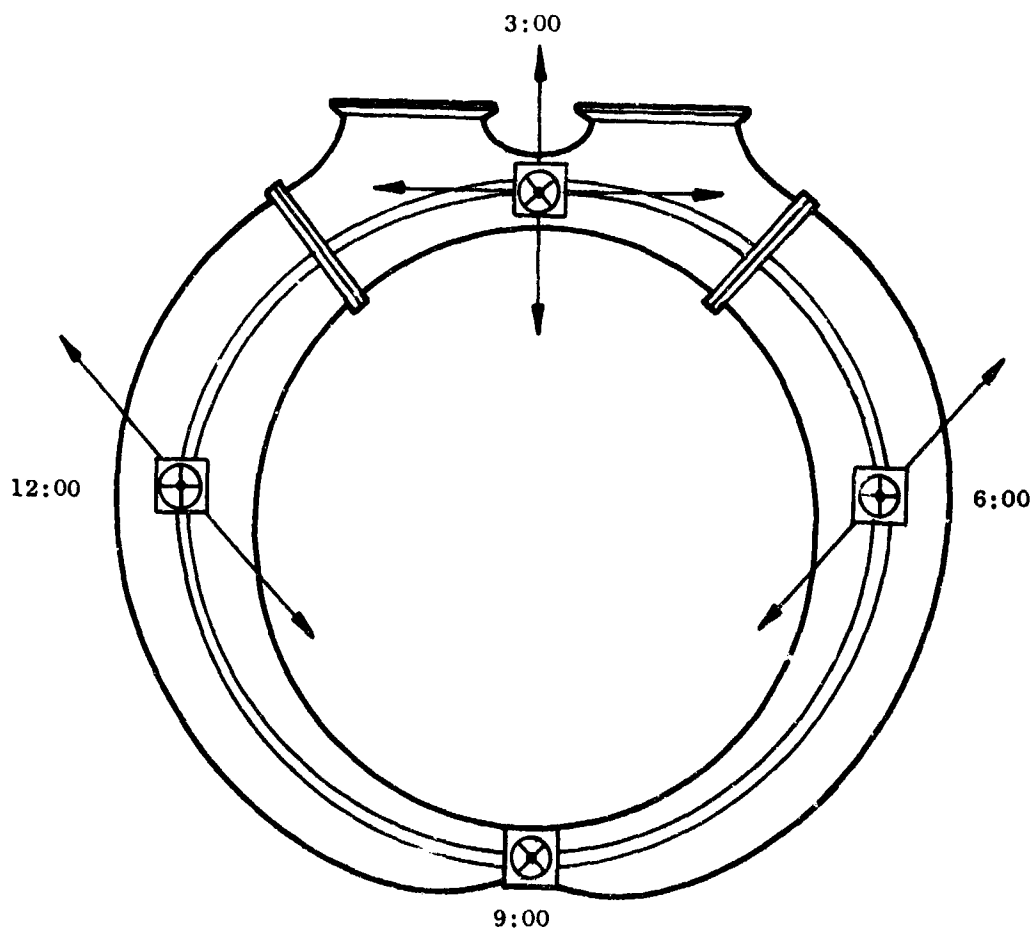
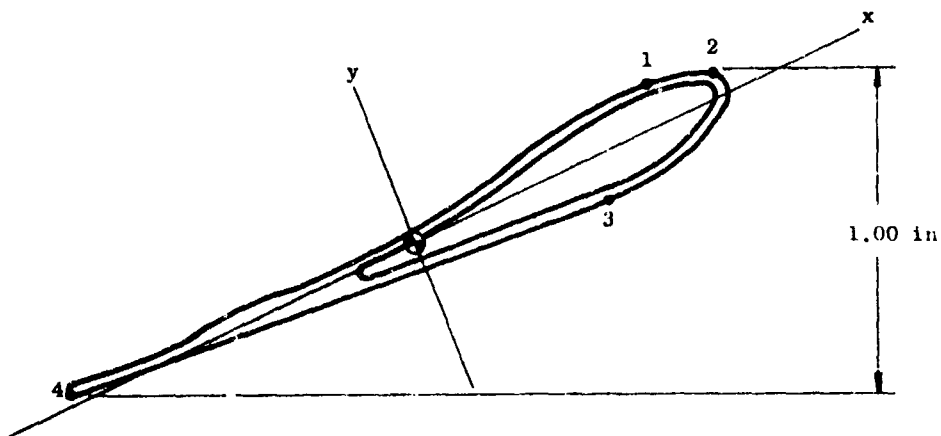
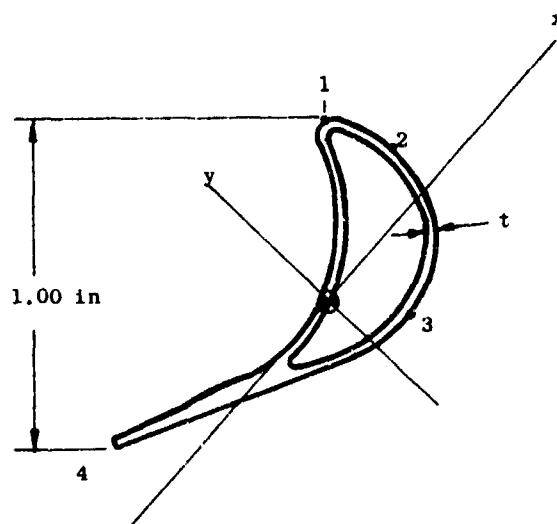


Figure 126. Alternate Scroll Split-Line
Concept - Close Inlets.



	I_{XX}	I_{YY}	NCT Area	$\frac{Y_1}{I_{XX}}$	$\frac{Y_3}{I_{XX}}$	$\frac{Y_4}{I_{XX}}$	$\frac{X_2}{I_{YY}}$	$\frac{X_4}{I_{YY}}$
t	(in. ⁴)	(in. ⁴)	(in. ²)					
Solid	0.01200	0.0943	0.327	116	120	41	10	14
0.039	0.00882	0.0654	0.180	158	163	56	15	20
0.027	0.00719	0.0542	0.137	192	195	62	20	23

Figure 127. Scroll Nozzle Partition (Type I)
Section Properties.



Reciprocal of Section Modulus								
t	I_{XX}	I_{YY}	Net Area	$\frac{Y_1}{I_{XX}}$	$\frac{Y_3}{I_{XX}}$	$\frac{Y_4}{I_{XX}}$	$\frac{X_2}{I_{YY}}$	$\frac{X_4}{I_{YY}}$
(in.)	(in. ⁴)	(in. ⁴)	(in. ²)	(in. ⁻³)	(in. ⁻³)	(in. ⁻³)	(in. ⁻³)	(in. ⁻³)
Solid	0.00352	0.01500	0.2320	95	91	142	29	70
0.038	0.00204	0.00958	0.0872	184	165	193	55	105
0.020	0.00150	0.00778	0.0674	241	220	215	69	122

Figure 128. Scroll Nozzle Partition (Type IV) Section Properties.

The physical size of the strut is governed by the geometry of the torque tube combined with the aerodynamic orientation angle of the strut. The strut contour itself is an NACA 0018 series airfoil. A spacing of 6 inches between struts was determined by the operating stresses given in Table XVIII.

Spout and Bubble

The scroll spout and bubble cross sections are circular arcs throughout the scroll periphery. The spout has a nearly constant radius, whereas the bubble radius is continually changing. Figure 129 shows the required scroll area around the scroll periphery.

Top Circumferential Hat Section

The top circumferential hat section, Figure 123, maintains reasonable membrane stresses in the spout and bubble skin. Because of the varying spout radius and bubble radius, the hat section is subjected to a varying in-plane load distribution. The normal-to-plane load occurs as a result of the pressure differential across the hat section. The portion of the hat section between the large struts at 6:00 and 12:00 was stiffened by welding a 0.140-inch-thick plate to the top of the hat section.

For this study the hypothetical 9-percent-thickness wing reduced the clearance between the top of the hat and bottom of the major strut spade; thus the hat section height could not be increased as desired. A thicker wing would allow more adequate clearance for mounting structure and insulation.

Inlet Hat Sections

The three-dimensional curvature of the scroll in the vicinity of the inlets makes it mandatory to use hat sections to prevent bending stresses in the shell. The hat sections shown in Zone C5 of Figure 123 represent the minimum hat section geometry required. The final hat section configuration will depend on the inlet spacing and orientation required for a given installation.

Inner Band Seal

The inner band seal consists of three independent layers of 0.005-inch and 0.010-inch sheet stock. The sheets will be overlapped radially, approximately every 6 inches, to prevent thermal buckling and to facilitate assembly. This type of seal has been demonstrated to be flexible and lightweight.

Although previous scrolls have utilized a seal rod attachment design (which allows seal sectors to be replaced), the short distance between the fan tip and bucket root does not leave adequate length to incorporate this design feature on the LFX scroll.

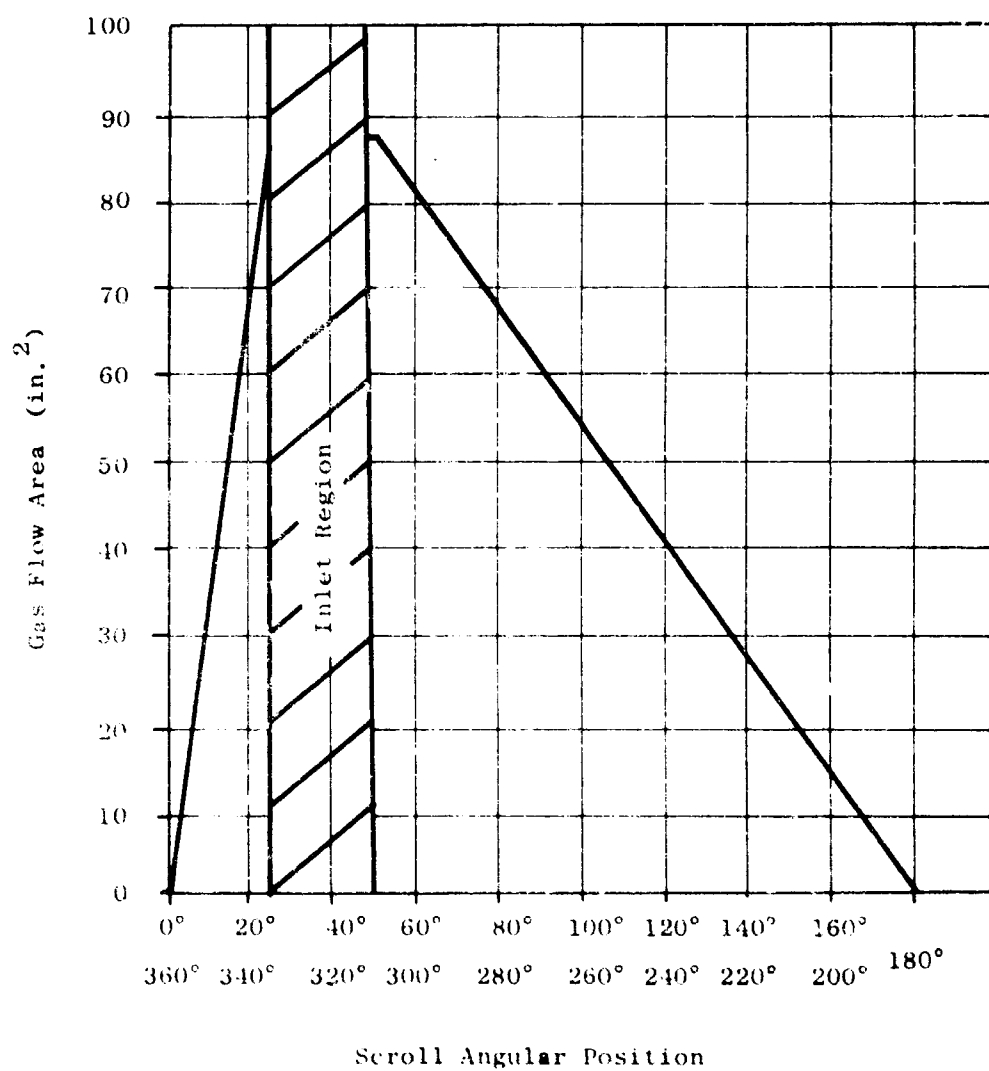


Figure 129. Scroll Area Distribution.

Skirt

The rear frame is attached to the scroll by a 360-degree skirt and the rear frame loads are thus transmitted to the front frame. The skirt consists of a 0.015-inch sheet metal shell with axial saw cuts reinforced by hat sections. The saw cuts are necessary to allow unrestrained thermal growth of the skirt. The hat sections are needed to carry axial compression and prevent leakage. The use of the skirt replaces the need for an outer-band rear frame slip-seal.

The utilization of a skirt requires that the thermal gradient from the scroll torque tube to the flange be close to linear. Any gradient other than linear will induce thermal stresses in the structure. A tapered insulation shield is provided to control the temperature distribution on the skirt. Also, induced cavity cooling between the scroll bubble and skirt is provided.

Variable Area Control System

The LFX variable area scroll has a maximum admission arc of 360 degrees and a minimum admission arc of 156 degrees ± 41 percent range of nozzle area variation. The variable admission arc is located on the inboard (3:00) portion of the scroll. This location was chosen primarily to maintain a constant scroll Mach number through the fixed portion of the scroll.

Nozzle area control is obtained by partially rotating a combination of splitter vanes and nozzle partition "flaps". Zones F19 and H19 of Figure 123 show the variable geometry in the nozzle diaphragm. The close spacing of the Type IV nozzle partitions (required to produce supersonic flow) does not provide sufficient clearance to completely utilize the splitter vane concept.

The close spacing of the nozzle partitions also results in a requirement for small bolts, i.e., #8-32, to connect the movable vane to its lever.

Actuation of the variable area mechanism can be accomplished by installing a single hydraulic actuator between the scroll inlets as shown in Zone E4 of Figure 123. This location was chosen because the wing is thickest in this region and the hat section provides ideal hard points for supporting the actuator.

The requirement for a fast response control system can be obtained by using a cam drive system similar to that used on the LF2 demonstrator vehicle. Figure 130 shows a section of the cam track, slide bracket and bellcrank which will rotate the movable vanes. Several vanes will be banked to each bellcrank, depending on their location in the system. Because the variable geometry is located on the inboard portion of the scroll, it will be necessary to consider a third type of movable vane to operate with the Type III nozzle partitions.

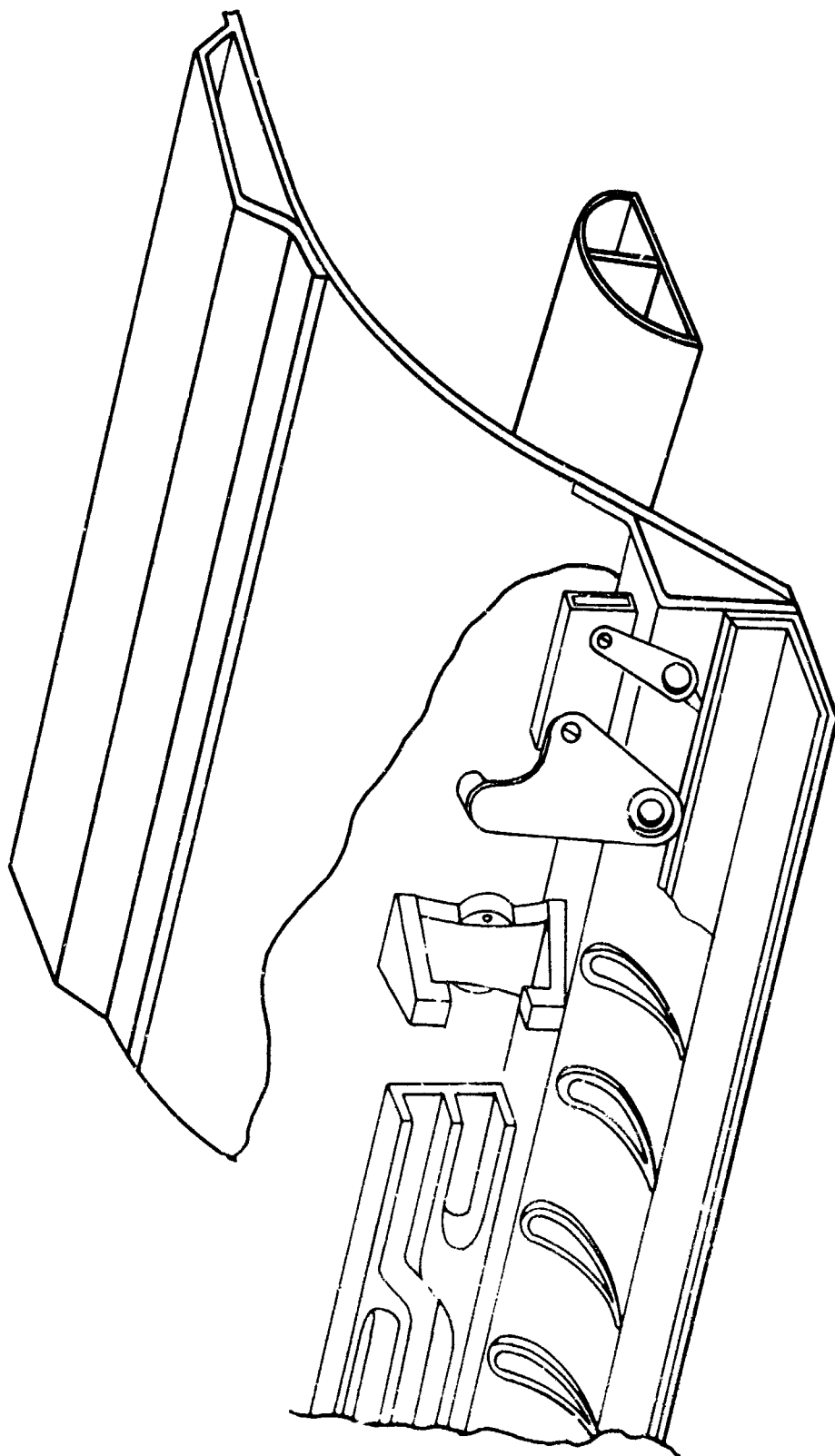


Figure 130. Variable Scroll Nozzle Area Actuation.

Design Analysis

The results of the design analyses conducted to define the scroll configuration and evaluate mechanical integrity are discussed below.

Nozzle partition stresses result from (1) nozzle reaction forces due to acceleration of the gases and (2) forces needed to support the spout skin. Table XVIII presents the effective nozzle partition stresses with and without the effects of the elastic end constraints (due to the inner band hat section and skin shear deformation). Prior to manufacturing release, the analysis should be verified in more detail, since the structure is highly indeterminate.

Because the nozzle partitions must produce supersonic velocities, there was a decrease in trailing edge thickness. Inherent with the thin trailing edge is the consideration of thermal shock during startup. To counter the induced thermal stress, the trailing edges of the nozzle partitions will be undercut at their intersection with the inner band hat section and torque tube. However, the cantilevered portion of the nozzle partition may be subject to thermal fatigue and therefore should undergo additional analysis and bench testing.

The trailing edges of the nozzle partitions are slanted in relation to the plane of the rotor. This slant is desirable for reducing the axial spacing required between the scroll and rotor buckets to accommodate gyroscopic rotor deflections. A more detailed analysis is required to determine the potential mechanical or weight advantages offered by nozzle partition cooling.

Although the primary scroll skin stress is membrane tension, the minimum wall thickness was established by a fabrication limitation rather than a stress limitation. To circumvent elastic instability, hat sections are required to stiffen the shell (Zone C5 of Figure 123).

Bending stresses on the shell during normal operation (full power transfer) are shown in Figures 131 and 132. These stresses were calculated using the scroll section properties shown in Figure 133.

The determination of the stress distribution in the top circumferential hat section is complicated by the elastic end constraints due to the struts and torque tube. For this study, it was assumed that the in-plane load was uniformly distributed around the periphery, and the restraints of the struts and torque tube are neglected. The resultant stresses are given in Table XVIII.

The scroll support strut stresses were calculated by assuming that all bending moments occurred about the minimum moment of inertia. Loads acting about the maximum moment of inertia axis would significantly reduce these calculated stresses. The exact operating stress requires further

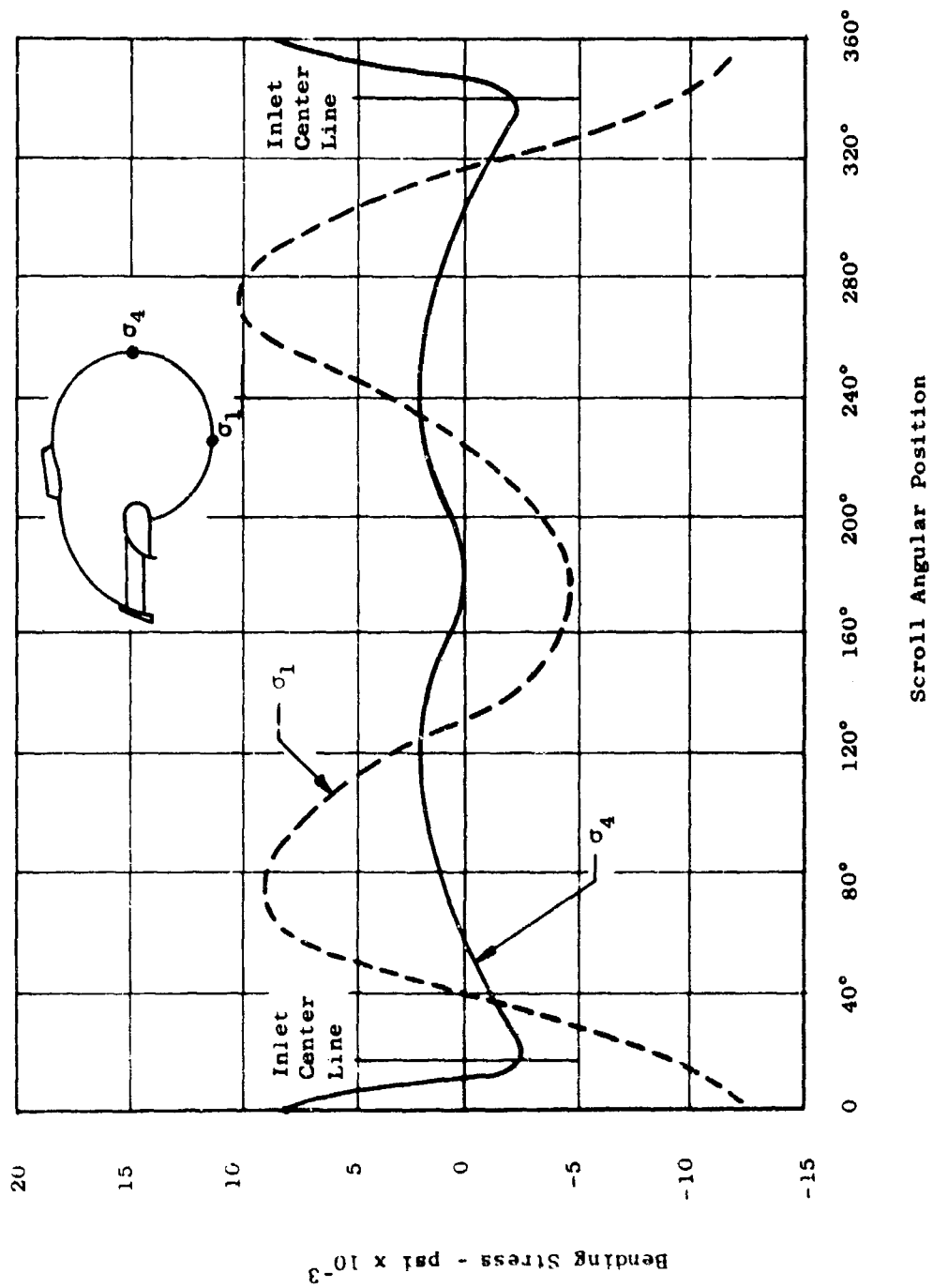


Figure 131. Scroll Bending Stress - Alternate Close Spaced Inlets.

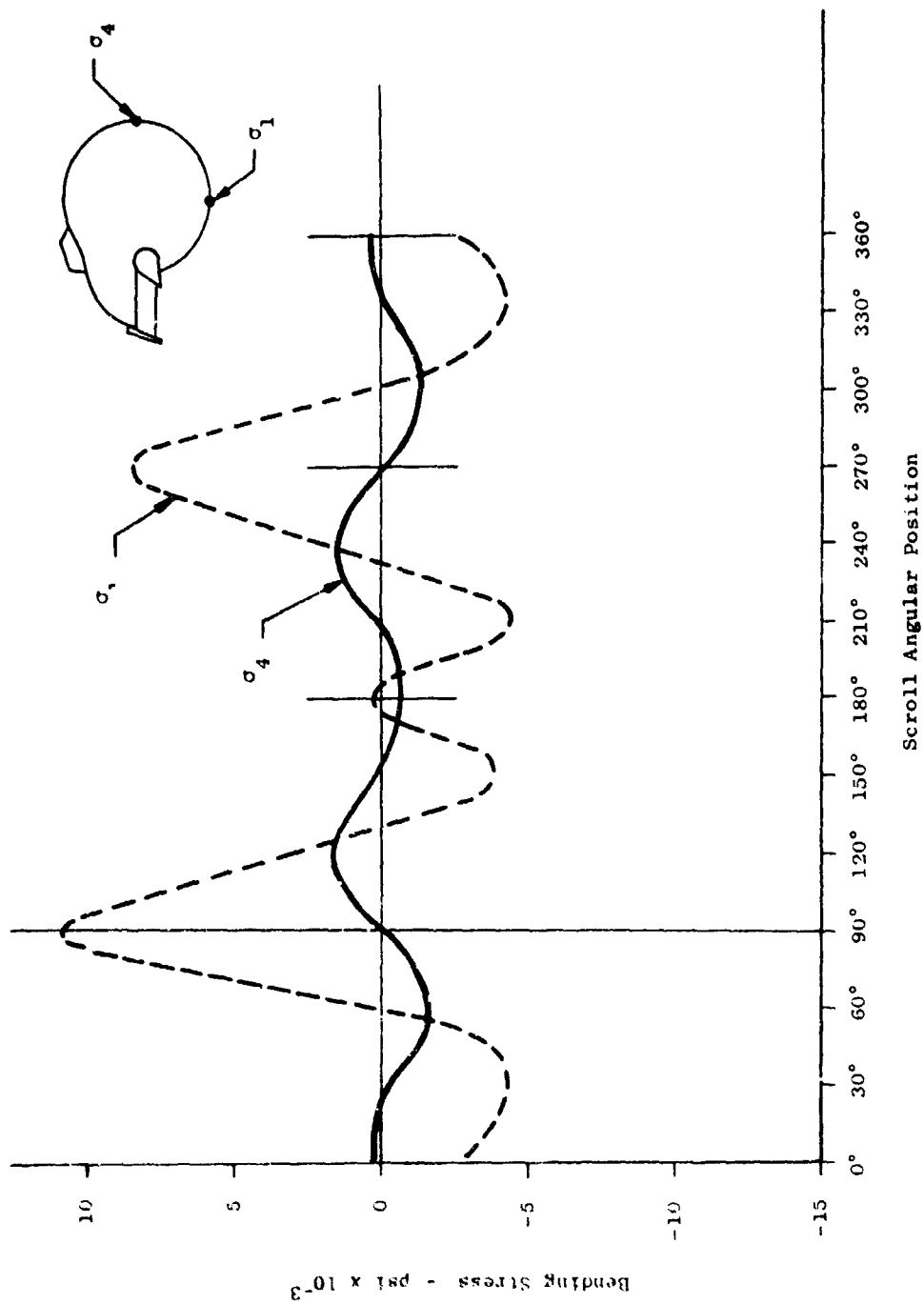


Figure 132. Scroll Bending Stress.

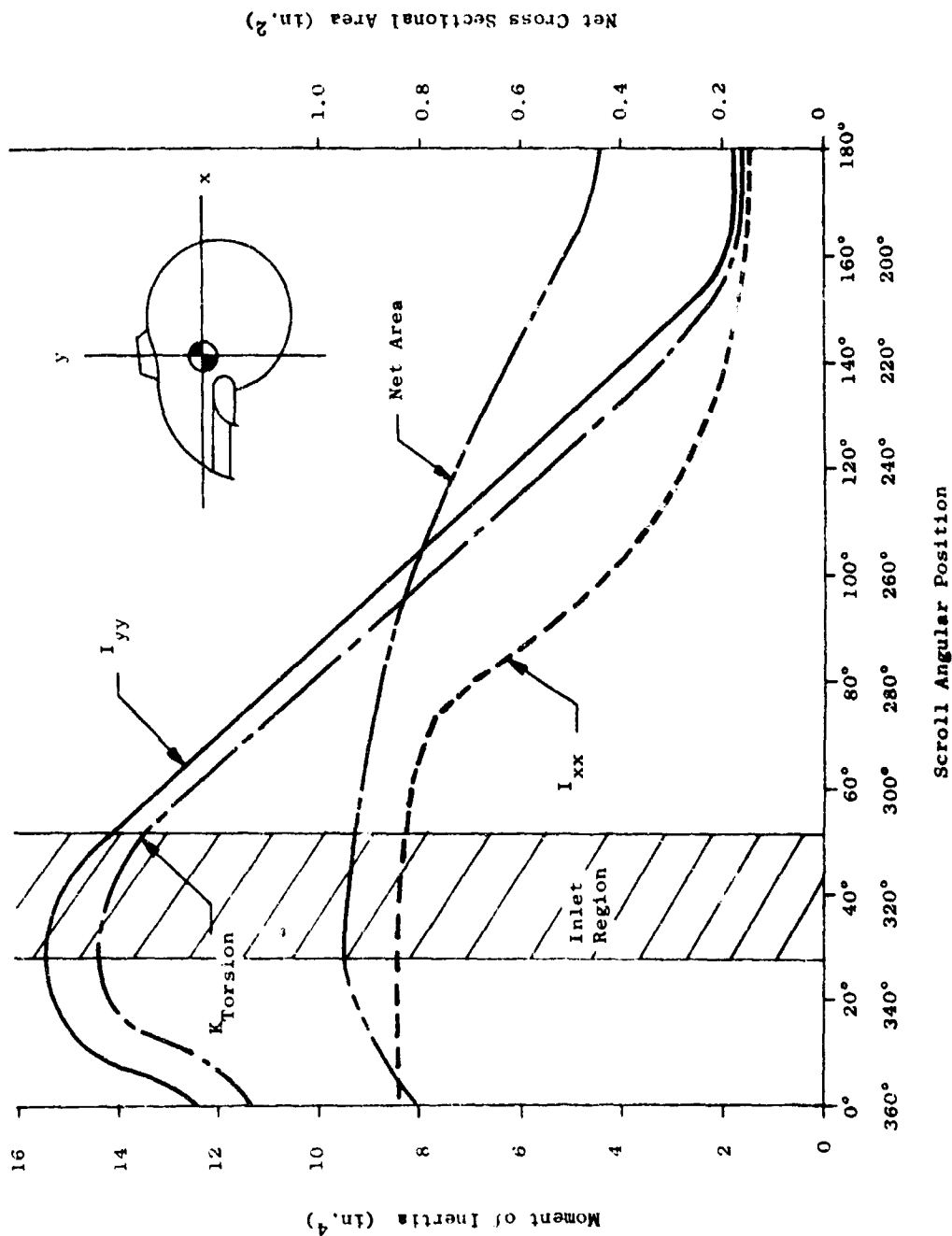


Figure 133. Scroll Section Properties.

investigation and detail analysis. However, as can be seen from the values in Table XVIII, the stresses on which the design was based (minimum moment of inertia) are not unacceptable.

In the region of the 6:00 and 12:00 mounts the strut chord is increased to support the concentrated mount loads. Since the exact load distribution is indeterminate and depends on the inlet centerline location, a conservative design approach was utilized. Detail design refinement could likely result in a weight reduction.

Variable area control mechanism leakage across the partitions can be minimized by designing the vane for a positive gas turning moment. Although this does induce higher bending stresses in the various components, it is a necessary consideration because of the large percent of admission arc being utilized. The inclination of the flow path creates additional leakage areas in the corners of the movable vanes; reducing the flow path inclination would reduce the size of the corners which must be omitted from the vanes for moving clearance.

The short distance between the fan tip and bucket root makes packaging of the mechanism and actuation a very challenging problem. Additional detail evaluation is required to determine if the area control system can be contained between the scroll and front frame in a 9-percent-thick wing. Increasing the wing thickness could provide additional space for the control system.

The utilization of high gas temperatures (1400° Fahrenheit) must be evaluated to determine the effects on material wear (actuation mechanism) resistance. Prior to the final selection of materials for the variable area components, a series of bench tests should be conducted to determine the effects of high temperature on the wear resistance. The close spacing of the nozzle partitions requires that small bolts be used, as noted previously. However, although the bolts are small, satisfactory operating stresses can be realized by controlling the unsupported length of the movable vane. Alternating bolt bending stresses of plus-or-minus 22,000 pounds per square inch will be induced for the unsupported length of 0.20 inch.

Splitter vane and flap thickness must be closely controlled to prevent high bending stresses. Typical bending stresses for the vanes are given in Table XVIII.

If the inlets were required to be close together and the mounting scheme shown in Figure 126 had to be used, then the scroll shell thickness would have to be increased in order to prevent structural buckling.

Areas Requiring Further Study

The areas outlined below warrant additional detail investigation to assure design integrity and reduce weight.

Figure 126 shows an alternate scroll mounting scheme which would be desirable if the scroll inlets were required to be close together. This mounting scheme is desirable because it prevents high bending stresses in the scroll skins due to the external gas piston force. Figure 131 shows the bending stress distribution around the scroll periphery for both mounting schemes, with the inlets spaced close together. Although the slip-seal design itself is not the most desirable, no other design has been conceived which satisfies all the requirements.

The scroll mounting scheme shown in Figure 134 was selected primarily to satisfy the mechanical sealing requirements between the scroll and front frame. The short distance between the tip of the fan blade and the root of the bucket, when combined with the flow-path inclination, does not leave satisfactory distance for scroll thermal growth. Since the unrestrained thermal growth of the outboard portion of the scroll shown in Figure 126 will be nearly twice that shown in Figure 134, it would be impossible to use the conventional slip seal approach.

If the inlets were required to be close together and the mounting scheme shown in Figure 134 had to be used, then the scroll shell thickness will have to be increased in order to prevent structural buckling.

The scroll mounting method finally selected will depend on the fan/air-frame interface definition.

As mentioned above, the cantilevered nozzle partitions may be subjected to flutter fatigue, and bench testing is desirable.

The variable area control mechanism should be evaluated in more detail to assure that a satisfactory system can be provided in a 9-percent-thick wing. The wearing parts of the variable area control mechanism should be subjected to cyclic bench tests at rated temperature to verify high temperature wear properties.

Materials

Table XIX presents the minimum strength properties, at 1400° Fahrenheit, of several materials which were considered applicable for the scroll assembly.

René 41 material was selected because of its superior stress rupture properties; the effects of aging during operation are also an important consideration.

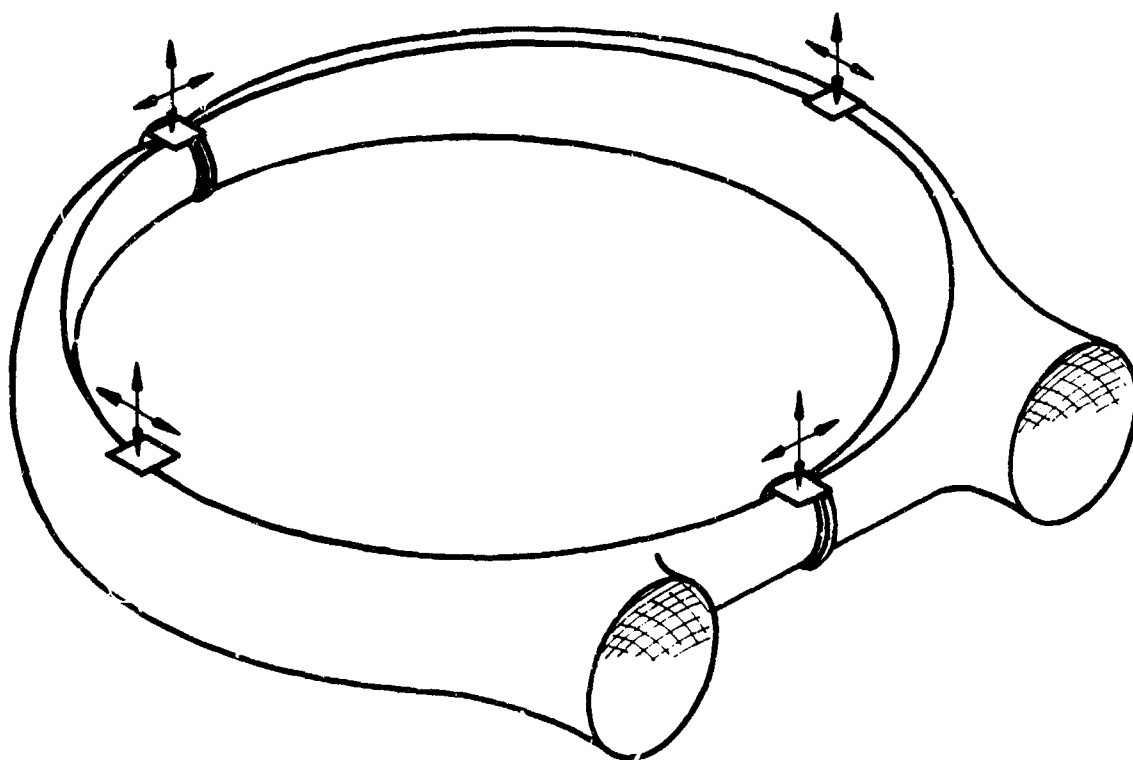


Figure 134. Conventional Scroll Mounting.

TABLE XVIII
SCROLL COMPONENT STRESSES

Nozzle Partitions	
Type I	42,100 psi (Unrestrained) 25,100 psi (Restrained)
Type IV	24,200 psi (Restrained)
Struts	30,360 psi
Top Circumferential Hat Section	21,700 psi
Torque Tube	27,300 psi
Shell	15,600 psi

TABLE XIX
SCROLL MATERIALS PROPERTIES

Material	0.02% Yield Strength (psi)	Ultimate Strength (psi)	1000-Hour Stress Rupture (psi)
Hastelloy X	28,600	43,500	11,200
L-605	15,000	45,000	24,800
René 41	85,000	127,000	30,400
Inconel X	50,000	74,000	25,000
Inconel 718	59,000	68,000	10,000

CONTROLS

Variable Area Scroll

The LFX basic design for control power modulation or power transfer utilizes a variable area scroll which was first tested on the LF-2 fan. The power to the fan can be increased by increasing the fan turbine nozzle area. However, in order for the gas generator to maintain a constant pressure ratio, it must be provided with a constant nozzle area. Consequently, when the nozzle area of one fan (or one-half the total nozzle area seen by the gas generator turbine discharge) is increased, the nozzle area of the other fan must be decreased an equivalent amount to maintain gas generator total discharge area constant. A schematic of this concept is shown in Figure 135.

The fan turbine nozzle area variation is accomplished by actuation of the split nozzle vanes and small auxiliary vanes shown in Figure 123. The movable vanes are ganged through a linkage which facilitates movement of the vanes in small groups, thus approaching a smooth area variation as a function of the command input. This variable area in turn minimizes throttling losses and provides an almost ideal thrust change with flow. The thrust variation according to the ideal fan laws would vary as the $2/3$ power of the ratio of turbine gas flows. Some deviations from this ideal result from ducting pressure loss variation, power (gas) losses in the inactive scroll arc and changes in fan turbine efficiencies and scroll leakage.

Dynamic Control Analyses

Steady-State Performance

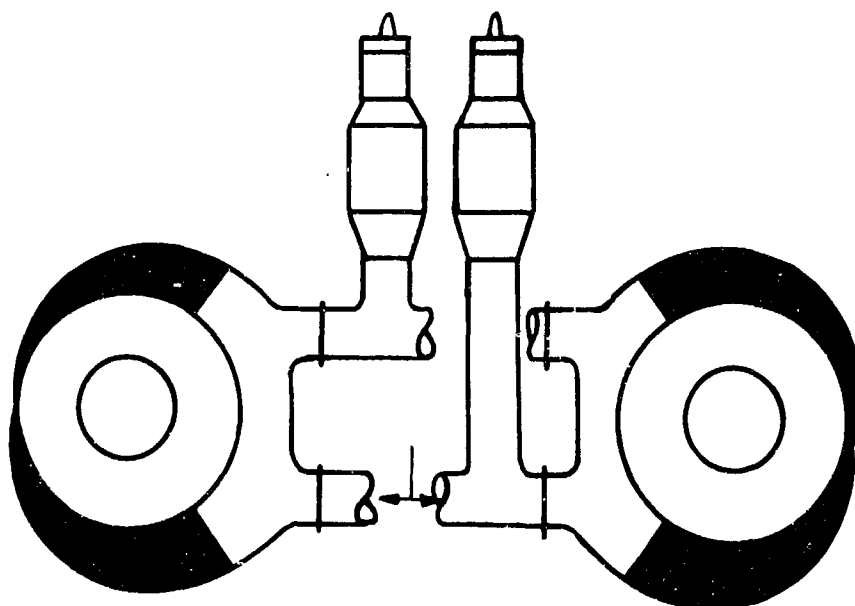
The gas power available to the fan may be controlled through variations in the turbine admission arc. Ideally, the power available to the fan would vary in direct proportion to the turbine admission arc, assuming fixed engine exhaust conditions. However, a number of secondary factors influence the actual power available to the fan with the result that the fan power varies in a nonlinear fashion with the turbine admission arc. Factors which have been considered in the calculation of steady-state lift and speed are as follows:

Variation of scroll pressure loss with gas flow

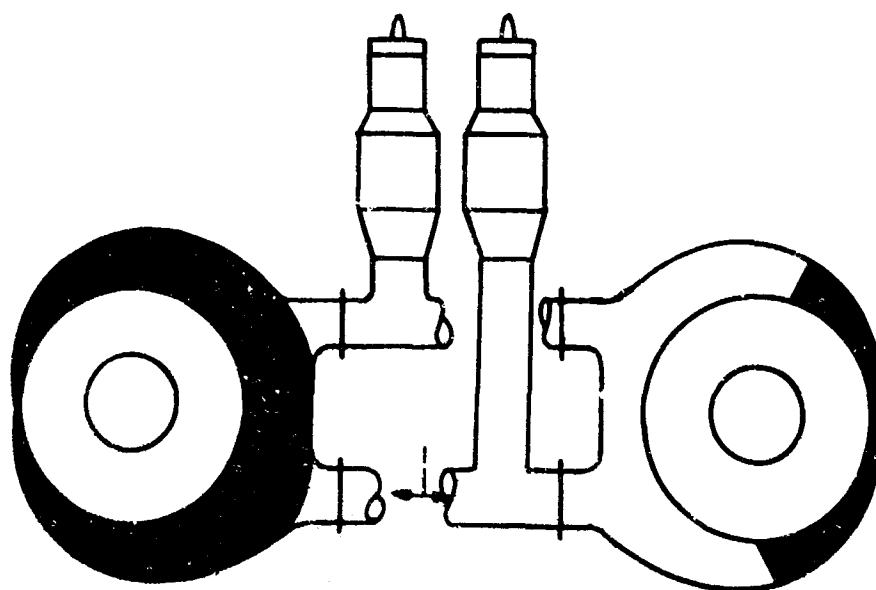
Variation of gas leakage with turbine arc

Variation of turbine efficiency with speed and admission arc

Table XX lists a number of significant fan parameters for the minimum, nominal and maximum admission arcs. Figure 136 shows how fan lift and speed vary with admission arc. Figure 137 shows how the combined lift of two fans varies with the amount of turbine flow transferred between them.



Nominal Lift Mode



Maximum Aircraft Roll Mode

Figure 135. Variable Area Scroll Schematic.

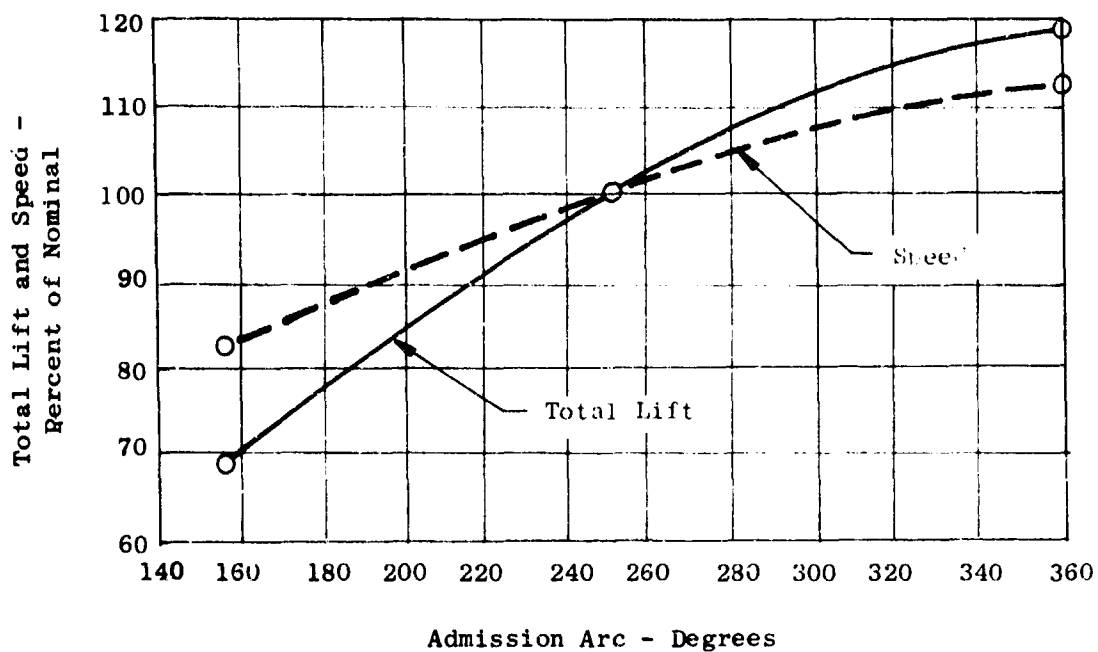


Figure 136. Lift and Variation With Power Transfer.

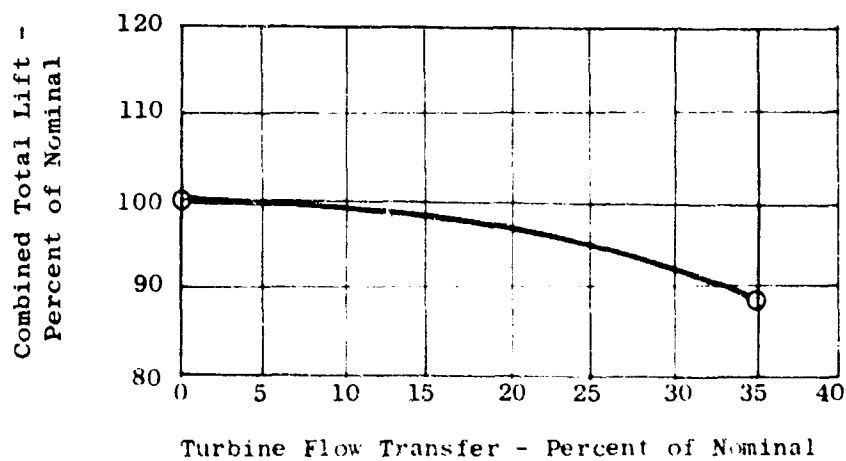


Figure 137. Power Transfer Lift Variation.

Dynamic Response Rates

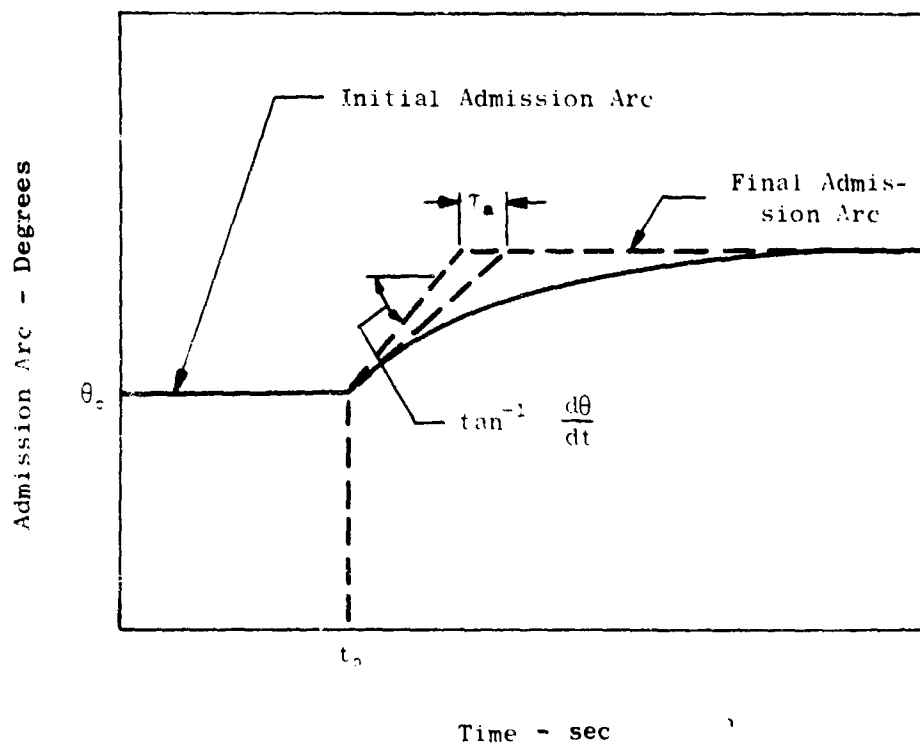
The dynamic response of a fan to a commanded change in admission arc is an extremely important factor in determining the overall controllability of an aircraft. Thus, studies were undertaken to determine the dynamic response of the LFX fan and its relation to a number of variables. For these studies it was assumed that the engine was unaffected by changes in admission arc, as would be the case with two perfectly matched fans with power transfer. Also, all response rates were based on step changes in the turbine arc command signal.

The fan is basically a nonlinear system and, thus, its dynamic response cannot be expressed in terms of system time constants in the same sense as can a linear system. For a linear system, the time constant represents the time required to reach 63.2 percent of the commanded change in any output variable. This definition has been arbitrarily extended to the nonlinear fan system for purposes of these studies. However, it must be realized that this definition is arbitrary and that the actual variation of any output variable with time will not follow exactly the exponential relation of a linear system. A further consequence of these nonlinearities is that various output variables will not have the same time constants when defined as above. Thus, we must distinguish between the speed time constant, τ_N , and the lift time constant, τ_F , as they will in general have different values.

The response rate of a given basic fan is affected primarily by two variables: the initial speed from which a change is to be made and the size of the commanded increment in speed or lift. In general, the response time of a fan may be expected to vary approximately in inverse proportion to the initial speed. This is basically due to the lower torque-to-inertia ratio at lower speeds. Because of the nonlinearity of the basic fan, the size of the commanded increment affects the response time such that a commanded increase in speed or lift will result in a decrease in response time and a commanded decrease in speed or lift will result in an increase in response time. The magnitude of these increases or decreases is approximately in proportion to the magnitude of the commanded changes.

In addition to the basic fan dynamic characteristics, the response rate of the total system is influenced by the dynamic characteristics of the variable turbine arc actuation and control mechanism. The characteristics of the actuation mechanism can be described adequately in terms of a simple time constant, τ_a , on the turbine arc and by a limiting rate of change of turbine arc representing actuator slew rate. The variation of turbine arc, θ , as a function of time is shown schematically in Figure 138.

The responsiveness of a fan system may be improved without resorting to closed loop speed control by including a lead network device commonly referred to as a jagger in its mechanical form. The jagger is a simple anticipatory device inserted into the fan control system. The device



τ_a = actuator time constant

$\frac{d\theta}{dt}$ = limiting arc rate, deg/sec

Figure 138. Turbine Admission Arc Variation With Time.

can be either mechanical or electrical. The mechanical jazzer system and an equivalent electrical circuit are shown in Figure 139. The electrical circuit is a simple resistance-capacitance network. The mechanical jazzer is a simple spring-dashpot device.

The response of a jazzer system to a step function input is of the following form:

$$\frac{\text{Output}}{\text{Input}} = 1 + M_j e^{-\frac{t}{\tau_j}}$$

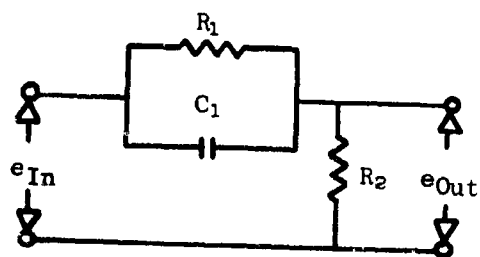
This relationship represents a function that is equal to unity plus a magnification factor, M_j , at time zero and is washed out exponentially to unity as time, t , increases. The rate of washout is controlled by the jazzer time constant, τ_j . Thus, the jazzer system initially magnifies a control input command, as a function of the input rate of change, to overcome fan inertia and quicken the fan response rate. It then exponentially washes out the input overshoot to the steady-state input proportional command level.

Figure 140 shows a typical jazzer response characteristic and its effect on fan system response. The upper figure shows a step input of unity occurring at time zero. The next figure shows the input command as modified by the jazzer. The initial level at zero time instantaneously achieves a level of one plus the magnification factor and exponentially decays to unity in about three time constants. The third figure shows the variation of the scroll actuator and consequently the area as a function of time. The initial ramp at zero time is due to actuator velocity limit, and the maximum level does not quite achieve the command level before the exponential washout occurs. The lower curve shows the fan system relative response. The jazzer improves the fan response by reducing the time required to achieve the commanded level of output.

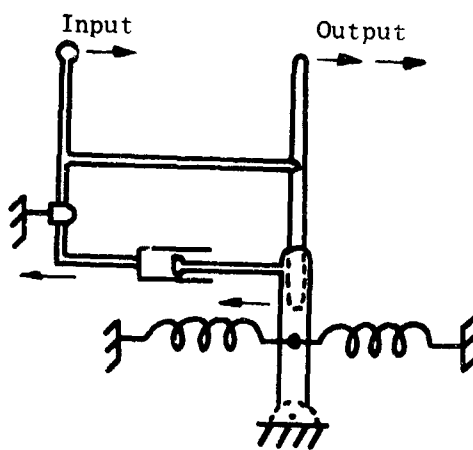
In order to evaluate the effects of the available variables on the fan response rate, two analytical studies of the LFX fan were conducted. Data were obtained for correlation by dynamically scaling analog computer results and hardware test results from the J85/LF2 lift fan [AVLABS Contract DA 44-177-AMC-220(T)]. These studies and their results are described in the following paragraphs.

Simplified Theoretical Analysis

First, a simplified theoretical analysis was conducted to determine the effect on fan response rate of variations in command step size, actuator velocity limits and initial fan speed. The jazzer was not included in this study, nor was the effect of the actuator time constant. The results of this analysis also yielded significant dimensionless ratios which should be maintained for proper dynamic scaling of analog and test results from other lift fans.



Electrical Circuit



Mechanical System

Figure 139. Electrical and Mechanical Jazzer Systems.

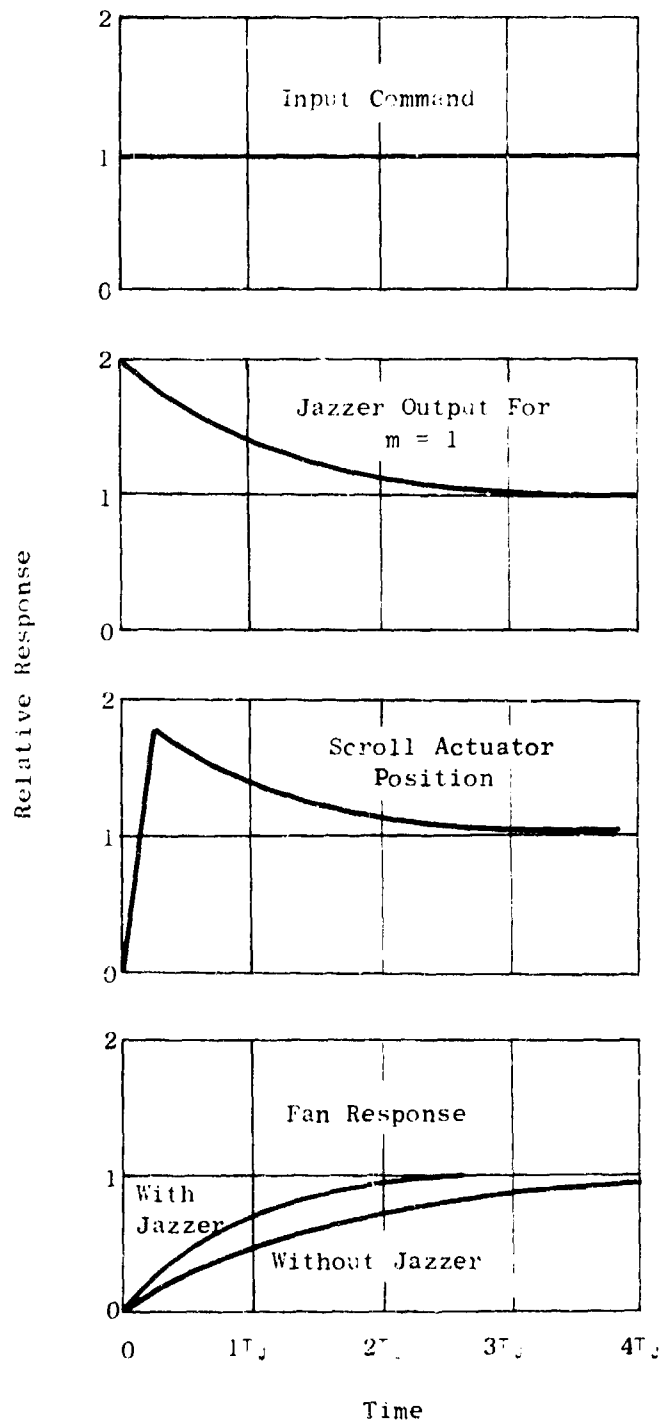


Figure 140. Jazzer Response Characteristics.

Figure 141 shows the turbine and fan torque versus speed characteristics assumed for the simplified mathematical model. Fan torque has been assumed to vary as the square of speed. Turbine torque has been assumed to be proportional to the admission arc and to vary linearly with speed as shown in Figure 141. Turbine admission arc was varied linearly with time at various rates as shown in Figure 142.

The above mathematical model results in two nonlinear differential equations for fan speed in terms of the above variables. The first equation applies during the time the turbine arc is changing while the second equation applies after the turbine arc reaches its commanded value. A numerical integration procedure was programmed on the General Electric Time Sharing Computer for these equations, and results were obtained for a range of input variables. These results are presented in Figure 143 which shows the fan speed time constant versus the commanded speed increment as a percent of initial speed. Curves are shown for various initial speeds as a percent of design speed and for two limit values of turbine arc rate of change. The fan lift time constant was not computed for this analysis, since the equations dealt only with speed and did not calculate separate turbine and fan stream thrusts.

Refined Theoretical Analysis

Use was made of an existing digital computer program "DYNASAR" (Dynamic Systems Analyzer) to make a more refined analysis of a few selected points. "DYNASAR" is a very elaborate and flexible program used for general dynamic systems analyses. With this program it was possible to include the effects of

- Scroll pressure drop variations
- Turbine partial admission losses
- A jaxzer circuit
- Scroll actuator time constant

and to calculate the lift time constant, T_L , as well as the speed time constant, T_N .

Figures 144, 145 and 146 show the speed time constant from this analysis for starting speeds of 100, 95 and 90 percent of design fan speed and for a range of commanded speed changes. The effect of the jaxzer magnification factor is also shown on Figure 144. These results are for a jaxzer time constant of

$$T_j = .110 \text{ second,}$$

an actuator time constant of

$$T_a = .037 \text{ second}$$

and a turbine arc rate of change limit of

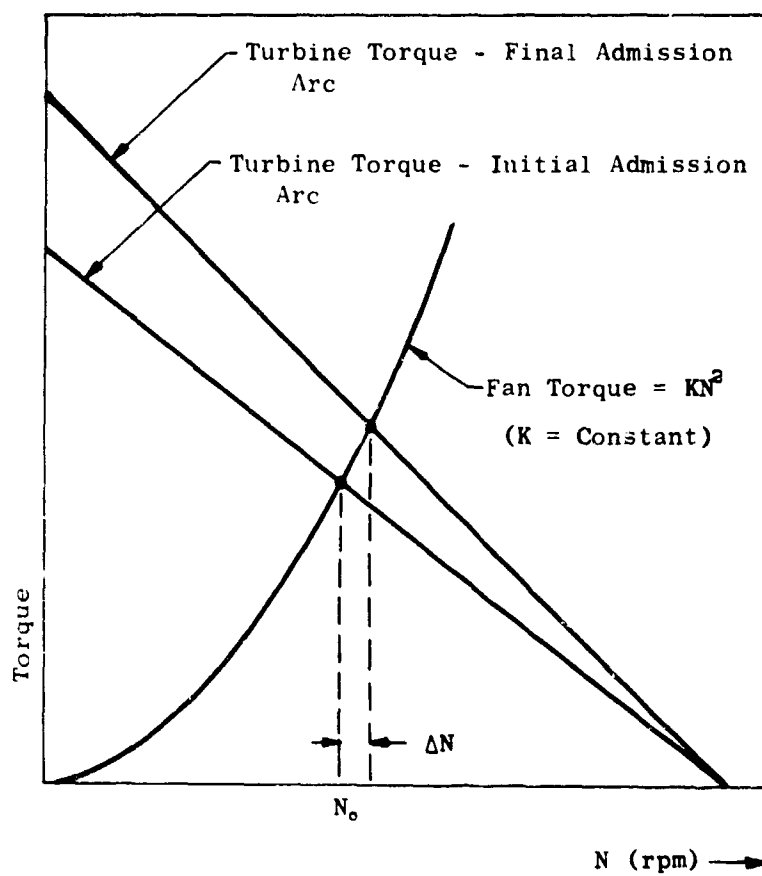


Figure 141. Torque-Speed Characteristics for Computer Input.

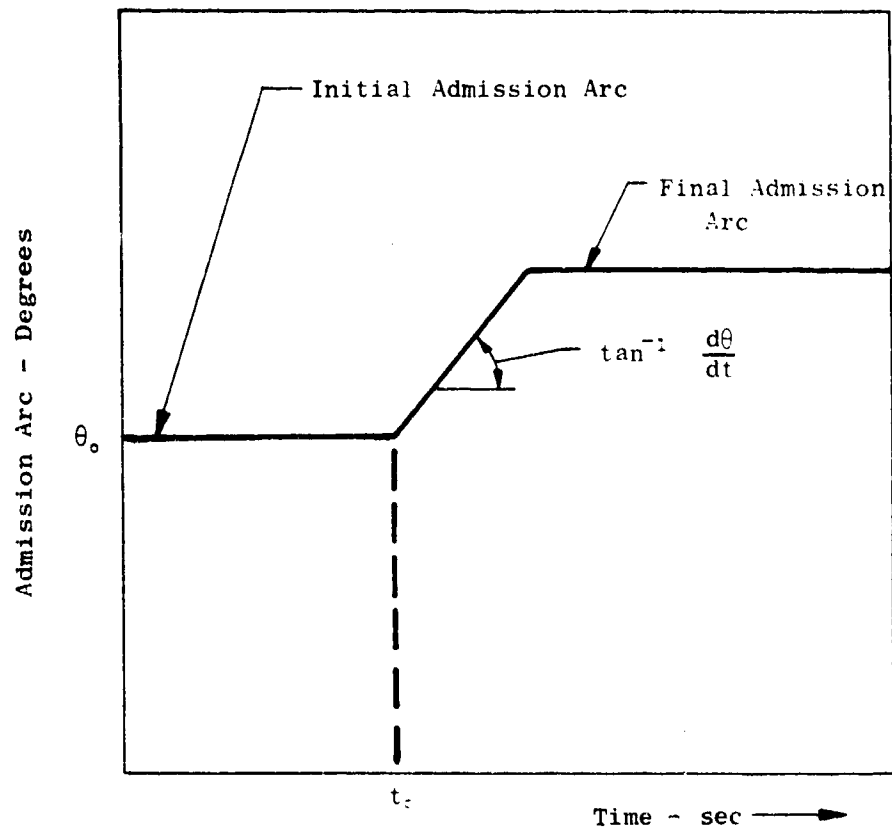


Figure 142. Turbine Admission Arc Time Rat. .

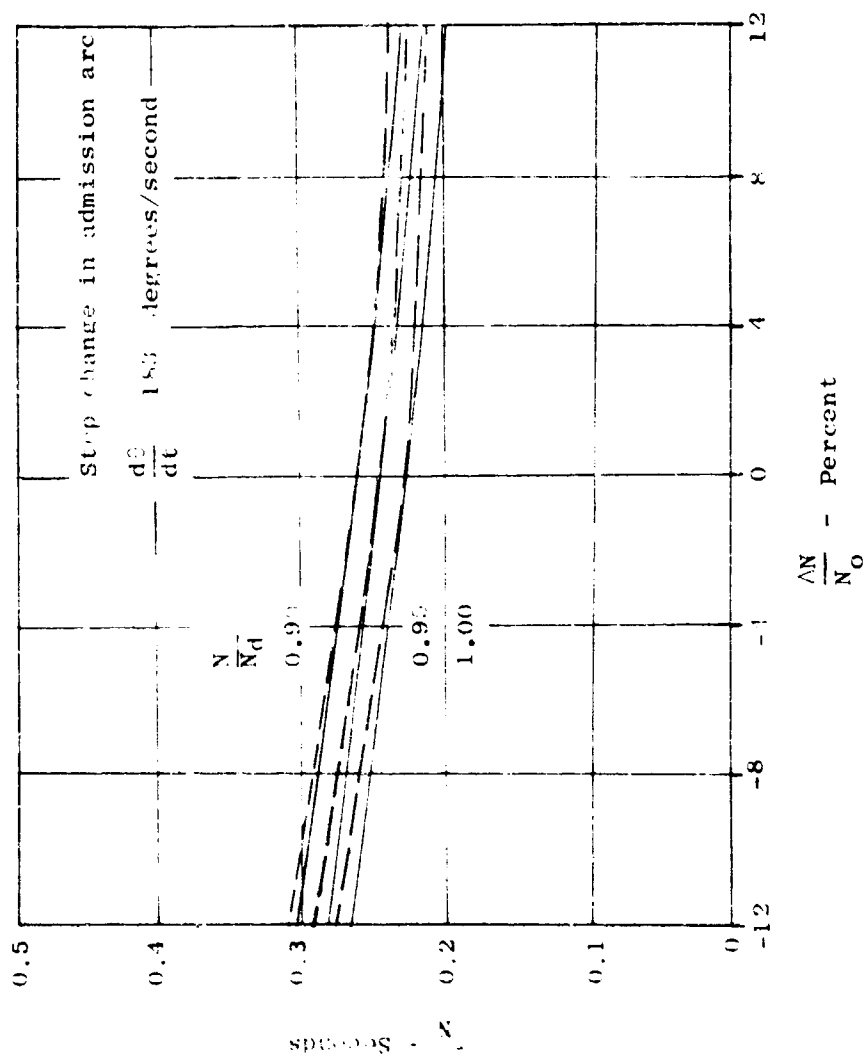


Figure 143. Speed-Time Constant for Changes in Turbine Arc.

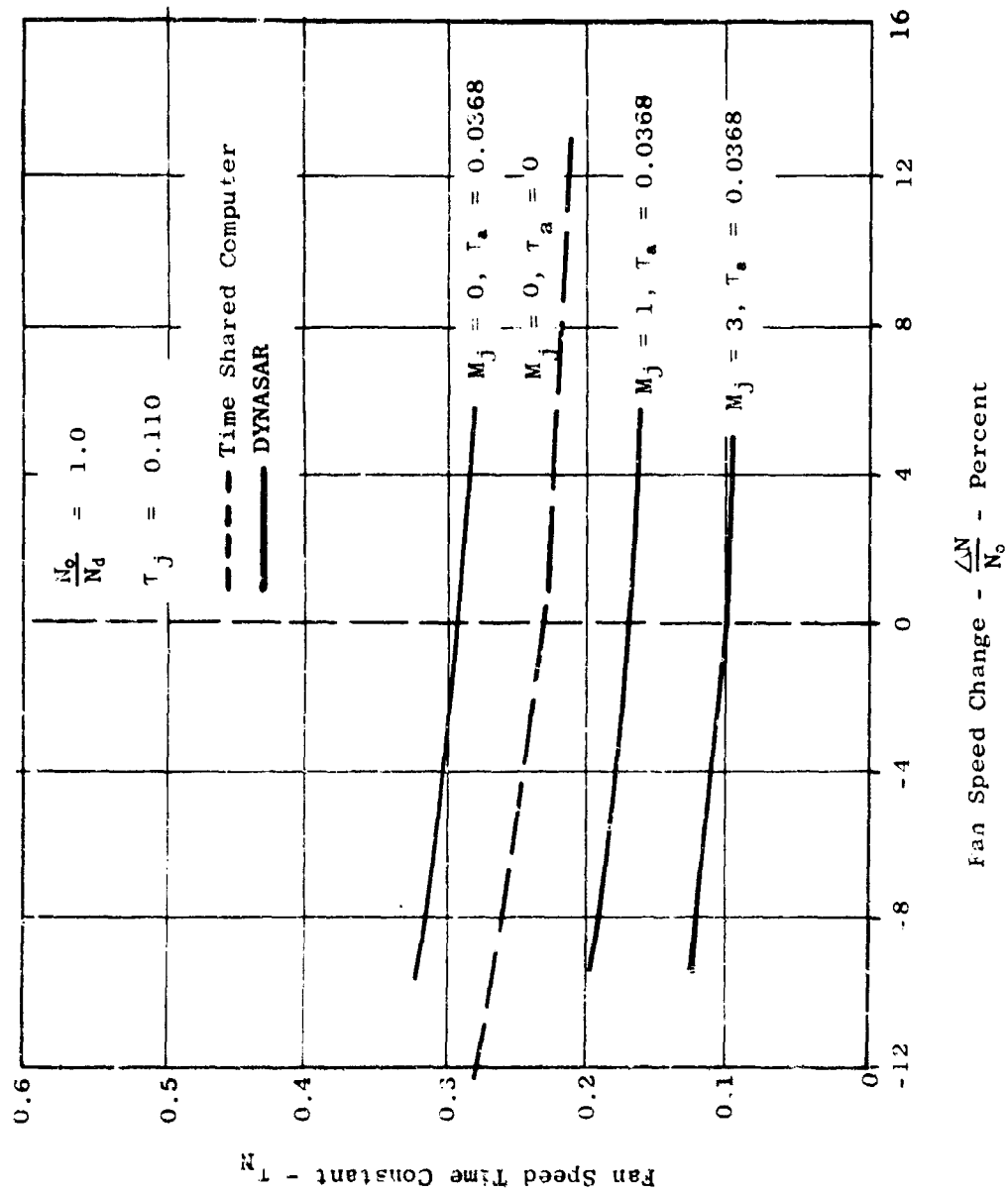


Figure 144. Speed Time Constant.

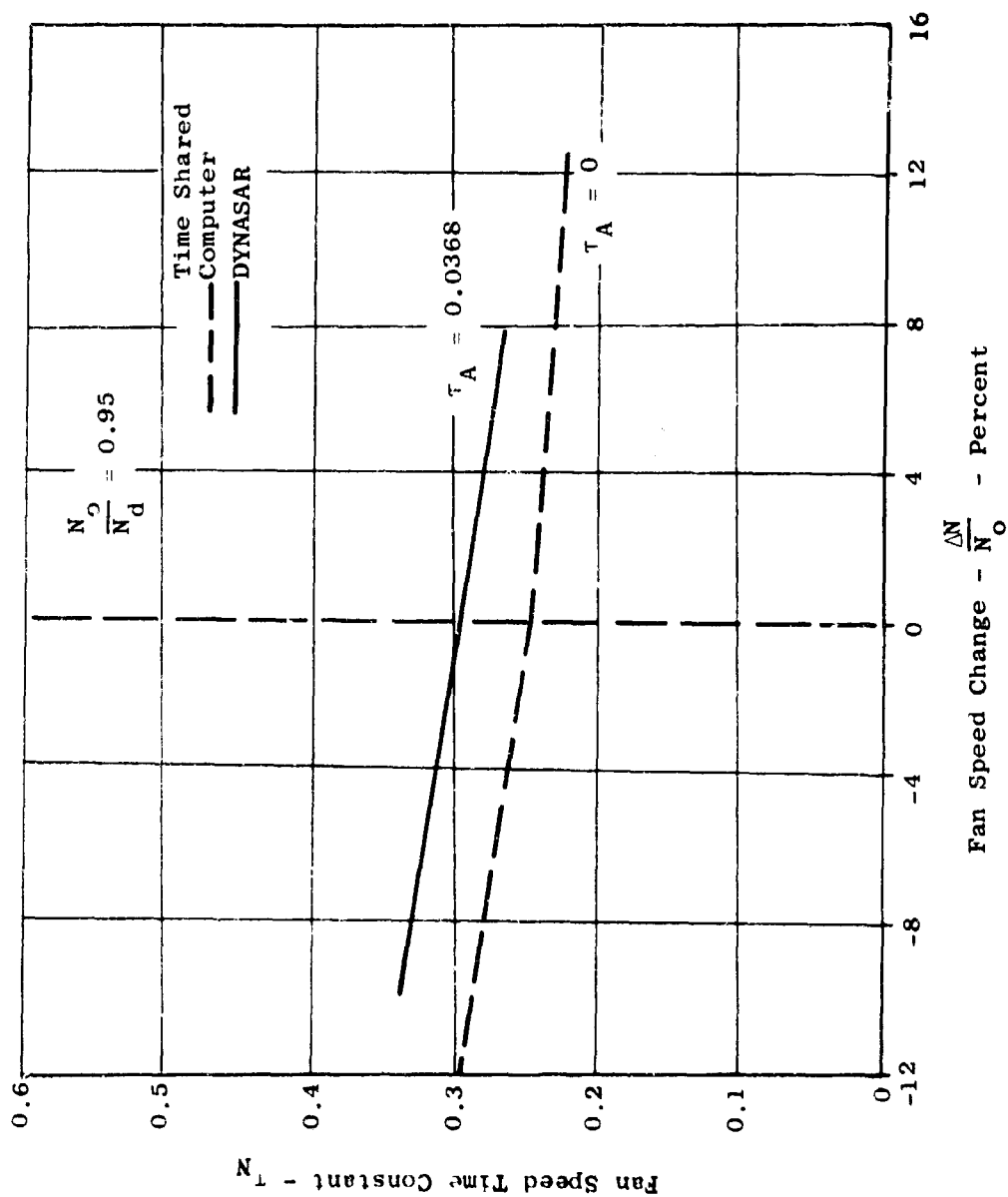


Figure 145. Speed Time Constant.

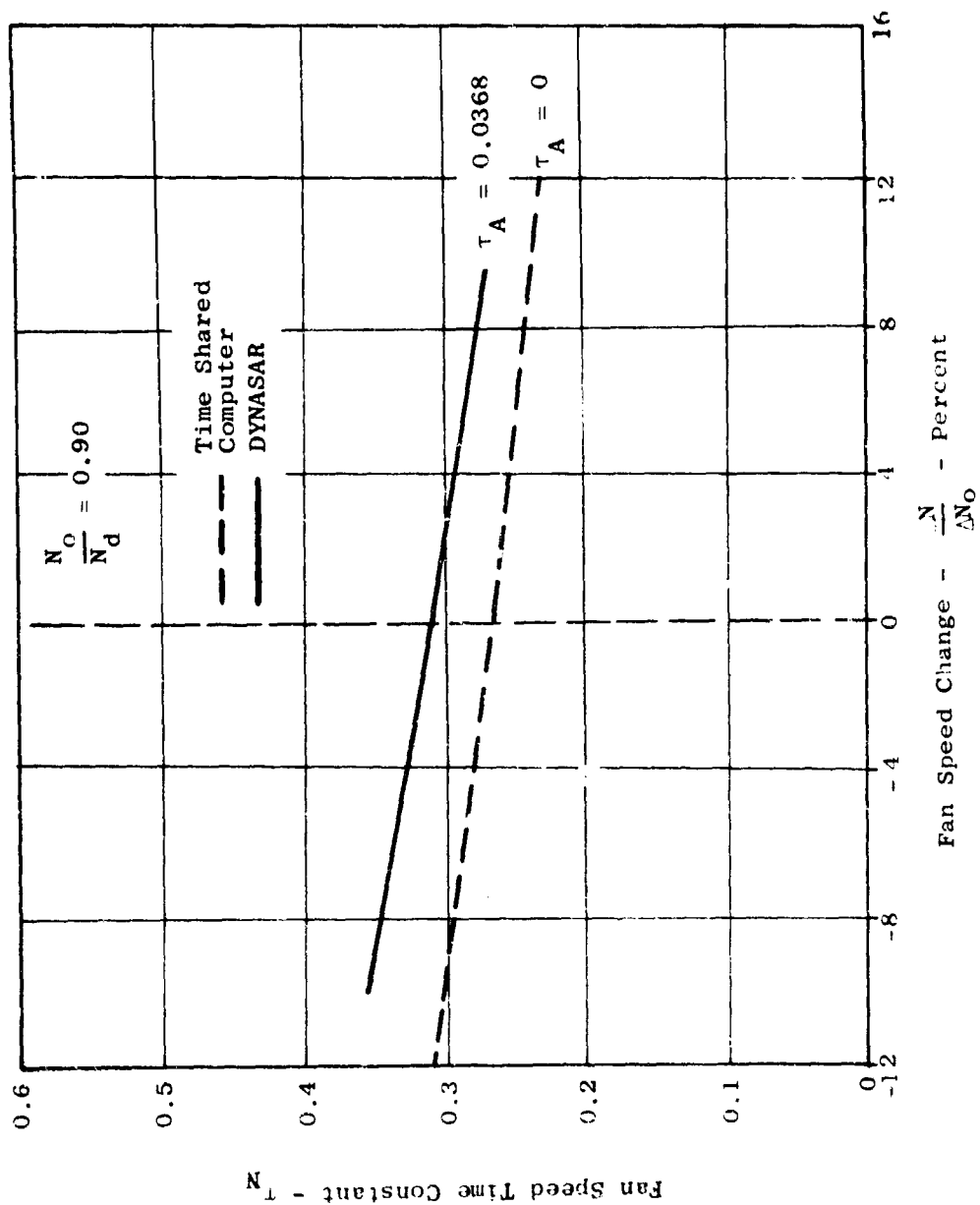


Figure 146. Speed Time Constant.

$$\frac{d\theta}{dt} = 1836 \text{ degrees/sec}$$

Also shown on these figures for comparison are the results of the simplified theoretical analysis for the same value of $d\theta/dt$. As can be seen, the "DYNASAR" analysis results in a somewhat higher value of the speed time constant than the simplified analysis. It is felt that the primary reason for this difference lies in the actuator time constant, T_a , which was zero in the simplified analysis.

In Figure 144 it can be seen that the jazer magnification factor, M_j , has a dramatic effect in reducing the time constant. The jazer magnification factor cannot be increased indefinitely, however, without introducing problems of speed and lift overshoot. Figure 147 shows plots of speed and lift versus time for different values of jazer magnification factor. It is apparent from these plots that a jazer magnification factor of 3 causes a substantial overshoot in both lift and speed while a magnification factor of 1 causes no overshoot. A small amount of overshoot in lift would be tolerable in most control systems. Thus, it would appear that a magnification factor of about 2 would be a near optimum value for this system; this value provides approximately 70 percent reduction in basic fan lift time constant.

The fan lift time constant differs from the speed time constant for two basic reasons. First, the fan lift exclusive of the turbine lift varies as the square of the speed. This tends to cause the lift time constant to be slightly higher than the speed time constant. Second, the turbine lift depends primarily on the turbine arc and is independent of the fan speed. Since the variation in turbine arc is considerably faster than the variation in fan speed this tends to cause the overall lift time constant to be lower than the speed time constant. The combination of these two effects usually results in a lift time constant which is smaller (quicker) than the corresponding speed time constant.

Figure 148 shows the effect of the jazer magnification factor on the ratio of lift time constant to speed time constant for an initial speed equal to the design speed. It can be seen that even with $M_j = 0$ the lift time constant is somewhat smaller than the speed time constant. As M_j is increased it is seen that the ratio of lift time constant to speed time constant is significantly reduced. Thus, the effect of the jazer magnification factor on the lift time constant is even more dramatic than its effect on the speed time constant as shown in Figure 144.

Figure 149 shows the ratio of lift time constant to speed time constant for several initial speeds. As can be seen, the effect of initial speed on this ratio is quite small for small commanded speed changes. For larger commanded speed increases there is an increase in the lift time constant relative to the speed time constant as the initial speed is reduced. The opposite effect is observed for commanded speed decreases.

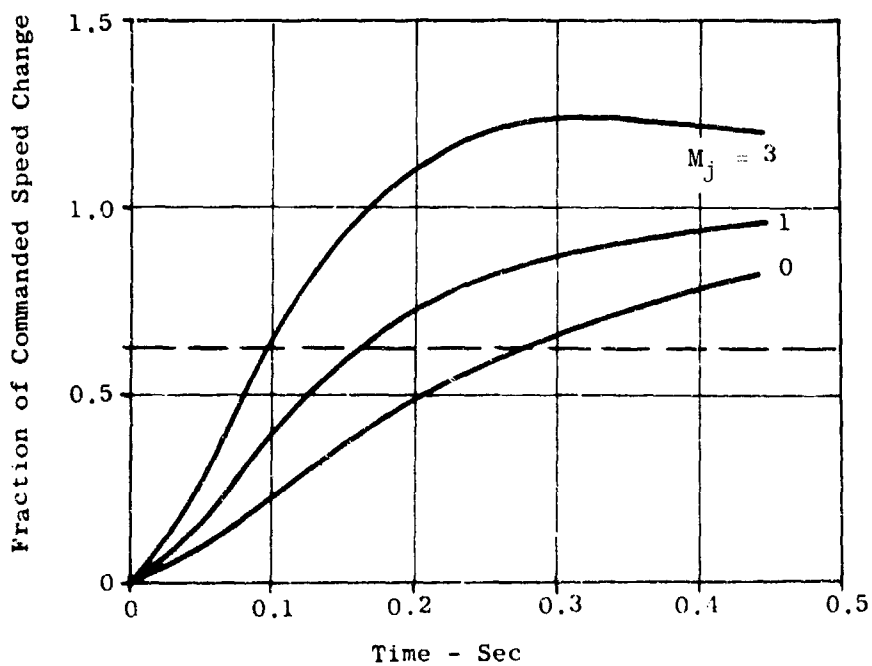
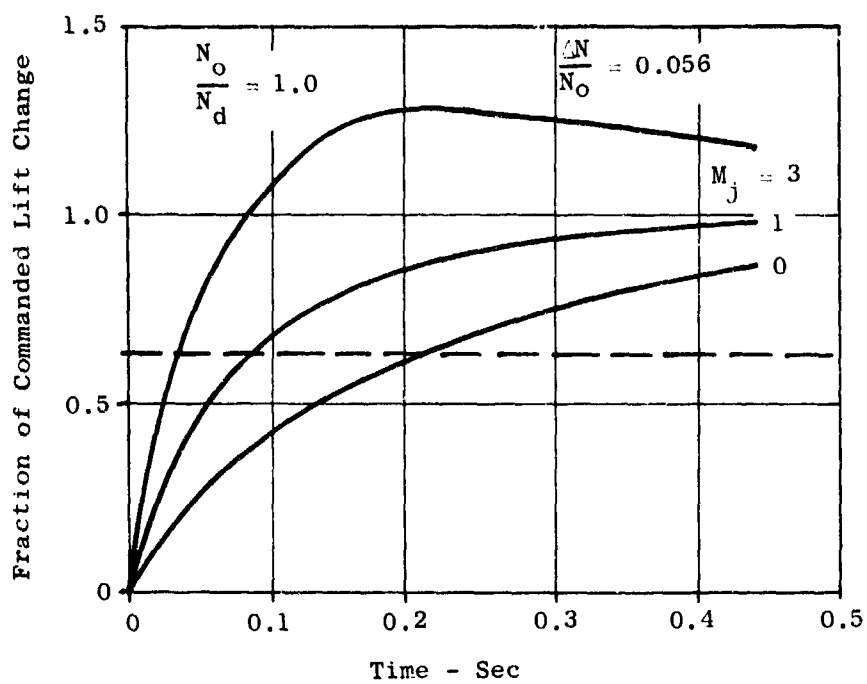


Figure 147. Effect of Jazzer Magnification.

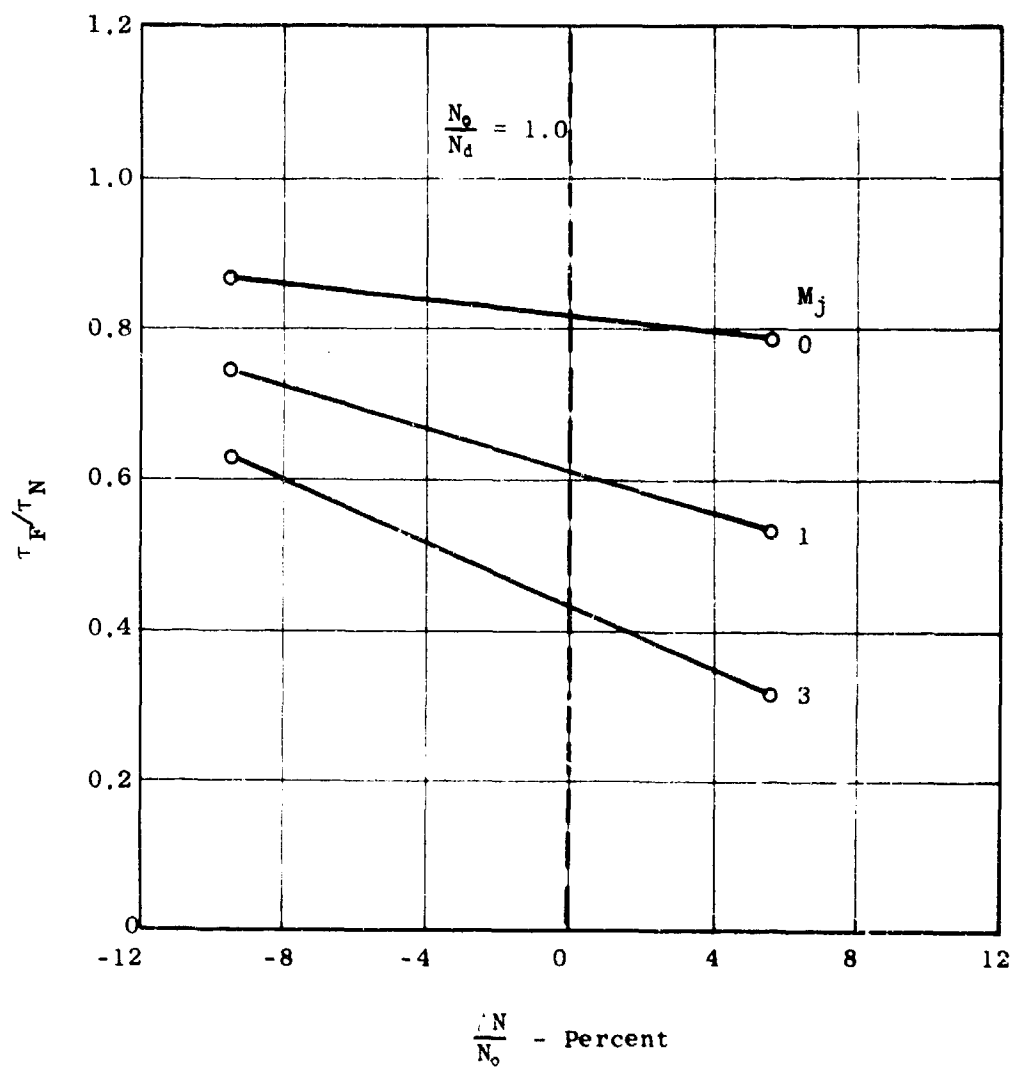


Figure 148. Jazzer Magnification Effect on Lift and Speed Time Constants.

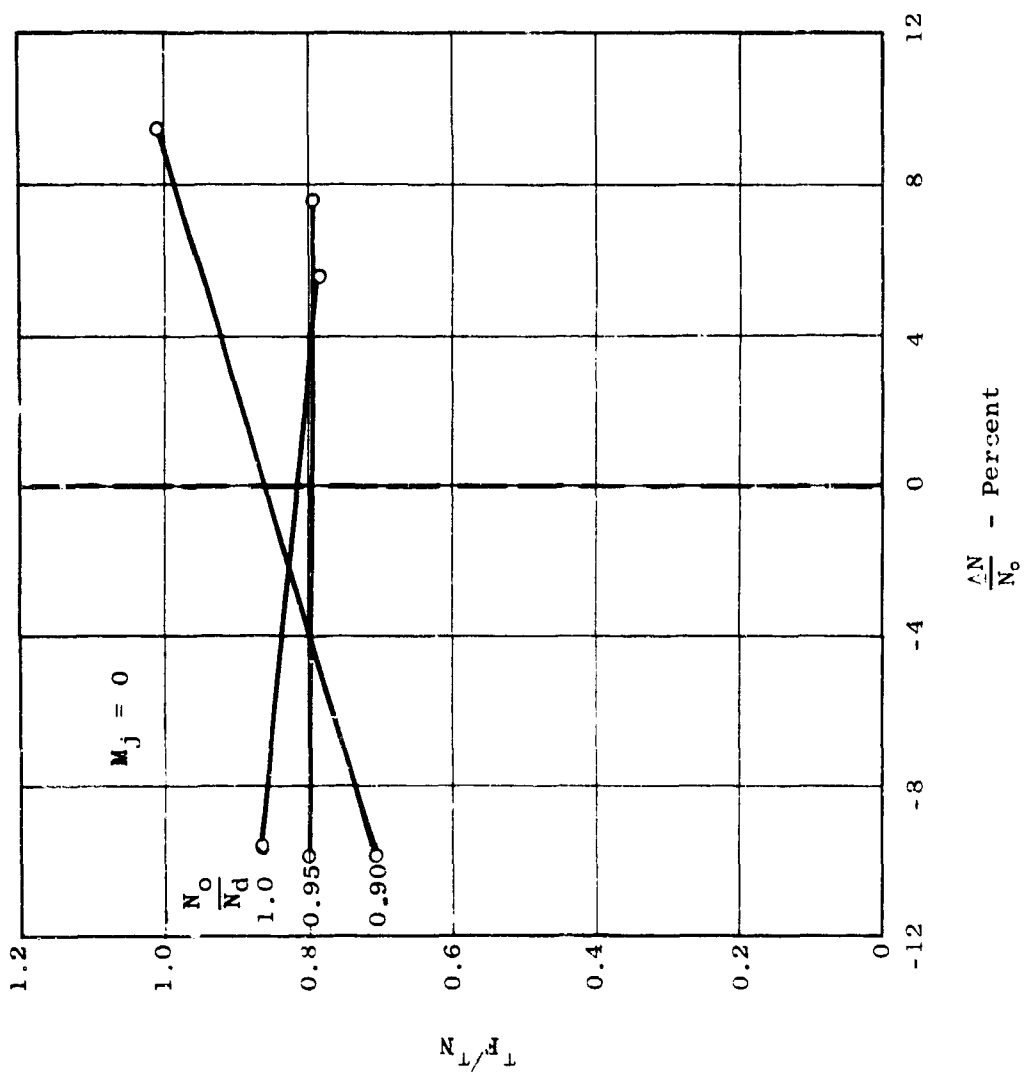


Figure 149. Initial Speed Effects.

Analog Computer Results

A study of the LF2 lift fan dynamic response has been completed on a rather elaborate analog computer setup. The mathematical model employed in this analysis was essentially identical to that of the refined theoretical analyses discussed previously. With the analog computer it was possible to study dynamic response to sinusoidally varying input command signals as well as response to step function command signals.

There are a number of significant differences between the LF2 fan and the LFX fan. These differences must be properly considered in any attempt to apply the results from the LF2 fan directly to the LFX fan. Table XXI lists the significant dynamic parameters for these two fans.

An elementary dimensional analysis of fan dynamic response shows that the fan speed time constant can be conveniently expressed in the following nondimensional form which may be called the time constant parameter.

$$Y_N = \frac{T_d T_N}{I_o W_d}$$

where

- Y_N = time constant parameter for speed
- T_d = design point torque, lb-ft
- T_N = speed time constant, sec
- I_o = rotor moment of inertia, lb-ft-sec²
- W_d = design point speed, rad/sec

The other significant fan time constants may also be similarly nondimensionalized. Thus,

$$Y_f = \frac{T_d T_f}{I_o W_d}$$

where

- Y_f = time constant parameter for lift

The values of Y_N and Y_f will be functions of other significant dimensionless ratios such as

$$\frac{N_o}{N_d} = \text{ratio of initial speed to design speed}$$

$$\frac{\Delta N}{N_o} = \text{ratio of speed change to initial speed}$$

$$Y_a = \text{time constant parameter for scroll actuator}$$

TABLE XX
FAN PERFORMANCE DURING POWER TRANSFER

Operating Point	Minimum	Nominal	Maximum
Fan Pressure Ratio	1.167	1.245	1.287
Fan Tip Speed, ft/sec	805	975	1090
Fan Speed, rpm	3358	4070	4558
Fan Speed, pct	82.5	100	112
Total Lift, lb	7420	10,750	12,750
Total Lift, pct	69	100	118.6
Arc of Admission, deg	156	250	360
Scroll Flow, lb/sec	32.50	50.01	67.52
Scroll Flow, pct	65	100	135
Scroll Nozzle Leakage, lb/sec	1.80	1	0
Turbine Flow, lb/sec	30.70	49.01	67.52
Scroll Total Pressure, psia	48.88	48.42	46.50

TABLE XXI
FAN DYNAMIC PARAMETERS

	<u>LFX</u>	<u>LF2</u>
Rotor Moment of Inertia, lb-ft-sec ²	12.5	21.5
Design Speed, rpm	4070	2740
Design Point Torque, lb-ft	8580	7320
Turbine Lift, Fraction of Total at Design Point	0.129	0.108
Turbine Velocity Ratio at Design Point	0.414	0.411
$I_o W_d / T_d$, sec	0.621	0.843

Y_j = time constant parameter for jazzer

turbine lift/total lift

Use of the above nondimensional parameters affords a rational means of dynamically scaling the LF2 data to the LFX design. As previously shown, all of the system time constants are proportional to the factor

$$\frac{I_o W_d}{T_d}$$

provided that all of the other dimensionless parameters are maintained. This factor is given in Table XXI for both fan designs and it is seen that this factor for the LFX is 73.8 percent of the factor for the LF2. Thus, the LF2 results can be applied to the LFX design if all system time constants are reduced by a factor of 0.738. Note that the turbine lift, as a fraction of total lift, is just slightly higher for the LFX design. The effect of this would be to decrease the lift time constant by slightly more than the above factor while not affecting the speed time constant. The significance of the turbine design point velocity ratio is that it determines the slope of the turbine torque-versus-speed curve. Since the turbine design point velocity ratios are similar it is expected that the torque curves will have similar slopes for the two fan designs.

Figures 150 and 151 show the LF2 analog results for lift and speed time constants without the jazzer and for a step change in admission arc command signal. Figure 151 may be compared to Figures 144, 145 and 146. Multiplication of the speed time constant values in Figure 151 by the factor of 0.738 gives values which agree reasonably well with those in Figures 144, 145 and 146 from the "DYNASAR" program, considering that the accuracy of the analog results is estimated to be about ± 5 to ± 10 percent. Some of the differences may also be attributed to the fact that the analog data were run with an equivalent value of

$$\frac{d\theta}{dt} = 850 \text{ degrees/second}$$

rather than the value of 1836 degrees/second used in the "DYNASAR" program. The jazzer time constant used for the analog was 0.05 second, which when multiplied by 0.738 is equivalent to the 0.0368-second value used in the "DYNASAR" program.

Figure 152 shows the effect on lift and speed time constant of the jazzer magnification factor, M_j . The jazzer time constant has been varied in this figure as follows. For the curves labeled "a" the jazzer time constant has been adjusted for each value of M_j to give zero overshoot in lift. For the curves labeled "b" the jazzer time constant has been adjusted for each value of M_j to give an overshoot in lift of 30 to 40 percent of the commanded lift change. Curves "a" and "b" both have the same value for $d\theta/dt$ as used in Figures 150 and 151, and are for an admission arc change of +5 percent and an initial speed of 100 percent of

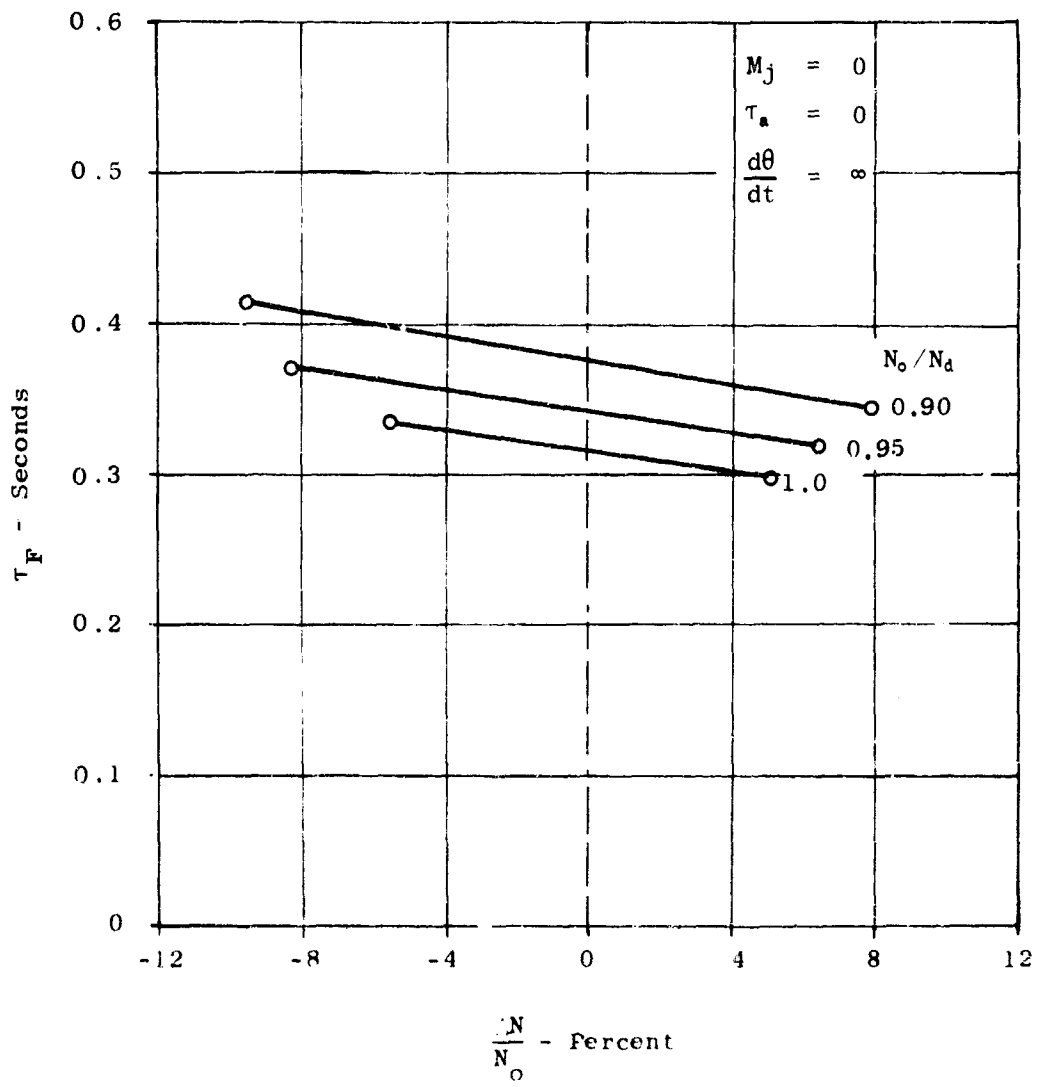


Figure 150. LF2 Analog Results.

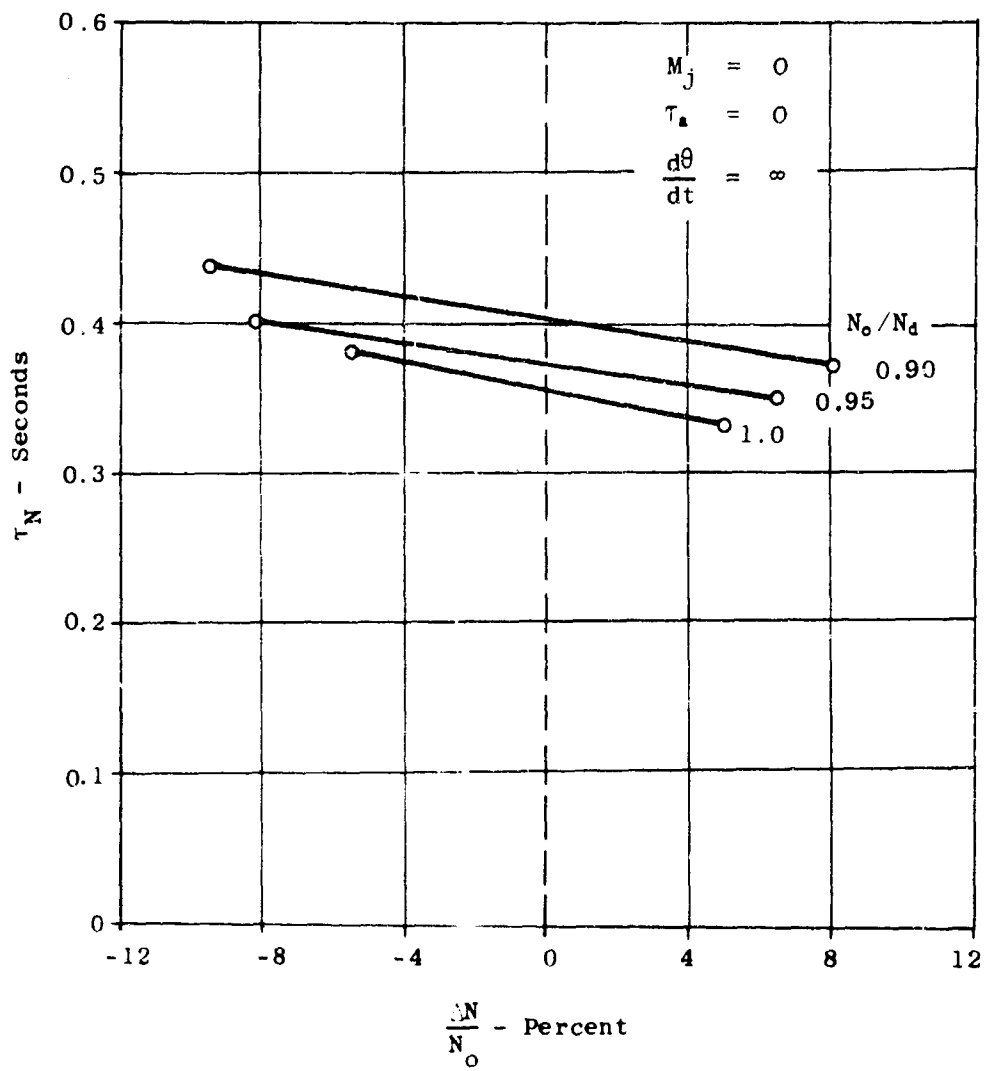


Figure 151. LF2 Analog Results.

- a = Fan response to step inputs with no overshoot
- b = Fan response to step inputs with overshoot
- c = Fan response to sine wave inputs with overshoot

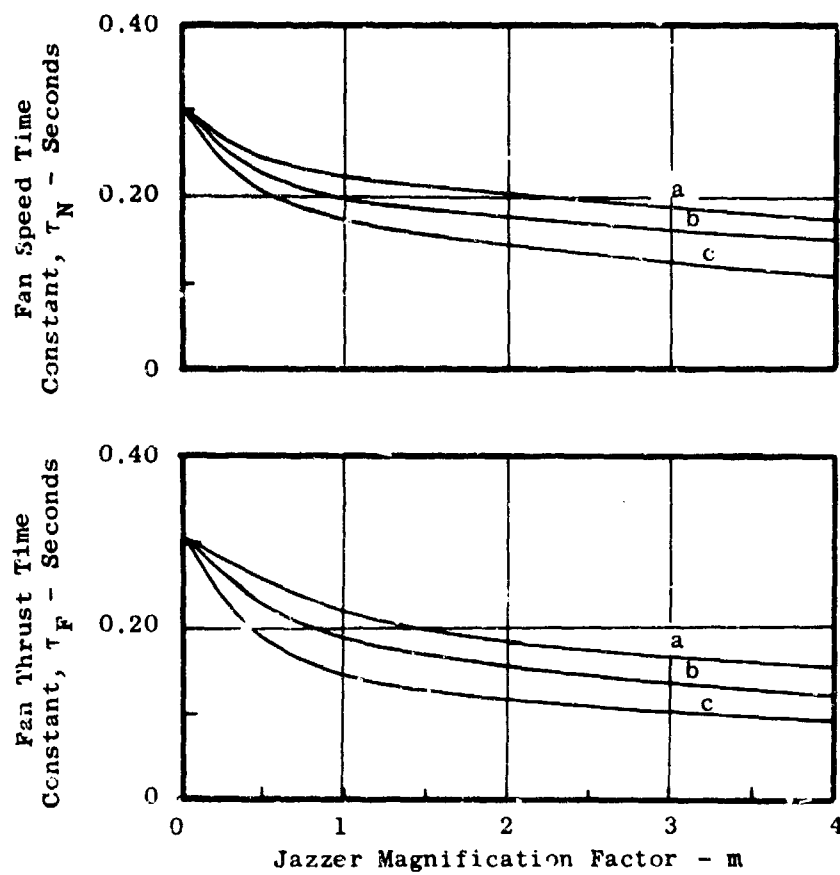


Figure 152. Analog Jazzer Magnification Factor Effects.

design speed. The curves labeled "c" show the lift and speed time constants as inferred from the steady-state frequency response to sine wave command signals with an amplitude of ± 5 percent of admission arc at the design speed. Curve "c" has the same jagger time constant at each M_j as does curve "b".

Figures 153, 154 and 155 show the steady-state frequency response to sine wave command signals with an amplitude of ± 5 percent of admission arc at design speed. Shown are both the amplitude and phase angle relationships versus impressed frequency. Figure 153 is for an M_j of 0, Figure 154 is for an M_j of 1 and Figure 155 is for an M_j of 3.

Figures 156, 157 and 158 show a comparison of test data from the LF2 variable area scroll test to analog results. Figure 156 shows the fan speed time constant as a function of initial fan speed and size of scroll area change. These results are without a jagger. Although there is some scatter in the test data, it can be seen that there is good agreement between the test data and the analog results.

Figures 157 and 158 show a comparison of steady-state frequency response for the actual fan and for the analog. Figure 157 is without a jagger and Figure 158 is for a jagger magnification factor of 1. Again, it can be seen that the test data and analog data are in good agreement.

A more extensive description of both the analog computer analysis and the LF2 fan test is given in Reference 11. This report also shows that there is generally good agreement between the analog and test results.

Potential Uses of Power Transfer Scroll

LFX Fan-In-Wing Aircraft

For an aircraft incorporating fans in wings plus pitch fan in fuselage, gas power transfer from variable area fan scrolls would be an extremely flexible and valuable design feature. For example, the following kinds of control could be obtained from power transfer with the incorporation of a simple mechanical mixer function between pilot commands and scroll area actuators.

<u>Commanded Function</u>	<u>Power Transfer Action</u>
Altitude Control	Collective area control of all fans
Roll Control and Trim	Differential area control of wing fans
Pitch Control and Trim	Differential control between pitch fan and collective wing fans
Engine EGT Trim	Collective area control of all fans
Pitch Reaction Control Phase-Out	Differential area control between pitch fan and collective wing fans

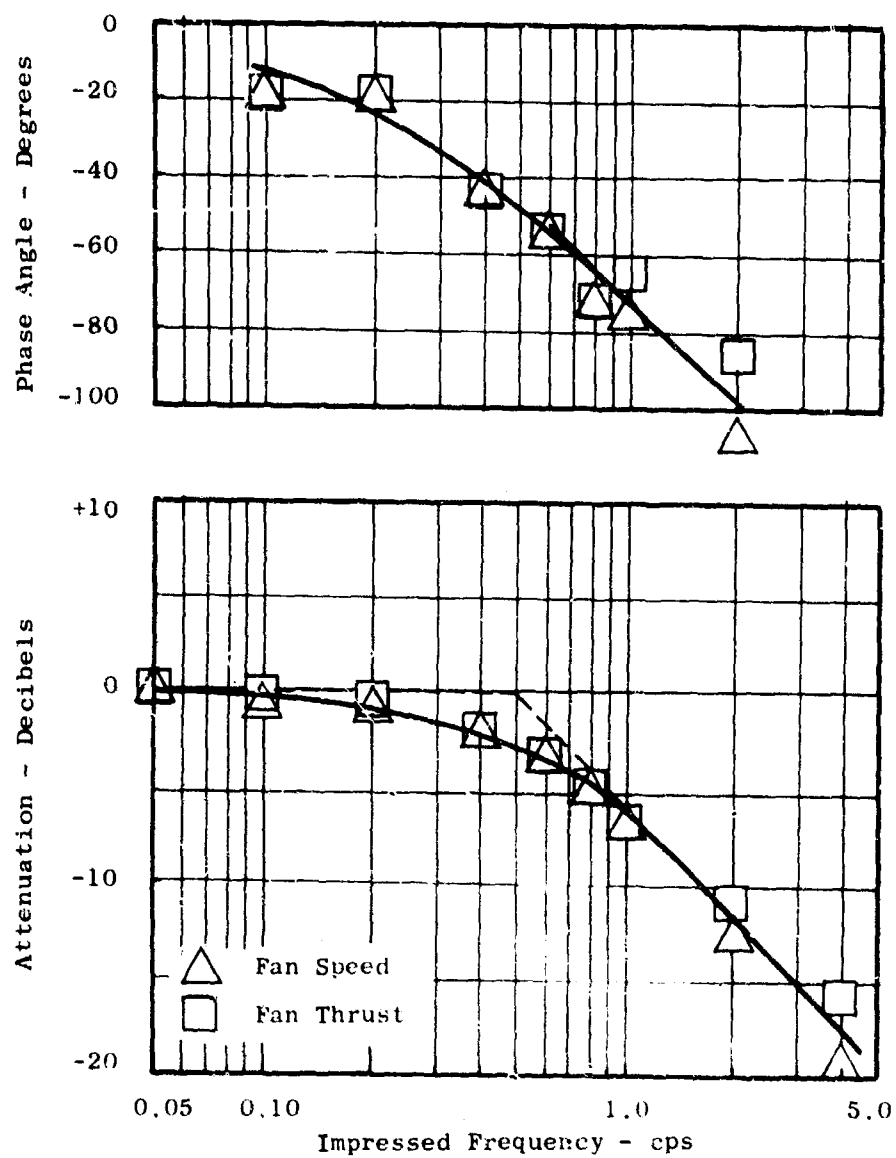


Figure 153. Steady-State Frequency Response - Analog Results for 100 \pm 5 Percent Area Without a Jazzer.

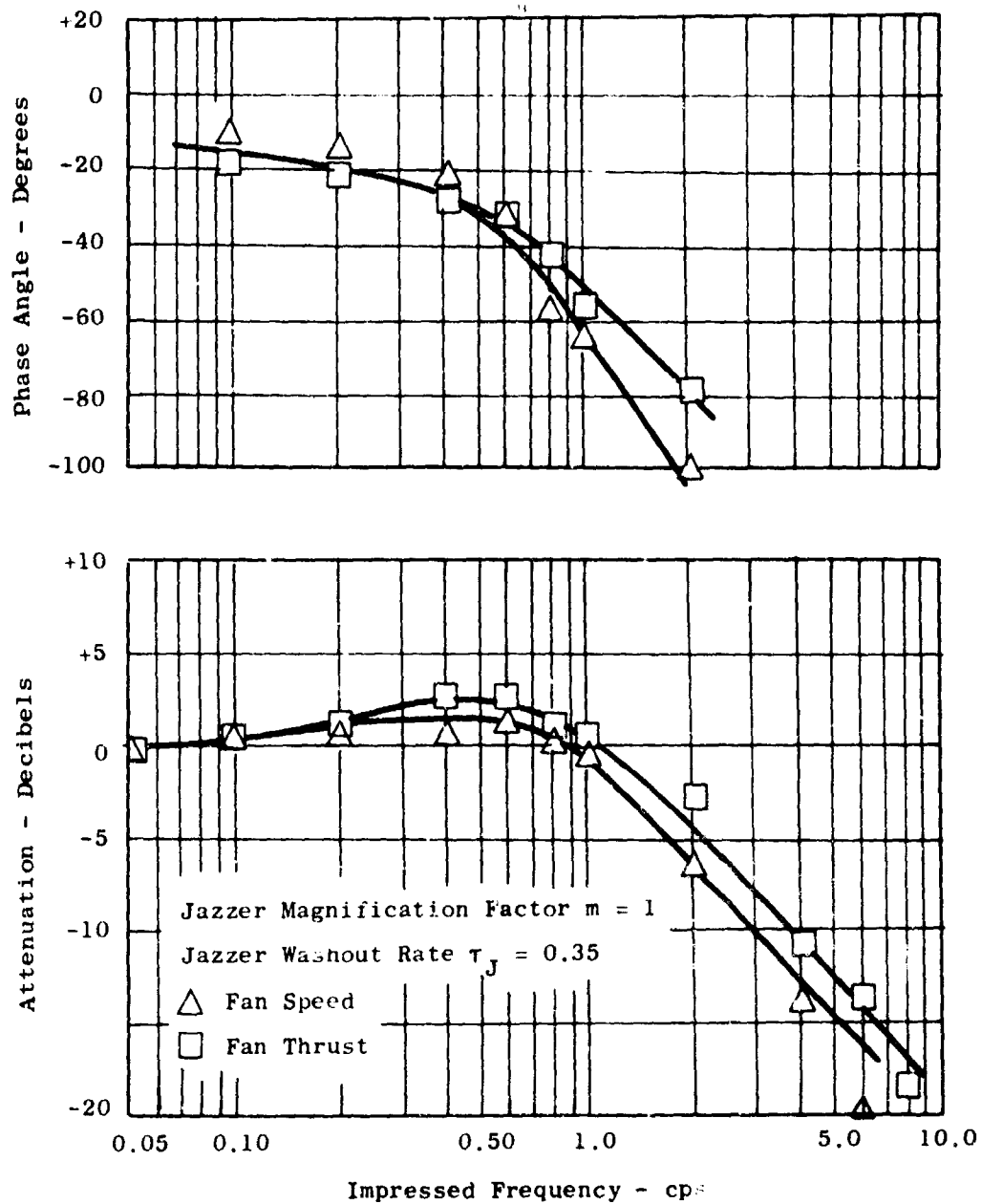


Figure 154. Steady-State Frequency Response - Analog Results for 100 \pm 5 Percent Area With a Jazzer Magnification Factor of 1.

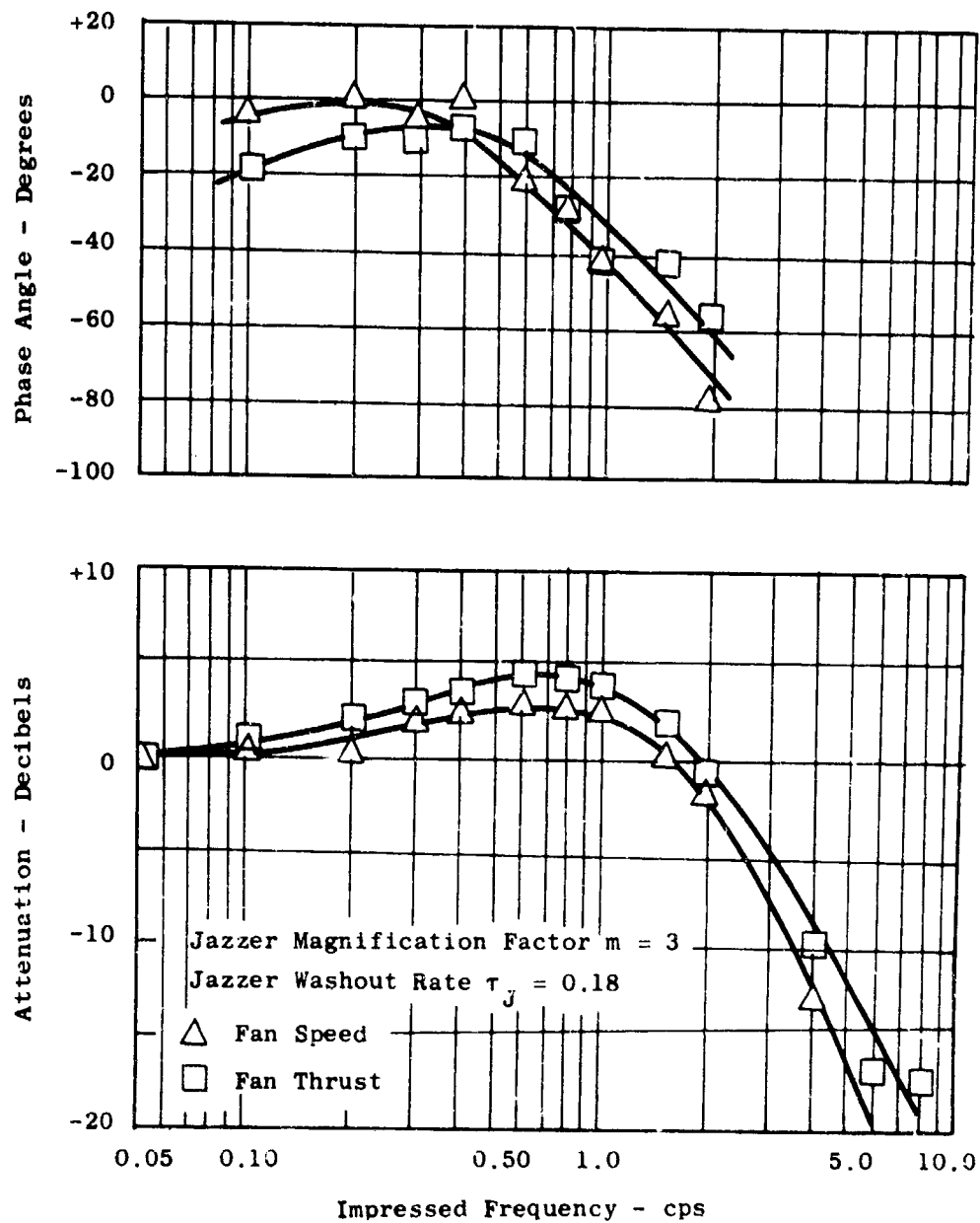


Figure 155. Steady-State Frequency Response - Analog Results for 100 \pm 50 Percent Area With a Jazzer Magnification Factor of 3.

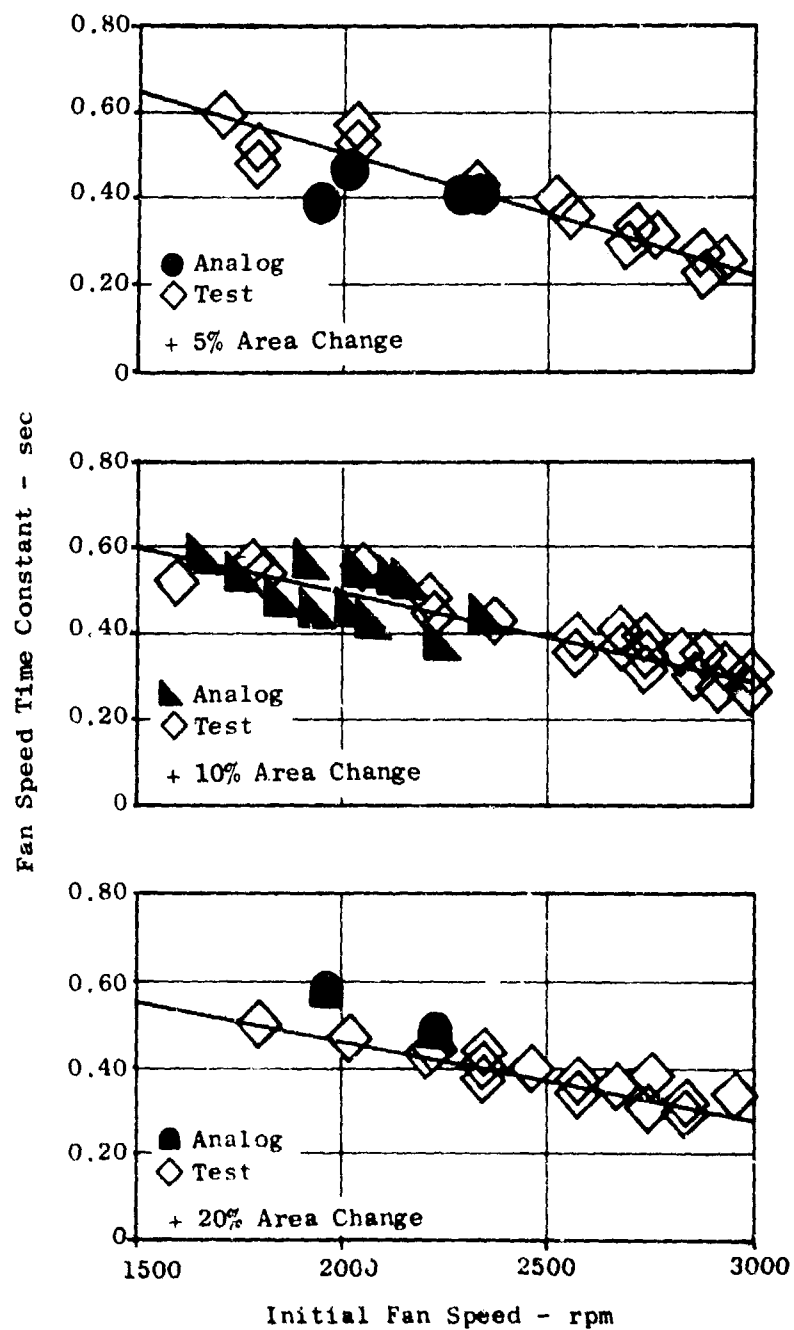


Figure 156. Comparison of Analog and Hardware Test Results - Fan Speed Time Constant for Positive Step Changes in Fan Area Without a Jazzer.

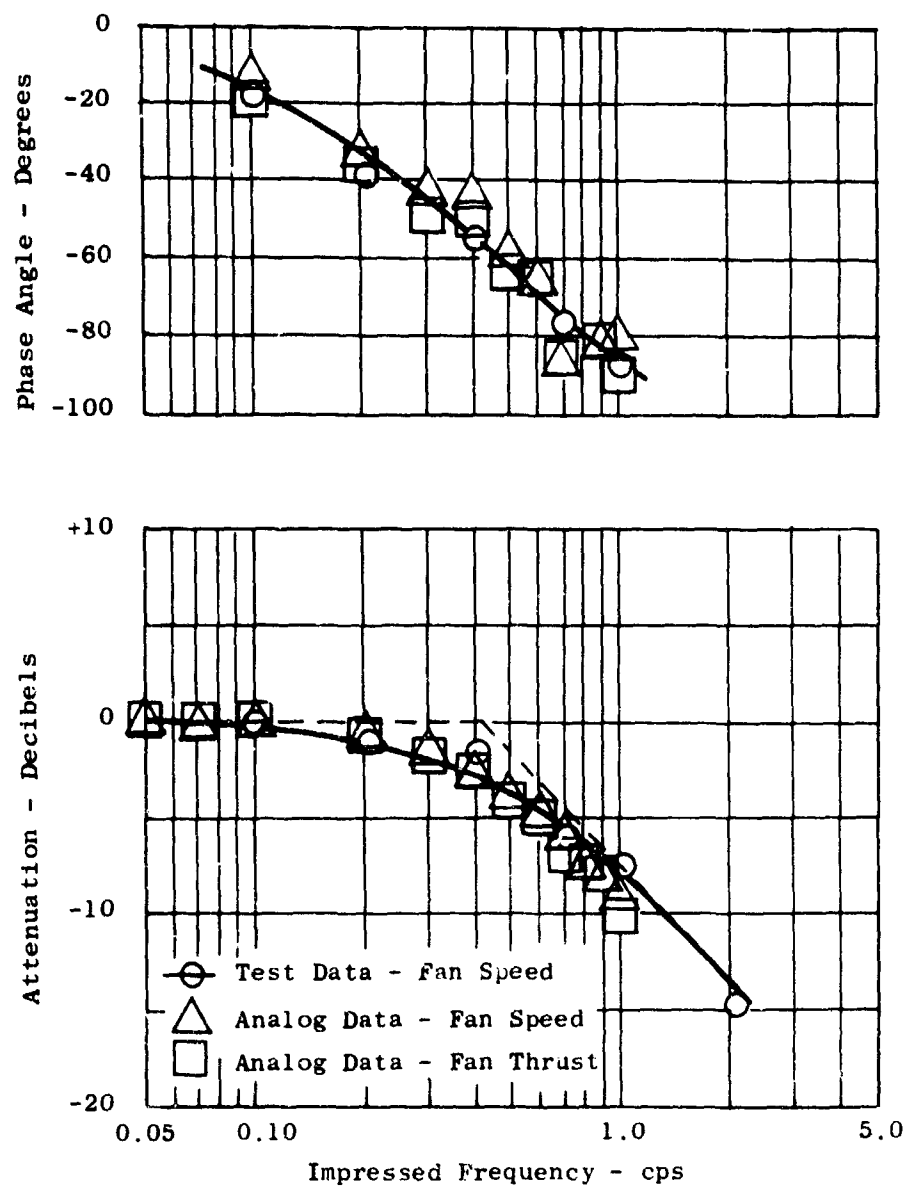


Figure 157. Steady-State Frequency Response - Comparison of Analog and Test Results for Test Actuator Stroke of 50 ± 20 Percent Without a Jazzer.

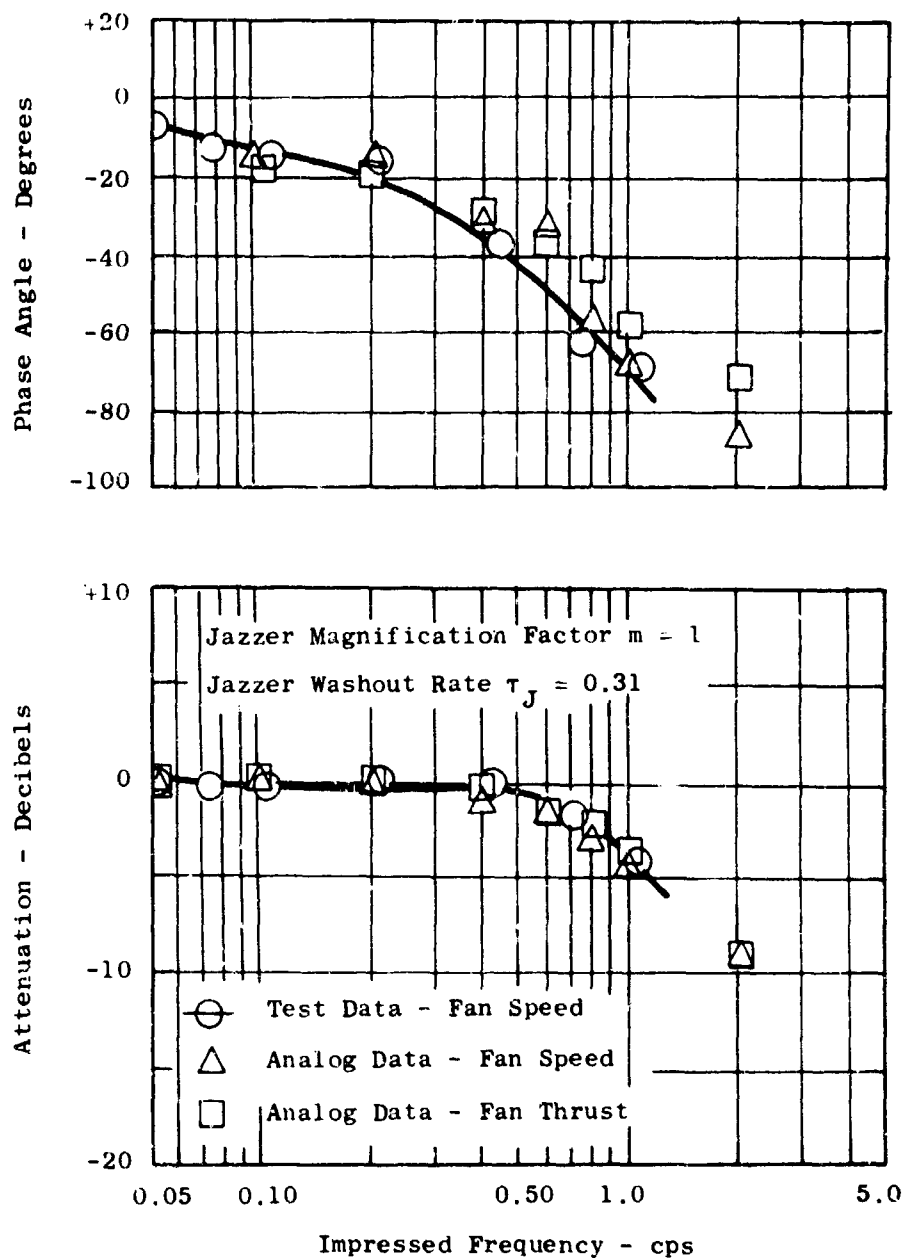


Figure 158. Steady-State Frequency Response - Comparison of Analog and Test Results for Actuator Stroke of 50 ± 20 Percent With Jazzer Magnification Factor of 1.

Aircraft Control Dynamic Requirements

Numerous airframe contractor and Government-sponsored studies have been aimed at defining the dynamic requirements for V/STOL aircraft reaction controls. The results of these studies can be summarized by categories of thrust control lag time constant for any type of propulsion system:

<u>Aircraft Control Function</u>	<u>Thrust Control Time Constant Range - Seconds</u>	<u>Expected Results</u>
Roll, Pitch and Yaw	0.0 to 0.20	Optimum control; effectively instantaneous; best pilot acceptance
Roll, Pitch and Yaw	0.2 to 0.6	Additional control power and more stability augmentation needed as lag increases
Roll, Pitch and Yaw	> 0.6	Unacceptable
Altitude	0.0 to 0.20	Optimum
Altitude	0.20 to 1.0	More installed lift needed
Altitude	> 1.0	Unacceptable

The LFX dynamic analyses have shown that the basic lift time constant is within the 0.20-second optimum response. Basic lift time constant in this definition is the time required for 63 percent of a small (< 5-percent lift) step change command to occur at or near the 100-percent speed fan design point without use of devices to quicken response. For the LFX fan, this value of $\tau_F = 0.187$ second. Including the effect of a practical scroll area hydraulic actuator and control, the value of τ_F increases to 0.236 second. Applying the jazzer to the LFX fan and scroll area control combination showed potential improvements to $\tau_F < 0.10$ second to be feasible. Thus, LFX fan dynamic thrust control can provide optimum V/STOL aircraft reaction control performance.

Cruise Propulsion Power Transfer

Use of LFX type fans in cruise propulsion applications can also provide flexible power control capability. For example, in compound rotorcraft, the ability to modulate gas drive energy between cruise fan and rotor drive may be advantageous in terms of minimizing total installed power requirements. The dynamic thrust requirements of such an application are not clearly defined at this time but the excellent response of LFX fans should meet almost any need.

Energy Modulation Concept

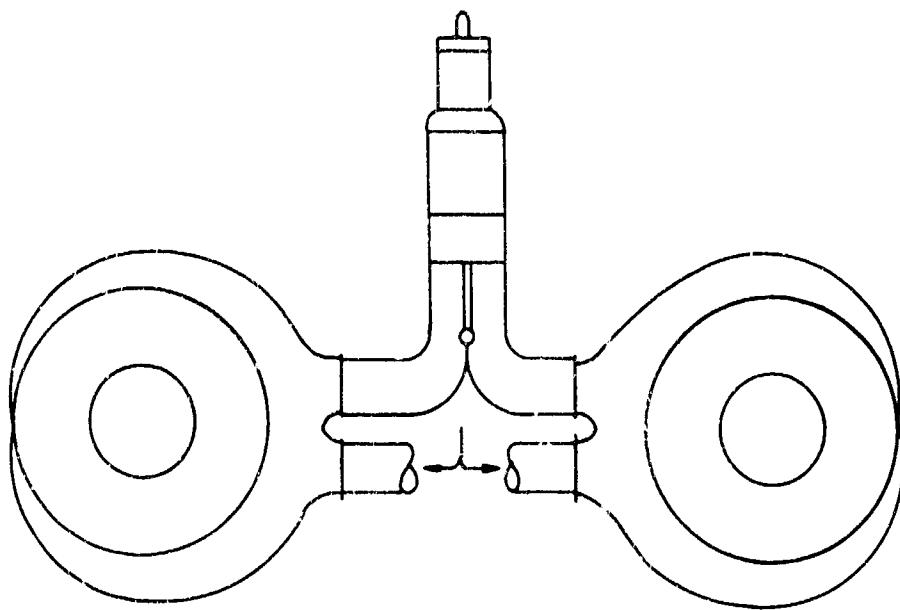
The shifting of power in a lift fan system can be accomplished by varying the turbine gas flow as described previously. Another technique for power modulation identified is the energy modulation concept. Fixed geometry fan scrolls are used with this concept with energy (area) modulation located at the gas generator discharge. With this technique, power transfer between fans is accomplished through the modulation of exhaust gas pressure and temperature in addition to flow transfer.

A schematic is shown in Figure 159. To understand how it works, consider the two separate exhaust flow-path areas to be equal at the point of expansion to atmospheric pressure: in this case, at the lift fan turbine scroll nozzles. With the gas generator exhaust divider (flow splitter) exactly centered so that total flow is divided into equal 180-degree sectors, each lift fan scroll receives equal flow, pressure, temperature, and therefore, equal energy. The result is equal thrust developed by the two lift fans.

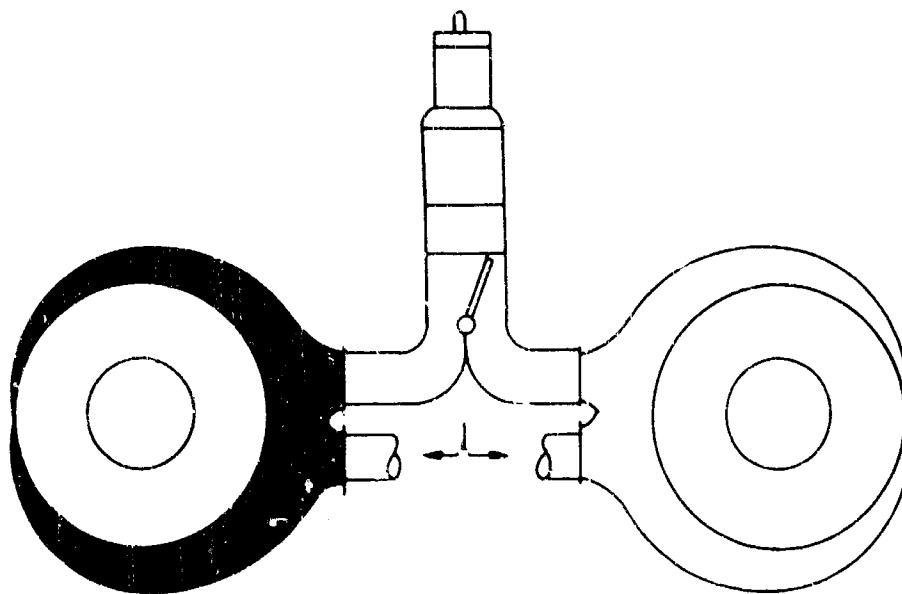
Now consider an unsymmetrical position of the flow splitter; say one sector of 160 degrees and the other sector of 200 degrees but no change to the downstream flow path. Assume that engine exhaust pressure ratio relative to ambient is greater than the critical pressure ratio of 1.85. Now there are unequal flows to the two equal area turbine scrolls, but continuity requires equal flow functions, $W/\sqrt{T}/P$. Therefore, as the flow, W , is decreased, so also must pressure, P , and temperature, T , decrease. Thus, the power ratio between the two lift fans is magnified far beyond the gas flow ratio, since gas internal energy and available energy are also affected in the same direction (sign) as flow. Flow, pressure and temperature effects in the larger, 200-degree sector are opposite in nature; i.e., more flow results in higher pressure and temperature.

Two tests were completed to demonstrate the thermodynamic feasibility of this concept. These tests were run on a YJ85 engine with a divided tail-pipe and a movable splitter located at the exhaust nozzle. The tests demonstrated the capability of transferring better than plus 50-percent power in one duct and minus 10-percent power in the other duct. No mechanical problems were encountered during the testing; however, more investigation of gas generator turbine stresses is required because of asymmetrical load induced in the turbine. The range of power reduction was limited by an annulus choke condition at the YJ85 turbine discharge. This is a limitation imposed by the test engine, and preliminary analysis has shown that it is not a problem in engines of advanced technology.

Results of the test with the YJ85 engine are shown in Figure 160. Percentage changes in horsepower per unit area for the separate ducts, as well as total horsepower, are shown as functions of area change. Application of these results assumes the scroll area to be constant with area change shown on the abscissa occurring at the gas generator turbine discharge.



Nominal Lift



Maximum Power Transfer

Figure 159. Energy Modulation Power Transfer Concept.

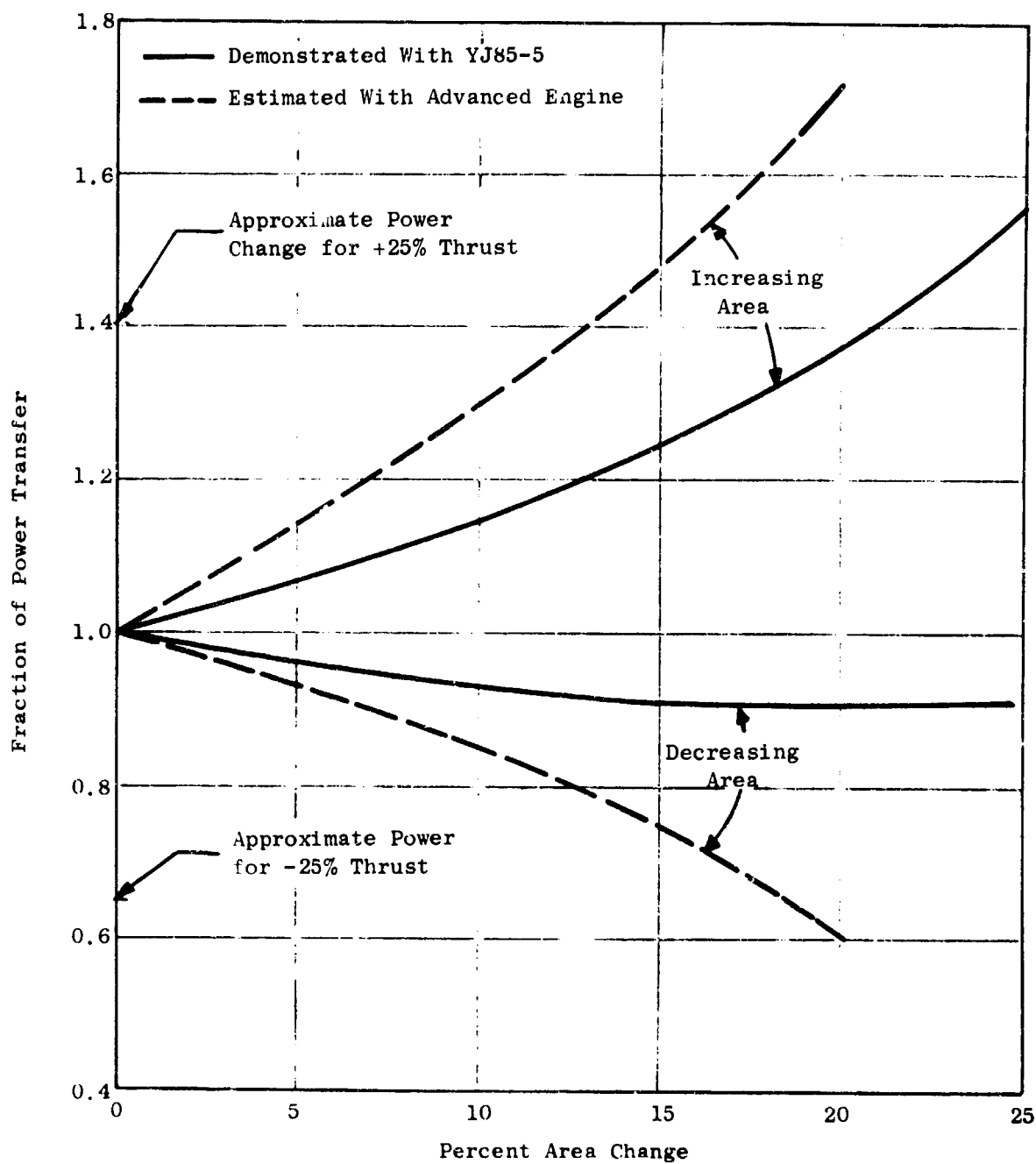


Figure 160. Energy Modulation Performance.

For comparison, a typical advanced technology engine characteristic is also shown without the limitation of annulus choke. A complete description of the tests is given in Reference 10.

ADVANCED FAN DEMONSTRATOR DEVELOPMENT PLAN

OBJECTIVES

The LFX Advanced Lift Fan study and the continuation design study herein reported provide the design basis for a level of turbotip fan technology offering significant improvements relative to demonstrated LF1 and LF2 hardware experience. When tailored specifically to the fan-in-wing convertible propulsion system typified generically by the XV-5A, the LFX twin-engine fan system has been shown to provide substantial utility and flexibility when integrated with an airframe for such tasks as surveillance, reconnaissance, target acquisition, or subsonic close support strike effort. Of more general interest, the LFX fan is the first design-in-depth of a fan compatible with a modern high energy engine. Therefore, the technology represented by the LFX fan coupled with the GE1 engine provides a sound base to fulfill a wide range of high bypass propulsion requirements including cruise as well as lift thrust generation.

Experience shows that propulsion development must precede aircraft development and even the establishment of mission requirements. Looking backward from the date a hypothetical V/STOL aircraft may be introduced to operational use, it is obvious that the longest hardware development lead time is needed for the basic prime mover gas generator. Next in sequence comes the lift propulsion hardware, then the airframe, and other equipment. Based on the conviction that a lift fan powered aircraft will be a vital asset to future military forces, it must be pointed out that development of a prime mover for such an aircraft is well under way and, in fact, approaching PFRT status. The limiting or pacing item is now the lift fan development, not engine development. As of the date of this report, it is not possible to develop the LFX fan within the GE1 engine PFRT schedule. It is even doubtful that LFX fan MQT status could be achieved within the potential GE1 MQT schedule.

To minimize the delay between availability of fans and engines, the LFX fan design represents a balance between technology advancement and risk. The overriding design criteria demand compatibility with the high energy GE1 engine and a lift/weight ratio in excess of 20:1. These criteria have been tempered with the necessity of achieving PFRT status within a 24-month schedule. Thus the LFX fan, as now defined, could be developed with the least possible risk in schedule. A development program could begin with detail component design as the first task. Subsequent sections of this report describe supporting technology programs which further diminish technical risk in an LFX fan development program.

As the next logical step in LFX fan development, it is recommended that a demonstrator program be undertaken. The program should include design and manufacture of two LFX fans as now defined. To fulfill objectives of the program, one fan should undergo extensive static tests to substantiate aero and mechanical design integrity. The second fan should be subjected to a realistic cross-flow environment typical of fan-in-wing installations.

XV-5A experience has shown that true verification of mechanical integrity and installed performance must include large scale cross flow testing. Both fans should be capable of developing objective lift/weight to provide a meaningful demonstration of LFX technology. It is also recommended that at least one of the fans include a variable area turbine scroll as defined in previous sections of this report. Static tests of this fan would provide dynamic thrust control performance extending the technology demonstrated in the J85-LF2 Variable Area Scroll Program to the energy level of GE1 engines and to the thrust control magnitudes required for typical aircraft.

MASTER SCHEDULE

The LFX program for technology acquisition and demonstration is divided into three phases: (1) advanced fan system study (completed with approval of the work described in this report), (2) detailed final design, component testing and hardware acquisition, and (3) demonstrator testing to lead to flight qualification of the hardware.

The master schedule for the major areas of effort involved in the LFX technology acquisition and demonstration program is shown in Figure 161. Other associated fan technology programs are integrated with the LFX master plan. The major milestones in the program are:

	<u>Months from Contract Initiation</u>
Detailed design complete	5
Fan assembly complete	16
Static fan testing complete	18
Wind tunnel testing complete	22
PFRT testing complete	24

The go-ahead date of 6-1-67 has been selected arbitrarily for purposes of planning. It is based on a projection from the date of submittal of this report of a period of time typical of that required for submittal of a proposal, evaluation and negotiation.

Phase I - Advanced Lift Fan Systems Studies

The Advanced Lift Fan System (LFX) Study was initiated in July, 1965. The initial portion of the studies was completed in January, 1966 and documented in a final report (Reference 1). Analytical design and mission studies were conducted to aid in identification of an advanced (1968-1970) lift fan propulsion system applicable to U.S. Army V/STOL surveillance and target acquisition mission concepts.

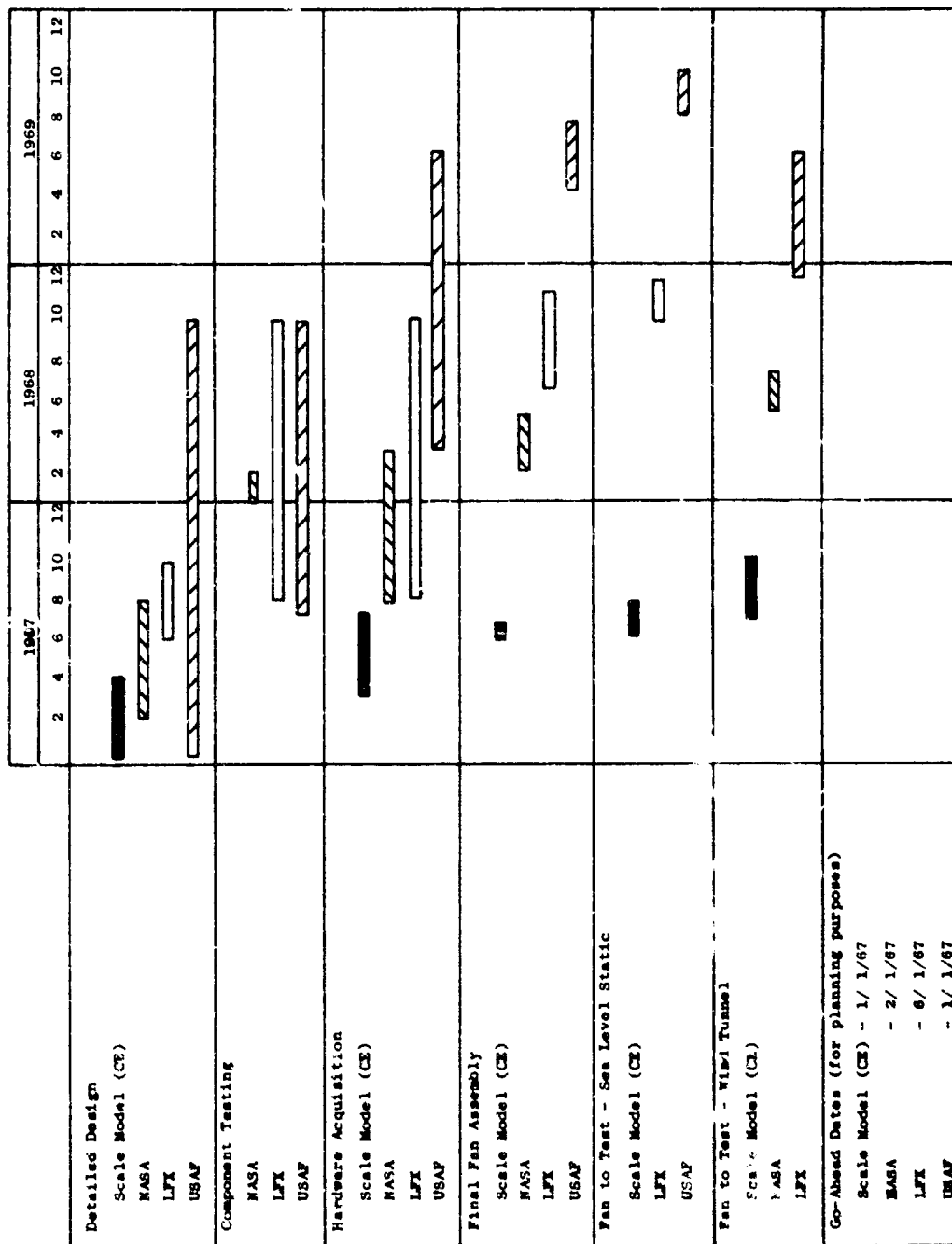


Figure 161. LFX Integrated Master Plan.

The successful XV-5A flight research vehicle was used as the progenitor for a family of turboprop fan-in-wing aircraft from which mission and aircraft design analyses identified an advanced turbojet as the logical choice from a stable of advanced engines either available or under development.

The conceptual aerodynamic and mechanical design of the LFX system was used to aid in identification of problem areas and critical technology.

The second portion of the advanced lift fan system study was initiated in May, 1966 and will be completed when approval of the work contained in this report is given. This continuation of the LFX studies has benefited from the technical momentum generated during the initial conceptual studies. A preliminary "design-in-depth" of the wing fan component of the LFX system was completed to permit realistic evaluation of weight and performance predictions and to better optimize aircraft/propulsion system interface requirements. A technically valuable base has been established for the continuing phases of the LFX technology acquisition and demonstration program.

Phase II - Detailed Final Design, Component Testing, Hardware Acquisition

Detail Design

The detail design phase of the program will utilize the technical base established during the completion of the technology identification phase. The layout drawings of the major wing fan components will be used as a preliminary aid to detailed aerodynamic and mechanical design analysis. Working layouts will be established using the detailed analyses in conjunction with suggestions generated during design and manufacturing review. With the working layouts available, detail prints will be completed to the degree necessary for introduction of the design into hardware.

The timing of the proposed LFX technology acquisition program will enable a maximum utilization and continuity of technical design effort associated with other anticipated Lift Fan Systems Operation programs. Some of the related component and demonstration programs are described in a subsequent section of this report.

Many computer programs are in common use which are applicable to lift fans generally as well as to the LFX fan specifically. During the Phase I LFX studies, specific subroutine modifications to existing programs were made for mission analysis, parametric fan optimization, performance calculations and weight calculations, and controls dynamics predictions. These programs, other existing computer programs and new programs will be extensively used both during the detail design phase and during the test verification phase.

The utilization of these computer programs was greatly enhanced when, in 1965, the General Electric Company completed Evendale substations and data links to a time-sharing computer whereby computers in Chicago, New York and Philadelphia are available through a convenient teletype link. This time-sharing computer link permits an individual engineer to prepare his own programs, subroutines or input to existing programs and input them directly to the computer via the teletype lines. Immediate answers are received for early checking and additional input modifications as necessary.

Component Testing

The component verification testing planned for the LFX program will utilize to the fullest extent the component programs from other portions of the technology acquisition shown in the integrated master plan (Figure 161). These tests will aid in identification of major problem areas in sufficient time to permit some modification of the LFX full-scale hardware prior to PFRT-type testing. The component programs included here will, in many cases, be started prior to the projected initiation of LFX detail design as a portion of other technology programs.

Compressor Aerodynamic Performance

The effects of cross flow on lift fans of medium to high pressure ratio have been extrapolated from the low pressure ratio LF1 and LF2 fan testing. Actual compressor component testing is required to verify the validity of these extrapolations and to predict the effects of such variables as exit louver back pressures, inlet geometry and wing configurations. This measurement of cross-flow effects is a vital part of the planned NASA advanced technology program. A continuous cross-feeding of data and results from NASA and other advanced technology programs will be utilized both to predict LFX performance and to identify the most promising areas for design improvement.

Turbine Aerodynamic Testing

The LFX turbine aerodynamic design features a converging-diverging turbine nozzle passage and near-sonic relative turbine bucket velocities in order to achieve maximum efficiency from the high specific energy of the gas generator flow. The impact of the aerodynamic design on the mechanical design capability needs to be evaluated through the medium of component testing. Cascade tests can be utilized to better identify the effects of normal shop tolerances on the optimum aerodynamic design. Rotating rig testing utilizing existing fan equipment such as the LF2 can be utilized to verify the effects of tip-seal leakage.

Turbine Mechanical Testing

The turbine design features sharp (0.020-inch) bucket leading and trailing edges. Aerodynamic requirements make even sharper (0.011-inch) leading and trailing edges desirable. Component testing is necessary to define the effects of erosion, foreign object damage, manufacturing variations, thermal gradients, and to optimize a manufacturing technique. Much of this component verification could be completed during the conduct of the previously noted aerodynamic component testing.

Scroll Aerodynamic and Mechanical Testing

The LFX scroll features a variable area power transfer concept similar to the proven LF2 fan but with much greater modulation capabilities. Component testing of the scroll to determine seal leakages, spring rates, actuation forces, full admission performance and partial admission performance needs to be completed.

Composite Structure Testing

The LFX fan design includes the use of materials with variant characteristics in close proximity or joined to each other. The aluminum honeycomb in the steel front frame strut is an example. Titanium bonded to steel in the rear frame is another. These uses of variant materials are feasible. However, bonding techniques, welding techniques and other methods of joining variant materials are an integral part of other Lift Fan Systems Operation programs which will be closely integrated with the LFX program.

Alternate Concepts

During the current LFX design studies, variations in basic fan mechanical design philosophy were identified and evaluated for potential weight savings, performance improvements or better aircraft interface integration. Some design innovations included a structural rear frame and no front frame, bonded turbine attachment in lieu of pins, composite compressor blade (Figure 162) and a combination bellmouth/scroll (Figure 163). The development time and necessary verification to achieve these concepts were not considered to be compatible with the planned LFX technology acquisition schedule. However, these advanced concepts and others will be included in other associated programs either currently in process or planned for the Lift Fan Systems Operation.

Hardware Acquisition

The hardware acquisition program is based on acquiring two complete fans in operating condition, spares necessary for testing at two different geographical sites and certain component parts for design analysis and verification.

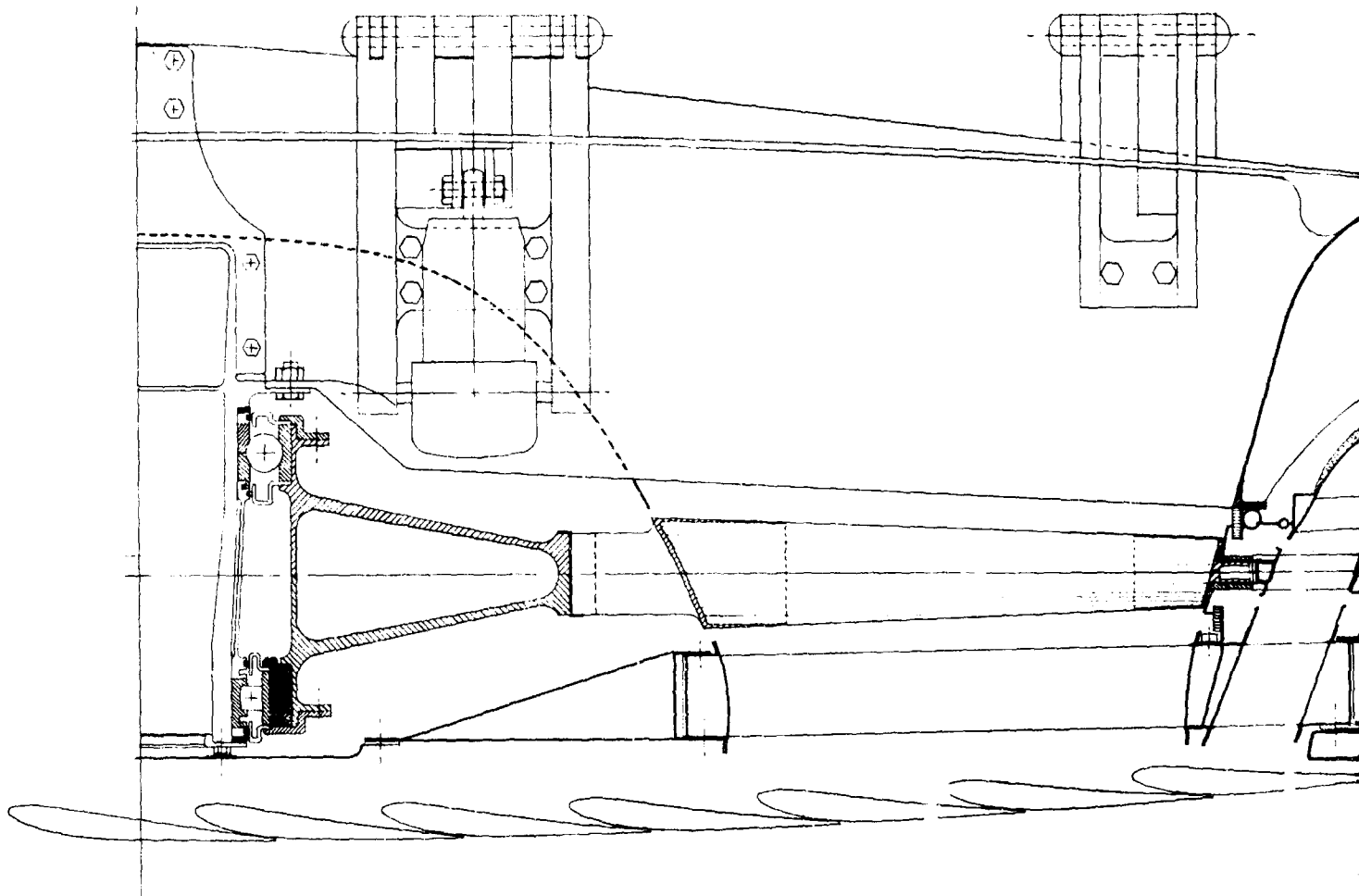


Figure 162. Composite Compressor Blade Concept.

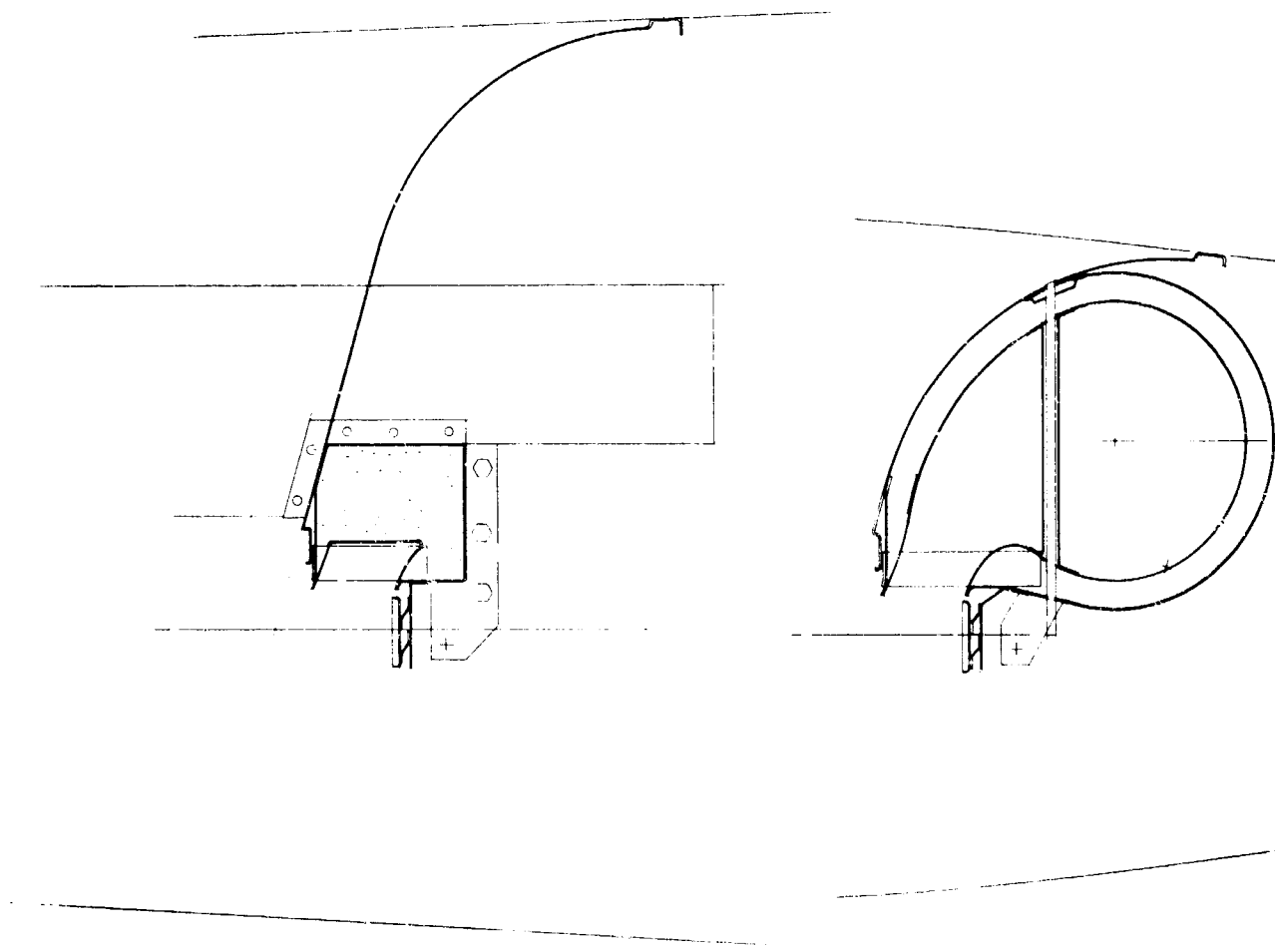
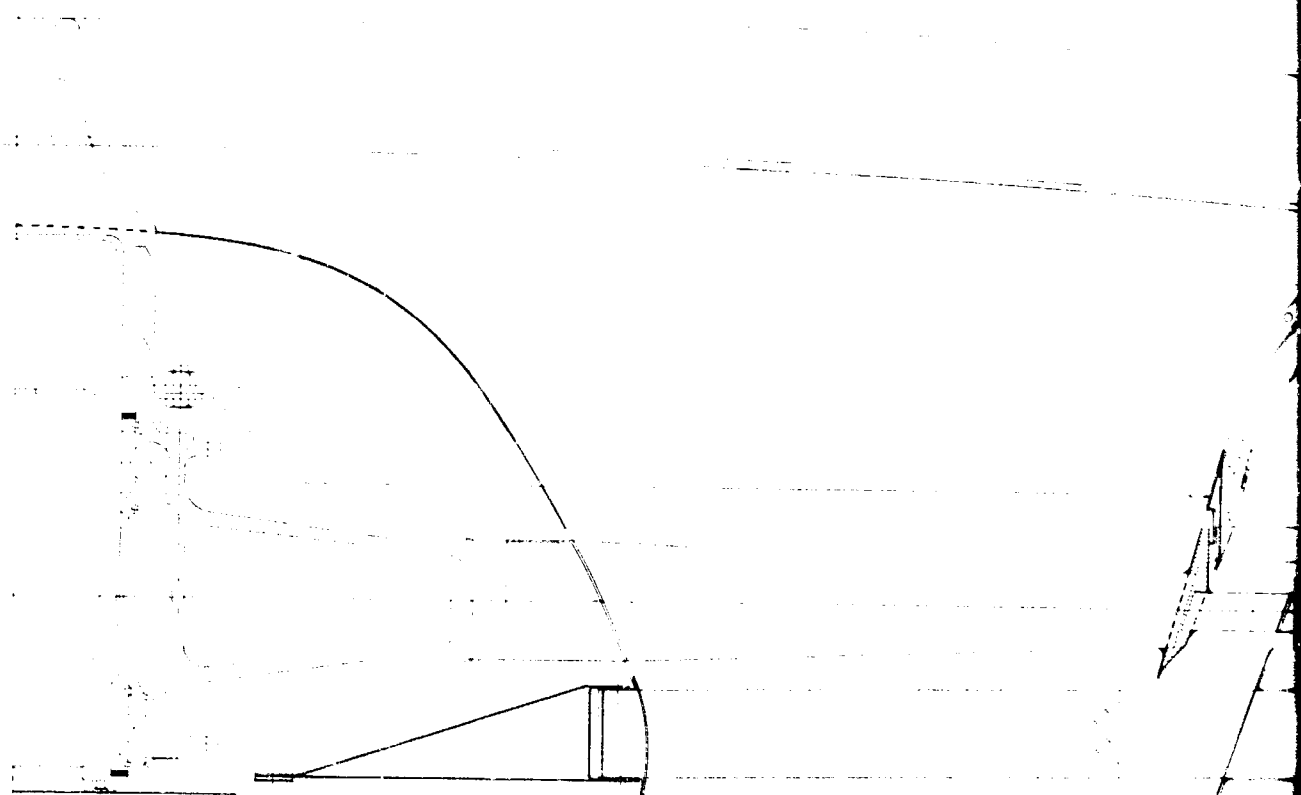
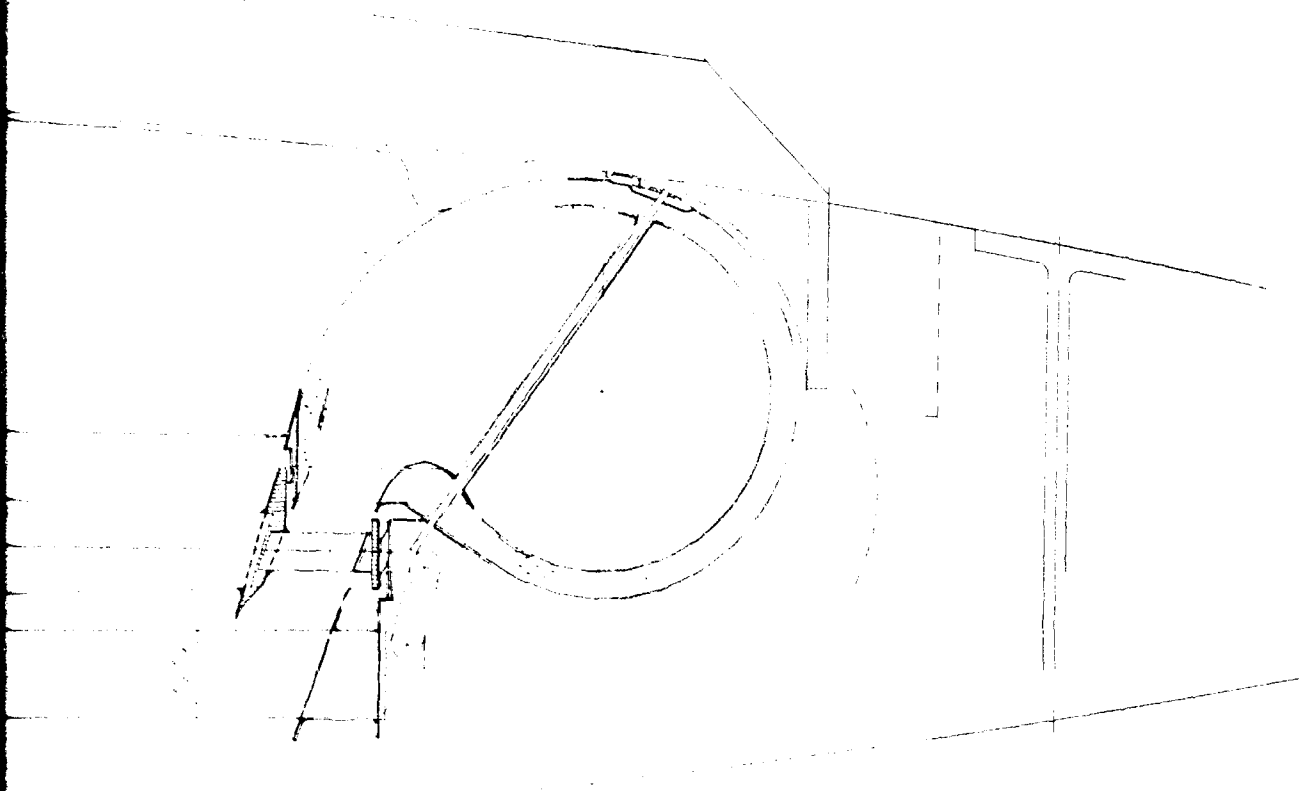


Figure 163. Combination Bellmouth/Scroll Concept.

A



0



PROJECT NUMBER	10000-663
PROJECT NAME	STUDY OF ADVANCED TECHNOLOGY
PROJECT OFFICE	EDWARDS
PROJECT ENGINEER	J. R. B. 10000-663
PROJECT MANAGER	J. R. B. 10000-663

6

The detailed design of hardware will be sufficiently advanced 2 months after initiation to permit release of long lead time items such as blade and disc forgings. Other shorter lead time items and associated tooling acquisition will be released on completion of the detail design 5 months after initiation.

Initial trial assemblies of major subcomponents such as the scroll, frames, etc., will begin 14 months after initiation of design with completion scheduled in time to permit initial testing on the Evendale Static Fan Test Facility 17 months after contract initiation.

A decision on the total number of spares for the program would be required not later than 5 months (or concurrent with detail design release) after program initiation. The actual quantity and specific spare components might be modified as the detail design and component test program. At the current time a minimum spares requirement estimate for one fan includes

- 10 compressor blades
- 5 turbine sectors
- 1 disc (wheel)
- 1 set of bearings
- 1 complete set of seals
- 10 rear frame stator vanes

A spares requirement for two complete fans with testing at different geographical locations includes

- 1 set of 50 compressor blades
- 25 turbine sectors
- 2 discs
- 2 sets of bearings
- 2 sets of seals
- 10 rear frame stator vanes

PHASE III - TEST PLAN

The LFX technology demonstration and development plan is intended to achieve the objectives of mechanical design verification and aerodynamic development and verification. The test plan is divided into two sections: static testing and cross-flow testing. The use of two fans will greatly enhance the probability of timely completion of both phases of this test plan.

Static Testing

The static testing of a lift fan in a controllable environment has been proven to be a valuable and useful tool both for mechanical evaluation and for aerothermodynamic evaluation and verification. A total of 35 to 40 hours running time on the initial static test would be necessary to permit a complete evaluation of full and part speed performance with and without power transfer. Some of the features which could be demonstrated include:

Performance of the high lift-to-weight ratio fan system with an advanced technology high exhaust energy gas generator

Thrust modulation equivalent to 50 percent of nominal thrust by variable area scroll actuation

Measurement of ground overpressure with a high pressure ratio lift fan system

Mechanical integrity at all operating speeds

Noise magnitude and attenuation

Fan inlet cover effects

Exit louver effects on fan mechanical and aerodynamic performance

Static Test Facility

The lift fan static test facility, located on the General Electric Evendale facility, was used for the initial concept evaluation and development testing of the LF1 fan. Its most recent use has been for the demonstration and performance measurement of the LF2 fan with an operable power transfer scroll.

The test stand has an outdoor column-mounted wing section with engine and fan mount capabilities and an indoor control room and instrumentation consoles. The stand thrust frame can measure both vertical and horizontal thrust. It is capable of accepting two gas generators, one wing fan and a fuselage fan for complete system demonstration, or it can be operated with one engine and wing fan for limited testing or demonstration.

Test Scope

The static test plan includes a functional check-out of the core engine gas generator prior to installation on the VTOL stand. Following installation on the VTOL stand, an additional functional check for leaks will be performed during idle power running.

After installation of the wing fan, a fan mechanical check-out will be performed through a series of gradually increasing fan speed runs. Complete readings of all fan mechanical parameters will be taken at each speed point up to the maximum attainable fan speed. Following the completion of each speed point, an inspection of the fan and gas generator will be completed.

After the mechanical check-out has been satisfactorily completed, a program for aerodynamic performance with maximum, nominal and minimum scroll area settings at all normal operating gas generator power settings will be initiated. Verification of the fan compressor map up to the stall line will be completed through suitable flow blockage of the fan discharge

stream. The effect of the exit louvers on the fan mechanical and aerodynamic performance will be measured.

Wind Tunnel Testing

In order to fully evaluate the potential of a lift fan system for aircraft propulsion, it is necessary not only to analyze static operation, but also to analyze the capability of the system to operate in a cross-flow environment such as that of the aircraft during transition to a forward speed sufficient for wing-supported flight. The excellent correlation of the XV-5A wind tunnel performance with the actual flight performance of the aircraft gives credence to the wind tunnel technique of fan evaluation. In addition to the verification of performance, the wind tunnel evaluation of the XV-5A fan system in the aircraft and in model installations afforded an excellent source of mechanical operational and reliability data.

The second fan in the LFX program would be mechanically checked at the Evendale VTOL static test facility prior to shipment for wind tunnel evaluation. Selection of a representative wing configuration for single fan testing or of a complete aircraft model for dual fan testing would permit a complete evaluation of the effects of cross flow on the fan aerodynamic and mechanical performance. Total testing hours for initial cross-flow testing could be as low as 25. More sophisticated evaluation of interaction effects might require running time in excess of 100 hours.

Program Milestones

A listing of major LFX program milestones projected to demonstrate the technology by fan running and acquire the technology through a successful flightworthiness (PFRT) test is as follows:

	<u>Months from Contract Initiation</u>
Initiate detailed design of lift fan and component test hardware	0
Initiate acquisition of long lead time hardware	2
Initiate component testing on selected critical components	3
Complete detailed designs	5
Initiate final fan assembly	14
Complete all component testing and final hardware acquisition	15

First fan to test - sea level static	17
Start sea level static fan testing	18
Complete sea level static fan testing	19
First fan to test - wind tunnel	19
Complete wind tunnel testing	22
Complete PFRT demonstration	24

SUPPORTING PROGRAMS

The master schedule section (Figure 161) includes the LFX program and other major lift fan programs. The interplay and exchange of data among all the LFSO programs will be integrated to result in the maximum amount of useful technology for the minimum amount of expended man-hours. There are two major programs, one under contract and one currently planned, that will indirectly and directly contribute to the efficient accomplishment of the LFX program objectives.

The highly significant progress in materials application and process application made under the Air Force sponsored ADO-26 and Contributing Engineering programs will represent a continuous source of technical innovation.

The programs alluded to in this paragraph will be covered separately in the following sections.

USAF Advanced Lift Fan and Lift/Cruise Fan Demonstrator Program

An Air Force RFQ PR (7) 25219 was issued by the Air Force Systems Command which called for technology advancement objectives in lift fan and lift/cruise fan designs compatible with missions envisioned for V/STOL transports in the 1975 time period. The program proposed by General Electric to fulfill the objectives stated in the RFQ defined a lift fan demonstrator of 73-inch diameter, with a pressure ratio of 1.4, a turbine inlet temperature capability of 1600°F, and a total lift rating of 27,500 pounds. This fan demonstrator, with the technology advancements required, would provide a major impetus to the acquisition of data applicable both to the LFX fan system as well as to the Air Force fan. An optimum fan for Air Force needs has been defined in the General Electric proposal (Reference 13). The design is drawn from a knowledge of USAF V/STOL assault transport needs and the specific operating environment imposed on lift fan propulsion, the latter gained through extensive experience with XV-5A operation.

The LFX program and the USAF advanced fan program are highly compatible with and complementary to each other. The attainment of the technical objectives of both programs would be more certain if both programs were simultaneously active. An equally important section of the Air Force

demonstrator program is the definition of a lift/cruise fan also needed to complete the studies toward a V/STOL transport aircraft of the mid-1970's.

NASA High Pressure Ratio Lift Fan Program

The NASA program requires the design, manufacture, and static test of two 1.3-pressure-ratio, 36-inch-diameter, tip turbine lift fans. The fans will be designed to a minimum thickness compatible with thin fan-in-wing installations; however, flexibility in front frame and scroll designs will also allow podded type installations. The fans are to be used to power research models for full-scale wind tunnel investigations of high-pressure-ratio lift fan aerodynamic and mechanical performance in cross-flow environment, and to determine overall fan-aircraft system performance as a function of aircraft and fan variables.

This program consists of three phases covering a period of 18 months.

The all-important data to be derived from this program and cross-fed into the LFX program lies primarily in aerodynamic and mechanical performance of high-pressure-ratio (1.3) fans in a cross-flow environment. Methods, procedures and perhaps design innovations would be defined and used in LFX development if the innovations proved to be practical and/or needed to successfully attain LFX performance goals.

Contributing Engineering Programs

In the common areas of component development, materials development, aerodynamic development and mechanical durability development, the technical groups contributing to the attainment of these objectives will make their results known to all participating LFSO engineers. The technical advancements thus discovered will mutually benefit all programs.

COST ESTIMATE

A preliminary cost estimate for the LFX technology demonstration and acquisition program has been completed as an aid to planning. The cost estimate, shown in Table XXII, is not intended to represent a commitment on the part of General Electric. It is based on the completion of two complete fans with power transfer scrolls and flight-weight components plus spares to support the static testing program and limited wind tunnel testing. The timing of the program is that indicated in the LFX master schedule, Figure 161.

TABLE XXII
LFX-6 PROGRAM COST ESTIMATE

Phase I	- Studies and preliminary design - Complete		
Phase II	- Detail design, component testing, manufacture hardware	\$2,880,300	
Phase III	- Assemble two fans, test one fan 40 hours static stand; one fan one hour static stand; ship to wind tunnel	837,800	
	M.C.	\$3,718,100	
	Plus G&A	3,978,400	
LFSO Design and Project		\$316,200	
Drafting		69,100	
ARADO		50,000	
MDLO		50,000	
Computations		55,000	
		<u>\$540,300</u>	
			540,300
Hardware (two sets plus spares)		\$1,418,900	
Tools		<u>785,300</u>	
		\$2,204,200	
			2,204,200
Evaluation		\$274,600	
Assembly		137,500	
Test		133,700	
Facilities		120,400	
Instrumentation		<u>171,600</u>	
		\$837,800	
			837,800
Component Testing		<u>135,800</u>	
MANUFACTURER'S COST		<u>\$3,718,100</u>	

CONCLUSIONS

PRINCIPAL CONCLUSIONS

1. The LFX propulsion system offers a flexible advanced technology V/STOL propulsion system which can be adapted to a wide variety of Army Air Mobility concepts.
2. The LFX wing fan can achieve lift-to-weight ratios as high as 23.5 to 1. The convertible LFX system including two gas generators, two wing fans and a fuselage fan can achieve a total system lift-to-weight ratio of 9.9. The wing fan can be installed in a representative 9-percent-thickness wing.
3. The LFX fan dynamic thrust control can provide optimum V/STOL aircraft reaction control performance.
4. A solid advanced technology foundation has been defined from which an advanced demonstrator lift fan could be produced to meet the LFX objectives. A principal LFX objective is the timely acquisition of fan technology appropriately compatible with the high energy GE1 (J97) engine.

The advanced technology demonstrator lift fan is a vehicle for lift fan, cruise fan and control fan technology advancement.

5. The LFX technology can be demonstrated through initial full-scale fan running in 1968. Complete acquisition of the LFX technology can be achieved through MQT tests by 1970. A PFRT status propulsion system based on GE1 (J97) engines and LFX fans could be available in 1969.

DETAILED CONCLUSIONS

Aircraft/Propulsion System Interface

1. The LFX wing fan should be an integral unit including the front frame, scroll, rotor, and rear frame. The wing fan should be capable of operation independent of wing structure.
2. The wing fan should be capable of mounting the split butterfly fan cover doors and door actuators on the front frame major strut.
3. The wing fan cover door latches should be arranged such that auxiliary struts in the compressor inlet flow path are not required.
4. The wing fan exit louvers can be mounted directly to the aircraft wing structure with a resultant weight savings for the overall aircraft/propulsion system weight. The exit louvers should be aerodynamically counterbalanced to the extent compatible with fan installation in a 9-percent-maximum-thickness wing.

5. The power transfer scroll should have the normally inactive a/c on the inboard side of a fan-in-wing installation. The scroll should be capable of accepting the total flow from one gas generator as its maximum flow position.
6. The wing fan should be capable of evacuating any flow leakage into the wing fan compartment during fan operation.

Specifications

1. The LFX preliminary design specification (USAAVLABS Technical Report No. 67-48) can be used as a basis for detailed design of the demonstrator fan.
2. The specification offers a useful tool to Government and industry for use in conceptual V/STOL aircraft evaluation.

Preliminary Design

1. The parametric optimization study using the conceptual LFX wing fan design as a base identified a 10-percent reduction in planform area coupled with a 7 $\frac{1}{2}$ -percent increase in maximum lift at no increase in weight.
2. The LFX weight objectives were sufficiently stringent to require ingenuity and innovation.
3. The LFX rotor preliminary design does not meet design objectives for dynamic characteristics. Further analysis is required prior to detailed design.
4. The LFX preliminary design layouts provide an excellent base for accurate cost and weight estimates.
5. The LFX aerodynamic design will benefit from other planned technology acquisition programs.
6. A possibility exists for a substantial weight improvement through combining the wing fan door cover with the fan front frame strut. Other weight and performance improvements can be realized through technology advances, innovations and development currently planned in other programs.

Master Plan

1. A plan for technology acquisition and demonstration of the LFX technology can be integrated with other Government and General Electric advanced fan technology programs to provide a minimum risk path to a high performance advanced lift fan system. The LFX technology acquisition is complementary to other advanced fan technology programs.

2. A qualified advanced technology gas generator will be available in a time period compatible with that projected for the LFX fan, i.e., 1970. A delay in instigation of the LFX fan technology program will result in the fan becoming the pacing item for a propulsion system with widely varied applications potential.

BIBLIOGRAPHY

1. Advanced Lift Fan System (LFX) Study, USAAVLABS Technical Report 66-51, U.S. Army Aviation Materiel Laboratories, Fort Eustis, Virginia, July 1966.
2. Study of Airframe Requirements for Lift Fan Technology Advancement, Ryan Report No. 29469-2, Ryan Aeronautical Company, San Diego, California, April 1966.
3. Summary of LFX/Airframe Interface Discussions, LFX Memorandum No. 66-4, General Electric Company, Evendale, Ohio, August 1966.
4. Lift Fan Technology Review, LFX Memorandum No. 66-3, General Electric Company, Evendale, Ohio, June 1966.
5. Conference on V/STOL and STOL Aircraft, NASA No. SP-116, April 1966.
6. Experimental Investigation of an Axial-Flow Compressor Inlet Stage, NACA RM E53G17, 1953
7. Investigation of an Axial-Flow Compressor Rotor, NACA RM E53D24, 1953
8. Use of Arbitrary Quasi-Orthogonals for Calculating Flow Distribution, NASA TN D-2546, 1964
9. Lift Fan Technology Studies, Part I, GE Report No. R66FPD304, General Electric Company, Evendale, Ohio, November 1966.
10. Test Results of Turbine Energy Division for Power Transfer, AC&S Memo No. 66-24, General Electric Company, Evendale, Ohio, August 1966.
11. Design, Test and Analog Simulation of the LF2 Fan System with Variable Area Scroll, General Electric Company, Evendale, Ohio, December 1966.
12. Revised Analysis of Single-Tang Dovetail Blade Attachments, GE Report No. R63FPD21, General Electric Company, Evendale, Ohio, February 1963.
13. Advanced Turbotip Lift Fan and Lift/Cruise Fan, Proposal P66-119, General Electric Company, Evendale, Ohio, November 1966.

UNCLASSIFIED

Security Classification

DOCUMENT CONTROL DATA - R & D		
(Security classification of title, body of abstract and indexing annotation must be entered when the overall report is classified)		
1. ORIGINATING ACTIVITY (Corporate author) General Electric Company Flight Propulsion Division Evendale, Ohio		2a. REPORT SECURITY CLASSIFICATION UNCLASSIFIED
3. REPORT TITLE Advanced Lift Fan System (LFX) Study Continuation.		2b. GROUP
4. DESCRIPTIVE NOTES (Type of report and inclusive dates) Final Report - May 1966-December 1966		
5. AUTHOR(S) (First name, middle initial, last name) Harris C. True		
6. REPORT DATE September 1967	7a. TOTAL NO. OF PAGES 336	7b. NO. OF REFS 13
8a. CONTRACT OR GRANT NO. DA 44-177-AMC-422(T)	8b. ORIGINATOR'S REPORT NUMBER(S) USAAVLABS Technical Report 67-45	
8c. PROJECT NO. Task 1M121401D14415	8d. OTHER REPORT NO(S) (Any other numbers that may be assigned this report) GE Company Report No. R66FPD342	
10. DISTRIBUTION STATEMENT This document is subject to special export controls and each transmittal to foreign governments or foreign nationals may be made only with prior approval of US Army Aviation Materiel Laboratories, Fort Eustis, Virginia 23604.		
11. SUPPLEMENTARY NOTES	12. SPONSORING MILITARY ACTIVITY U.S. Army Aviation Materiel Laboratories Fort Eustis, Virginia	
13. ABSTRACT A preliminary design of an advanced lift fan propulsion system is presented. The V/STOL system is designed to utilize the General Electric J97 gas generator, together with fans having a high degree of inherent control capability during vertical mode flight. A technology development and acquisition plan leading to MQT in 1970 is identified.		

DD FORM 1473

REPLACES DD FORM 1473, 1 JAN 64, WHICH IS OBSOLETE FOR ARMY USE.

UNCLASSIFIED
Security Classification

UNCLASSIFIED
Security Classification

14. KEY WORDS	LINK A		LINK B		LINK C	
	ROLE	WT	ROLE	WT	ROLE	WT
Lift fans Propulsion system Tip-turbine-driven lift fan V/STOL propulsion system Wing fan LFX						

UNCLASSIFIED
Security Classification